CRYSTAL ENGINEERING IN THE GEM-ALKYNOLS. PSEUDOPOLYMORPHISM AS A MODEL FOR CRYSTALLIZATION

A Thesis
Submitted for the Degree of
Doctor of Philosophy

By
RAHUL BANERJEE

School of Chemistry
University of Hyderabad
Hyderabad 500 046
India

January 2006

To
Ma and Baba

CHAPTER ONE

CRYSTAL ENGINEERING – FROM CRYSTAL NUCLEATION TO CRYSTAL STRUCTURE

1.1 Overview

The synthesis of organic compounds relies on the strengths of covalent bonds and the relative rates of formation of these bonds in order to lead to the final product via a rational, multi-step process [1.1]. In supramolecular synthesis, supermolecules are synthesized through self-assembly with many non-covalent interactions in a single step. For supramolecular synthetic chemists, the motivation is to control the ability of the supramolecular assembly to exhibit desirable chemical and physical properties [1.2]. These properties are dependent on the nature of the individual molecules present, as well as on the manner in which they are arranged within the supramolecular assembly [1.3].

The field of crystal engineering [1.4], a sub-discipline of supramolecular chemistry [1.5], is concerned with the construction of crystalline materials from molecules or ions using non-covalent interactions [1.6]. The supramolecular assembly is a single crystal in this case. It is noted in crystals that the same type of association between two or more specified molecular fragments is observed in a variety of systems that contain these fragments. This suggests that these interaction patterns are relatively robust and are therefore likely to be observed in other systems containing these fragments. In other words, the patterns are specific to this combination of molecular fragments. Such observations motivated Desiraju to introduce the term *supramolecular synthon* which may be defined as *a structural unit within supermolecules, which can be formed and/or assembled by known or conceivable synthetic operations involving intermolecular interactions* [1.7]. The term *synthon* was introduced by Corey in 1967 [1.8] to represent the key structural features of a target molecule in organic synthesis [1.9]. A synthon is usually smaller and less complex than the target molecule and yet contains most of the information required to synthesize the target substance [1.10]. The supramolecular synthon concept combines the idea of the synthon, proposed by Corey

for organic synthesis, with Lehn's definition of supramolecular chemistry as the chemistry of intermolecular bond.

The supramolecular synthon concept draws an analogy between classical organic synthesis and supramolecular synthesis. It attempts to describe the recognition events that take place when molecules assemble into a supermolecule and provides an important illustration of the similarities between organic retrosynthesis and crystal engineering [1.11]. The supramolecular synthon is an aid to understand the means by which groups of molecules communicate, bind and organize themselves in solution. As crystallization is a kinetic phenomenon, the best possible synthons prefer to assemble first and form the core of the crystal structure that finally results. The idea that supramolecular synthons are the critical building blocks in crystal engineering has provided a working definition, which includes all types of intermolecular interactions like hydrogen bonds, van der Waals interactions and polarization based interactions within a general framework. Desiraju's idea in proposing the term *supramolecular synthon* was to simplify the analysis of a complex crystal structure and to understand the subtle chemical and geometrical effects on the overall crystal packing. Today, this concept has diversified into all corners of crystal engineering starting from an understanding of synthetic crystallography [1.12], molecular tectonics [1.13], crystal nucleation [1.14], crystal structure prediction [1.15] and to reticular synthesis [1.16]. Thus, crystal engineering has at its heart a synthetic endeavour that begins with the identification of suitable supramolecular synthons, which can be combined in a directed manner by self-assembly methods to yield a crystalline supermolecule [1.17].

Identifying supramolecular synthons is clearly as important to crystal engineering as is an understanding of reaction mechanisms and reagents to conventional covalent organic synthesis. So it is important to find out the conditions under which molecular recognition can be used to assemble structures with precise topologies. Such insight is most effectively obtained through rationalization, analysis, design and prediction. Recent progress in crystallography both in terms of diffraction hardware and software have provided extraordinary access to structural information. Among them the Cambridge Structural Database (CSD) [1.18], which houses more than 3,50,000 organic

and metal-organic crystal structures, contains numerous examples of almost every kind of intermolecular contacts and has been used by crystal engineers to analyze and identify important trends in crystal packing. Today, crystal engineering has implications that extend into areas as diverse as pharmaceutical development [1.19] and synthetic chemistry [1.20]. The recent huge stimulus of crystal engineering also owes to its applications in non-linear optics [1.21], microporous materials [1.22], electronic materials and sensors [1.23] and molecular modelling [1.24].

1.2 Intermolecular interactions

The hydrogen bond, defined in the standard formulation as an X–H…A interaction, plays a dominant role in crystal engineering, biological recognition and drug design [1.25]. Hydrogen bonds combine, in addition to specificity, strength with directionality. These features, in combination, control the design of various molecular assemblies. Hydrogen bonding provides an explanation of conformational preferences of molecules, their properties and their reactivities in the gas, liquid and solid phases. The packing of molecules in a crystalline organic solid, directed by conventional hydrogen bonds, where both X and A are electronegative atoms (O–H…O, N–H…O, O–H…N, and N–H…N) has been well studied [1.26]. The binding energies of strong hydrogen bonds are normally greater than 5 kcal mol^{-1} and the distance between the proton and the acceptor atom (H…A) is significantly shorter than the sum of their respective van der Waals radii. For unusually activated donors and acceptors, say as in the case of the inorganic fluoride ion F–H…F^{-}, and the charged O–H…O^{-}, N^{+}–H…N or O^{+}–H…O, O^{+}–H…N^{-} systems, the hydrogen bonds are very strong and show similarities to covalent bonds [1.27]. On the other hand, for systems in which both X and A or only one of them are of moderate to low electronegativity, the bond energy drops significantly to below 10 kcal mol^{-1} and approaches values typical of van der Waals interactions (weak hydrogen bonds) [1.28]. Thus, one may distinguish between systems with: (a) weak donors and strong acceptors, for example, C–H…N/O/S [1.29], (b) strong donors and weak acceptors, such as O/N–H…Cl/F–C, O/N–H…π [1.30] and (c) weak donors and weak acceptors, such as C–H…Cl/F–C, C–H…π interactions [1.31] based on their hydrogen

bond energies. In crystal structures it is sometimes difficult to say if the stronger hydrogen bonds are more significant than the weaker ones or not. Each is probably important for the viability of the overall structural motif, and for this type of interaction, Desiraju recently suggested a different term "hydrogen bridge" instead of "hydrogen bond" [1.32].

A crystal structure is a result of a balance between various non-covalent interactions in the solid-state. When geometrical requirements of two interactions can be fulfilled in isolated regions of a structure, these interactions are said to be structurally *insulated*. If the geometric demands of two interactions come into conflict, optimization of one interaction changes the normal pattern of the other, and this phenomenon is termed *interaction interference* [1.33]. It is difficult to anticipate when a particular chemical modification will conserve a synthon and when a structure will be disturbed. Interaction interference can be minimized through structural insulation, i.e. by having structurally orthogonal domains in a crystal. The family of geminal alkynols is a good example of interaction interference and structural insulation.

1.3 Hydroxy and ethynyl (*gem*-alkynol) recognition and their interaction patterns

The family of geminal alkynols or *gem*-alkynols, molecules that contain equal stoichiometries of hydroxyl and ethynyl groups attached to the same carbon atom, offers an assorted structural behaviour, which is suited to the effective exploration of the relationships between molecular functionality and crystal packing [1.34]. The lack of structural repetition among the 158 published crystal structures in this family is an additional challenge. Failure to find repeating structural relationships in this family arises from the close juxtaposition of two hydrogen bond donors (O–**H**, C–**H**) and two acceptors (**O**–H, **C**≡**C**–H). In this sterically hindered situation, the four interactions that are possible, namely O–H…O, C–H…O, O–H…π and C–H…π, become competitive. This leads to high levels of interference among these four interaction types (Scheme 1). Most of these structures do not contain traditional hydrogen bonds (*e.g.* O–H…O) as the dominant intermolecular interaction. The packing pattern in any particular crystal structure in this family is highly sensitive with respect to changes in the substitution

pattern of the molecular skeleton. As a result, attempts to establish a molecule–supermolecule correspondence via the supramolecular synthon approach are extremely difficult [1.35].

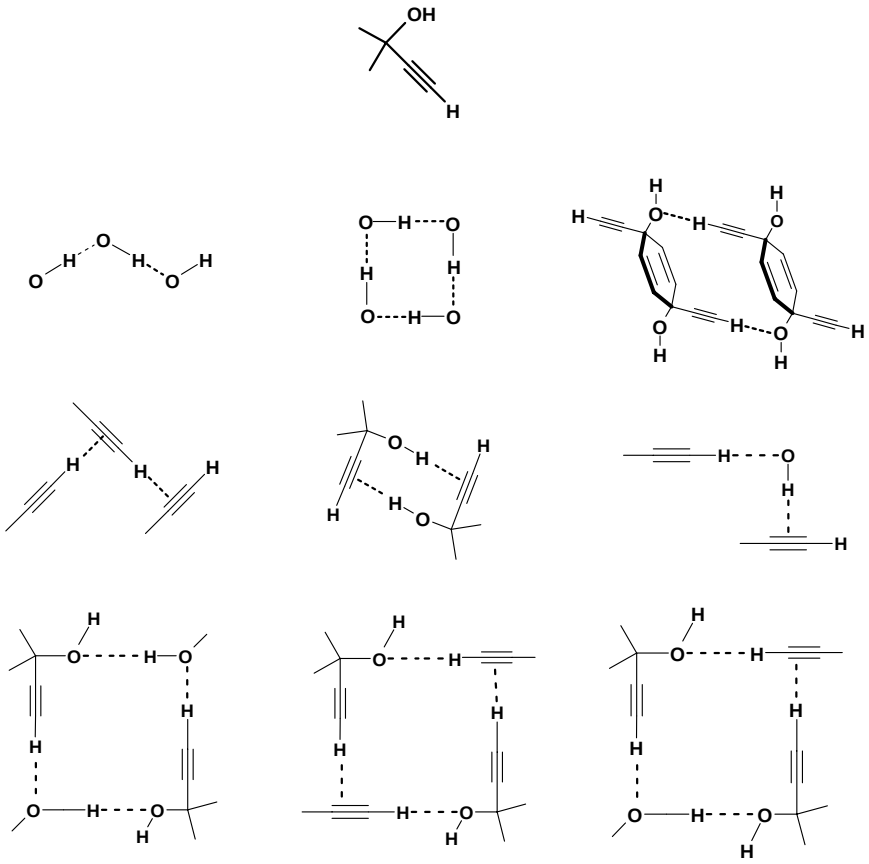

Scheme 1. Some supramolecular synthons discussed in this thesis.

1.4 Mechanism of crystallization

Solution crystallization is considered to be a two-step process: nucleation, or the birth of crystals, and crystal growth, which involves subsequent growth of existing nucleii. Among these two, nucleation is more important because it plays the decisive role in determining the structural variations and properties of the solid in its final state [1.36].

Surprisingly, little attention has been paid so far to the structural modulations during nucleation and crystallisation. It is, however, Davey who has tried to explore the structural aspects of the nucleation process in a range of small molecule systems. According to him, several crystal packing possibilities exist in solution via variations in intermolecular interactions of different functional groups. This structural landscape that is encountered during the crystallization of a molecular solid from solvent could be considered to begin with the solvated molecules. These solvated molecules associate via supramolecular synthons to give growth units, the essential building blocks that transfer structural information from the solution to the crystal, followed by nucleation and the crystal growth [1.37]. Although the experimental measurements of the overall crystal growth rate are relatively simple, those of the nucleation rate may be quite difficult, primarily because the small size of a nucleus is not measurable by current experimental techniques. In a recent review, Leiserowitz, Lahav and co-workers have described the use of grazing incidence X-ray diffraction technique to understand crystal nucleation [1.38]. The basis of their work is the hypothesis that supersaturated solutions containing molecular clusters adopt various arrangements and shapes, some of which resemble the crystal they grow into. Myerson et al. have used the cluster size distribution theory via refractive index measurements to analyze nucleation [1.39]. Their results show that glycine exists mostly as dimers in supersaturated solutions and that urea exists as oligomers. Other common methods that have been utilized to measure nucleation rates are time-resolved simultaneous SAXS-WAXS experiments [1.40], laser polarized turbidimetry [1.41] and in situ atomic force microscopy [1.42]. These experimental techniques indirectly point out the beginning of nucleation. In a recent paper, Datta and Grant described a method to estimate the relative nucleation rate of two pharmaceutically relevant compounds, phenylbutazone and sulfamerazine, in selected solvents using molecular dynamics simulations [1.43].

The occurrence of more than one molecule in the asymmetric unit of a crystal ($Z' > 1$) is a phenomenon of interest from a fundamental standpoint, because the factors leading to its occurrence are not well understood [1.44]. Desiraju recently emphasized that high Z' structures (possibly with solvent incorporated in the lattice) are reflective of

'frozen' or 'interrupted crystallization' [1.45]. Steed suggested that these structures could also be considered as fossil relics of the crystal nucleus [1.46]. Hence, an understanding of these structures may help one to visualize the structural modulations during the early stages of crystallization. Nangia and co-workers in a study of polymorphism of 4,4-diphenyl-2,5-cyclohexadienone have emphasized the importance of kinetic factors during crystallization by understanding the relationship between C–H···O strength and the occurrence of high *Z′* polymorphs [1.47]. On the whole, such crystals with Z' > 1 may represent stages in a pathway towards more stable crystals where the symmetry is more neatly expressed.

Matzger and co-workers have taken a reductionist approach to understand crystallization [1.48]. This promising model uses the idea of two-dimensional crystallization and decreases the dimensionality of the problem. Some complexities found in three-dimensional crystallization remain in this model system, including the possibility of finding more than one crystallographically unique molecule in a given crystal structure (Z' > 1) and multiple energetically achievable packing motifs (polymorphs). However, an important simplification in the two-dimensional crystal packing problem is that only 17 space groups are needed to describe the possible symmetry element combinations instead of the 230 required to describe packing in three-dimensions.

1.5 Solvation

Nangia and Desiraju analyzed the relative solvate-forming propensities of 20 common solvates, and highlighted the need for systematic studies of the formation and structure of solvates [1.49]. According to them, solvation is an entropically disfavoured process during crystallization, being observed in only around 15% of non-ionic organic compounds in the CSD. This observation may be rationalized by assuming that crystallization begins with solute–solvent aggregates that contain solute–solute, solute–solvent and solvent–solvent interactions. The entropic gain in eliminating solvent molecules from these aggregates into the bulk solution, and the simultaneous enthalpic gain in forming stable solute species that contain robust supramolecular synthons,

provides an adequate driving force for nucleation and crystallization leading to solvent-free crystals.

There are many reasons for the inclusion of solvent in organic crystals and these depend on the nature of both solute and solvent. The formation of a solvated crystal may be considered with reference to the mechanism for crystallization sketched above. If solute–solvent interactions are unusually important, say because of multipoint recognition, the entropic advantage associated with solvent expulsion into the bulk may be overridden by these additional enthalpic factors resulting in retention of some solvent in the crystal. Indeed, multi-point recognition between solvent and solute appears to be a critical factor that determines ease of solvation, especially for organic solvents capable of strong and/or weak hydrogen bonding. For instance, the CSD study showed that the likelihood of solvation by 1,4-dioxane DMSO and DMF is unusually high because these solvents are able to act donor/acceptor of strong and/or weak hydrogen bonds.

1.5.1 Solvates and Hydrates

Solvates, defined as crystalline forms of a compound that includes solvent molecules in the crystal lattice, have been deemed to be of great importance in the pharmaceutical industry [1.50]. The drug development process exposes active pharmaceutical ingredients (APIs) to organic and aqueous solvents during crystallization, wet granulation, storage and dissolution and can lead to the formation of solvated crystals by design or by accident. Crystalline forms of APIs with included solvent molecules differ in pharmaceutical performance like mechanical behaviour, stability, dissolution and often bioavailability [1.51]. Choice of development of solvated or unsolvated form will depend on its pharmaceutical properties, like how long it can survive and under what conditions. The most important point is that some APIs form solvates while others do not. The propensity of an API molecule to form solvates has been related to molecular structures, hydrogen bond patterns, and crystal packing. Matzger et al. successfully used the CSD to analyze the nature of supramolecular networks in solvated crystals and to identify molecular recognition events that lead to incorporation of solvents in crystal structures [1.52]. They found that water is

incorporated into organic crystals far more frequently than any other solvent [1.53]. It is surprising that about one third of the entries for solvates are hydrates although water is not a good solvent for crystallization of many of these compounds and other solvents are commonly used for crystallization.

Hydrated forms of pharmaceutical solids are more common than other solvates due to the abundance of water in the atmosphere, its small size, its ability to act as both hydrogen bond donor and hydrogen bond acceptor, and the water activity of solvents or vapor with which APIs come in contact [1.54]. Accordingly, it is not necessary to conclude that a hydrate will form, if and only if, a compound is crystallized from water. A CSD study of the environments of water molecules, hydrogen bonded to N- and O-atoms within organic hydrates, revealed that water prefers to maximize its hydrogen bonding interactions within a hydrate structure [1.55]. In a recent study, Infantes and Motherwell examined the patterns of water clusters in more than 1400 hydrated structures and classified them as discrete rings, chains, infinite chains, tapes and layer structures [1.56]. Regardless of the hydrate class, the removal of water from the crystal lattice leads to more or less distinct internal structural changes. Most hydrates dehydrate to anhydrous solids whose crystal structures differ from those of the original hydrate phase. Some even become amorphous when dehydrated [1.57]. Ultimately, the structural changes will be reflected as altered physical and chemical properties of APIs with corresponding effects on their dissolution rate, bioavailability, tabletting properties and stability. An understanding of the mechanisms involved in the dehydration of a hydrate is a prerequisite, therefore, to controlling the manufacturing process and storage conditions of a drug product.

1.5.2 Pseudopolymorphs

In a paper that describes more than 100 solvates of sulfathiazole, Hursthouse, Threlfall and co-workers have indicated the need for a large collection of data in order to get an overview of the structural characteristics and of the factors determining solvate formation [1.58]. In general, solvates can be classified into two categories: (a) *host–guest compounds*, *clathrates*, or, more generally *inclusion compounds*, in which the main

function of the guest molecule is cavity filling, with or without additional weak hydrogen bonding, in a host molecule [1.59] and; (b) *pseudopolymorphs* wherein different solvated crystal structures of a particular compound have the same/different solute to solvent ratio [1.60]. The physical property changes during solvate formation are similar to those related to polymorphism [1.61] and therefore solvates are often referred to as pseudopolymorphs to distinguish them from true polymorphs. This subject has not been treated systematically although it is of general importance in the pharmaceutical industry. Thermodynamics of pseudopolymorphic transitions are very complex because different possible phase transitions can occur [1.62]. Desolvation or dehydration of pseudopolymorphs can often cause rearrangement of the crystal lattice. Hence the principle aim of any pharmaceutical industry is the preparation of a dosage form that includes a pseudopolymorph that has a long shelf life.

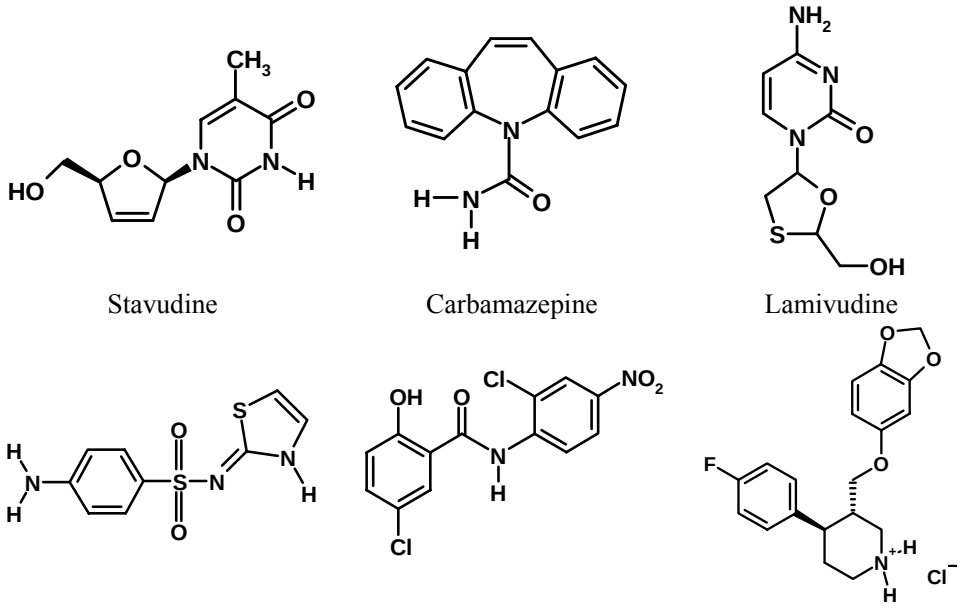

Scheme 2. Some APIs that form hydrates during crystallization.

This thesis as a whole is concerned with solvation and the intermolecular interactions that are important in solvation. In the following chapters I have tried to describe several aspects of crystal engineering that may help one to understand the link between the crystal nucleation and crystal structure.

CHAPTER TWO

SYNTHON ROBUSTNESS IN SUBSTITUTED *gem*-ALKYNOLS

2.1 Introduction

The family of geminal alkynols or *gem*-alkynols, molecules that contain equal stoichiometries of hydroxyl and ethynyl groups attached to the same carbon atom, offers an assorted structural behaviour, which is suited to the effective exploration of the relationships between molecular functionality and crystal packing [1.34]. The lack of structural repetition among the 144 published *gem*-alkynol crystal structures is an additional challenge to an understanding of this family. Failure to find repeating structural relationships in this group of structures arises from the juxtaposition of two hydrogen bond donors (O–**H**, C–**H**) and two acceptors (**O**–H, **C≡C**–H). In this sterically hindered situation the four possible interactions O–H…O, C–H…O, O–H…π and C–H…π become competitive, leading to high levels of interference (Scheme 1) [1.33]. Accordingly, one finds 95 O–H…O, 78 C–H…O, 18 O–H…π, and 88 C–H…π hydrogen bonds present in these 144 crystal structures. It is noted that the packing pattern in any particular crystal structure in this family is highly sensitive with respect to substitutional perturbation. As a result, attempts to establish a molecule–supermolecule correspondence [1.11] via the supramolecular synthon [1.7] approach are extremely difficult. Previous studies from this group include a discussion of *trans*-1,4-diethynyl-1,4-dihydroxy-2,5-cyclohexadiene, **1a**, *trans*-1,4-diethynyl-1,4-dihydronaphthalene-1,4-diol, **2a** and *trans*-9,10-diethynyl-9,10-dihydroanthracene-9,10-diol, **4a**, which are the prototype compounds [1.34d]. Crystal structures of a further 14 related compounds (Scheme 2) have been discussed in this chapter to assess the structural similarities in this family. These 14 compounds are classified according to the quinones from which they were synthesized. Alkynols **1a**-**1f** are based on benzoquinone (BQ), **2a**-**2f** on naphthoquinone (NQ), **3a** and **3b** on 1,4-anthraquinone and **4a**-**4d** on 9,10-anthraquinone (AQ). Essentially, the compounds described in this chapter are the chloro and methyl derivatives in the BQ, NQ and AQ series.

In this chapter the formation, modulation and robustness of weak supramolecular synthons with respect to the substitutional changes in BQ, NQ and AQ molecular cores have been described. One finds that observed crystal structures result from a balance between several factors and that interaction interference [1.33] can at least be understood if not completely controlled.

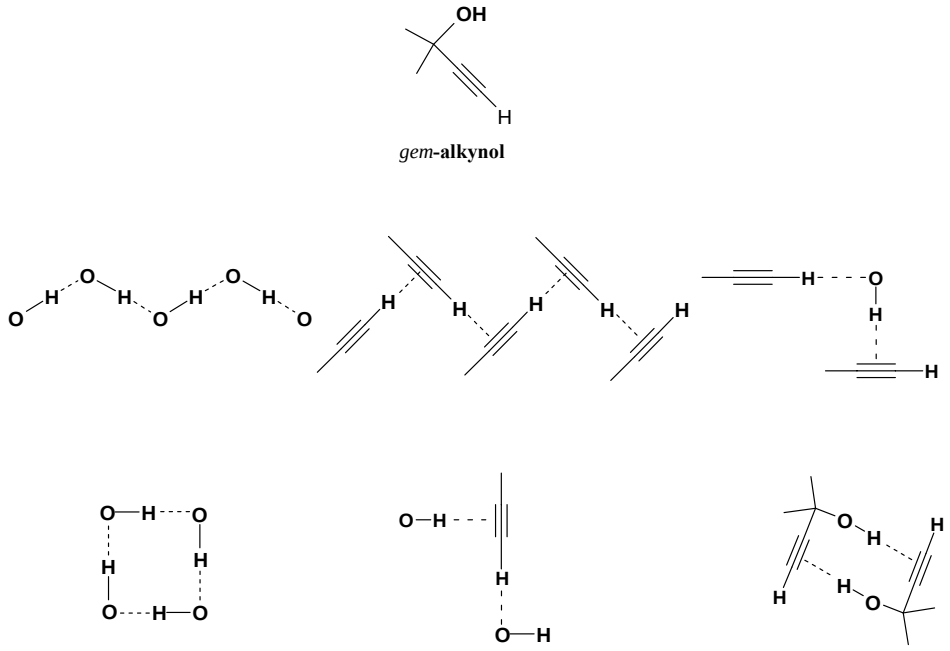

Scheme 1. Supramolecular synthons observed previously in the *gem*-alkynol family.

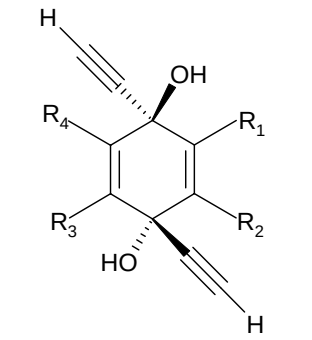

1a, $R_1=R_2=R_3=R_4=H$
1b, $R_1=R_3=H$, $R_2=R_4=CH_3$
1c, $R_1=R_2=H$, $R_3=R_4=CH_3$
1d, $R_1=R_2=R_3=R_4=CH_3$
1e, $R_1=R_2=H$, $R_3=R_4=Cl$
1f, $R_1=R_2=R_3=R_4=Cl$

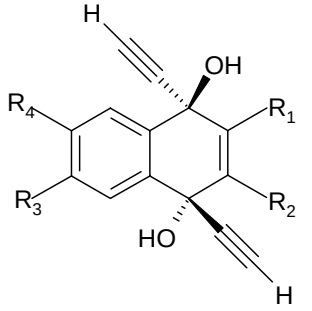

2a, $R_1=R_2=R_3=R_4=H$
2b, $R_1=R_2=CH_3$, $R_3=R_4=H$
2c, $R_1=R_2=Cl$, $R_3=R_4=H$
2d, $R_1=R_2=H$, $R_3=R_4=CH_3$
2e, $R_1=R_2=Cl$, $R_3=R_4=CH_3$
2f, $R_1=R_2=Br$, $R_3=R_4=CH_3$

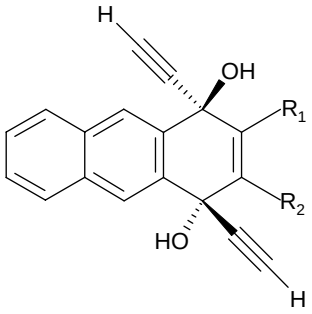

3a, $R_1=R_2=H$
3b, $R_1=R_2=Cl$

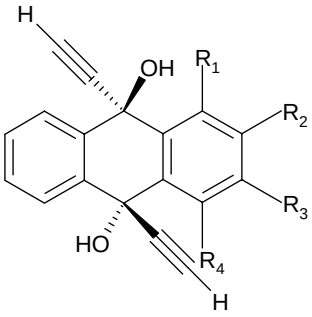

4a, $R_1=R_2=R_3=R_4=H$
4b, $R_1=R_3=R_4=H$, $R_2=CH_3$
4c, $R_2=R_3=H$, $R_1=R_4=CH_3$
4d, $R_1=R_4=H$, $R_2=R_3=CH_3$

Scheme 2. Schematic drawing of *gem*-alkynols in this study.

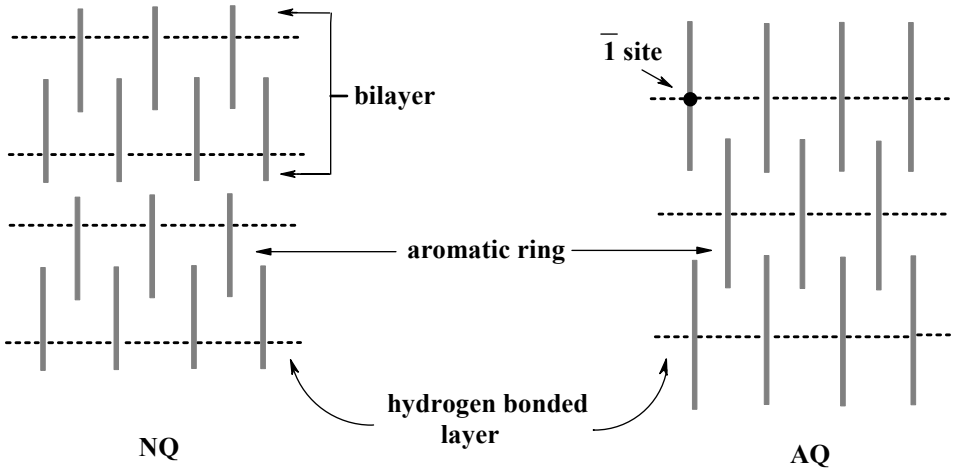

Scheme 3. Interdigitation of aromatic residues in the NQ and AQ prototypes **2a** and **4a**. Note that the hydrogen bonded layers and the aromatic residues are perpendicular.

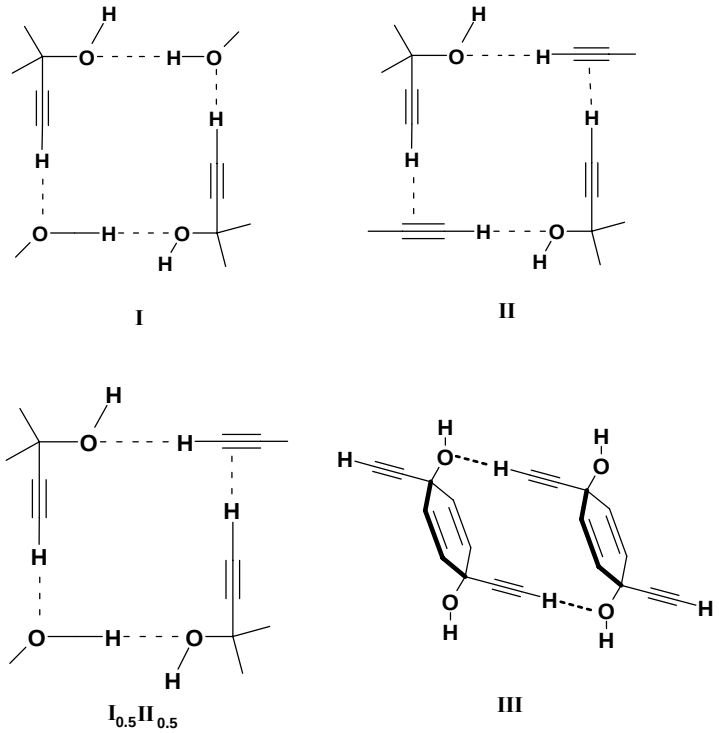

Scheme 4. Supramolecular synthons discussed in this chapter.

Table 1. Geometrical parameters of hydrogen bridges of the alkynols in this study.

Alkynol	H-bridge	*d*/Å (H…A)	*D*/Å (X…A)	*θ*/deg ∠X–H…A
1a	O–H…O	2.12	3.075(1)	162.1
	C–H…O	2.39	3.305(1)	141.2
	C–H… π	2.98	3.654	127.6
1b	O–H…O	1.88	2.851(1)	166.4
	C–H…O	2.08	3.153(1)	168.2
	O–H…π	2.58	3.395	158.2
	C–H…π	2.92	3.791	155.1
1c	O–H…O	1.84	2.811(1)	169.5
	C–H…O	2.09	3.173(1)	171.2
	O–H…π	2.38	3.271	171.9
	C–H… π	3.06	3.893	150.4
1d	O–H…O	1.84	2.781(1)	159.5
	O–H…O	1.92	2.882(1)	162.5
	C–H…O	2.08	3.160(2)	178.9
	O–H…π	2.62	3.442	159.1
	C–H… π	3.00	3.886	154.5
1e	O–H…O	1.89	2.809(2)	155.7
	C–H…O	2.44	3.414(2)	147.3
2a	O–H…O	1.89	2.836(2)	162.7
	C–H…O	2.06	3.140(2)	169.2
	O–H…π	2.68	3.486	149.5
	C–H… π	2.90	3.805	156.5
2b	O–H…O	1.92	2.860(2)	159.8
	C–H…O	2.12	3.181(3)	167.5
	O–H…π	2.59	3.391	162.1
	C–H… π	3.05	3.948	156.5
2c	O–H…O	1.82	2.788(1)	166.3
	C–H…O	2.22	3.274(1)	164.4
	O–H…π	2.73	3.508	172.3
2d	O–H…O	1.83	2.797(1)	169.6
	C–H…O	2.12	3.191(1)	170.4
	O–H…π	2.37	3.255	170.8
	C–H… π	3.20	4.044	152.3

2e	O–H…O	1.92	2.864(2)	160.9
	O–H…Cl	2.62	3.382(1)	133.9
2f	O–H…O	1.83	2.801(2)	169.8
	C–H…O	2.22	3.197(2)	148.8
	O–H…π	2.69	3.469	169.4
	C–H…π	3.07	3.976	146.9
3a	O–H…O	1.86	2.813(2)	161.4
	O–H…O	1.91	2.826(2)	152.3
	C–H…O	2.04	3.085(2)	160.8
	O–H…π	2.50	3.311	169.7
	C–H…π	2.86	3.745	159.8
3b	O–H…O	1.81	2.787(2)	170.2
	C–H…O	2.43	3.446(1)	156.1
4a	O–H…O	1.90	2.845(2)	158.8
	C–H…O	2.06	3.120(3)	162.5
	O–H…π	2.42	3.372	162.3
	C–H… π	2.97	3.863	157.7
4b	O–H…O	1.69	2.665(4)	169.8
	O–H…O	1.71	2.659(4)	161.6
	C–H…O	2.02	3.013(6)	172.9
	C–H…O	2.03	3.095(6)	165.6
	O–H…π	2.79	3.613	161.8
	C–H…π	3.26	4.092	149.2
4c	O–H…O	1.89	2.849(1)	163.4
	O–H…π	2.29	3.170	170.6
	C–H…π	2.80	3.681	160.8
4d	O–H…O	1.83	2.738(2)	151.9
	C–H…O	2.16	3.217(2)	165.2

[a] O–H and C–H distances are neutron normalized to 0.983 and 1.083 Å.

2.2 Prototype structures

Figure 1 shows the crystal structures of the prototype alkynols **1a**, **2a** and **4a** that have been published previously [1.34d]. The unsubstituted BQ compound **1a** has a unique structure with an infinite cooperative O–H…O–H…O–H chain and additional C–

H…O and C–H…π bridges in a perpendicular plane so that all the interactions form a 3-D network.

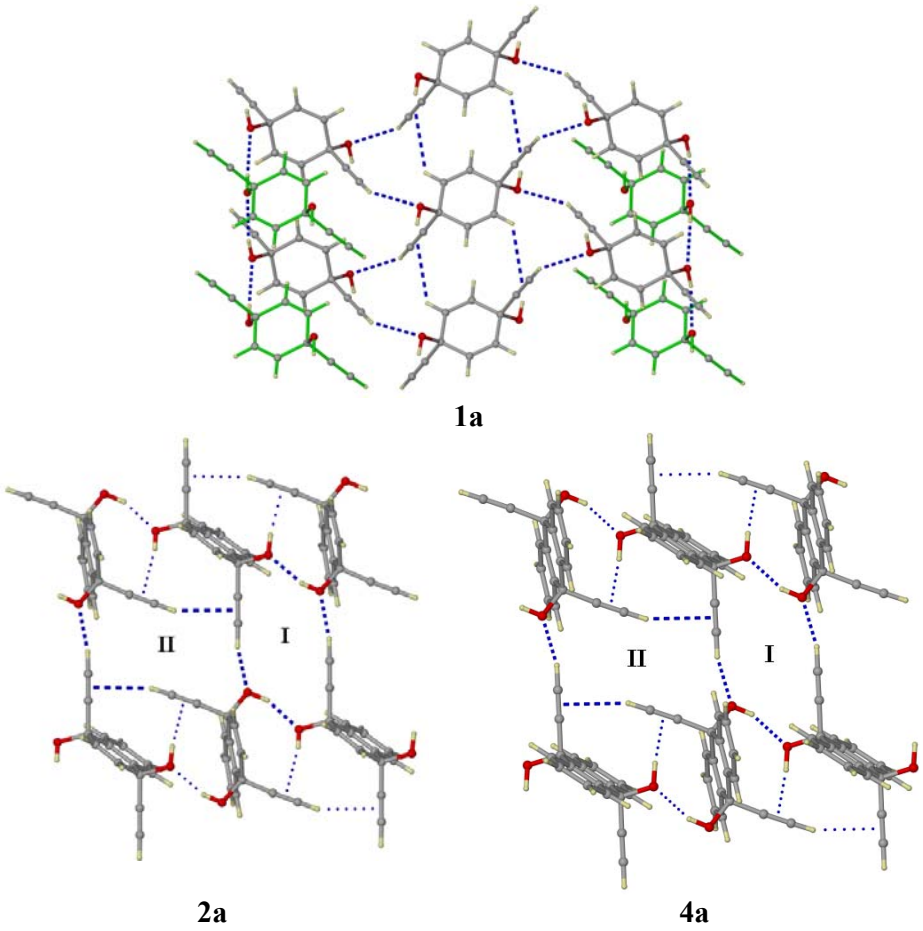

Figure 1. Crystal structures of the prototype compounds **1a**, **2a** and **4a**. In **1a**, the figure shows the C–H…O and C–H…π interactions between grey coloured molecules and O–H…O interactions between grey and green molecules. The orthogonality of these sets of hydrogen bonds renders this crystal structure incapable of further modulation. In **2a** and **4a**, however, all the hydrogen bonds are in the same layer making structural modulation possible. Note that structures **2a** and **4a** are nearly the same with synthons **I** and **II**, and the manner in which they are attached, being identical.

Effectively, the various functional groups in **1a** (hydroxy, ethynyl, alkene) are intimately involved with each other in the packing. Accordingly, any substitutional perturbation of this molecule is expected to alter the packing completely. In contrast, the NQ prototype, **2a**, and the 9,10-AQ prototype, **4a** have more generic packings because the O–H…O, C–H…O and C–H…π hydrogen bonds form a 2-D network with the hydrocarbon residues perpendicular to this plane (Scheme 3). It should be noted that the O–H…O, C–H…O and C–H…π bridges (Table 2) form the clearly defined centrosymmetric synthons **I** and **II** (Scheme 4) in **2a** and **4a**. Also the manner in which these synthons are fused together to generate a planar hydrogen bonded sheet is identical in both structures. Scheme 3 shows that the aromatic residues interdigitate to form a bilayer structure in NQ and a continuous structure in 9,10-AQ. This orthogonality of the hydrogen bonded and hydrocarbon regions leads to *structural insulation* so that it is not difficult to understand that the addition of an extra fused ring in going from **2a** to **4a** leaves the structure unaltered. In principle, substitution on these rings might also preserve this structure with orthogonal hydrogen bonding and aromatic interdigitation. Lastly, it is to be noted that two molecules of the symmetrical **4a** lie on distinct crystal inversion centres such that $Z' = (0.5 + 0.5)$ whereas for the unsymmetrical **2a**, $Z' = (1 + 1)$ to maintain the same packing.

2.3 Benzoquinone (BQ) based structures

To understand the modulation of the packing in terms of geometrical and chemical effects the alkenic protons in **1a** were systematically replaced with Cl- and Me-groups to obtain **1b**-**1f**.

2.3.1 Crystal structure of 2,5-dimethyl-*trans*-1,4-diethynyl-1,4-dihydroxy-2,5-cyclohexadiene, 1b

2,5-Dimethyl-*trans*-1,4-diethynyl-1,4-dihydroxy-2,5-cyclohexadiene, **1b**, adopts space group $P\bar{1}$ with $Z' = (0.5 + 0.5)$. The packing of this symmetrical molecule is exactly the same as in **4a** (also $P\bar{1}$) and indeed, one can visualize the two Me-groups as vestigial benzo rings; the cell edges in **1b** (6.6905, 8.6781, 10.1446 Å) and **4a** (8.7684,

8.9558, 10.315 Å) show a close correspondence with the *a*-axis being the direction of the Me-groups in **1b** and of the benzo rings in **4a**. Synthons **I** and **II** occur as previously noted in **2a** and **4a** (Figure 2). As before, these synthons involve both symmetry independent molecules (A and B). Synthon **I** is constituted with O–H…O and C–H…O hydrogen bonds, while **II** contains C–H…O and C–H…π bonds. It is noteworthy that the fusion of synthons **I** and **II** is accompanied by a characteristic cooperative chain of hydrogen bridges, O–H…O–H…C≡C–H…C≡C–H…O–H…which forms an infinite pattern.

2.3.2 Crystal structure of 2,3-dimethyl-*trans*-1,4-diethynyl-1,4-dihydroxy-2,5-cyclohexadiene, 1c

In principle, the packing of 2,3-dimethyl-*trans*-1,4-diethynyl-1,4-dihydroxy-2,5-cyclohexadiene, **1c**, could follow that of **1b** except that the molecule is unsymmetrical like **2a**. Indeed, the packing in space group $P2_1/c$ is generally similar (Figure 3) but there is a very interesting variation in the synthon structure. A new synthon [$\mathbf{(I)_{0.5}(II)_{0.5}}$], $\mathcal{H}$, is observed, which is obtained by bisecting synthons **I** and **II** and joining the distinct halves (Scheme 5). This hybrid synthon is constituted with one O–H…O, two C–H…O and one C–H…π interactions. Synthon [$\mathbf{(I)_{0.5}(II)_{0.5}}$] is comparable thermodynamically with synthons **I** and **II**, containing as it does the same elaborate cooperative network of strong and weak hydrogen bonds, O–H…O–H…C≡C–H…C≡C–H…O–H… and the supramolecular transformation involved in going from **I** and **II** to [$\mathbf{(I)_{0.5}(II)_{0.5}}$] is given in figure 4. Suggestively, the symmetrical **1b** gives the centrosymmetric synthons **I** and **II** while the unsymmetrical **1c** leads to the unsymmetrical hybrid. The hybrid [$\mathbf{(I)_{0.5}(II)_{0.5}}$] has a close parallel in the *heterosynthons* that were first identified by Zaworotko in his studies of hydrogen bonded molecular complexes [2.1]. Scheme 5 shows that if synthons **I** and **II** are taken as homosynthons, then [$\mathbf{(I)_{0.5}(II)_{0.5}}$] becomes the corresponding heterosynthon.

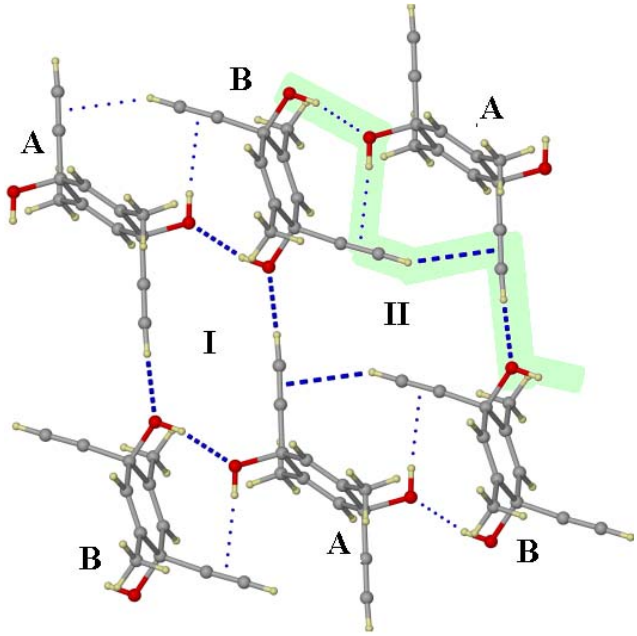

Figure 2. Crystal structure of **1b**. Note the cooperative network of strong and weak interactions in synthons **I** and **II**. **A** and **B** represent the two distinct molecules in the asymmetric unit.

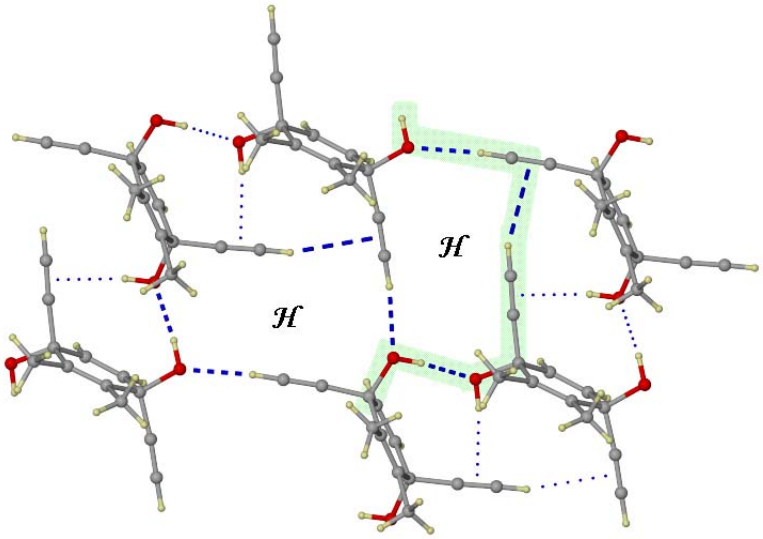

Figure 3. Supramolecular synthon $[(\mathbf{I})_{0.5}\ (\mathbf{II})_{0.5}]$ in **1c**. Note the unsymmetrical nature of this hybrid synthon, denoted $\mathcal{H}$ in the figure.

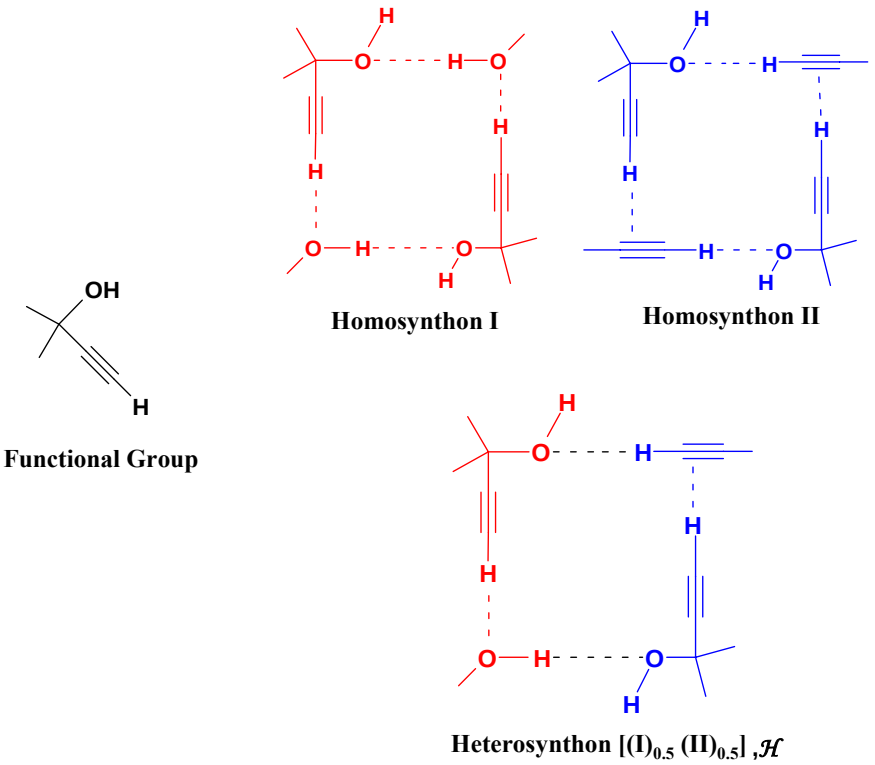

Scheme 5. Representation of hybrid [**(I)$_{0.5}$(II)$_{0.5}$**] as a heterosynthon.

2.3.3 Crystal structure of 2,3,5,6-tetramethyl-*trans*-1,4-diethynyl-1,4-dihydroxy-2,5-cyclohexadiene, 1d

2,3,5,6-Tetramethyl-*trans*-1,4-diethynyl-1,4-dihydroxy-2,5-cyclohexadiene, **1d**, is a symmetrical molecule and is an extension of **1b** or **1c** in which all the H-atoms in the cyclohexadiene ring are replaced by Me-groups (Figure 5). The packing is similar to that of **1b** with synthons **I** and **II** observed instead of hybrid [**(I)$_{0.5}$(II)$_{0.5}$**]. Curiously, for a symmetrical molecule, which adopts a crystal structure with symmetrical synthons, the space group is non-centrosymmetric (*Fdd*2, $Z' = 0.5 + 0.5 + 1 + 1$).

Encouraged by the fact that the synthon structure and packing arrangement is preserved in the BQ series so far, the dichloro and tetrachloro derivatives, **1e** and **1f** were considered next. The latter structure ($I4_1/a$) has been published previously and an O–

H…O hydrogen bonded tetramer ring has been noted [1.34c]. The importance of O–H…O hydrogen bonding is rationalized by the fact that the O–H group is activated as a donor by the Cl-atoms.

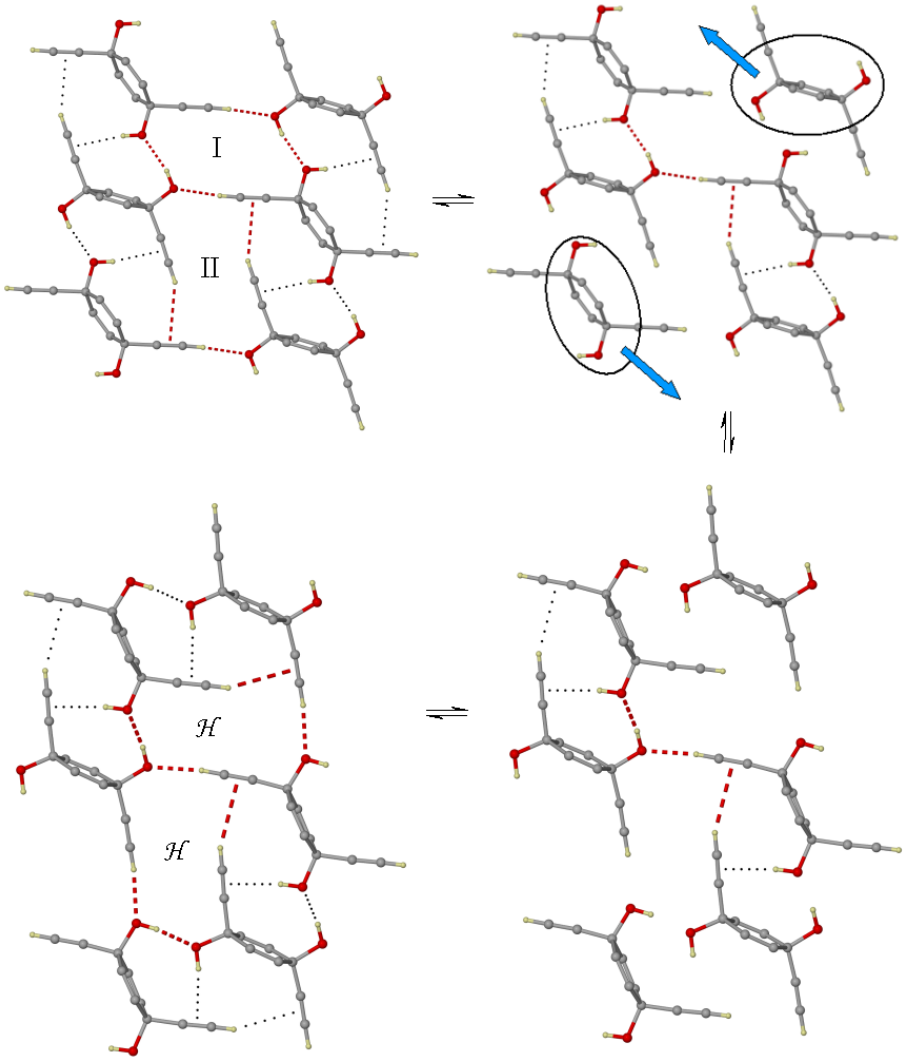

Figure 4. Transformation of homosynthons **I** and **II** to the hybrid [$\mathbf{(I)_{0.5}(II)_{0.5}}$]. Minimal molecular movement is required for this supramolecular transformation.

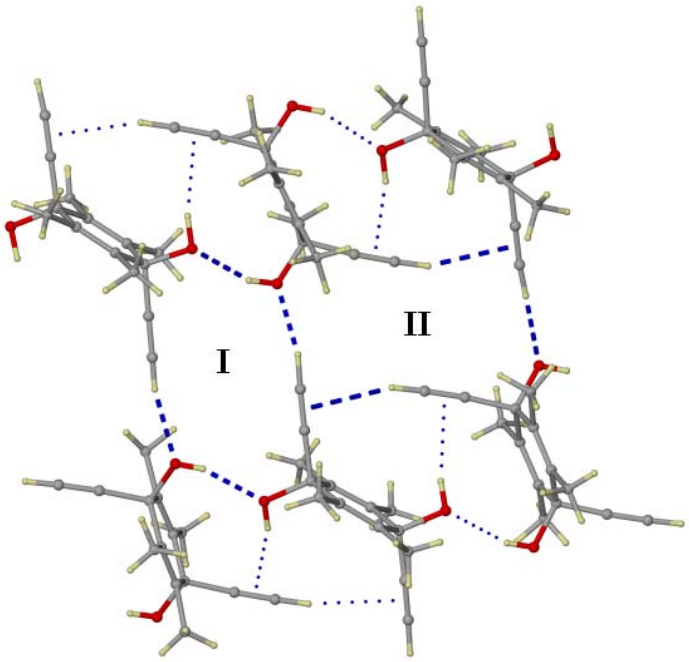

Figure 5. Crystal structure of **1d**. Note the presence of synthons **I** and **II** as in **1b**.

2.3.4 Crystal structure of 2,3,-dichloro-*trans*-1,4-diethynyl-1,4-dihydroxy-2,5-cyclohexadiene, 1e

2,3,-Dichloro-*trans*-1,4-diethynyl-1,4-dihydroxy-2,5-cyclohexadiene, **1e**, ($P2_1/c$, $Z' = 1$) shares features of both the tetrachloro **1f** and the methyl derivatives **1b**-**1d** (Figure 6). It is like **1f** in that the dominant interaction pattern is the O–H…O tetramer. It resembles the methyl derivatives in that (a distorted) synthon **I** is present. Therefore, the Cl/Me exchange rule does not operate in the BQ series [2.2]. This suggests a chemical role for these substituents in the crystal packing; this is hardly surprising when interactions involving these groups are so intimately and implicitly involved in the structural organization.

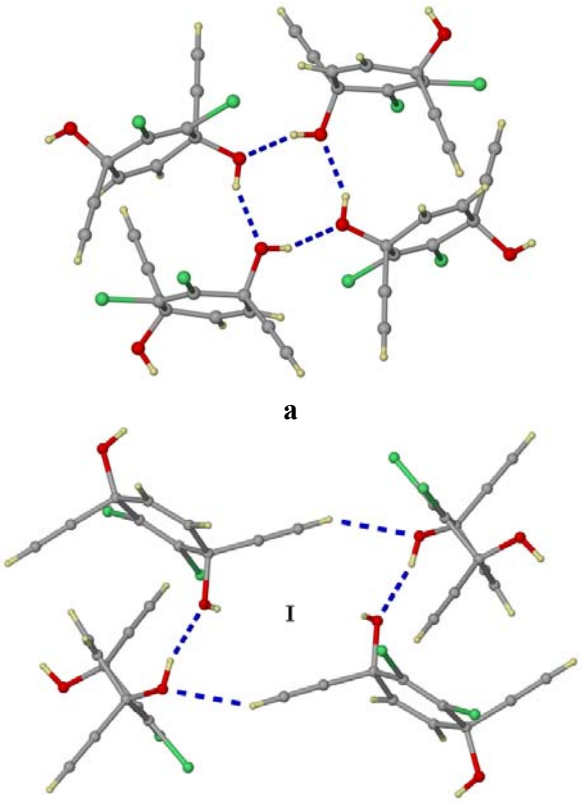

Figure 6. Perspective views of **1e** displaying (a) O–H…O tetrameric synthon and (b) distorted synthon **I**.

2.4 Naphthoquinone (NQ) based structures

Crystal structures of the naphthoquinone based compounds have been analyzed. In the prototype, **2a**, the disposition of the fused benzo rings is such that the rings are situated on the same side of the hydrogen bonded sheets (Scheme 3). These rings interdigitate with aromatic edge-to-face interactions to give a bilayer of molecules that close pack. The packing behaviour of methyl and halogen substituted NQ derivatives have been explored. Compounds **2b**-**2f** constitute the NQ group and their crystal structures show the limits to which the prototype structures **2a** and **4a** may be conserved, and when and why this structural domain is exceeded.

2.4.1 Crystal structure of 2,3-dimethyl-*trans*-1,4-diethynyl-1,4-dihydronaphtha alene-1,4-diol, 2b

The packing of 2,3-dimethyl-*trans*-1,4-diethynyl-1,4-dihydronaphthalene-1,4-diol, **2b**, ($P\bar{1}$, Z' = 0.5+0.5) contains synthons **I** and **II** as seen previously in **2a** and **4a** (Figure 7). Because of a disorder between the methyl groups and the benzo ring, the structure is almost identical to that of the AQ derivative **4a** and the cell edges (8.4194, 8.7817, 10.3302 Å) are nearly the same. Alkynol **2b** is closer to **4a** than is **1b** (which has a similar mimicry but is not disordered). The interdigitation of rings is similar to **4a**.

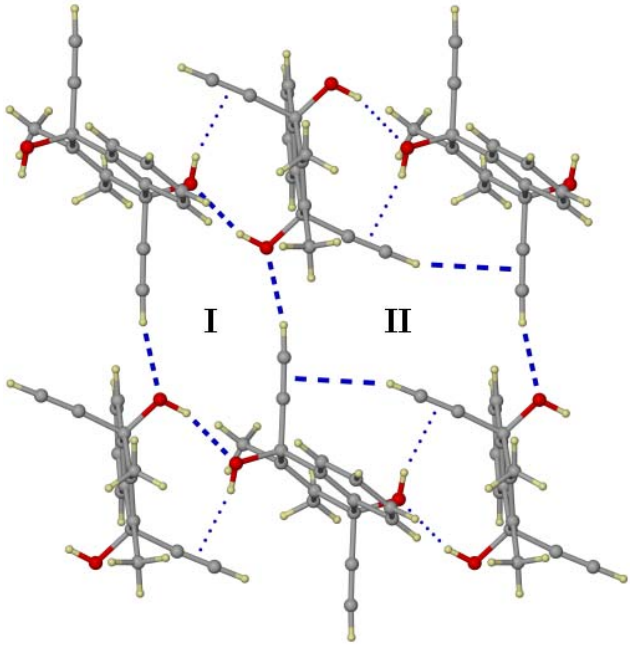

Figure 7. Crystal structure of **2b** to show synthons **I** and **II**.

2.4.2 Crystal structure of 2,3-dichloro-*trans*-1,4-diethynyl-1,4-dihydronaphtha lene-1,4-diol, 2c

A comparison of **2b** with alkynol **2c**, 2,3-dichloro-*trans*-1,4-diethynyl-1,4-dihydronaphthalene-1,4-diol, ($P2_1/c$, Z' = 1) is more interesting (Figure 8). While

synthon **I** (with its O–H…O bonds) is preserved, **II** has disappeared and is replaced by a new C–H…O dimer synthon **III** (Scheme 3), and an additional O–H…π and type-II Cl…Cl contact [2.3]. In contrast to the BQ series wherein replacement of Me-groups by Cl-groups changed the structure completely (**1c → 1e, 1d → 1f**), Cl/Me exchange in the NQ series (**2b → 2c**) perturbs only some elements of the crystal packing. Still, chloro substitution enhances the significance of O–H…O hydrogen bonding as in the BQ series.

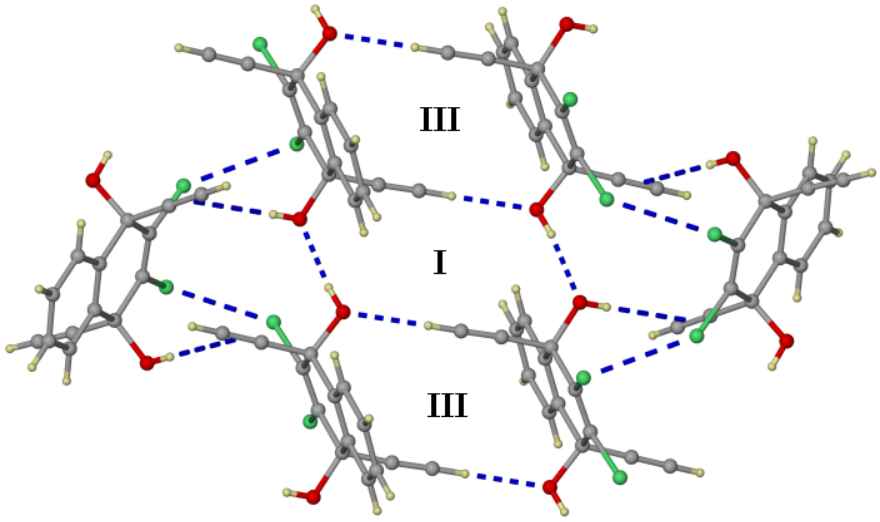

Figure 8. Crystal structure of **2c**. Note how synthon **I** has changed its shape and is engaged in a ladder network with synthon **III**. Note the additional Cl…Cl interactions.

2.4.3 Crystal structure of 6,7-dimethyl-*trans*-1,4-diethynyl-1,4-dihydronaphtha lene-1,4-diol, 2d

6,7-Dimethyl-*trans*-1,4-diethynyl-1,4-dihydronaphthalene-1,4-diol, **2d**, ($P2_1/c$, $Z' = 1$) may be compared with the unsubstituted NQ compound **2a** and the dimethyl BQ derivative **1c** both of which are unsymmetrical. The packing is similar to **1c** in that the hybrid synthon [$\mathbf{(I)_{0.5}(II)_{0.5}}$] is present (Figure 9).

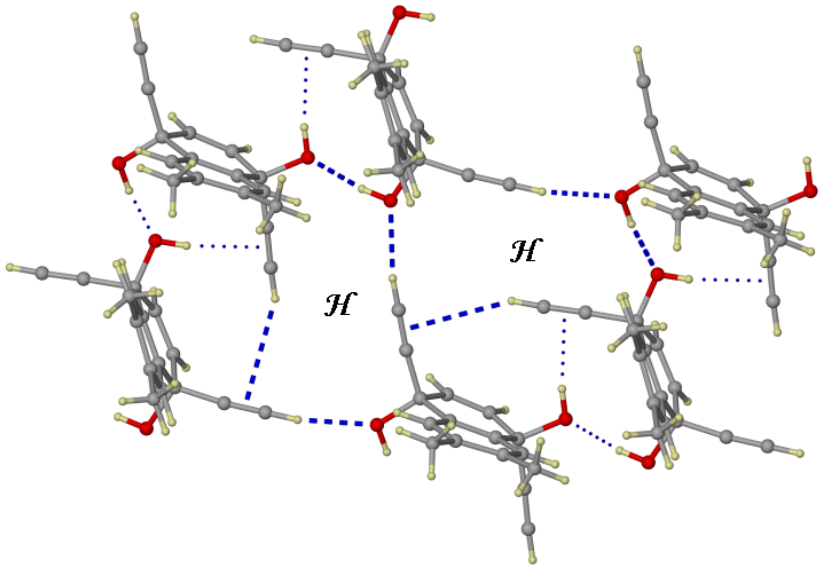

Figure 9. Crystal structure of **2d**. Note the recurrence of hybrid synthon $[(\mathbf{I})_{0.5}\ (\mathbf{II})_{0.5}]$.

2.4.4 Crystal structure of 2,3-dichloro-6,7-dimethyl-*trans*-1,4-diethynyl-1,4-dihydronaphthalene-1,4-diol, 2e

In alkynol **2e**, 2,3-dichloro-6,7-dimethyl-*trans*-1,4-diethynyl-1,4-dihydronaphthalene-1,4-diol, ($P2_1/c$, $Z' = 1$), the effect of two Cl-groups is sufficient to ensure total disruption of the NQ prototype structure. The structure (Figure 10) is completely different with a new tetramer loop synthon consisting of O–H…O, C–H…O and C–H…π bridges. The interdigitation of aromatic residues has also vanished. It should be noted that dichloro substitution in going from **2a** to **2c** is insufficient to perturb synthon **I**; only the more feeble synthon **II** is affected. However, a similar dichloro substitution on **2d** to give **2e** has exceeded the structural limits of the NQ family.

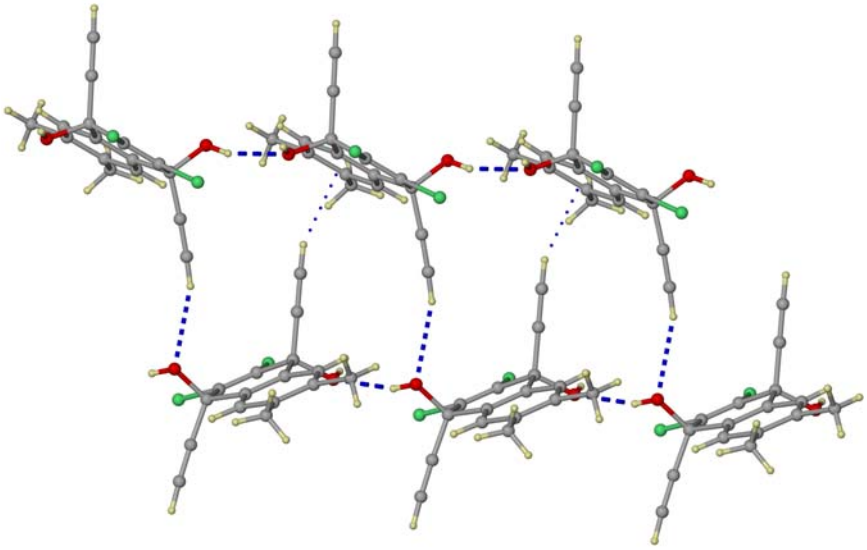

Figure 10. Tetramer loop synthon in **2e** consisting O–H…O, C–H…O and C–H…π interactions. Note that the structure is completely different from **2a** through **2d**.

2.4.5 Crystal structure of 2,3-dibromo-6,7-dimethyl-*trans*-1,4-diethynyl-1,4-dihydronaphthalene-1,4-diol, 2f

2,3-dibromo-6,7-dimethyl-*trans*-1,4-diethynyl-1,4-dihydronaphthalene-1,4-di ol, **2f**, ($P2_12_12_1$, $Z' = 1$) conserves the layer interdigitated structure of **2d** along with the hybrid [$\mathbf{(I)_{0.5}(II)_{0.5}}$]. These results clearly indicate that the nature of the halogen atom (Br, Cl) affects the donor and acceptor properties of the hydrogen bonding functionalities in these molecules in very subtle ways. Because the systems are structurally very fragile, the slightly different effects of Br and Cl are amplified in the final outcome. Put another way, the Br-groups are chemically not as aggressive as Cl and are unable to change the **2d** packing; they revert to a space filling role (Figure 11). This crystal structure is an interesting example of the relative importance of geometrical and chemical factors [2.4] in determining the overall packing.

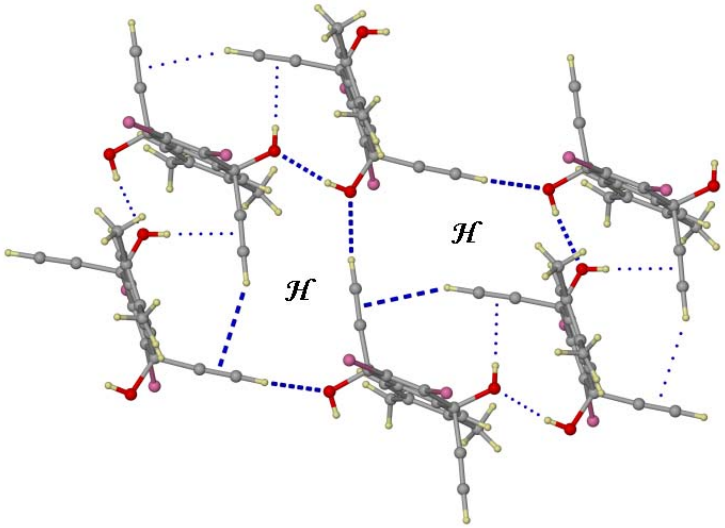

Figure 11. Crystal structure of the dibromo NQ derivative **2f**. Br-atoms (pink) here play a space filling role and the crystal structure is same as the non-brominated **2d**.

2.5 Anthraquinone (AQ) based structures

Two sets of compounds were studied, based on 1,4-anthraquinone (**3a** and **3b)** and on 9,10-anthraquinone (**4a**, **4b**, **4c** and **4d**).

2.5.1 Crystal structure of *trans*-1,4-diethynyl-1,4-dihydroanthracene-1,4-diol, 3a

Alkynol **3a**, *trans*-1,4-diethynyl-1,4-dihydroanthracene-1,4-diol, is the benzo extension of the NQ prototype **2a**, and it is interesting to note that it has the same packing ($P2_1/c$, $Z' = 1 + 1$) with a corresponding increase in one of the axial lengths (**3a**, 10.8363, 27.5202, 10.3894; **2a**, 10.8247, 22.6384, 10.4783). In **3a**, the alternating centrosymmetric synthons **I** and **II** characterize the packing along with aromatic edge-to-face interdigitation (Scheme 4, Figure 12).

2.5.2 Crystal structure of 2,3-dichloro-*trans*-1,4-diethynyl-1,4-dihydroanthracene -1,4-diol, 3b

2,3-dichloro-*trans*-1,4-diethynyl-1,4-dihydroanthracene-1,4-diol, **3b**, ($P2_12_12_1$, Z'=1) is the benzo extension of **2c** and its crystal structure is also similar to that of **2c**

($P2_1/c$) with the expected axial length relationships (**3b**, 6.7139, 7.4777, 29.8603; **2c**, 7.4303, 23.2596, 7.5476). Such homology [2.5], across different sets of structures, is impressive and shows that modularity can be found even in the alkynol family, which is well known for interaction interference and the concomitant synthon fragility (Figure 13).

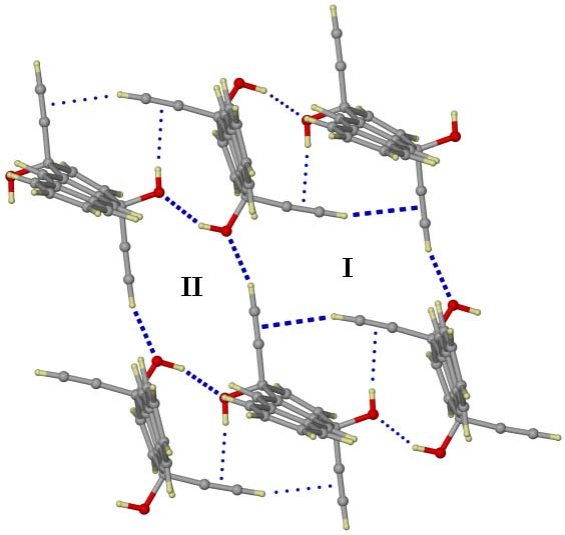

Figure 12. Crystal structure of alkynol **3a**. Note synthons **I** and **II**.

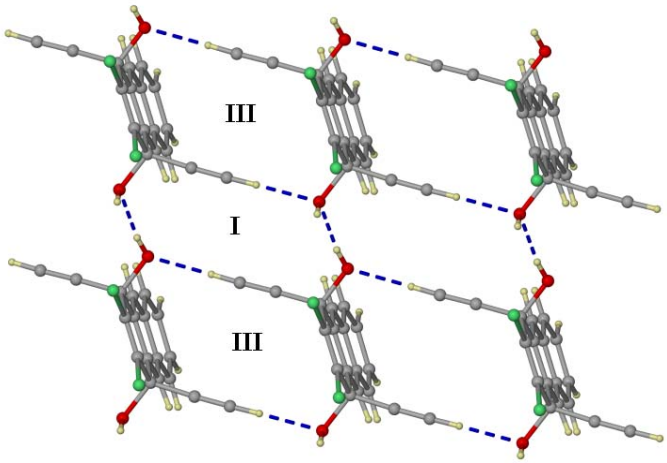

Figure 13. Crystal structure of alkynol **3b**. Note the similarity to **2c**.

2.5.3 Crystal structures of 9,10-anthraquinone (9,10 AQ) compounds

The modularity shown in most of the NQ and 1,4 AQ derivatives begins to break down in the 9,10 AQ derivatives. The unsubstituted **4a** has been discussed previously, and it is related to the NQ derivatives. Monomethyl substitution gives **4b**, 2-methyl-*trans*-9,10-diethynyl-9,10-dihydroanthracene-9,10-diol which has a related structure ($P2_1/c$, $Z' = 1$) with synthons **I** and **II** (Figure 14). However, while synthon **I** is undistorted, the C–H…π bridges in **II** are distorted (d= 3.26) and this is a prelude to the process of synthon disruption which is complete in **4c** and **4d** (Figure 15), although some elements of a cooperative network of hydrogen bonds are seen in the form of a finite O–H…O–H…C≡C–H…C≡C–H…π chain.

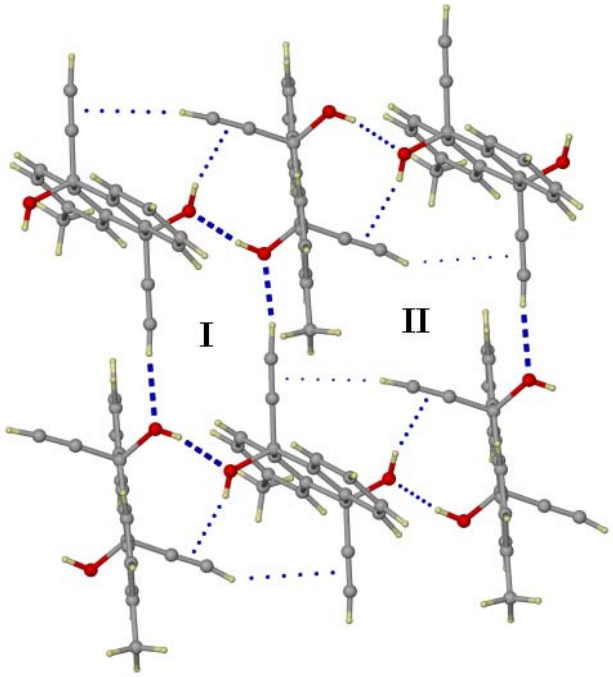

Figure 14. Crystal structure of **4b**. Distortion of synthon **II** is because of the Me-group.

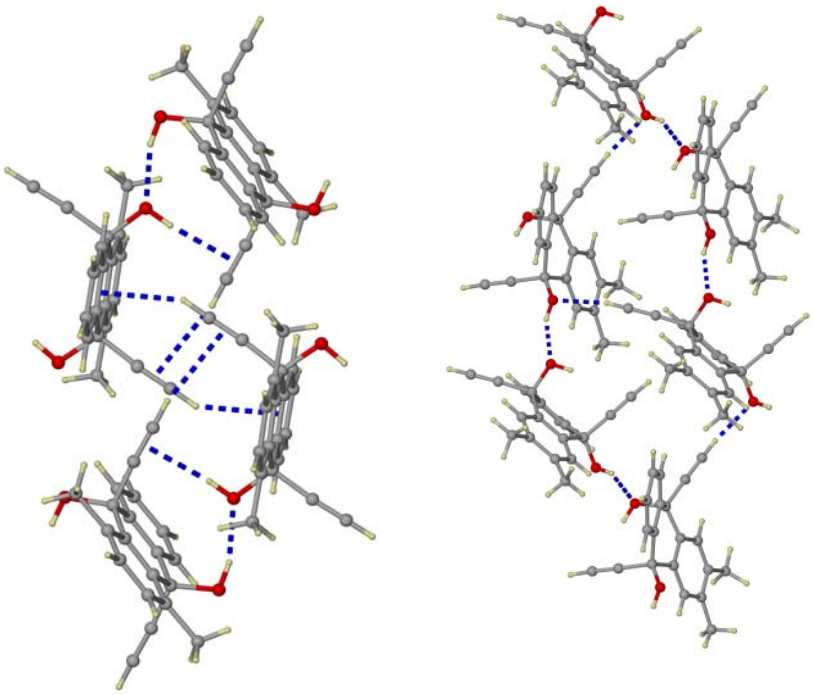

Figure 15. Packing diagram of **4c** (left) and **4d** (right). Synthons **I** and **II** are absent.

Robustness or lack of structural interference is a sought after goal in synthon based crystal engineering. In the *gem*-alkynol family, there are several structural options based on different types of hydrogen bonds. Identifying a robust supramolecular synthon and proving its repetition is in itself a challenging task in a system as fragile as this: it will be noted that there is no repetition of a major hydrogen bonded supramolecular synthon in the 144 *gem*-alkynols the structures of which have been published prior to this work. In this context, the crystal structures of alkynols **1a**-**1f**, **2a**-**2f**, **3a**, **3b**, **4a** and **4b** prove the robustness and repetitive character of synthons **I**, **II** and their near equivalent [$\mathbf{(I)_{0.5}(II)_{0.5}}$].

The following observations are noteworthy in this series: (i) The main structure type is obtained in which the hydrogen bonds occur in a planar arrangement, and the aromatic residues are perpendicular to this plane; (ii) This hydrogen bond arrangement manifests itself as a combination of synthons **I** and **II**, or alternatively their hybrid

[$\mathbf{(I)_{0.5}(II)_{0.5}}$]; (iii) In both these cases, an infinite chain O–H…O–H…C≡C–H…C≡C–H…O–H… is the basis of the structure and is probably the kinetically relevant synthon; (iv) The aromatic residues emerge from one or both sides of the hydrogen bonded layer and interdigitate with similar residues from adjacent layers; (v) Addition of a fused benzo residue, say **2a→3a** or **2c→3b** does not perturb the structure because it is a manifestation of naphtha/anthra homology; (vi) The addition of one or two Me-groups is akin to benzo annelation, and explains the similarities between pairs of structures like 1b and **4a**, **1d** and **4a**, or **2b** and **4a**; (vii) Cl-substitution results in more deep seated chemical changes and pairs of compounds like **1c** and **1e**, **1d** and **1f**, or **2b** and **2c** are not isostructural; (viii) A rare case of Br/H mimicry is seen in the pair of compounds **2d** and **2f**. Bromine is able to fulfill a space filling role that chlorine cannot; (ix) At a subtle level, the preference for the formation of synthons **I** and **II** versus the hybrid [$\mathbf{(I)_{0.5}(II)_{0.5}}$] does not seem to be directly related to molecular symmetry. However, it is noted that no centrosymmetric molecule takes the hybrid synthon.

Each intermolecular force will have some influence on the result of the crystallization process but it is evident that some intermolecular interactions will be more significant than the others in the final crystal. The probability that a certain synthon will emerge in the end could be taken as a measure of the yield of a supramolecular reaction [2.6]. That synthon **I**, **II** or synthon [$\mathbf{(I)_{0.5}(II)_{0.5}}$] emerges as a robust supramolecular synthon in the *gem*-alkynol crystal structures is in itself a significant result because such robustness has not been previously observed in this family. However, the question still remains as to why synthon **I**, **II** or synthon [$\mathbf{(I)_{0.5}(II)_{0.5}}$] are formed, and not something else. Synthons **I**, **II** and [$\mathbf{(I)_{0.5}(II)_{0.5}}$] appear to be very similar or indeed almost identical when they are considered in terms of the individual interactions. The major structural element in both cases is the infinite cooperative network of strong and weak hydrogen bonds O–H…O–H…C≡C–H…C≡C–H…O–H… running in two directions. This infinite chain is the key to the structural similarity in this family.

Finally, it is necessary to comment about polymorphism or the lack of it in this family. Polymorphism is a rare phenomenon in the *gem*-alkynols and the crystallization batches have been searched adequately to be able to make this assertion. Why is this the

case, and whether polymorphism may eventually be found in this family of structures, it cannot be said. In principle, **1b** and **1c** should be good candidates for polymorphic behaviour, as they are kinetically and thermodynamically very similar (hydrogen bond energy and packing coefficient for **1b** is −3.65 kcal mol^{-1} and 0.68 and for **1c** it is −3.59 kcal mol^{-1} and 0.66). But no polymorphs were found for these compounds. It is possible that the infinite chain referred to above is both kinetically and thermodynamically preferred leading thereby to a single stable crystal form. This behaviour is reminiscent of the aminophenols wherein a similar role has been ascribed to an infinite $(O–H…N–H…)_n$ chain [1.35b].

2.6 Conclusions

The value of a supramolecular synthon as an indicator of crystal packing arises from its frequency of occurrence. However, another indicator that should be used while assessing the utility of a synthon is its size. A synthon symbolizes a carry-over of structural information from a molecule to a crystal and between crystal structures: as its size increases, so does its information content. So larger synthons are potentially more informative than smaller ones (**I**, **II**, and $[\mathbf{(I)_{0.5}(II)_{0.5}}]$ as opposed to say, the O–H…O tetramer). But as synthon size increases its occurrence becomes less frequent. The real challenge in crystal engineering is to find a big enough synthon that occurs often enough. There must lie an optimal region between the extremes of small size and numerous occurrences, and large size and infrequent occurrences. *It is in this domain that the synthons are the most useful*, and where the visualization of crystal structures in terms of supramolecular synthons and the comparison of crystal structures is most effectively accomplished. Such a domain has been identified in this family of *gem*-alkynols, a group of compounds well known for their structural inconsistency.

2.7 Experimental section

Synthesis

All *gem*-alkynols were synthesized from the respective quinones using a two-step procedure. The operations were carried out in a dry N_2 atmosphere using standard

syringe-septum techniques. (i) A solution of $Me_3SiC{\equiv}CH$ (4.4 mmol) in THF (15 mL) was mixed with ^{n}BuLi (4.2 mmol) at –78 °C. After stirring for 15 min a solution of the respective quinone (1mmol) in THF, was added dropwise and stirring continued for 30 minutes at – 78 °C and for a further 1 h at room temperature. The product was obtained after standard work-up. (ii) The solid product from step (i) was dissolved in MeOH and methanolic KOH was added slowly and the mixture was stirred for 1 h at room temperature. Water was added to the reaction mixture and the product was extracted with EtOAc. The product was dried over $MgSO_4$ and the solvent was removed. All these compounds were characterized with NMR (Bruker ACF200 MHz) and IR (Jasco 5300) spectra. All melting points were measured in Fisher-Jones melting point instrument. Crystals for X-ray work were obtained by purification of the crude material (column chromatography) followed by recrystallization from 1:1 $CHCl_3$–benzene.

1b ^{1}H NMR (200 MHz $CDCl_3$): δ 6.06 (s, 2H), 2.53 (s, 2H), 2.07 (s, 2H), 1.99 (s, 6H); IR (cm^{-1}): 3395, 3296, 3059, 2924, 2118, 1722, 1657, 1612, 1477, 1450, 1265, 1159, 1024, 949, 916, 825. mp 172 °C

1c ^{1}H NMR (200 MHz $CDCl_3$): δ 6.01 (s, 2H), 2.49 (s, 2H), 2.02 (s, 2H), 1.99 (s, 6H); IR (cm^{-1}): 3395, 3296, 3059, 2924, 2118, 1722, 1657, 1612, 1477, 1450, 1265, 1159, 1024, 949, 916, 825. mp 126 °C

1d ^{1}H NMR (200 MHz $CDCl_3$): δ 2.47 (s, 2H), 1.99 (s, 12H), 1.87 (s, 2H); IR (cm^{-1}): 3501, 3385, 3271, 2928, 2108, 1614, 1386, 1226, 1168, 1033, 958. mp 186 °C

1e ^{1}H NMR (200 MHz $CDCl_3$): δ 6.09 (s, 2H), 2.96 (s, 2H), 2.69 (s, 2H), IR (cm^{-1}): 3377, 3300, 2118, 1674, 1624, 1373, 1232, 1197, 1103, 1028, 839, 792, 756. mp 128 °C

2b ^{1}H NMR (200 MHz $CDCl_3$): δ 7.85 (m, 2H), 7.47 (m, 2H), 2.59 (s, 2H), 2.32 (s, 2H), 2.12 (s, 6H), IR (cm^{-1}): 3454, 3067, 3030, 2957, 2870, 2145, 1668, 1597, 1456, 1377, 1300, 1249, 1120, 845. mp 162 °C

2c ^{1}H NMR (200 MHz $CDCl_3$): δ 7.91 (m, 2H), 7.51 (m, 2H), 3.29 (s, 2H), 2.74 (s, 2H); IR (cm^{-1}): 3396, 3294, 3065, 2959, 2930, 2870, 2119, 1641, 1491, 1450, 1338, 1221, 1151, 1030. mp 187 °C

2d ^{1}H NMR (200 MHz $CDCl_3$): δ 7.61 (s, 2H), 6.21 (s, 2H), 2.62 (s, 2H), 2.44 (s, 2H), 2.32 (s, 6H); IR (cm^{-1}): 3412, 3371, 2960, 2120, 1666, 1608, 1500, 1492, 1408, 1249, 1022, 842, 760. mp 170 °C

2e ^{1}H NMR (200 MHz $CDCl_3$): δ 7.60 (s, 2H), 3.15 (s, 2H), 2.72 (s, 2H), 2.33 (s, 6H); IR (cm^{-1}): 3501, 3387, 3273, 2926, 2108, 1628, 1385, 1321, 1032, 958, 864, 723, 673. mp 194 °C

2f ^{1}H NMR (200 MHz $CDCl_3$): δ 7.61 (s, 2H), 2.76 (s, 2H), 2.45 (s, 2H), 2.33 (s, 6H); IR (cm^{-1}): 3530, 3439, 3271, 2108, 1649, 1626, 1454, 1329, 1180, 1103, 1093, 885, 806, 742. mp 201 °C

3a ^{1}H NMR (200 MHz $CDCl_3$): δ 8.40 (s, 2H), 7.93 (m, 2H), 7.55 (m, 2H) 6.33 (s, 2H), 2.69 (s, 2H), 2.33 (s, 2H); IR (cm^{-1}): 3557, 3400, 3055, 3000, 2961, 2305, 2118, 1685, 1626, 1597, 1502, 1388, 1321, 1265, 1163, 1016, 960. mp 163 °C

3b ^{1}H NMR (200 MHz $CDCl_3$): δ 8.43 (s, 2H), 7.96 (m, 2H), 7.58 (m, 2H), 3.36 (s, 2H), 2.80 (s, 2H); IR (cm^{-1}): 3557, 3400, 3055, 2960, 2305, 2120, 1670, 1626, 1587, 1376, 1232, 1197, 1103, 1028. mp 183 °C

4b ^{1}H NMR (200 MHz $CDCl_3$): δ 8.01 (m, 4H), 7.97 (d, 1H), 7.87 (s, 1H) 7.56 (d, 1H), 2.82 (m, 4H), 2.51 (s, 3H); IR (cm^{-1}): 3375, 3067, 3263, 2961, 2901, 2874, 2108, 1614, 1475, 1452, 1410, 1249, 1145, 1045, 976, 949, 914. mp 227 °C

4c ^{1}H NMR (200 MHz $CDCl_3$): δ 8.01 (m, 2H), 7.57 (m, 2H), 7.26 (s, 2H), 2.92 (s, 6H), 2.70 (s, 2H), 2.60 (s, 2H); IR (cm^{-1}): 3479,3441, 3277, 3263, 2108, 1460, 1383, 1352, 1251, 1203, 1174, 1043, 1008, 956, 835, 765, 702. mp 234 °C

4d ^{1}H NMR (200 MHz $CDCl_3$): δ 8.10 (m, 2H), 7.87 (s, 2H), 7.46 (m, 2H), 2.82 (s, 2H), 2.71 (s, 2H) 2.46 (s, 6H); IR (cm^{-1}): 3489, 3277, 3294, 3069, 3030, 2957, 2932, 2114, 1932, 1724, 1658, 1604, 1450, 1321, 1259, 1122, 1024, 968. mp 208 °C

X-ray crystallography

The X-ray data were collected at the University of Durham, U.K. by Dr. R. Mondal under the supervision of Prof. J. A. K. Howard. The X-ray diffraction were carried out on a Bruker SMART–1000 diffractometer using Mo K_α radiation (λ = 0.71073 Å) [2.7].

The structure solution and refinements were carried out using SHELXTL (Version 5.1) programs [2.8]. Structures of all the compounds were solved by direct methods and refined by full-matrix least squares on F^2. H-atoms were located in all six structures and refined freely with isotropic displacement parameters. The relevant crystallographic information is given in the appendix.

Calculations

All calculations were carried out on Indigo Solid Impact and Indy workstations from Silicon Graphics in Hyderabad [2.9]. All interatomic distances and related calculations were carried out with the PLATON programme [2.10].

CHAPTER THREE

ORGANIC CHLORINE AS A HYDROGEN BRIDGE ACCEPTOR

3.1 Introduction

The role of intermolecular interactions in the context of designing organic and organic/inorganic crystal structures is a topic of much current interest [1.6]. The packing of molecules in crystalline solids, generated by conventional hydrogen bonds like O–H…O, O–H…N, N–H…O and N–H…N (energy 5 to 15 kcal mol^{-1}), has been well studied [1.26]. More recently, weak hydrogen bonds (energy less than 5 kcal mol^{-1}) like C–H…O, C–H…π, X…X (X= halogens) and π…π have attracted attention [1.28]. For these types of interactions, a different term *hydrogen bridge* instead of *hydrogen bond* has been suggested [1.32].

Halogens have their common presence in both inorganic and organic chemistry, serving as bridging ligands for a wide variety of coordination compounds as well as being common substituents in a large number of organic compounds [3.1]. CSD studies by Seddon and Aakeröy [3.2], by Brammer and co-workers [1.31 b-d] and by Thallapally and Nangia [1.31a] show that the X–H…Cl–Y interaction is viable for metal-bound chlorines (Cl–M) as well as chloride ions (Cl^-), or as carbon-bound chlorines (Cl–C) with suitable activating groups present. Dunitz and Taylor [3.3] showed that the hydrogen bonding capability of the C–F moiety is very poor and X–H…F–C (X = O, N, *etc*.) hydrogen bonding interactions are too weak to be of significance in molecular recognition processes in biological chemistry or crystal engineering. The acceptor property of organic fluorine was also studied by Howard et al. [1.30b] and by Boese, Desiraju and co-workers [1.30c]. There are recent studies, which show that the C–H…F–C interaction is necessary in transition-metal-catalysed alkene polymerisation, [3.4] ligand enzyme binding and molecular conformation [3.5].

O–H…Cl–C hydrogen bridges occur very rarely and there are only a few examples that emerge from a literature survey [3.6]. The work of Hantzsch [3.7] on dimethyl 3,6-dichloro-2,5 dihydroxyterephthalate and of Wulf et al. [3.8] on the ortho-halogenated phenols are some of the classical examples of O–H…Cl–C interactions in

the solid state. O–H…Cl–C interactions have been invoked in solution, for example, to explain the appearance of polymorphs of 2,6-dihydroxybenzoic acid during recrystallization from $CHCl_3$ [1.37a]. Crystalline diterpenoid briarein A is another instance where a hydroxyl group forms an O–H…Cl–C interaction instead of any intermolecular O–H…O hydrogen bridges [3.9]. An unusual intramolecular O–H…O–H…Cl–C cooperative network of hydroxy groups of a ferrocene derivative has also been reported [3.10].

In this chapter, a combined approach of crystallographic, spectroscopic and computational methods has been used to quantify intramolecular O–H…Cl–C hydrogen bridges in the crystal structures of a series of Cl-substituted *gem*-alkynols. Since the chloro-substituent in this group of compounds may not be considered to be a good hydrogen bond acceptor, such a study was expected to be useful.

3.2 CSD study

To assess the hydrogen-bonding capabilities of the C–Cl unit, the CSD (Version 5.26, May 2005) [1.18] was used to search for structures containing O–H as well as the C–Cl fragment. The search showed that out of 1536 crystal structures, only 181 contain one or more O–H…Cl–C interactions [3.11]. Of these interactions, 76 are intermolecular while 118 are intramolecular. Our objective was to compare the geometry of O–H…Cl–C interaction in these crystal structures as well as to assess the relative probability of such contacts being formed (Figure 1). Not only is the interaction observed infrequently but it is also reported to be weak. Rowland and Taylor mentioned that while values of *d*(H...A) for (O,N)–H…N(O) interactions are markedly smaller than those for C–H…O(N), these preferences are actually inverted when organic chlorine is an acceptor. Values of *d* for (O,N)–H…Cl(Br) are larger than those for C–H…Cl(Br). This inversion is rationalized by the fact that interactions like O–H…Cl–C are often minor components in a bifurcated hydrogen bond while the C–H…Cl–C are stand-alone interactions [3.12].

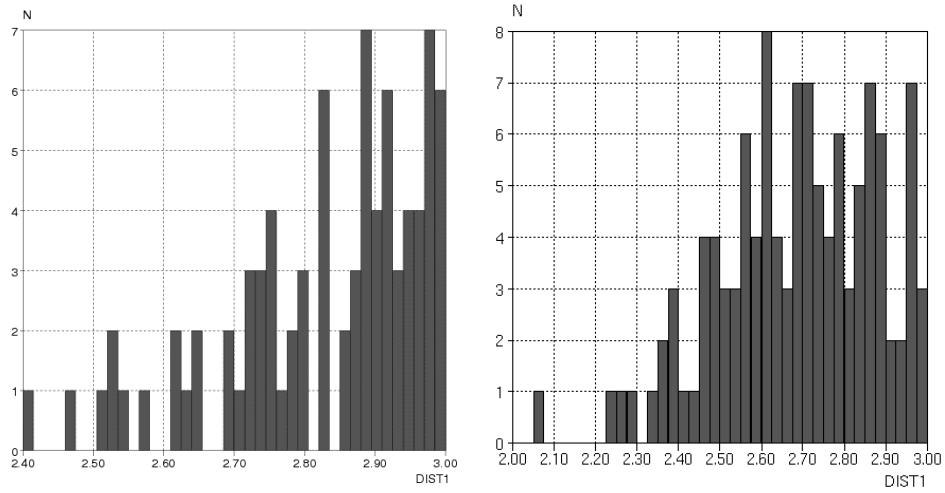

Figure 1. Histograms of intramolecular (right) and intermolecular (left) O–H...Cl–C interactions.

3.3 Molecular structures

The parent compound *trans*-9,10-diethynyl-9,10-dihydroanthracene-9,10-diol is labelled DDA and the other compounds are given suitable related acronyms (Scheme 1). In chapter 2 it was mentioned that it is a general feature in the *gem*-alkynol family that the combination of two hydrogen bond donors and two acceptors in close proximity and in a sterically hindered situation results in a wide variety of hydrogen bond patterns [1.34]. It is extremely difficult to envisage in advance what the hydrogen bond pattern will be for a particular compound. It has been noted that five of the six chloro derivatives under consideration (CDDA, 14DDDA, 15DDDA, 18DDDA, 15MKA) showed an intramolecular O–H…Cl–C interaction and that in the 15DDDA only one of the two Cl-groups does so. TDDA does not show an intramolecular O–H…Cl–C interaction in the solid state. Scheme 1 gives the structural formulas of the six *gem*-alkynols in this study with the intramolecular O–H…Cl–C interactions that occur in the solid state being shown in Figure 2. The short H…Cl distances (d) and the hydrogen bond angles (θ) are also indicated in Scheme 1. The approach of the hydroxyl group toward the Cl-atom is very nearly the same in all five structures (Figure 2). Figure 3 is an

overlay diagram of CDDA, 14DDDA, 15DDDA, 18DDDA and 15MKA. The figure shows that these interactions are highly conserved in this group of compounds.

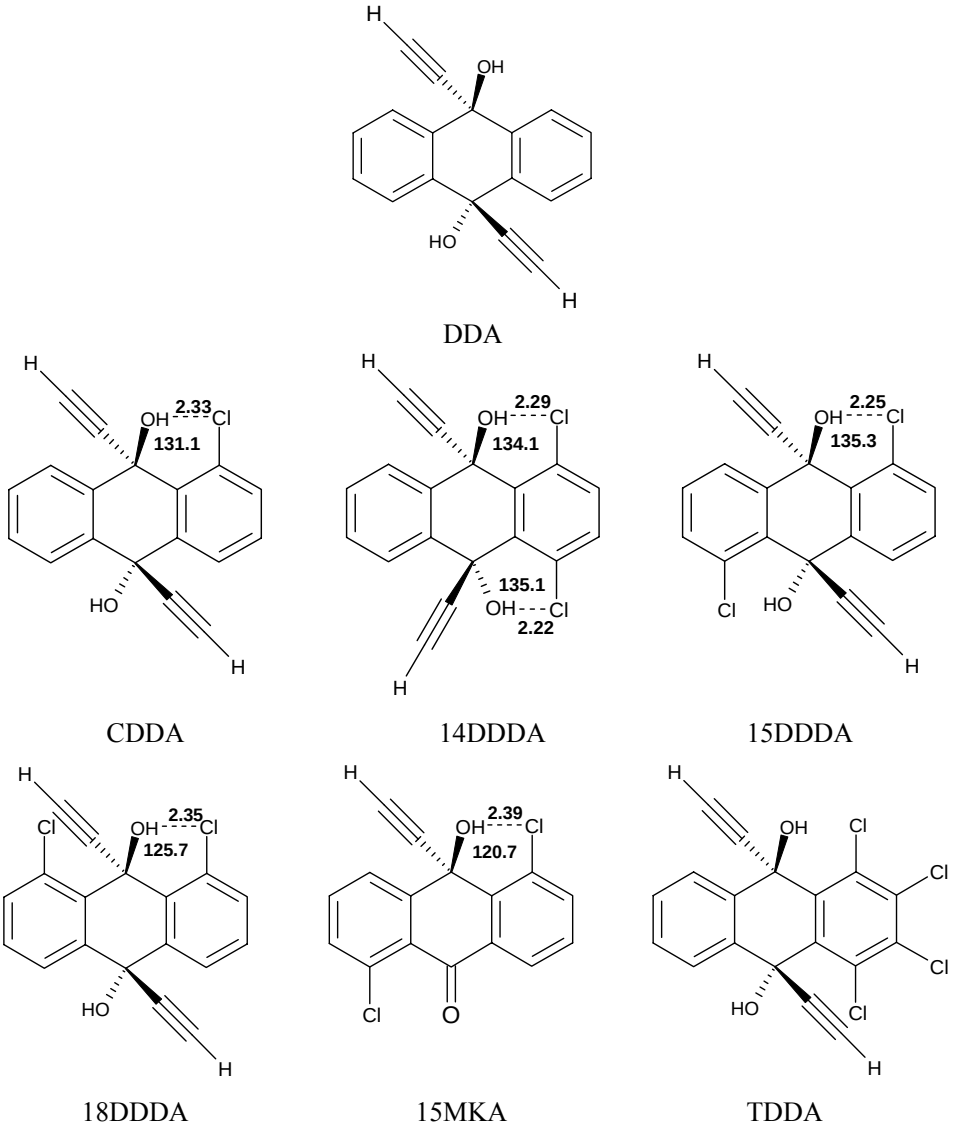

Scheme 1. Compounds in this study with the metrics of the solid state O–H…Cl–C interactions marked.

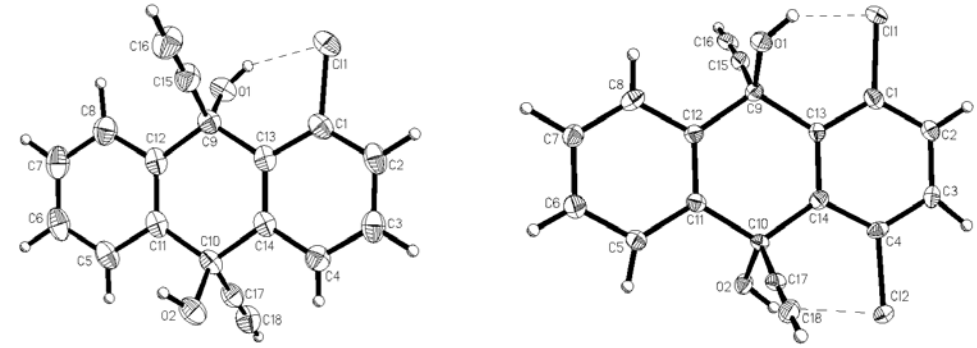

CDDA 14DDDA

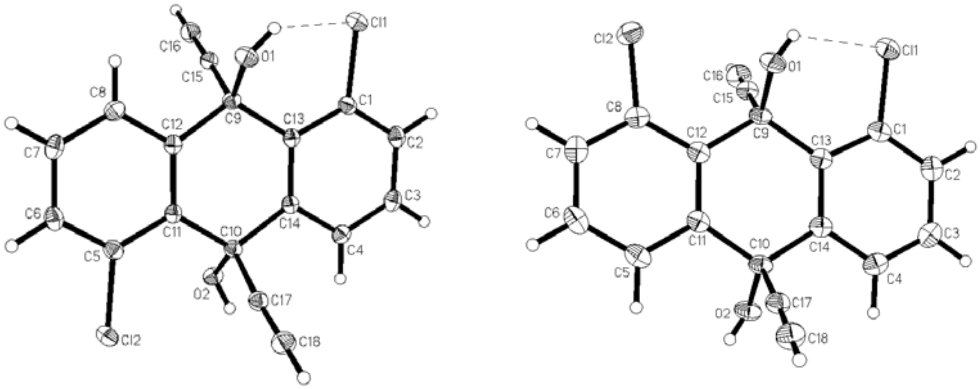

15DDDA 18DDDA

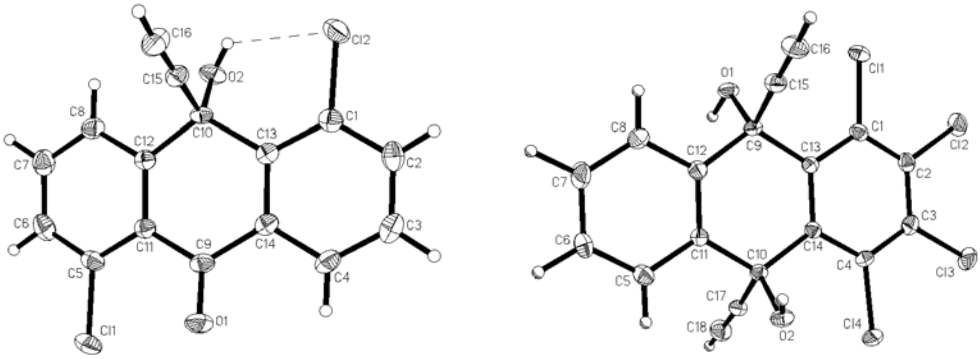

15MKA TDDA

Figure 2. Single molecule ORTEP drawings of the molecules in this study. The O–H…Cl–C interactions are shown as dotted lines. Note that the symmetrical 15DDDA does not sit on an inversion centre in the crystal and that TDDA does not form O–H…Cl–C interactions.

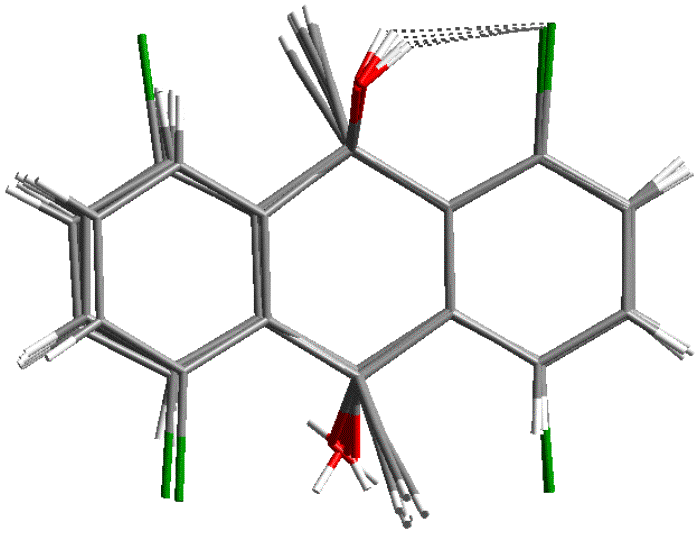

Figure 3. Overlay diagram of CDDA, 14DDDA, 15DDDA, 18DDDA and 15MKA. 14DDDA has been superimposed twice to show the intramolecular O–H…Cl–C interaction for each of the symmetry independent hydroxyl groups.

3.4 NMR spectroscopy

Solution NMR data ($CDCl_3$) of the five molecules studied (Table 1) further strengthens the idea of an intramolecular O–H…Cl–C interaction. Unlike in the solid state, all O–H groups that can participate in intramolecular O–H…Cl–C interactions (both groups in 15DDDA and TDDA) do so in solution. The hydroxyl H-atom shifts routinely from δ = 2.6 ppm in *gem*-alkynols that lack an adjacent Cl-group to about δ = 4.5 ppm. This downfield shift is surprisingly large, but it is consistent and there is some precedent [3.13]. The lack of further change in intensity or position of the peaks on dilution confirms the intramolecular nature of the interaction (Figure 4). D_2O exchange confirms the assignment of the δ = 4.5 ppm peak to the hydroxyl H-atom. A further experiment with CDDA provides very clear evidence of the hydrogen-bond nature of this intramolecular interaction. In this compound, there are two nonequivalent O–H groups, with only one able to form an O–H…Cl–C interaction. Addition of D_2O showed that while the free O–H group exchanges immediately, the hydrogen bonded O–H requires

one hour for complete exchange (Figure 5). Our observation on the slow exchange of the δ = 4.5 ppm peak shows that this weak acceptor, organic chlorine, is well able to sustain an attractive and stabilizing intramolecular hydrogen bridge. In summary, the NMR data show that the intramolecular O–H…Cl–C interaction is the preferred mode of association in appropriately chloro-substituted *gem*-alkynols.

Table 1. ^{1}H NMR chemical shifts of hydroxyl H-atoms in *gem*-alkynols showing the existence of intramolecular O–**H**…Cl–C interactions.

Compound	δ(O–H…Cl–C) hydrogen bonded hydroxyl proton	δ (free O–H)
DDA	—	2.80
CDDA	4.51	2.78
14DDDA	4.39	—
15DDDA	4.46	—
18DDDA	4.51	2.79
TDDA	4.40	—
15MKA	4.71	—

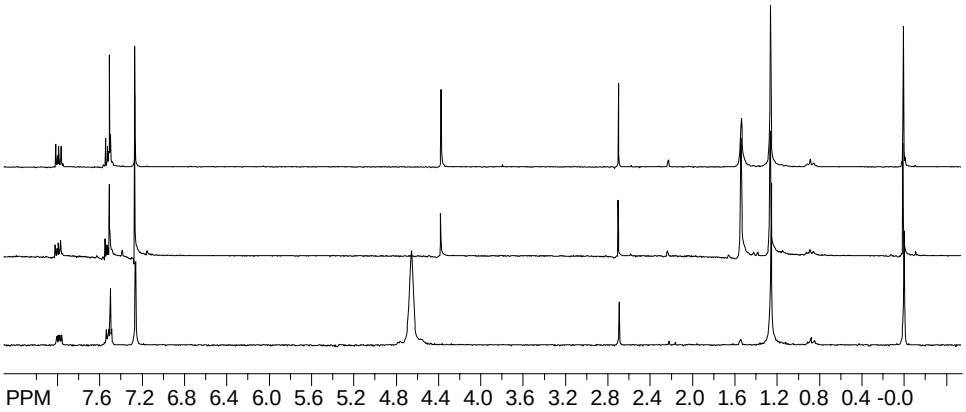

Figure 4. ^{1}H NMR spectra of 14DDDA ($CDCl_3$). Top: Initial spectrum; Middle: twice diluted; Bottom: D_2O added.

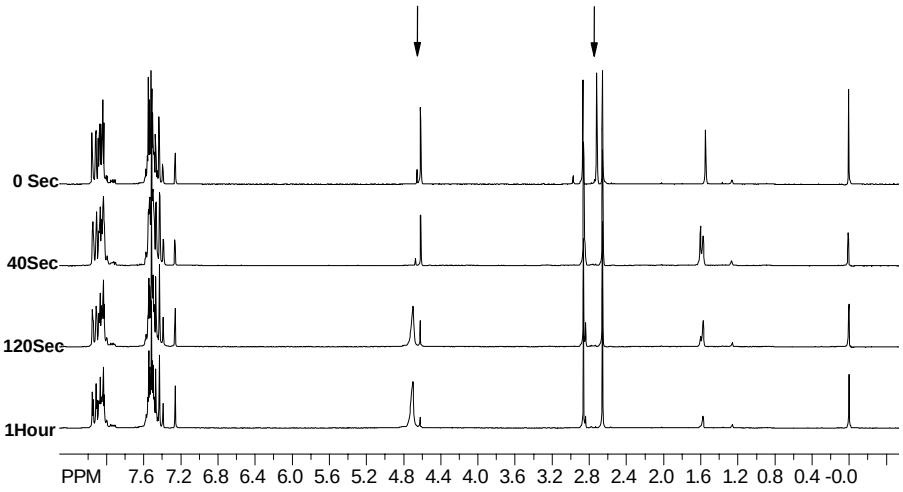

Figure 5. Time resolved D_2O exchange NMR spectra of CDDA. Note that the intramolecular O–**H**...Cl hydrogen bonded proton (δ 4.51) exchanges slowly when compared with the 'free' hydroxyl proton at δ 2.78 that exchanges immediately.

3.5 Theoretical calculations

The above observations show that organic chlorine is a good acceptor of hydrogen bonds. Therefore the energy of the O–H…Cl–C interaction was calculated [3.14]. The results in Table 2 pertain to both the Hartree-Fock ab initio method (PC Spartan; 6-31G*) [3.15] and to DFT (GAMESS; B3LYP/6-31G*) [3.16]. The Hartree-Fock optimized structure corresponds quite well with the molecule obtained crystallographically. This trial molecule was taken and the hydroxyl group H-atom(s) were rotated anti compared to the Cl–C bond so that the O–H…Cl–C interaction is excluded. The hydroxyl H-atoms were fixed in their new position and the structure optimized at the 6-31G* level. The difference in the total energy of both the optimized conformational isomers gives the O–H…Cl–C bond energy. A similar strategy was employed for the DFT calculations. Respective geometries of the trial molecules with and without O–H…Cl–C hydrogen bonds optimized at the AM1 level were then input into GAMESS for DFT calculations. The results show that the stabilization energy for the interaction is surprisingly high (that too for an intramolecular interaction), and that it occurs at the upper end for weak hydrogen bonding (0.5-4.0 kcal mol^{-1}) [1.25d].

Table 2. O–H…Cl–C hydrogen bond energies in the simulated structures.

Compound	Hartree-Fock method kcal mol^{-1}	DFT method kcal mol^{-1}
CDDA	4.446	4.320
14DDDA	3.558	4.384
15DDDA	4.150	4.681
18DDDA	3.662	2.889

3.6 Crystal structures

The crystal structures of the four molecules (14DDDA, 15DDDA, 18DDDA, CDDA) may be considered in terms of how: (a) the intramolecular O–H…Cl–C interactions fit into the overall hydrogen bridge scheme; (b) these structures may be derived from that of the unsubstituted compound DDA via synthon exchange and (c) the O–H…Cl–C interaction fares in the presence of competing acceptors. Table 3 gives the geometrical parameters of the hydrogen bridges in these structures.

3.6.1 Hydrogen bridge patterns

The most notable structural feature in 14DDDA is the absence of O–H…O hydrogen bonds (Figure 6a). There is a cooperative assistance to the O–H…Cl–C interaction from a C–H…O interaction and the O–H…Cl–C distance (*d*, 2.22 Å; *θ*, 135.1°) is the shortest in the series.

In the crystal structure of 18DDDA, there is a cooperative arrangement of the type C–H...O–H…O–H…Cl–C (intermolecular, intermolecular, intramolecular). In this case, the cooperative assistance to the O–H…Cl–C interaction arises from a C–H…O and an O–H…O interaction (Figure 6b). To summarise, one should note that the appearance of a C–H…O dimer synthon results in a general similarity in the overall packing in all three structures (14DDDA, 15DDDA, 18DDDA). The intramolecular O–H…Cl–C interaction gets cooperative assistance from other hydrogen bridges. Whatever be the situation in solution (and the NMR results show that the interaction is far from negligible there), this cooperative assistance can only further stabilize the interaction in the solid state.

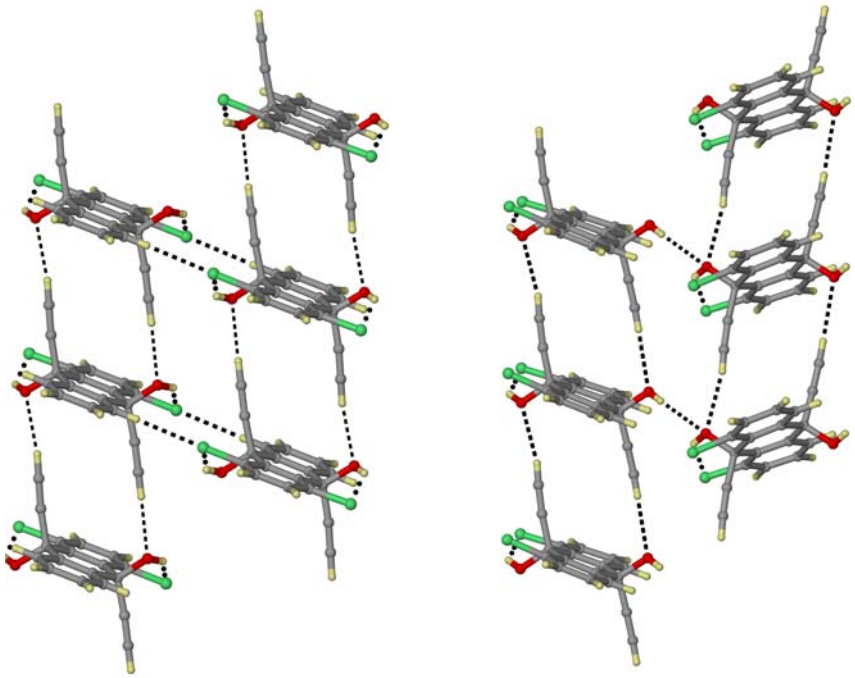

a **b**

Figure 6. (a) Packing diagram of 14DDDA. Notice the intramolecular O–H…Cl–C interaction. The planar C–H...O dimer synthon and intermolecular C–H...Cl hydrogen bridge are also shown. (b) Packing diagram of 18DDDA to show the hydrogen bridges.

Once again the dominant interaction pattern in 15DDDA is a cooperative arrangement of three hydrogen bridges (Figure 7), an intermolecular C–H…O from the ethynyl group (2.22 Å; 160.5°), an intermolecular O–H…O between hydroxyl groups (1.83 Å; 173.8°) and an intramolecular O–H…Cl–C (2.25 Å; 135.3°) [1.60h].

It should be remembered that crystalline TDDA does not form an intramolecular hydrogen bond. Perhaps the high extent of chlorination makes the O–H groups so activated that O–H…O hydrogen bridge formation competes in a favourable manner. The packing of the TDDA molecules is reminiscent of the packing of one of the CDDA molecules that does not form an intramolecular O–H…Cl–C bridge and in which a cooperative O–H…O–H…π arrangement is seen.

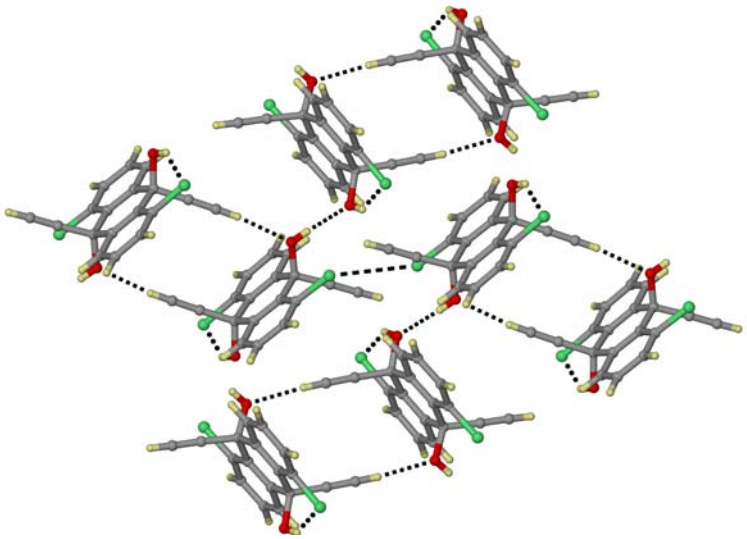

Figure 7. Packing diagram of 15DDDA to show the intramolecular O–H…Cl–C interaction. Notice the C–H...O dimer synthon in this crystal structure also.

Table 3. Geometrical parameters of H-bridges in the crystal structures in this study.

Compound	H-bridge	*d*/Å (H…A)	*D*/Å (X…A)	*θ*/deg ∠X–H…A
CDDA	O–H…Cl	2.33	3.071(1)	131.1
	O–H…O	1.87	2.819(8)	162.3
	C–H…O	2.03	3.106(1)	174.1
	C–H…O	2.35	3.376(2)	158.3
14DDDA	O–H…Cl	2.29	3.055(5)	134.1
	O–H…Cl	2.22	3.000(5)	135.1
	C–H…O	2.40	3.436(9)	160.1
	C–H…O	2.44	3.453(9)	156.0
15DDDA	O–H…Cl	2.25	3.025(1)	135.3
	O–H…O	1.83	2.814(2)	173.8
	C–H…O	2.44	3.501(1)	164.7
	C–H…O	2.22	3.021(1)	160.5
18DDDA	O–H…Cl	2.35	3.021(1)	124.4
	O–H…O	2.14	2.894(2)	132.2
15MKA	O–H…Cl	2.39	3.017(1)	120.7
	O–H…O	2.06	2.801(2)	130.2

	C–H…O	2.44	3.254(2)	131.1
	C–H…O	2.42	3.331(2)	140.4
TDDA	O–H…O	2.33	3.071(1)	131.1
	O–H…O	1.87	2.819(8)	162.3
	C–H…O	2.03	3.106(1)	174.1
	C–H…π [b]	2.89	3.876(2)	154.3
	O–H…π	2.85	3.776(2)	158.3

[a] O–H and C–H distances are neutron normalized to 0.983 and 1.083 Å.
[b] π denotes the centroid of the ethynyl linkage.

3.6.2 Synthon distortion and replacement

The representative synthon **I** in DDA is composed of alternating strong O–H…O and weak C–H…O bridges, while synthon **II** is made up of a loop of alternating C–H…O and C–H…π hydrogen bridges (Scheme 2). It should be noted that the structure of DDA is related to those of 14DDDA, 15DDDA and 18DDDA via that of the monochloro derivative CDDA. It is, therefore, useful to discuss this latter compound in detail.

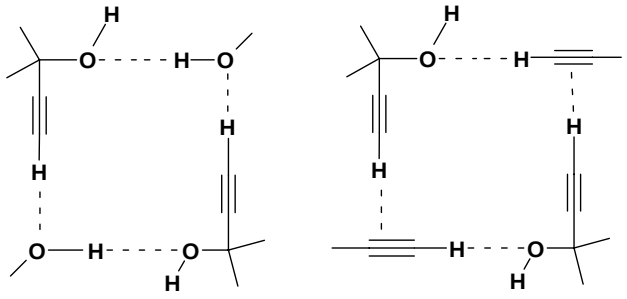

I **II**

Scheme 2. Representative synthons in DDA.

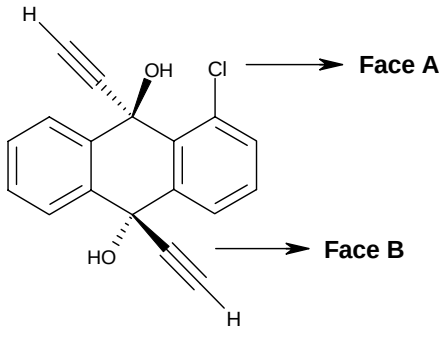

Scheme 3. CDDA molecule with a chlorine-rich face (**A**) and a hydrogen-rich face (**B**).

There are two symmetry-independent molecules in the asymmetric unit of CDDA ($P\bar{1}$, Z'=1.5). The one that lies on a general position forms an intramolecular O–H…Cl–C interaction while the one that lies on the special position does not. The molecule of CDDA exposes a chlorine-rich face (**A**) and a hydrogen-rich face (**B**) (Scheme 3). Face **B** forms synthon **II** characteristic of the unsubstituted DDA while on face **A** the intramolecular O–H…Cl–C bond disturbs the formation of synthon **I** in part that leading to the C–H…O dimer already seen in the three dichloro derivatives. In effect, the packing of CDDA is a composite of the crystal structures of DDA and of the dichloro compounds (Figure 8). Compound CDDA may be therefore be considered as a supramolecular intermediate between DDA and the dichloro derivatives (Scheme 4).

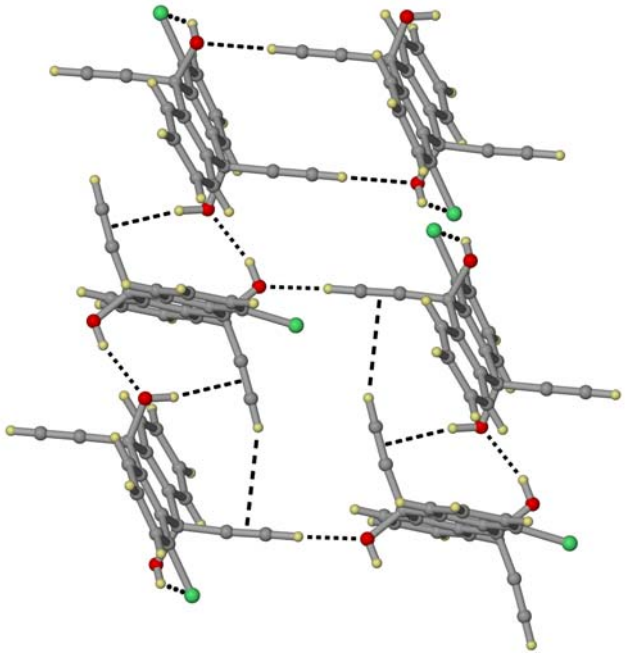

Figure 8. Packing diagram of CDDA. Notice the planar C–H...O dimer synthon, seen in all three dichloro isomers, and synthon **II** seen in DDA.

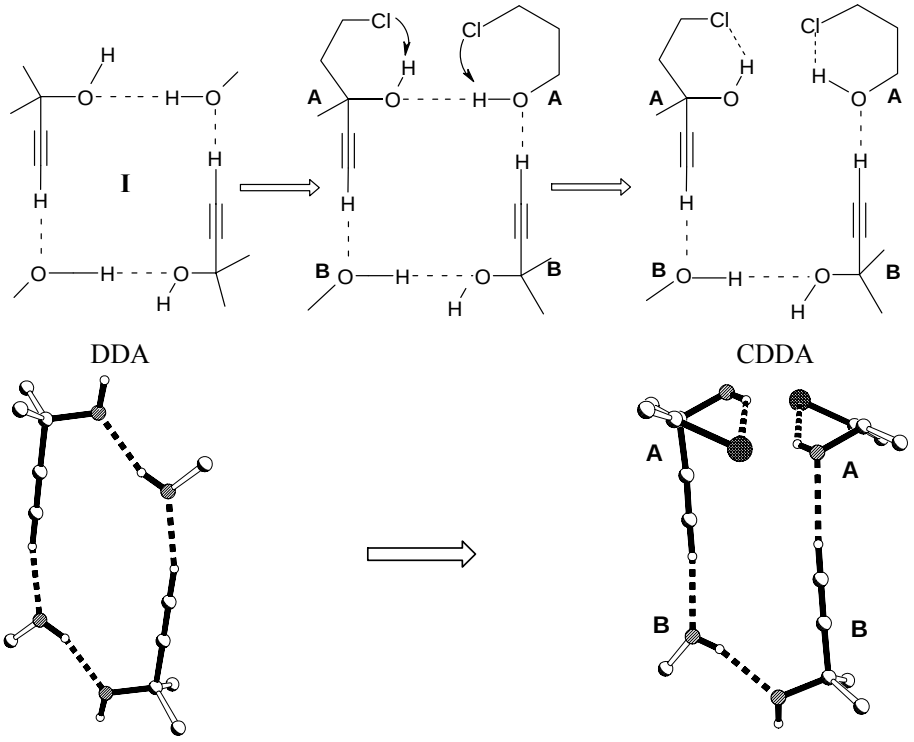

Scheme 4. Supramolecular distortion of synthon **I** in CDDA by the Cl-group via intramolecular O–H…Cl–C interaction. Note how the vestigial synthon on the hydrogen rich side **B** of the molecule retains its original identity.

Two Cl-groups in 14DDDA makes both faces chlorine-rich and therefore, synthon **I** and with it O–H…O hydrogen bonding completely cease to exist (Scheme 5).

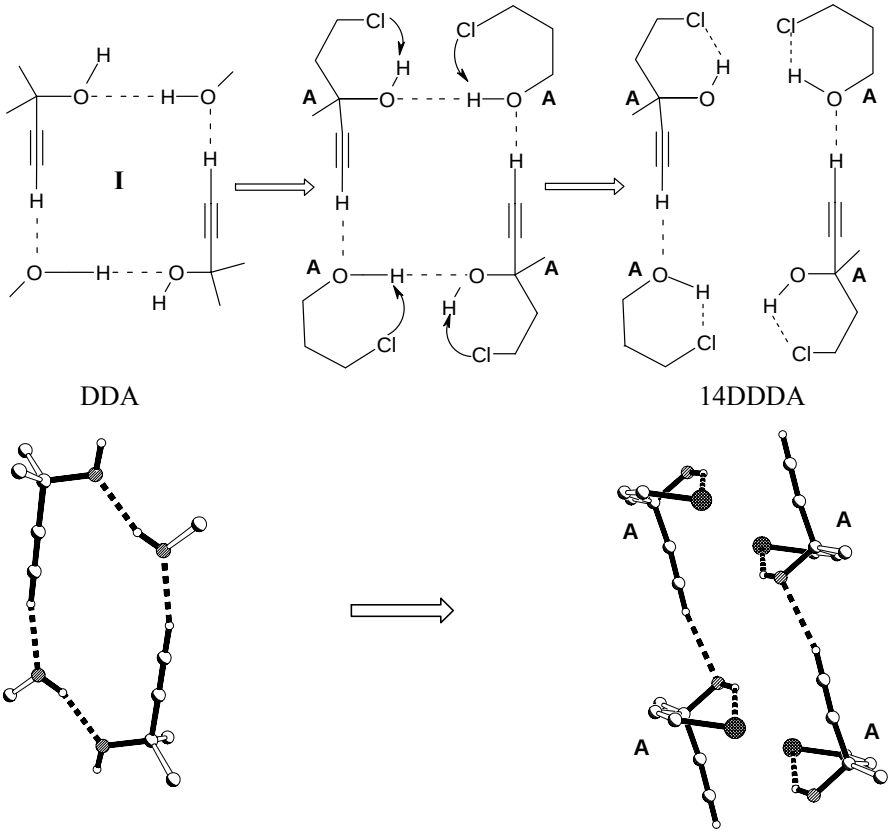

Scheme 5. Supramolecular distortion of synthon **I** by two Cl-groups in 14DDDA.

In 18DDDA, there are again chlorine rich and hydrogen rich faces and an orderly shuffling of hydrogen bonded synthons leads to the observed packing. O–H…Cl–C hydrogen bonding once again modifies the prototype DDA structure in a reasonable way (Scheme 6). The major structural feature in 15DDDA is the Cl_4 supramolecular synthon which is composed of two Cl atoms that are intramolecularly hydrogen bonded to O–H groups and two which are not. However, the notable feature is the absence of synthons **I** and **II**, which may be ascribed to the presence of intramolecular O–H…Cl–C bridges (Figure 6).

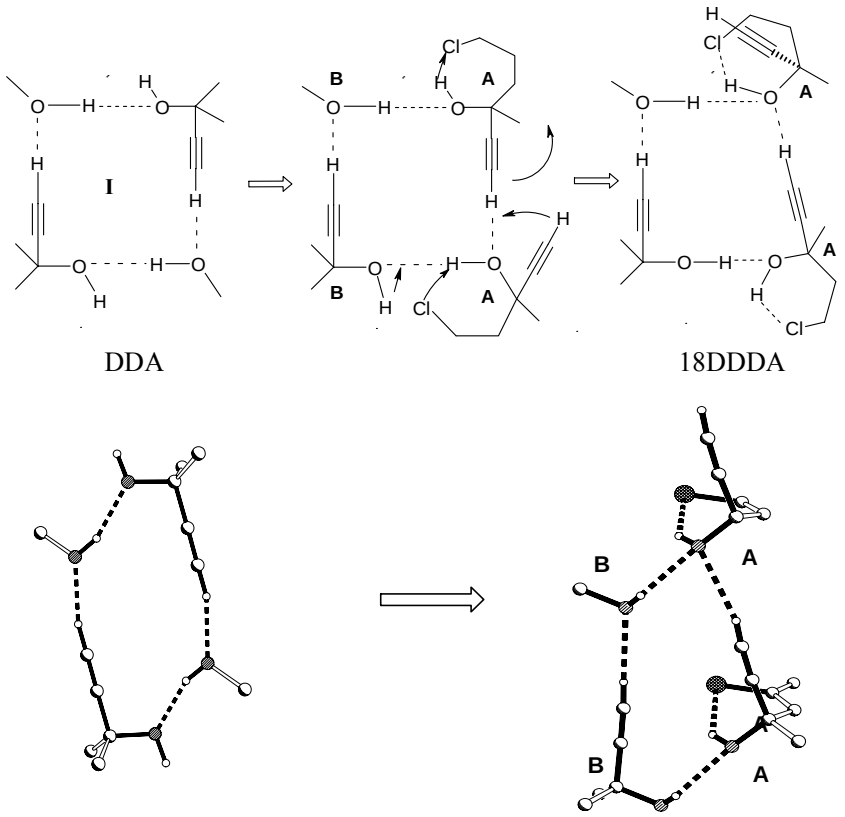

Scheme 6. Supramolecular relationship between DDA and 18DDDA.

3.6.3 Competition between organic chlorine and a stronger acceptor

The keto-alcohol 15MKA has been studied to understand the effectiveness of an intramolecular O–H…Cl–C interaction in which a much stronger acceptor (C=O) is present in a sterically unhindered situation (Figure 9). One would expect a strong O–H…O=C interaction if interaction hierarchy is to be followed. On the contrary, there is a long O–H…O=C interaction (*d*, 2.06 Å; *θ*, 130.2°) in the crystal structure of 15MKA, because the bifurcated donor (O–H) also participates in a short intramolecular O–H…Cl–C hydrogen bridge (2.39 Å; 120.7°). As if to 'make up' for its 'unfulfilled' acceptor capability, the C=O group accepts a weak hydrogen bridge from ethynyl hydrogen (2.44 Å; 131.1°). This latter H-atom is also bifurcated to hydroxyl oxygen (2.42 Å; 140.4°).

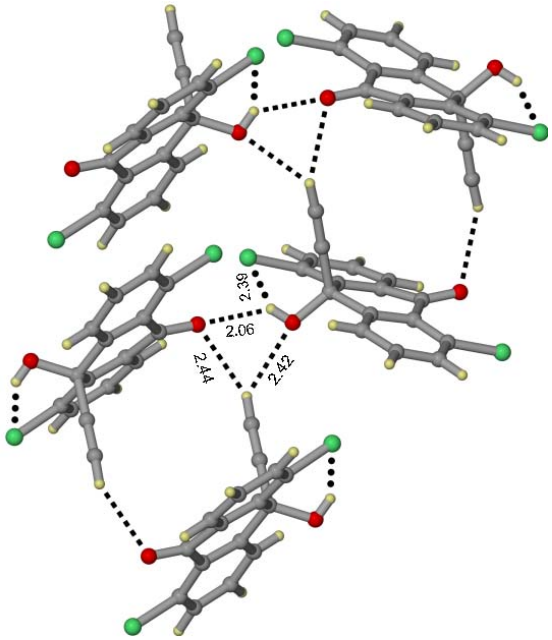

Figure 9. Packing diagram of 15MKA. Notice the four distinct hydrogen bridges.

3.7 Conclusions

Crystal structures in a family of chloro substituted *gem*-alkynols were examined to understand competition and interplay between intermolecular O–H…O–H and a competing intramolecular O–H…Cl–C interaction. This work establishes that O–H…Cl–C interaction is a notable example of a hydrogen bridge, despite the fact that unactivated organic chlorine is not considered to be a good acceptor and the interaction is of the hard donor–soft acceptor type. The significance of the interaction is estimated by the fact that its effects on intramolecular and intermolecular structure are steady and consistent. The NMR results argue in favour of an attractive interaction and theoretical studies show that it is stabilizing to the extent of ~ 4.0 kcal mol^{-1}. We conclude that O–H…Cl–C hydrogen bridges are of more significance than it has been previously thought, and these examples argue for the use of the term ‘hydrogen bridge’ rather than ‘hydrogen bond’ in describing the phenomenon.

3.8 Experimental section

Synthesis

All operations were carried out in a dry N_2 atmosphere. CDDA, 14DDDA, 15DDDA, 18DDDA, and TDDA were synthesized from the respective quinones using a two-step procedure. A solution of trimethylsilylacetylene (4.4 mmol) in THF (15mL) was mixed with *n*-butyllithium (4.2 mmol) at –78 °C. After stirring for 15 min a solution of the respective quinone in THF (15mL) was added dropwise and stirring was continued for 30 minutes at –78 °C and for a further 1h at room temperature. The solid product recovered after workup was treated with methanolic KOH to yield the desired compound. All these compounds were characterized with NMR (Bruker ACF200 MHz) and IR (Jasco 5300) spectra. All melting points were measured in Fisher-Jones melting point instrument. Crystals for X-ray analysis were obtained by purification of the crude material (column chromatography 30% EtOAc/hexane) followed by recrystallization from 1:1 $CHCl_3$/benzene or 1:1 EtOH/benzene.

CDDA ^{1}H NMR ($CDCl_3$): δ 8.15 (m, 3H), 7.58 (m, 4H), 4.61 (s, 1H), 2.87 (s, 1H), 2.78 (s, 1H), 2.68 (s, 1H); IR (cm^{-1}) 3508, 3387, 3252, 3215, 2108, 1591, 1568, 1489, 1435, 1356, 1286, 1248, 1228, 1149, 1111, 1026. Mp: 250 °C

14DDDA ^{1}H NMR ($CDCl_3$): δ 8.01 (s, 2H), 7.58 (m, 2H), 7.51 (m, 2H), 4.39 (s, 2H), 2.70 (s, 2H); IR (cm^{-1}) 3530, 3248, 2100, 1435, 1336, 1219, 1151, 1026. Mp: 281°C

15DDDA ^{1}H NMR ($CDCl_3$): δ 8.10 (dd, *J* 8, 3 Hz, peri 2H), 7.51 (m, 4H), 4.46 (s, 2H) 2.70 (s, 2H); IR (cm^{-1}) 3312, 3288, 3177, 3001, 2881, 2116, 1973, 1811, 1595, 1562, 1456, 1300, 1205, 1039. Mp: 280 °C

18DDDA ^{1}H NMR ($CDCl_3$): δ 8.08 (m, peri 2H), 7.60 (m, 2H), 7.48 (m, 2H), 4.51 (s, 1H), 2.85 (s, 1H), 2.79 (s, 1H), 2.68 (s, 1H); IR (cm^{-1}) 3530, 3256, 3048, 2106, 1591, 1562, 1437, 1340, 1222, 1176, 1149, 1024. Mp: 228 °C

TDDA ^{1}H NMR ($CDCl_3$): δ 8.01 (dd, *J* 8, 3 Hz, 2H), 7.58 (dd, *J* 8, 3 Hz, 4H), 4.40 (s, 2H), 2.70 (s, 2H); IR (cm^{-1}) 3485, 3414, 3271, 3229, 2110, 1444, 1396, 1356, 1249, 1165. Mp: 233 °C

15MKA Obtained as a side product during the preparation of 15DDDA. ^{1}H NMR ($CDCl_3$): δ 8.27 (dd, *J* 8, 3 Hz, 1H), 8.15 (dd, *J* 8, 3 Hz, 1H), 7.73 (m, 4H), 4.71 (s, 1H), 2.66 (s, 1H); IR (cm^{-1}) 3518, 3271, 2926, 1168, 1585, 1442, 1278, 1138. Mp: 197 °C

X-ray crystallography

The X-ray data were collected at the University of Durham, U.K. by Dr. R. Mondal under the supervision of Prof. J. A. K. Howard. The X-ray diffraction were carried out on a Bruker SMART–1000 diffractometer using Mo K_α radiation (λ = 0.71073 Å). The structure solution and refinements were carried out using SHELXTL (Version 5.1) programs [2.8]. Structures of all the compounds were solved by direct methods and refined by full-matrix least squares on F^2. H-atoms were located in all six structures and refined freely with isotropic displacement parameters. The relevant crystallographic information is given in the appendix.

Calculations

All calculations were carried out on Indigo Solid Impact and Indy workstations from Silicon Graphics in Hyderabad [2.9]. All interatomic distances and related calculations were carried out with the PLATON programme [2.10]. Details of the *ab initio* calculations are given in the results section.

CHAPTER FOUR

STRUCTURAL STUDIES OF *trans*-1,5-DICHLORO-9,10-DIETHYNYL-9,10-DIHYDROANTHRACENE-9,10-DIOL AND ITS PSEUDOPOLYMORPHS

4.1 Introduction

The theory of close-packing forms the basic framework of our understanding of the ways in which organic molecules assemble into crystals [4.1]. A simple model of crystal packing could be rationalized in terms of how well the symmetry operators of a particular space group fit the molecules together [4.2]. This is a powerful tool to understand how molecular crystal structures are formed and stabilized. However, a crystal structure is, in general, the result of a subtle balance between the isotropic/anisotropic interactions present within it [1.6]. These isotropic/anisotropic forces select the experimental space group that gives the highest enthalpic stability and closest packing. Formation of anisotropic forces in the crystals is governed by the interactions that have preferred directionality. These anisotropic forces administrate the formation of intermolecular interactions even in solution, and the resulting crystal structures deviate from closest packing in some way or the other [1.37]. An important challenge in crystal engineering is to dissect and isolate different kinds of intermolecular interactions (isotropic/anisotropic) so that the consequences of any one kind towards the overall crystal packing are easier to predict and control [4.3].

Kitaigorodskii [4.1c] proposed that popular space groups would be those that provide good conditions for the close packing of molecules, taking into consideration the role of molecular symmetry. The majority of organic compounds utilize only about 20 of the theoretically possible 230 space groups [4.4]. In this context, three consequences are pertinent: (1) centrosymmetric space groups are preferred; (2) space groups that contain translational symmetry elements like screw axes and glide planes are preferred, and (3) the inversion centre is the only molecular symmetry element that is routinely carried over into the crystal because it is the only crystal symmetry element that does not lead to any loss of packing efficiency by its presence [4.5]. However, the shape factor is also important and when the molecular shape exceeds a certain awkwardness, close-packing

may become problematic leading to the formation of open frameworks, in which a second molecular species is included as a guest to improve packing efficiency [4.6].

The molecule, *trans*-1,5-dichloro-9,10-diethynyl-9,10-dihydroanthracene-9,10-diol (15DDDA) that we had discussed briefly in the previous chapter has a molecular inversion centre, does not occupy this site symmetry in the crystal. Although the space group is centrosymmetric ($P2_1/n$), the symmetrical molecule lies on a general position in the unit cell. However, in the crystal structures of different solvates of 15DDDA, the molecule is able to occupy an ***i*** site and form strong and linear O–H…O, O–H…N, N–H…O hydrogen bonds with the solvent molecules. These solvents are divided into two different categories: (a) dipolar aprotic solvents (DMSO, NMP, Pyrrolidinone, HMPA, DMF) and (b) amine solvents (1˚, 2˚ and 3˚ amines). This sufficiently uncommon occurrence is discussed in detail in this chapter.

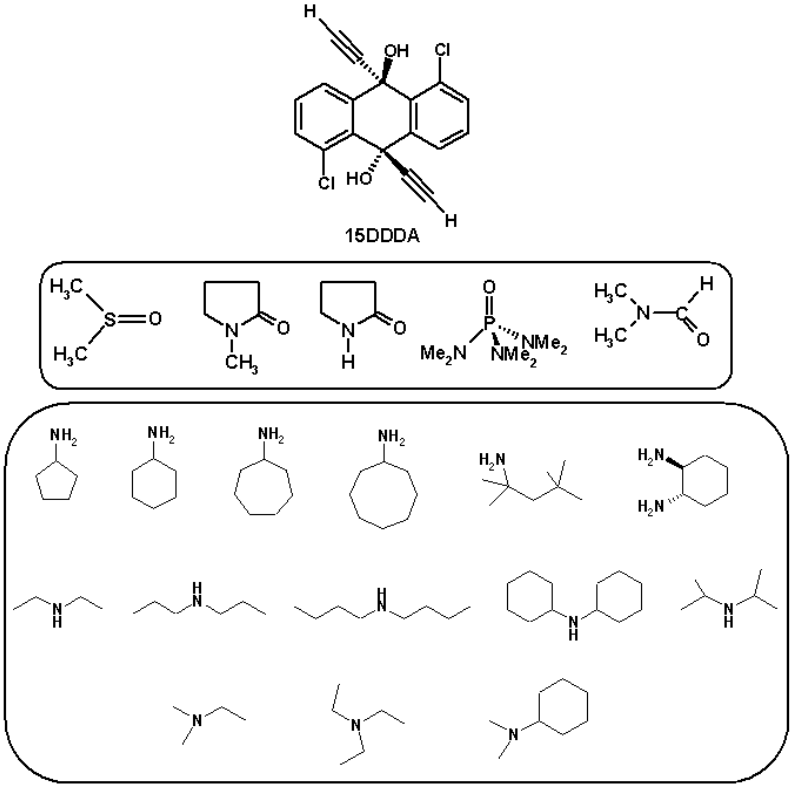

Scheme 1. Various pseudopolymorphs of 15DDDA discussed in this chapter.

4.2 *CSDSymmetry*. A relational database

The Cambridge Structural Database (CSD) [1.18] may be used as a unique source of information about relationships between molecular and crystallographic symmetry. Motherwell and coworkers have applied a molecular-symmetry perception algorithm to approximately 200000 molecules retrieved from the CSD. The resulting data, together with crystallographic properties such as space group, symmetry of occupied Wyckoff positions and Z', have been collected and entered into a relational database, *CSDSymmetry* [4.7]. Queries may be posed to this database to obtain information on relationships between molecular and crystal symmetry. It was found that 18008 molecules belong to point groups containing the symmetry element ***i***. Of these, 17152 molecules (95.2%) crystallize in space groups containing a Wyckoff position of symmetry ***i***, and of these 15156 molecules (88.4%) lie on a crystallographic inversion centre. Additionally, if the molecule contains ***i*** as the *only* molecular symmetry element (like 15DDDA), 99% of such molecules lie on an inversion centre in the crystal [4.8]. These numbers indicate that the behaviour of 15DDDA is not unique but it is certainly unusual.

4.3 Molecular and supramolecular symmetry

15DDDA is one among the 144 published crystal structures in the *gem*-alkynol family [1.34]. Combination of two hydrogen bond donors (O–**H**, C–**H**) and two acceptors (**O**–H, **C≡C**–H) in close proximity and in a sterically hindered situation, makes the four possible interactions O–H…O, C–H…O, O–H…π and C–H… π competitive. The unusually high levels of interaction interference that are therefore possible may generate different and unpredictable hydrogen bond networks.

The asymmetric unit of 15DDDA clearly shows that the molecule does not lie on a crystallographic inversion centre (Figure 1). No other symmetrical *gem*-alkynol present in the CSD and/or studied by us displayed such behaviour. An important molecule for comparison is the non-chloro analogue *trans*-9,10-diethynyl-9,10-dihydroanthracene-9,10-diol (DDA), which lies on an inversion centre in space group $P\bar{1}$ (Scheme 2) [1.34d]. Substitution of hydrogen atoms by the –Cl functionality in 15DDDA changes

the geometrical and chemical effects that lead to the crystal packing adopted. This explains that the relationships between molecular and crystal structure are far from regular and that a particular system is amenable to the techniques of crystal engineering to that extent where changes in the molecular structure cause predictable effects in the crystal structure [4.9].

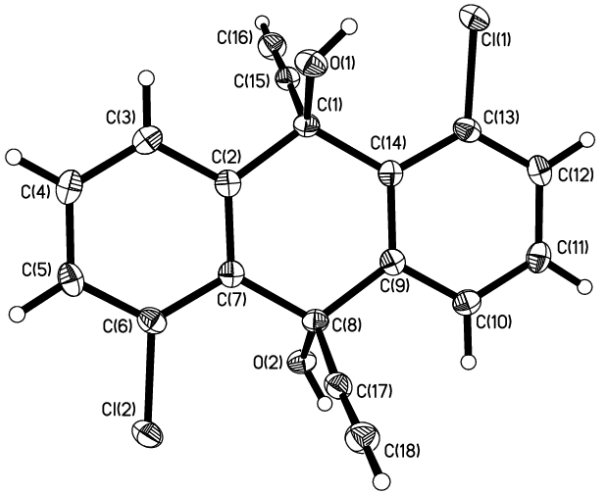

Figure 1. ORTEP drawing of 15DDDA

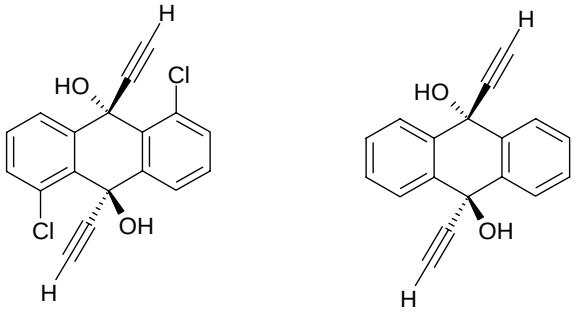

15DDDA DDA

Scheme 2. Schematic drawing of 15DDDA (left) and its non-chloro analogue DDA (right).

4.3.1 Crystal structure of 1,5-dichloro-*trans*-9,10-diethynyl-9,10-dihydroanthracene -9,10-diol (15DDDA)

15DDDA crystallizes in the monoclinic space group $P2_1/n$ with one symmetry independent molecule in the asymmetric unit. 15DDDA contains ***i*** as the *only* molecular symmetry element, yet it fails to occupy the inversion centre in the crystal. This indicates that there should be other compensating factors in the crystal packing that reduce the free energy and stabilize the structure. Hence, the hydrogen bonds and other intermolecular interactions were closely examined. Figure 2 shows the packing diagram of 15DDDA and the two main patterns of interactions present within. There is a cooperative arrangement of three hydrogen bonds, an intermolecular C–H…O from the ethynyl group (*d*, 2.44 Å; *θ*, 164.7°), an intermolecular O–H…O between hydroxy groups (1.83 Å; 173.8°) and a weak intramolecular O–H…Cl–C (2.25 Å; 135.4°) interaction [3.6]. The second distinctive pattern is the supramolecular synthon consisting of four Cl-atoms. This four-atom synthon is built up with two quasi type-II Cl…Cl contacts (3.56 Å) and one type-I Cl…Cl contact (3.64 Å) [4.10]. The local environment of the two hydroxy groups in the molecule is different. One forms an intermolecular O–H…O bond while the other forms an intramolecular O–H…Cl–C bond. A third synthon may be derived from the first in that it is a C–H…O dimer formed between two inversion-related interactions (Figure 2).

4.3.2 Supramolecular synthon and crystal symmetry

Supramolecular synthons may be considered as being equivalent to molecules [1.7]. Supramolecular synthons can be used as modules for close-packing provided they are sufficiently compact. 15DDDA is an example where all the special positions are occupied by synthons rather than the molecules with little loss in close-packing efficiency (C_k 0.716). The four-atom Cl_4 synthons occupy one set of inversion centres and the C–H…O dimer synthons occupy the other set of inversion centres in the structure (Figure 2). It has been noted that crystal symmetry may be analyzed as a convolution of molecular symmetry and supramolecular synthon (or void) symmetry [4.11]. The underlying reason why centrosymmetric molecules tend to lie on inversion

centres in the crystal is that the largest number of atoms are then able to aggregate with the shortest possible separations. Cl_4 synthons and the C–H…O dimer synthons are two densely packed and symmetrical supramolecular synthons that occupy inversion centres in the structure. An example which is similar to 15DDDA, is the equivalence of the crystal structures of $[C(C_6H_4Br)_4]$ and 1:1 molecular complex of tetraphenylmethane and CBr_4. Here the tetrahedral synthon 'Br_4' in $[C(C_6H_4Br)_4]$ may be replaced by the molecular synthon CBr_4 in $[C(C_6H_5)_4{:}CBr_4]$ without any loss of symmetry and therefore leading to an equivalent structure [4.12].

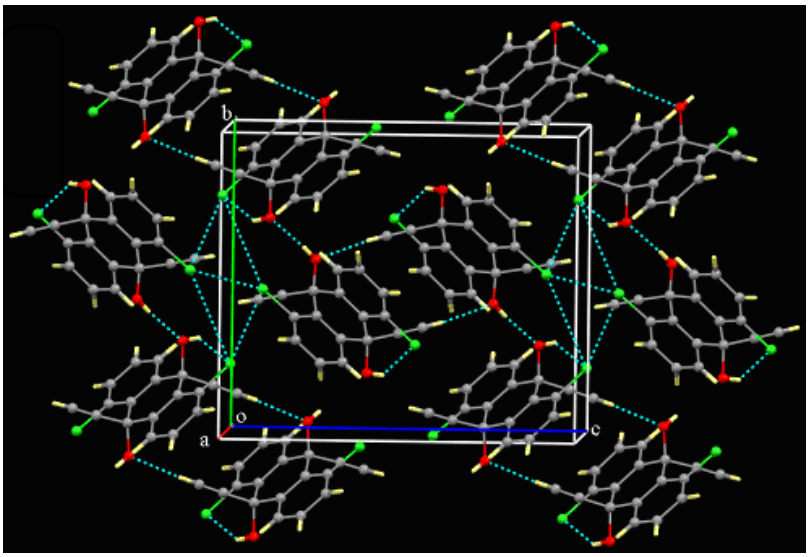

Figure 2. Packing diagram of 15DDDA. Notice the planar Cl_4 synthon (highlighted). C–H...O and O–H...Cl–C hydrogen bridges are also shown.

In most *gem*-alkynols the dominant mode of association is a cooperative chain of O–H…O hydrogen bonds and/or loops of weak and strong hydrogen bonds to give elaborate networks. Chloro substituents in 15DDDA make the already crowded environment of this *gem*-alkynol moiety even more crowded. Therefore, extensive hydrogen bond networks are not possible. In the crystal structure of 15DDDA only one of the two hydroxy groups participates in strong O–H…O hydrogen bonding; the second

one forms a weak intramolecular O–H…Cl–C interaction. One of the two ethynyl groups forms a C–H…O hydrogen bond; the other is completely free. To overcome this situation, the chloro groups assemble into the centrosymmetric Cl_4 synthon. A detailed CSD (Con Quest 1.7 version 5.26, May 2005) search has been carried out for this four-atom cluster. Of the 3517 hits with an aromatic chloro substituent, there are 307 cases of the Cl_4 tetramer. This respectable number shows that this synthon could easily become structure determining.

4.4 Pseudopolymorphism

Polymorphism and pseudopolymorphism offer opportunities to investigate the effects of crystal packing and solvent on the self-organization of hydrogen bonded motifs, leading to supramolecular networks. Polymorphs or pseudopolymorphs usually exhibit different physicochemical properties, which is of essential importance for several practical applications. Pseudopolymorphism is most commonly defined as the existence of different crystalline modifications of a compound, embracing both unsolvated forms and various solvates [1.60]. In general, molecules with unsatisfied hydrogen bonding potential tend to form solvates from solvent with complementary hydrogen bonding capacity. It was highlighted previously that only 15% among all organic crystals are solvates [1.46]. Hydrogen bonding is less than optimum in the crystal structure of 15DDDA and because of this, 15DDDA was crystallized from strongly hydrogen bond accepting solvents (like dipolar aprotic solvents and aliphatic amines) in the search for pseudopolymorphs. Nineteen solvates were obtained in this way and all the solvates provide an excellent demonstration of directed inclusion of small molecular guests (Scheme 1). In all solvates, there are strong O–H…O and O–H…N hydrogen bonds formed by both the hydroxy groups of 15DDDA and the O/N-atom acceptor of the solvent, whereas in the apo-host only one among two hydroxy groups is engaged in O–H…O hydrogen bonding. These strong intermolecular interactions with the solvate molecules justify the hypothesis that the hydrogen bonding in the unsolvated crystal is somehow insufficient or unsatisfactory.

4.4.1 (15DDDA).(DMSO)$_2$

DMSO, DMF and dioxane form solvates very easily because they interact with the solute *via* multi point recognition of strong and weak hydrogen bonding. DMSO has one of the highest tendency for inclusion in crystals because of its small size and good hydrogen bonding ability [4.13]. In the crystal structure, the 15DDDA molecule lies on an inversion centre (space group $P\bar{1}$) and donates strong O–H…O bonds to the S=O groups of DMSO molecules (Figure 3a). This constitutes the centrosymmetric 1:2 solute–solvent module. The dominant hydrogen bond pattern is the centrosymmetric dimer formed by short and linear C–H…O bonds along [100]. The C–H…O bond is from the acidic ethynyl group to the hydroxy group of 15DDDA and is cooperative with the O–H…O bond. Self-association of two DMSO molecules via C–H…O bonds form a dimeric supramolecular synthon (Figure 3b).

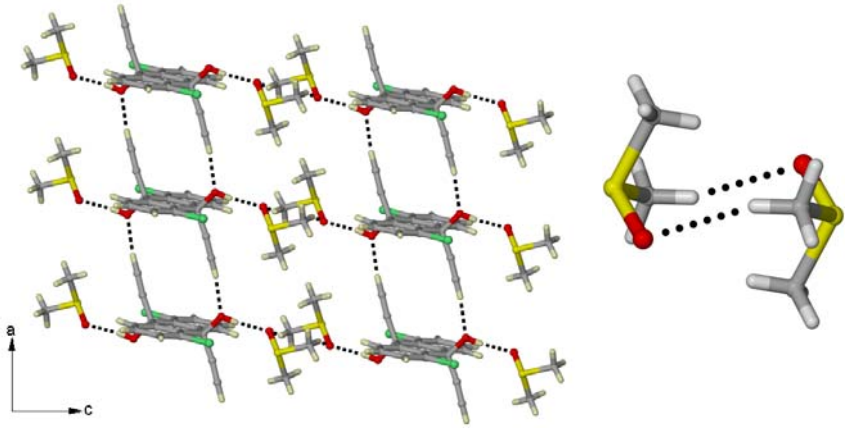

a **b**

Figure 3. (a) Crystal structure of (15DDDA).(DMSO)$_2$. Note the C–H…O and the O–H…O interactions between the solute-solvent modules. (b) C–H…O dimer between two DMSO molecules.

4.4.2 (15DDDA).(DMSO)

(15DDDA).(DMSO) is a variation of the 1:2 solvate. Crystals of (15DDDA).(DMSO) were obtained when 15DDDA was crystallized from a mixture of DMSO and DMF. It crystallizes in the centrosymmetric space group $P\bar{1}$ with two solute molecules (in special positions) and one DMSO molecule in the asymmetric unit. An

'extra' molecule of 15DDDA interleaves between the 1:2 modules via O–H…O bonds to give a host rich structure (Figure 4). The ethynyl groups become 'free' as a consequence. There is a C–H…O–H…O–H…O=S cooperative chain between two solute-solvent modules starting from the activated methyl group of a DMSO.

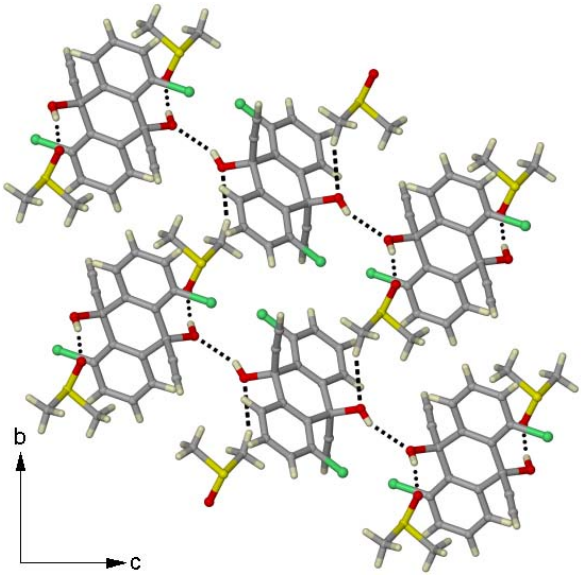

Figure 4. Crystal structure of (15DDDA).(DMSO)$_2$. Note the C–H…O and the O–H…O interactions between the solute-solvent modules.

4.4.3 (15DDDA).(NMP)$_2$

(15DDDA).(NMP)$_2$ crystallizes in the centrosymmetric space group $P\bar{1}$. The 1:2 solute-solvent module is again found on an inversion centre and these modules are connected to each other via C–H…Cl–C bonds. As in (15DDDA).(DMSO)$_2$, the host and guest domains are distinct. Like other solvates, 15DDDA donates strong O–H…O bonds to the C=O groups of two NMP molecules (Figure 5a). Self-association of two NMP molecules via C–H…O bonds form a dimeric supramolecular synthon.

4.4.4 (15DDDA).(pyrrolidinone)$_2$

(15DDDA).(pyrrolidinone)$_2$ crystallizes in the centrosymmetric space group $P\bar{1}$. The 15DDDA molecule occupies an inversion centre and these 1:2 solute–solvent

modules are connected to each other via the N–H…O and O–H…O tetramer synthon. 15DDDA molecules interact with the pyrrolidinone molecules via strong O–H…O bonds (Figure 5b).

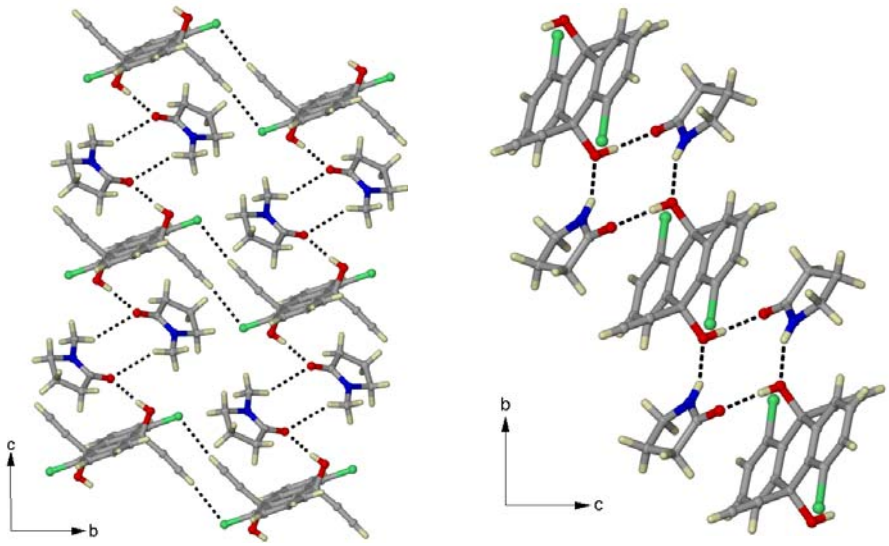

a **b**

Figure 5. (a) Crystal structure of (15DDDA).$(NMP)_2$. Note the C–H…Cl–C interaction between two 15DDDA molecules. (b) Crystal structure of (15DDDA).$(pyrrolidinone)_2$. Note the solute-solvent modules are connected by N–H…O and O–H…O hydrogen bonds.

4.4.5 (15DDDA).$(HMPA)_2$

In this structure too, the 1:2 solute–solvent module is found and these modules are connected to each other via C–H…Cl–C bonds. Like other solvates, there are strong O–H…O bonds between 1:2 solute–solvent modules (Figure 6a). The structure is triclinic (space group $P\bar{1}$) and centrosymmetric, and from a packing viewpoint, it is hardly distinguishable from the 1:2 solvate with NMP.

4.4.6 (15DDDA).$(DMF)_2$

(15DDDA).$(DMF)_2$ crystallizes in the non-centrosymmetric space group $P2_1$. The structure is pseudo-centrosymmetric [4.14], and the 1:2 module is a recurring theme.

As in (DDDA).$(DMSO)_2$ the modules are linked with C–H…O bonds to form a criss-cross arrangement in which solute and solvent domains are integrated (Figure 6b).

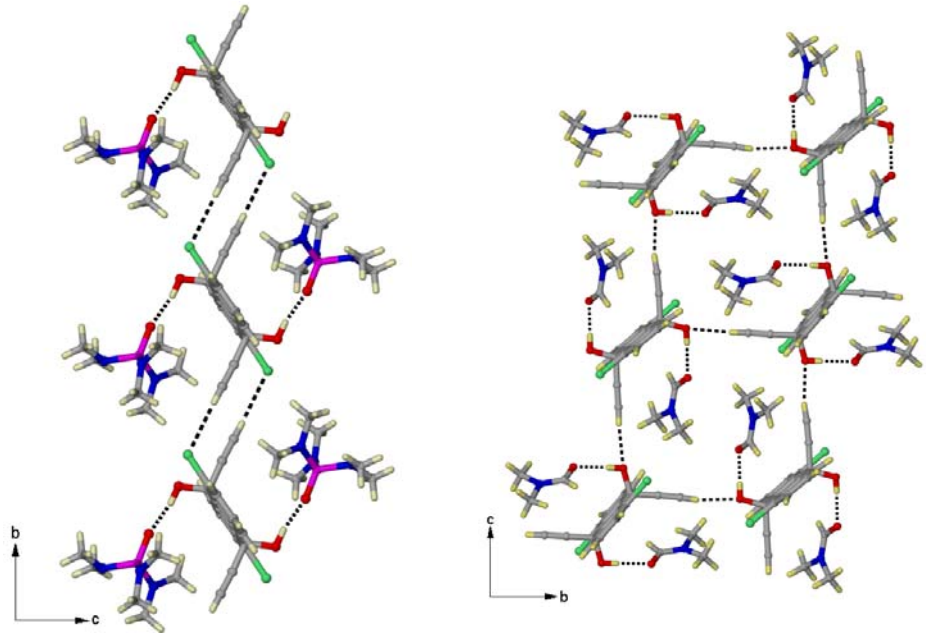

a **b**

Figure 6. (a) Crystal structure of (15DDDA).$(HMPA)_2$. Note the C–H…Cl–C interaction between two15DDDA molecules. (b) Crystal structure of (15DDDA).$(DMF)_2$. Note the C–H…Cl–C interaction between two 15DDDA molecules.

Table 1. Geometrical parameters of H-bridges of the crystal structures in this study.

Compound	H-bridge	*d*/Å (H…A)	*D*/Å (X…A)	*θ*/deg ∠X–H…A
(15DDDA).(DMSO)	O–H…O	1.76	2.733(2)	169.5
	O–H…O	1.96	2.853(2)	149.8
	C–H…O	2.32	3.258(2)	142.9
	C–H…O	2.45	3.491(2)	159.1
(15DDDA).$(DMSO)_2$	O–H…O	1.71	2.682(2)	172.4
	C–H…O	2.14	3.184(2)	163.9
	C–H…O	2.42	3.538(2)	167.2
(15DDDA).$(pyrrolidinone)_2$	O–H…Cl	2.25	3.025(1)	135.3
	O–H…O	1.83	2.814(2)	173.8

	C–H…O	2.44	3.501(1)	164.7
	C–H…O	2.22	3.021(1)	160.5
(15DDDA).(NMP)$_2$	O–H…O	1.74	2.726(2)	172.4
	C–H…O	2.45	3.443(2)	150.9
	C–H…O	2.41	3.277(2)	135.3
	C–H…Cl	2.67	3.752(1)	172.4
(15DDDA).(HMPA)$_2$	O–H…O	1.71	2.667(4)	161.4
	O–H…O	1.70	2.667(4)	165.9
	C–H…O	2.36	3.343(5)	149.9
	C–H…O	2.27	3.274(5)	153.2
	C–H…Cl	2.62	3.706(6)	176.1
(15DDDA).(DMF)$_2$	O–H…O	1.70	2.689(5)	176.1
	O–H…O	1.71	2.695(4)	173.8
	C–H…O	2.19	3.227(5)	159.3
	C–H…O	2.30	3.312(5)	154.3

[a] O–H and C–H distances are neutron normalized to 0.983 and 1.083 Å.

4.4.7 Competition experiment

These six crystal structures show that the presence of a dipolar aprotic solvent allows for better hydrogen bonding by 15DDDA. In every case except one, a 1:2 solute–solvent module is seen, mediated by strong O–H…O hydrogen bonds. This 1:2 solute–solvent module lies on an inversion centre (or a pseudo-inversion centre) and any packing deficiencies that might be present in the unsolvated 15DDDA are seemingly avoided. To complete the study, a competition experiment was carried out in which 15DDDA was crystallised from solvent mixtures. The mixtures selected were DMSO+DMF, DMSO+HMPA, DMSO+pyrrolidinone, HMPA+DMF, NMP+pyrrolidinone, NMP+HMPA and NMP+DMF. In each experiment, several crystals were selected (>6) and examined on the diffractometer. In every case, only a single pseudopolymorph was obtained. These were the 1:2 solvates with, respectively, DMSO, DMSO, DMSO, HMPA, pyrrolidinone, NMP and NMP. Accordingly, one can conclude that the preference for solvent inclusion in this system is in the following order: DMSO>Pyrrolidinone>NMP>HMPA>DMF. This order may be rationalized on the basis of the size of the solvent molecule and its hydrogen bond acceptor ability (Table 2).

Generally, a smaller solvent molecule with a greater acceptor ability is included more easily and the hydrogen bonds formed are correspondingly better.

Table 2. A comparison of the six solvates with regard to selected solvent properties

Solvent	Host/Guest ratio	Space group	C_K	Solvent surface Area Å^2/u.c	Solvent volume Å^3/u.c	Acceptor strength	
						Electrostatic	Mulliken
DMSO	1:1	$P\bar{1}$	73.0	101.04	72.05	–0.521	–0.784
DMSO	1:2	$P\bar{1}$	70.6	101.04	72.05	–0.521	–0.784
Pyrrolidinone	1:2	$P\bar{1}$	71.2	105.83	79.89	–0.642	–0.638
NMP	1:2	$P\bar{1}$	70.2	134.45	102.72	–0.622	–0.620
HMPA	1:2	$P\bar{1}$	68.7	221.53	179.35	–0.702	–0.579
DMF	1:2	$P2_1$ ($P2_1/n$)	72.5	108.40	78.65	–0.553	–0.579

4.5 Structural Studies of amine pseudopolymorphs of 15DDDA

15DDDA occupies an ***i*** site in all six solvates discussed so far and forms strong and linear O–H…O hydrogen bonds with solvent molecules. Amines were selected for theses studies for two reasons. Firstly, the hydrogen bond acceptor capability of amines would promote solvation effectively. Secondly, even though 15% of entries in CSD are solvates, only a few of them contain amine as solvent. As a part of the ongoing projects in crystal engineering, hydrogen bond patterns of hydroxy (–OH), amine (–NH_2) and alkyne (–C≡C–H) functionalities in two distinct families of compounds, viz. supraminols (amine-hydroxy) [1.35b] and *gem*-alkynols (ethynyl-hydroxy) [1.34], were analysed. Notwithstanding this, the structural interplay among all these three functional groups together has not been studied so far. Therefore this work should be considered in the background of a better understanding of hydrogen bonding. In this sense, this particular series justifies the strategy of using amines not simply as solvents but as an essential 'component' molecule for the competitive study of the interplay of strong and weak hydrogen bonding among the hydroxy (–OH), amine (–NH_2) and alkyne (–C≡C–H) functionalities. Amine solvates are subdivided in three groups, based on the number of donor amine hydrogen atom(s) available: (a) primary, 1˚ (b) secondary, 2˚ and (c)

tertiary, 3˚ amine solvates. Amines with variable donor protons have been used to understand the importance of the number of donor amine hydrogen atom(s) towards synthon selection and overall packing.

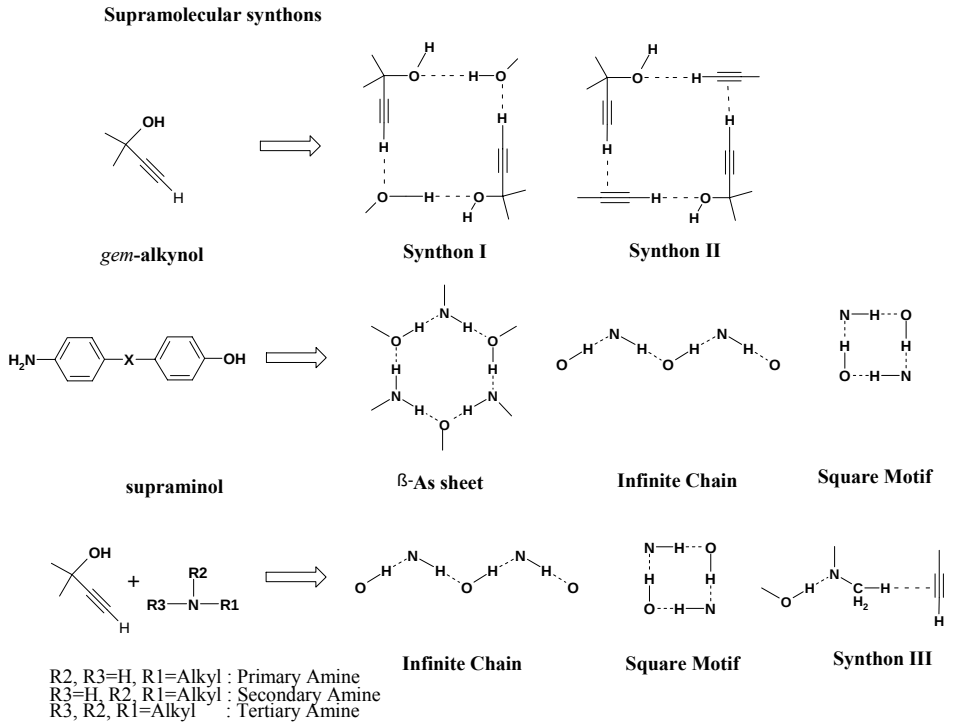

Scheme 3. Supramolecular synthons in 15DDDA: amine pseudopolymorphs.

4.5.1 15DDDA.(1˚ amine)

Three different types of 1˚ amines were used, cyclic, acyclic and cyclic diamines. Cyclopentylamine, cyclohexylamine, cycloheptylamine, and cyclooctylamine are among the cyclic amines. 1,1,3,3-Tetramethyl-butylamine (acyclic amine) and *trans*-1,2 diaminocyclohexane (cyclic diamine) were used to study the effect of interaction interferences on crystal packing. Crystal structures of 15DDDA.(1˚ amine) show an interesting trend of composite crystal packing of *gem*-alkynols and supraminols. From a supraminol point of view, amine and hydroxyl groups are perfectly complementary to

each other. Recent studies on supraminols show that mutually parallel orientation of the C–O and C–N vector (as in the archetypal 4-aminophenol) is a prerequisite for the complete saturation of hydrogen bond potential and the resultant *β*-As sheet [4.15]. Absence of such linearity leads to supramolecular synthons like the infinite chain and square motifs. Structures containing *β*-As network usually lack the 2_1 screw axis, whereas for structures containing only infinite chains, the 2_1 screw axis is quite important. 1° amine solvates containing the infinite chains crystallize in a space group that contains a 2_1 screw axis (like $P2_1/c$). In all 1° amine solvates, 15DDDA molecule occupies an inversion centre, whereas the corresponding amine molecule sits in the general position. This makes C–O (alkynol) and C–N (amine) vectors almost perpendicular to each other, with the smallest probability of forming a *β*-As network. Figure 7 shows the packing diagram of 15DDDA.(cyclopentylamine)$_2$ with an infinite N(H)O chain as a representative case. Interestingly, these infinite chain patterns closely resemble those of supraminols. Here, an ethynyl group takes part in the N–H...π interaction instead of a benzene ring. However, as the solvent becomes bulky, increased steric bulk of the solvent molecule terminates the infinite chain and generates synthon **III** (1,1,3,3-tetramethyl-butylamine) or a N(H)O square synthon (*trans*-1,2 diaminocyclohexane).

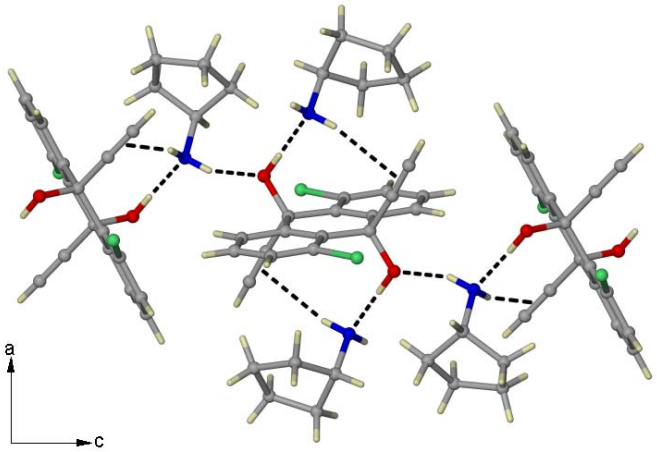

Figure 7. Packing diagram of 15DDDA.(cyclopentylamine)$_2$. Notice the infinite N(H)O chain supported by N–H...π interactions.

4.5.2 15DDDA.(2˚ amine)

The crystal packing of 15DDDA.(2˚amine) pseudopolymorphs should be different from 1˚ amines because the number of amine hydrogen atoms is restricted to one. A strained system like 2˚ amine may not be able to generate an infinite chain, because it needs much more flexibility. Accordingly, five different 2˚ amine solvates were investigated with increasing steric bulk. 15DDDA.(2˚ amine) pseudopolymorphs do not form an infinite N(H)O chain like the 1˚ amine pseudopolymorphs. All the structures except one are based on a four fold arrangement of N(H)O square motif. Figure 8 shows the packing diagram of 15DDDA.(diethylamine) with N(H)O square synthon as a representative case.

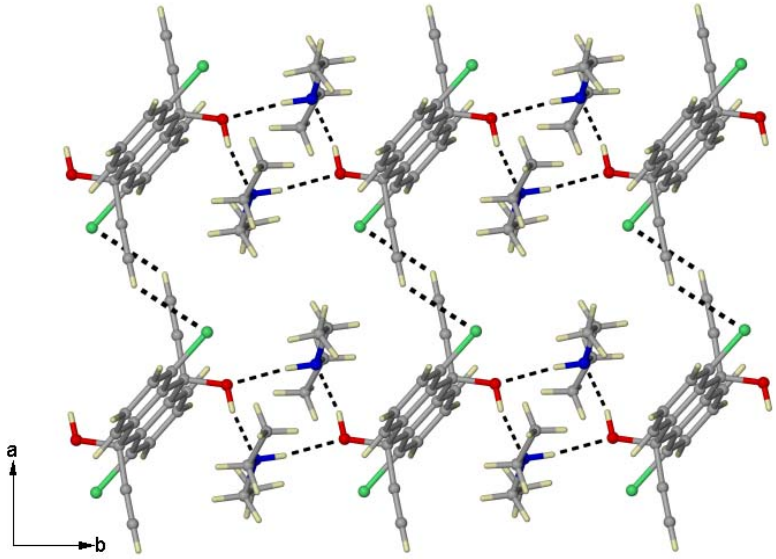

Figure 8. Packing diagram of 15DDDA.(diethylamine)$_2$. Notice the N(H)O tetramer.

4.5.3 15DDDA.(3˚ amine)

Structural analysis of 1˚ and 2˚ amine pseudopolymorphs of 15DDDA show a clear correspondence between the adopted crystal structure and the number of amine hydrogen atoms. It was therefore thought that the 3˚ amines, being devoid of any donor

amine hydrogen atom, should neither form any infinite chains nor square motifs. All the tertiary amine pseudopolymorphs crystallize with a single O–H…N interaction. Figure 9 shows the packing diagram of 15DDDA.(triethylamine)$_2$ as a representative case.

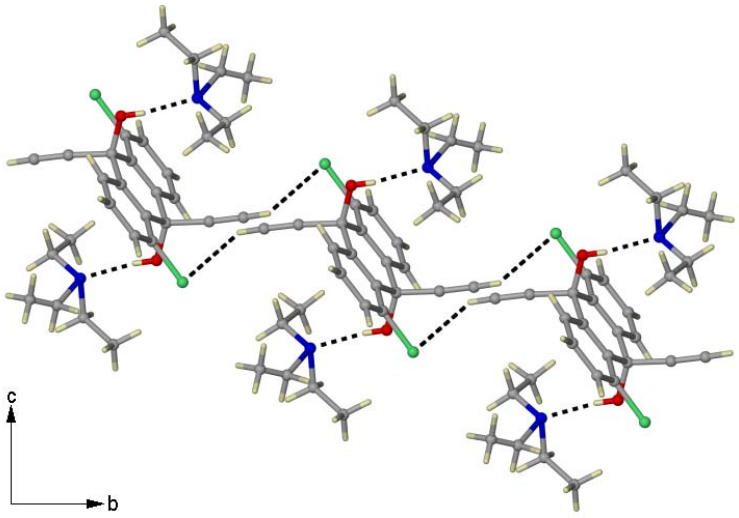

Figure 9. Packing diagram of 15DDDA.(triethylamine)$_2$

4.6 Conclusions

In most crystallizations wherein a single-component ordered crystal is obtained, solvent is expelled from a solute–solvent cluster into the bulk at the time of nucleation, because of the entropic advantage that would accrue. Solvation implies that this entropic gain is more than offset by the enthalpic gain in retaining the solvent in the crystal. This is especially true if the solvent is able to form strong and directional interactions like hydrogen bonding with the solute. So, solvation can also be termed 'interrupted crystallization' [1.45]. We have described the crystal structure of 15DDDA and have noted an unusual occurrence, namely, its presence on a general position in a centrosymmetric space group. This has been ascribed to unsatisfactory hydrogen bonding brought about by steric hindrance of the hydrogen bond donor and acceptor groups in the molecule. Solvates of 15DDDA, in which it can form strong O–H…O and O–H…N hydrogen bonds to the solvent, avoid this problem. In these cases, the 15DDDA

molecule can lie on an inversion (or pseudo-inversion) centre to give a more or less 'normal' structure.

4.7 Experimental section

Synthesis and Crystallization

Synthetic details, IR and ^{1}H NMR spectra of 15DDDA have been given in the experimental section of Chapter 3. Crystals of 15DDDA were grown from 1:1 ethanol/benzene at room temperature. Diffraction quality crystals of all pseudopolymorphs of 15DDDA were prepared by crystallizing 15DDDA from the respective solvents. Special care has been taken to grow the crystals of all amine pseudopolymorphs of 15DDDA. However most of the amines used are either volatile or have low boiling points and the corresponding solvates are mostly unstable. Due to the volatile nature of the amines when the crystals removed from the mother liquor, some of the crystals lose solvent, resulting in polycrystalline or opaque material. In order to overcome this problem, once the crystals were taken out of the sample vial, they were soaked immediately into oil with a high surface tension and mounted on a goniometer using this oil directly into a cold N_2 gas stream at 120K.

X-ray crystallography

The X-ray data 15DDDA and its pseudopolymorphs were collected at the University of Durham, U.K. by Dr. R. Mondal under the supervision of Prof. J. A. K. Howard. The X-ray diffraction were carried out on a Bruker SMART–1000 diffractometer using Mo K_α radiation (λ = 0.71073 Å) [2.7]. The structure solution and refinements were carried out using SHELXTL (Version 5.1) programs [2.8]. Structures of all the compounds were solved by direct methods and refined by full-matrix least squares on F^2. H-atoms were located in all six structures and refined freely with isotropic displacement parameters. The relevant crystallographic information is given in the appendix.

Calculations

All calculations were carried out on Indigo Solid Impact and Indy workstations from Silicon Graphics [2.9]. All interatomic distances and related calculations were carried out with the PLATON programme [2.10].

CHAPTER FIVE

CONFORMATIONAL PSEUDOPOLYMORPHISM IN *cis*-1,5-DICHLORO-9,10-DIETHYNYL-9,10-DIHYDROANTHACENE-9,10-DIOL

5.1 Introduction

Incorporation of solvent into the lattice of crystalline solids results in the formation of molecular adducts known as solvates [1.49, 1.50]. When the incorporated solvent is water, the solvates are called hydrates [1.53, 1.54]. A different unit cell, often leading to different physical properties, i.e., density, solubility, dissolution rate, and bioavailability, results with solvate formation. These physical property changes are similar to those related with polymorphism [1.61], and therefore, solvates are often referred to as pseudopolymorphs to distinguish them from polymorphs [1.60]. Pseudopolymorphism is commonly defined as the existence of structurally different crystalline modifications of a host compound, which embrace both unsolvated forms and various solvates. Pseudopolymorphs can also be considered as polymorphic modifications of the host component that are stabilized by the presence of a templating guest. Some hosts persistently form the same architecture with a wide range of guests [1.59], while others may exhibit a number of inclusion architectures to accommodate different guests [5.1]. In addition, there are examples where the same host forms two/more crystalline forms with the same guest [5.2]. Some pseudopolymorphs even have the same composition but different crystal structures [5.3].

Pseudopolymorphism is a common phenomenon in pharmaceutical and biological molecules [1.60]. Recently, the existence of pseudopolymorphism in a number of organic compounds has been reported. Multipoint recognition involving strong (O–H…O, O–H…N, N–H…O) and weak (C–H…O) hydrogen bonds exist between the solvent and the solute molecules; therefore, solvent molecules are retained and integrated in the crystal lattice. The phenomenon of pseudopolymorphism highlights the role of solvent control in the organic molecular packing arrangement [1.49]. In order to obtain different polymorphs of particular compounds, crystallization from solutions in various

solvents, at different temperatures, pressures and concentrations are used. A similar approach should be suitable for searching for the pseudopolymorphs as well.

Conformational pseudopolymorphism may be defined as different structural modifications of the same solute-solvent system that may/may not have the same stoichiometry but differs in the conformation of the solute or the solvent [5.4]. There are examples where the crystal structures of different solvates of the same solute molecule (host) are different because of the different conformations of the host. More rare is when the crystal lattice of a solute molecule traps a conformationally flexible solvent molecule (guest) in one of its higher energy conformations [5.5]. In none of these cases, however, has a solvate with the solvent in a more stable conformation in the same host ever been reported.

In the previous chapter pseudopolymorphism of *trans*-15DDDA was described. This compound posses a remarkable solvate forming ability. In this chapter a unique observation of both gauche and staggered rotamers of diethylamine, **1a** and **1b**, in two distinct 1:1 solvates, **2a** and **2b**, of the host compound 1,5-dichloro-*cis*-9,10-diethynyl-9,10-dihydroanthracene-9,10-diol (*cis*-15DDDA) is described. These solvates were isolated only after an analysis of the crystal structure of unsolvated *cis*-15DDDA, which is also reported in this chapter (Scheme 1).

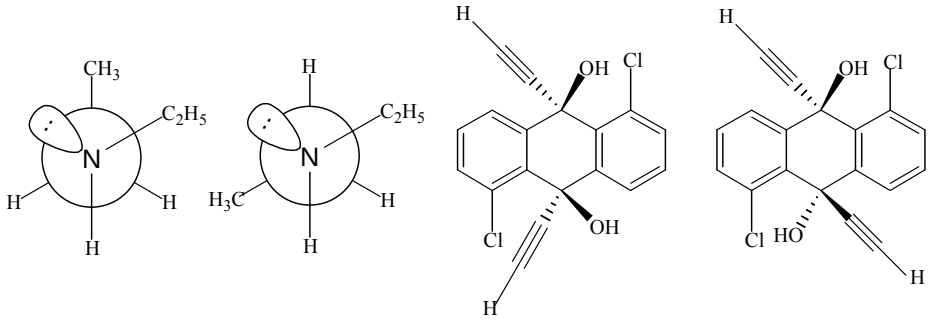

1a **1b** *cis*-15DDDA *trans*-15DDDA

2a = (**1a**).(*cis*-15DDDA) **2b** = (**1b**).(*cis*-15DDDA)

Scheme 1. Schematic drawing of gauche and staggered rotamers of diethylamine.

5.2 Conformational pseudopolymorphism

Different polymorphic modifications of a molecule that possess torsional degrees of freedom and exhibit different molecular conformations are known as conformational polymorphs [5.6]. The differences between the lattice energies of different polymorphic modifications of an organic compound may be expected to be in the range of 1-3 kcal mol^{-1}. Similar conclusions can be drawn for conformational pseudopolymorphs as well, if the solute-solvent stoichiometries of two or more solvates are the same. One should keep in mind that the energetic relationship between two solvates is not so simple because the number of components is more than one. It is not easy to isolate a conformational pseudopolymorph that has conformational variations of the guest molecule at room temperature due to dynamic equilibrium between different conformers. This is so because each solute–solvent cluster will try to achieve maximum enthalpic stability during the final stage of crystallization. Accordingly, the solvent will get trapped in its stable conformation. If at all the solvent molecules get trapped into its higher energy conformation due to other stabilizing factors, most of the conformational pseudopolymorphs should be obtained as concomitant mixtures of crystals.

Conformational pseudopolymorphism has been rarely reported in the literature. Among the very few papers, the work of Glaser et al. on (–) scopolamine hydrobromide/hydrochloride salts [5.4a] and of Muthiah et al. on benzthiazide anhydrate and monohydrate [5.4c] are important. Recently, Howard et al. reported an unusual occurrence of two different conformers of cyclooctylamine in two different pseudopolymorphs of *trans*-15DDDA [1.45c]. In another report, Harris and coworkers described different structural variations of two 1:1 solvates of *p*, *p*'-biphenol/DMSO and mentioned this phenomenon as “true polymorphism among co-crystals” [5.4b]. Matzger et al. have used this term to describe two-dimensional crystallization. According to them, conformationally flexible monolayers of a given compound that differ in conformations and stoichiometry with the surface are conformational pseudopolymorphs [5.4e,f]. Figure 1 gives an overview of different conformational pseudopolymorphs reported till date.

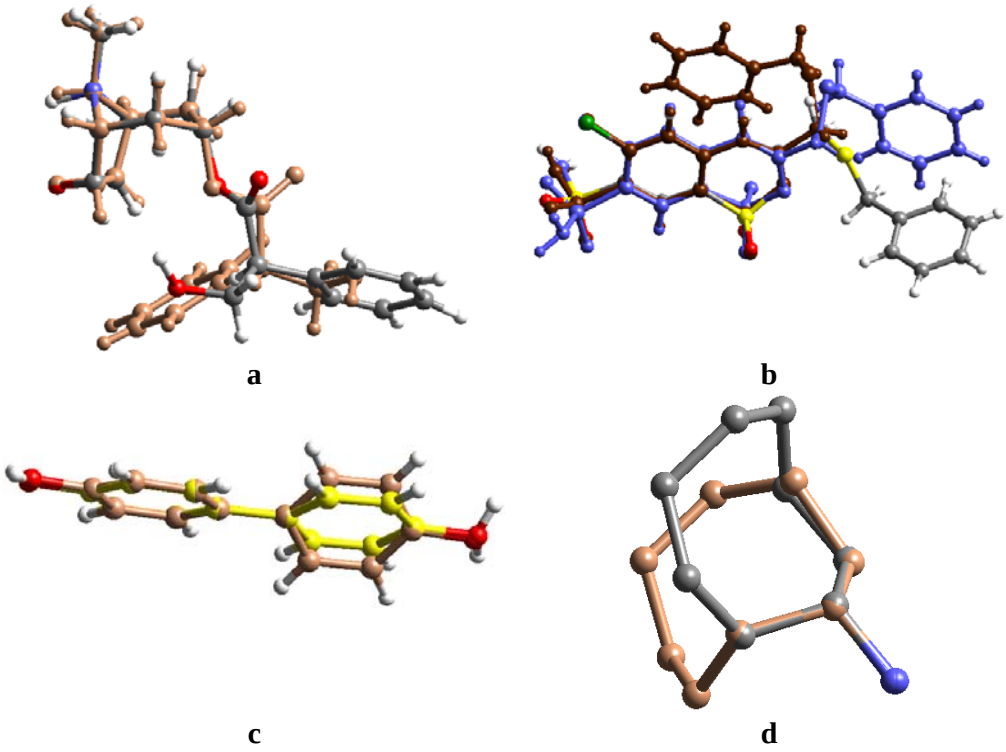

Figure 1. Overlay diagram of conformational variations of (a) Scopolamine molecule in scopolamine hydrobromide anhydrate and sesquihydrate, (b) Benzthiazide in benzthiazide anhydrate and monohydrate, (c) *p,p*'-Biphenol in 1:1 solvates of *p,p*'-Biphenol/DMSO and (d) Cyclooctylamine in (*trans*-15DDDA).(cyclooctylamine) pseudopolymorphs. Hydrogen atoms for the cyclooctylamine have been removed for clarity.

5.3 Crystal structure of 1,5-dichloro-*cis*-9,10-diethynyl-9,10-dihydroanthracene-9,10-diol

1,5-dichloro-*cis*-9,10-diethynyl-9,10-dihydroanthracene-9,10-diol(*cis*-15DDDA) crystallizes in the centrosymmetric space group $P2_1/n$ with one molecule in the asymmetric unit. In *cis*-15DDDA, one of the hydroxyl groups forms an intramolecular O–H…Cl–C hydrogen bridge (*d* 2.32 Å, θ 129°), while the other donates to an intermolecular O–H…π interaction (2.78 Å, 144°; to the triple bond centroid), with some synthon features seen previously (Figure 2) [1.34a]. There is an intermolecular C–H…O–H (2.13 Å, 145°) interaction, which is by far the best interaction in the structure,

and also an intermolecular C–H…Cl–C bridge (3.67 Å, 2.72 Å, 146°). Although this *cis*-diol contains two hydroxyl groups, there is no evidence of an O–H…O hydrogen bond in the crystal structure.

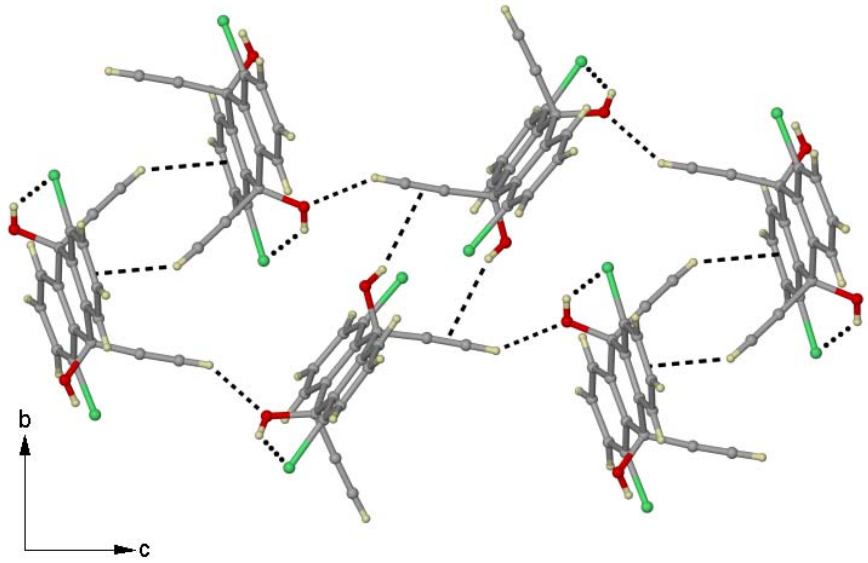

Figure 2. Crystal structure of *cis*-diol **3**. Notice the absence of O–H...O interactions.

5.4 Crystal structures of diethyl amine solvates

It has been noted in chapter 4 that an awkward hydrogen bond pattern of *trans*-diol (*trans*-15DDDA) results from the sterically constrained environment of hydroxyl and ethynyl groups. This uncomfortable pattern can relax via solvation. Noting further that the unusual hydrogen bond pattern in *cis*-diol (*cis*-15DDDA) is reminiscent to that in the *trans*-diol, the crude mixture of isomers was crystallized from diethylamine, since these organic bases have been found to promote solvation very effectively (as described in chapter 4). Crystals with different morphologies, cuboid and plate-like, were obtained. Two different crystals from this batch with clearly different unit cell measurements were found to correspond to the 1:1 solvates **2a** and **2b**. *trans*-15DDDA with diethylamine was also obtained in the same flask and the structure has been described in chapter 4. Interestingly, the hydrogen bonding pattern in the (*trans*-diol).(diethylamine) is quite different from that seen in the crystals of the amine with the *cis* isomer (**2a** and **2b**).

(*trans*-diol).(diethylamine) forms a familiar N(H)O square motif, as seen in the supraminol series [1.26n].

5.4.1 (*cis*-15DDDA).(Et_2NH), 2a

(*cis*-15DDDA).(Et_2NH), **2a** adopts the centrosymmetric space group $P2_1/n$ in the monoclinic crystal system. The asymmetric unit contains one molecule of *cis*-15DDDA and one molecule of diethylamine. The two hydroxyl groups of the solute molecule are hydrogen bonded to the diethylamine solvent and form an infinite cooperative array of O–H…N (1.70 Å, 172.5°), N–H…O (2.19 Å, 166.4°) and O–H…O (1.81 Å, 170.5°) interactions along [010] as shown in Figure 3. In the previous chapter, it has been discussed that, supraminols form infinite N(H)O chains or N(H)O square motifs. Interestingly, there is only one report of O–H…O interactions in the supraminol series [1.26n]. This is the first report of an infinite cooperative array of O–H…N–H…O–H…O hydrogen bonds in an amine hydroxy system where an O–H…O interaction interlinks two O–H…N–H…O synthons.

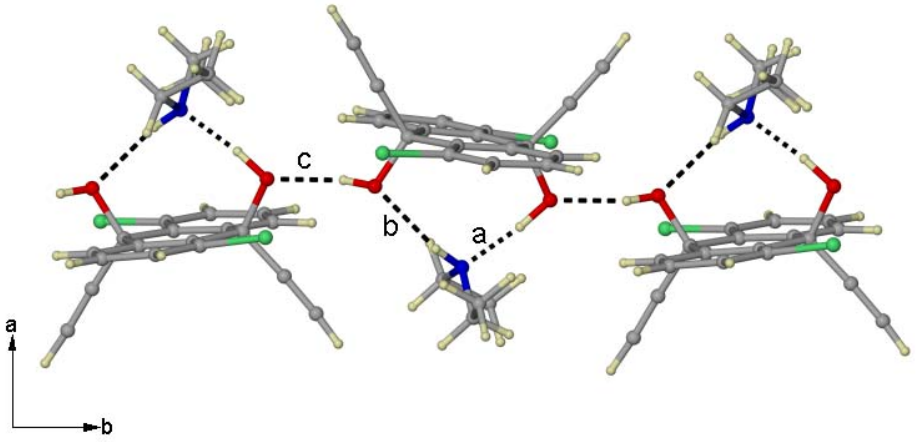

Figure 3. Crystal structure of solvate **2a**. Notice how the solvent enters the space between hydroxyl groups in the same molecule. Notice also the infinite cooperative arrangement of O–H…N–H…O–H…O interactions (**a**, **b**, **c** respectively in the figure) those are formed thereby.

5.4.2 (*cis*-15DDDA).(Et_2NH), 2b

The crystal structure of (*cis*-15DDDA).(Et_2NH), **2b** in the orthorhombic system (space group *Pbca*) also has one symmetry independent *cis*-diol molecule and one diethylamine molecule in the asymmetric unit. Symmetry-independent *cis*-15DDDA and diethylamine molecules constitute the same infinite cooperative array of O–H…N (1.72 Å, 175.5°), N–H…O (2.39 Å, 156.8°) and O–H…O (1.78 Å, 173.9°) hydrogen bonds along [010] (Figure 4).

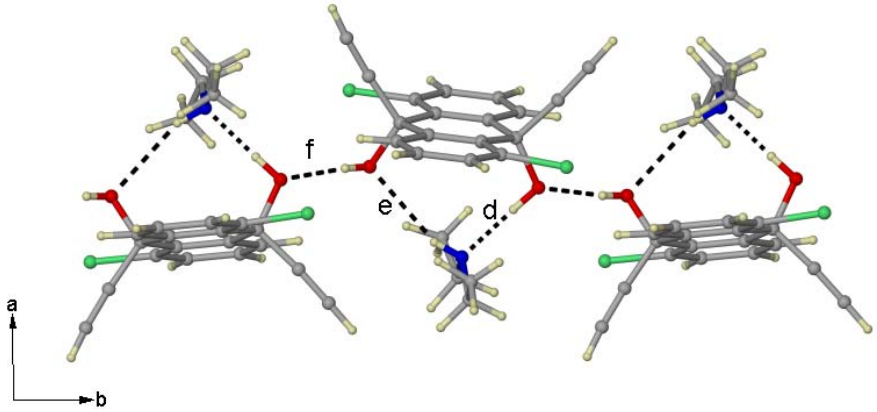

Figure 4. Crystal structure of solvate **2b**. Compare this with Figure 2. The cooperative array is formed with interactions, **d**, **e** and **f**.

Table 1. Geometrical parameters of H-bridges of the crystal structures in this study.

Compound	H-bridge	*d*/Å (H…A)	*D*/Å (X…A)	*θ*/deg ∠X–H…A
(*cis*-15DDDA)	C–H…O	2.13	3.084(3)	144.2
	O–H…Cl	2.32	3.040(2)	128.9
	O–H…π	2.78	3.442	144.1
	C–H…Cl	2.72	3.668(2)	145.9
2a	O–H…O	1.81	2.782(2)	170.5
	O–H…N	1.70	2.677(2)	172.5
	N–H…O	2.19	3.178(2)	166.4
2b	O–H…O	1.78	2.764(3)	173.9
	O–H…N	1.72	2.709(3)	175.5
	N–H…O	2.39	3.350(3)	156.8

[a] O–H, N–H and C–H distances are neutron normalized to 0.983, 1.009 and 1.083 Å.

The role of solvent in improving the hydrogen bond arrangement in *cis*-15DDDA is without doubt. In solvate **2a**, the (gauche) Et_2NH molecule links the intramolecular hydroxyl groups of the diol and there is an infinite cooperative array of O–H…N–H…O–H…O hydrogen bonds. In solvate **2b** too, the (staggered) Et_2NH molecule performs the same function. The cooperative array is topologically the same but the metrics are different. While the O–H…N and O–H…O interactions are comparable in **2a** and **2b**, the N–H…O hydrogen bond is distinctly longer in **2b** (interaction **e** longer than interaction **b**). This lengthening of the N–H…O interaction seems to arise from steric hindrance between one of the ethyl groups of the diethylamine and the aromatic ring of the *cis*-diol (Figure 5). When the methyl fragment in this ethyl group swings away from the ring in the gauche conformation, steric hindrance is reduced and the N–H…O hydrogen bond can become optimally shorter (Figure 5). The solvent being in its most stable staggered conformation compensates the enthalpic loss due to the N–H…O lengthening in **2b**. Alternatively, one can say that a better N–H…O hydrogen bond network, stabilizes the more energetic gauche conformation in solvate **2a**. All other packing features in the two solvates are very similar. The energy difference between two conformers is of the order of ~ 4 kJ mol^{-1} and it is reasonable to equate this energy difference with a difference of around 0.3 Å in an N–H…O hydrogen bond [5.7].

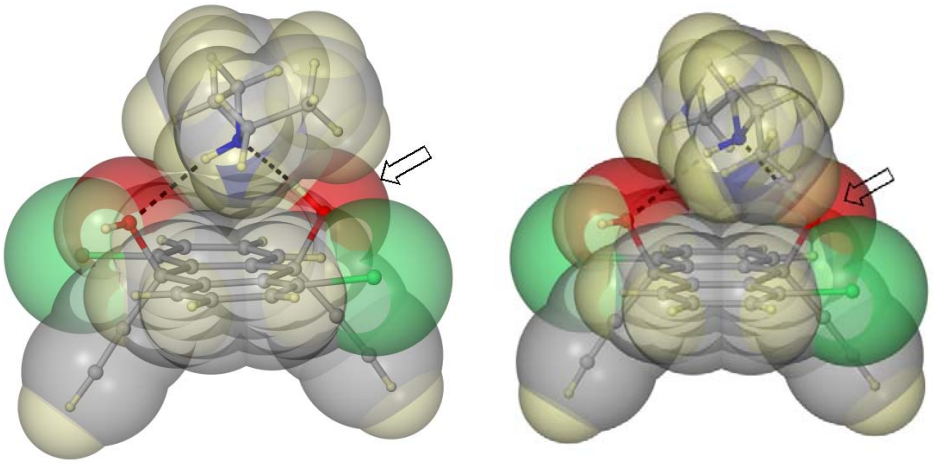

Figure 5. Spacefill model of solute solvent cluster in solvate **2a** (left) and **2b** (right). Note the steric hindrance between one of the ethyl groups of the diethylamine and the aromatic ring of the *cis*-diol (indicated by an arrow) is much relaxed for **2a**.

5.5 CSD Study and computational details

Figure 6 shows the conformations of diethylamine in solvates **2a** and **2b**. The dihedral angle between the two best planes in the gauche and staggered conformers is 70° and 171°. This is the first example of the isolation of the gauche conformer of diethylamine in a pure state. It is easier to isolate the relatively stable staggered conformer rather than the unstable gauche conformer. In all seven diethylamine solvates in the CSD [1.18] (version 5.26, May 2005), the molecule adopts the more stable staggered conformation. The energy difference between the staggered and the gauche conformations was estimated to be 3.26 kJ mol^{-1} (DFT) and 5.06 kJ mol^{-1} (HF). In order to obtain a rationale as to why the two crystal forms were obtained, the packing energies, packing coefficient (C_k) and other computational details of the apo-host and the diethylamine pseudopolymorphs were examined more carefully.

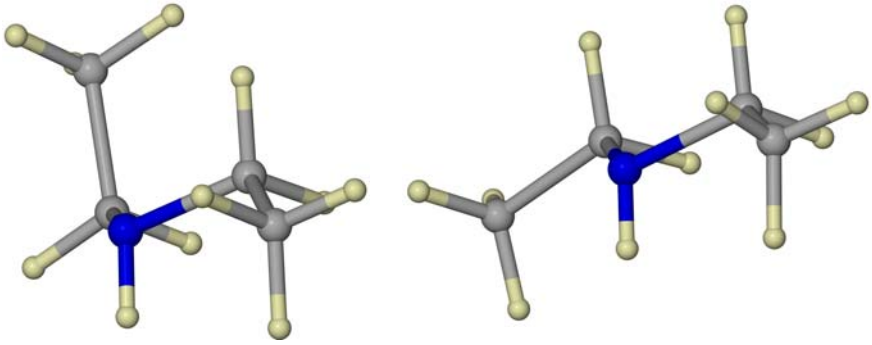

Figure 6. Gauche, **1a**, (left) and staggered, **1b**, (right) conformations of Et_2NH in solvates **2a** and **2b**.

Analysis of all the computational details reveals that the *cis*-diol is energetically unstable than **2a** and **2b** (Table 1). However it should be remembered that these computations are qualitative and one should not draw a conclusion from these as the compositions of *cis*-15DDDA and **2a** and **2b** are different. Energy calculations show that the enthalpic gain in both the solvates are very high due to a better packing and stronger hydrogen bonds.

Table 1. Lattice energies [kcal mol^{-1}] of *cis*-5DDDA and its pseudopolymorphs computed in Cerius^2 by COMPASS (COM) and DREIDING 2.21 (DRE) force fields.

	***cis*-15DDDA**		**2a**		**2b**	
Force field	**COM**	**DRE**	**COM**	**DRE**	**COM**	**DRE**
Total	51.49	51.85	60.49	84.93	57.03	85.19
van der Waals	29.22	28.19	38.01	35.35	39.18	33.93
Coulombic	22.27	19.07	22.34	39.70	17.85	41.49
Hydrogen bond	—	3.95	—	9.87	—	9.76
C_k	69.0		69.9		73.7	

5.6 Confusion in terminology

Recently there has been a considerable debate on the issue of crystal engineering nomenclature [5.8]. Can these solvates also be referred to as pseudopolymorphs? McCrone originally suggested the term pseudopolymorph and it has become standard in the pharmaceutical literature for more than two decades [5.9]. Both Byrn [1.51b] and Bernstein [1.61f] have mentioned this term in their respective books although Bernstein has subsequently maintained that his mention of the term in his book is not equivalent to his endorsing the term. Threlfall mentions several difficulties in its usage [1.61a]. The term seems to suggest that there are at least two structures, the unsolvated and solvated forms with different crystal structures. Since the systems being considered are different chemical entities, the 'polymorphism' is not real but 'pseudo'. On the other hand, it has been argued that a crystal and its solvates are not related by a 'morphic' relationship but by a 'composition' relationship. A compound and its solvate must necessarily have different crystal structures, and since they are not chemically identical, there is no question of polymorphism, pseudo or otherwise.

Desiraju has noted that there are some points that are worthy of mention in this context. Difficulties seem to arise when the term *polymorph* is applied to crystals that contain more than one chemical component [5.10]. Ideally, the term *polymorph* should be restricted to crystals of a single compound. Then it is easier to state if two or more crystal structures are the same or different. In multi-component crystals, there are two structural possibilities. In the first case, one of the components could be inactive in

determining the crystal structure whereas in the other case, the role of the two components in the crystal packing is complementary. In this context, the term *pseudopolymorphism* has virtues that need to be considered on a case-by-case basis. This term brings to attention the fact that certain related multi-component crystals, with the same or different chemical composition, have distinct crystal structures.

In the present case, **2a** and **2b** may be called "polymorphs of a solvate" according to currently proposed definition [5.8e]. But the major features in the packing of the major component are virtually the same. The differences occur in the minor component. Another possibility for **2a** and **2b** is to call them *conformational polymorphs*. But this term is more appropriate when the major component has a different conformation in both forms. However, it will be appropriate to refer **2a** and **2b** as *conformational pseudopolymorphs* of *cis*-15DDDA, given that it is the minor component in these solvates that has the conformational variations.

Presumably, however, there is very little possibility of erasing a word like pseudopolymorph [5.11], which describes a technical phenomenon, from the established literature [5.12] even if the word is not the best choice. There are many such examples in the technical literature that one has to live with. For example the phenomenon of *inclusion compound* is quite similar to the term *host−guest*, in which the main function of the guest molecule is cavity filling, with or without additional weak hydrogen bonding in a host molecule assembly. However, there are more important things to do than having a discussion on words (names) well knowing that the term pseudopolymorph will never disappear completely because of its citation of around 40 years in the scientific field. All we can and should do is to watch that in future things get as clear as possible.

5.7 Conclusions

The constraints of the crystal lattice usually do not trap conformationally flexible molecules into one of the multiple low-energy conformers existing in solution. Efficient molecular packing within the extended array is a very important factor. However, similar two-dimensional and three-dimensional packing in **2a** and **2b** strongly suggests that lattice-packing considerations alone cannot explain the observation of a conformational

variation of diethylamine molecules in these crystals. Still the reason for this particular conformational choice remains unclear although it might involve attractive O–H…N hydrogen bonding and removal of unfavorable H_2C–H…π interactions as noted above.

5.8 Experimental section

Synthesis

Hydroxy ethynylation of 1,5-dichloroanthraquinone (TMSC≡CLi, KOH) gave predominantly the *trans*-isomer (*trans*-15DDDA) with the amount of *cis*-isomer (*cis*-15DDDA) being so small that it could never be separated satisfactorily with chromatography. Synthetic details, IR and ^{1}H NMR spectra of *trans*-15DDDA have been given in the experimental section of Chapter 3.

Crystallization

Isolation of single crystals of **2a**, **2b** and **3** was achieved only with careful experimentation. When the crude product was crystallized from 1:1 acetone–benzene, two different crystal morphologies were obtained, prisms and needles, corresponding to the *cis* and *trans* isomers, respectively. Since diethylamine is a low boiling solvent once the crystals were taken out of the sample vial, they were soaked immediately into oil with a high surface tension and mounted on a goniometer using this oil directly into a cold N_2 gas stream at 120K.

X-ray crystallography

The X-ray data *cis*-15DDDA and its amine pseudopolymorphs were collected at the University of Durham, U.K. by Dr. R. Mondal under the supervision of Prof. J. A. K. Howard. The X-ray diffraction were carried out on a Bruker SMART–1000 diffractometer using Mo K_α radiation (λ = 0.71073 Å) [2.7]. The structure solution and refinements were carried out using SHELXTL (Version 5.1) programs [2.8]. Structures of all the compounds were solved by direct methods and refined by full-matrix least squares on F^2. H-atoms were located in all three structures and refined freely with

isotropic displacement parameters. The relevant crystallographic information is given in the appendix.

Calculations

All calculations were carried out on Indigo Solid Impact and Indy workstations from Silicon Graphics [2.9]. Lattice energy calculations are corrected to per molecule. All interatomic distances and related calculations were carried out with the PLATON programme [2.10].

CHAPTER SIX

PSEUDOPOLYMORPHISM IN SILDENAFIL SACCHARINATE. A NEW HOST MATERIAL

6.1 Introduction

A solvate is defined as a solid adduct in which solvent molecules are incorporated into the crystal lattice [1.50]. The incorporated solvent is often termed as *guest* and the major component is termed as *host* [1.59]. The presence of solvent molecules in the crystal lattice confers unique physical properties to solvates [1.62]. For example, the solubility and dissolution rate of a hydrate are different from those of the corresponding anhydrate and can result in a difference in the bioavailability of a drug. In some solvates, the solvent molecules act as space fillers, whereas in others the solvent molecules become essential components of the lattice by interacting with the host molecules with specific intermolecular interactions such as hydrogen bonds. The majority of drugs are administered as solids. This means that apart from the molecular structure of the API, solid-state properties significantly influence the performance of the final product [1.61]. Solvation has a huge commercial and practical impact on APIs at all stages of development. Identifying all the relevant solvates/pseudopolymorphs at an early stage of drug development is therefore crucial [1.60].

Certain molecular shapes and intermolecular interactions favour the formation of solvated crystals. The ease of formation and subsequent stabilization of a solvate depend on its crystal structure and that of the unsolvated host. A solvate is stabilized when the incorporated solvent molecule either improves the packing or strengthens the intermolecular interactions in the crystal. Many of the early examples of host lattices were discovered by chance. These include urea inclusion compounds, β-hydroquinone clathrates, trimesic acid, the hydrogen-bonded hexamer of phenol, hydroquinone and Dianin's compound [1.59]. Weber proposed rules for the design of new host frameworks based on an examination of several host–guest systems [6.1]. According to him, a typical host molecule should have four characteristics: (1) bulky in constitution and awkward shape; (2) rigid structure to maintain the cavity so that it does not collapse to a close-

packed structure; (3) high affinity functional groups like –OH, –COOH, –CONH2, for specific and directional hydrogen bonding and; (4) an overall balanced shape so that the host–guest crystal can achieve maximized close packing. Desiraju suggested that crystal engineering principles can be applied for the design of host lattices by a consideration of molecular and crystal symmetry and supramolecular synthon concept and the phenomenon of solvation in crystals (pseudopolymorphism) [1.4a].

This chapter describes the crystal structures of 12 solvates of the saccharin salt of sildenafil, which is an anti-impotency drug. Sildenafil citrate is used to treat male erectile dysfunction under the trade name Viagra [6.2]. Although this block-bluster drug was in the news for several years, relatively little work has been done on its structural aspects except for a recent report on sildenafil citrate dihydrate [6.3]. While studying the crystallization of sildenafil saccharinate from different solvents, solvates with the following solvents were obtained: acetonitrile, dimethylformamide, dimethylsulfoxide, 1,4-dioxane, ethanol, ethylene glycol, formamide, methanol, nitromethane, pyrrolidinone, tetrahydrofuran and water. One of the N-atoms of the piperazine ring, to which is attached the methyl group, is protonated and the saccharinate molecule exists as an anion. Several C–H…O hydrogen bonds, between the $(\text{sildenafil})^{+}$ cation and $(\text{saccharin})^{-}$ anion stabilize the host lattice. All the inclusion complexes, except methanol, are isostructural [6.4] and are mediated by various host–guest C–H…O or O–H…O interactions. Guest atoms are disordered in some solvates. Scheme 1 shows the lists of solvents. Complete crystallographic information of all these solvates are provided in the appendix.

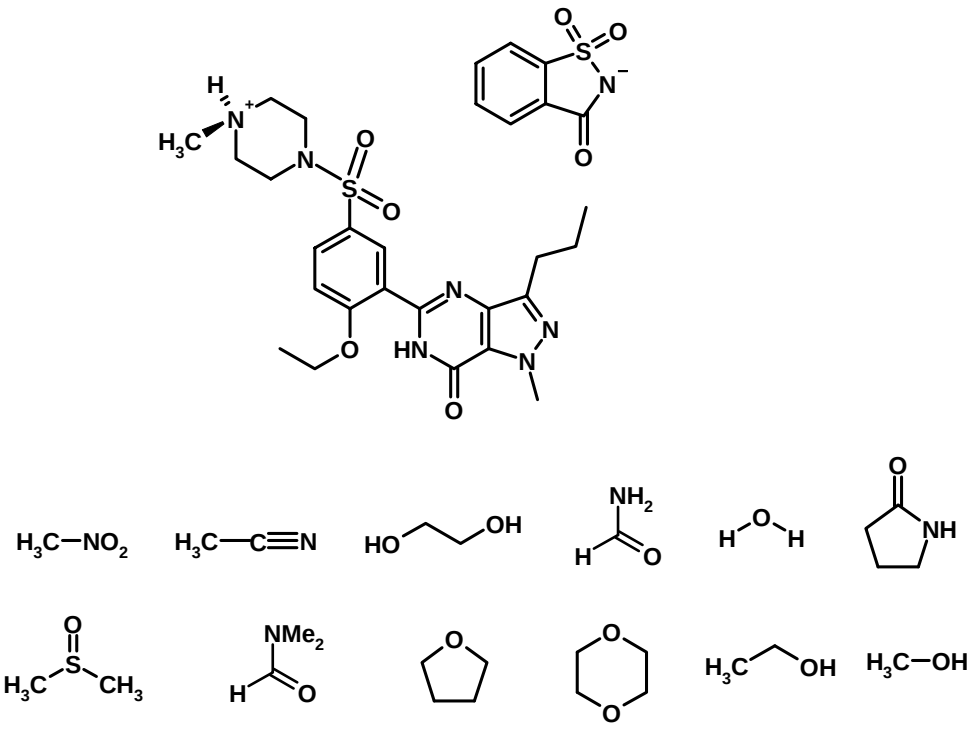

Scheme 1. Schematic drawing of sildenafil saccharinate and below lists of all solvents incorporated in the lattice.

6.2 Crystal structure of sildenafil saccharinate apohost

Saccharinate salt of sildenafil was prepared by grinding 1:1 molar proportions of sildenafil and saccharin. Quantitative conversion to the sildenafil saccharinate (**SS**) was achieved when a dry mixture of appropriate quantities of the sildenafil and saccharin were hand ground in a mortar and pestle (typically 50 to 300 mg were ground for time periods ranging from 15 min to 1 h). A good indication for complete **SS** formation is obtained from the bathochromic shift in the C=O stretching frequency (1720 cm^{-1} in saccharin to 1690 cm^{-1} in the salt) of the IR spectrum [6.5]. However, this procedure led to mixtures of crystalline and amorphous forms. X-ray powder diffraction [6.6] patterns indicated that the amorphous content in the sample obtained by grinding is considerable at room temperature. When this hand ground sample was heated, DSC traces showed that

a crystallization exotherm was observed at 120 ºC. Melting occurs normally at 208 ºC with no further event (Figure 1). The hand ground sample was heated slowly to 150 ºC in an oil bath. The temperature settings of the oil bath were set at T = 60, 90, 120, 150 °C. Approximately, 50 mg of the sample were taken from the flask when the system reached the respective temperature. The material was cooled to room temperature and X-ray data was collected. The X-ray powder patterns showed that the peak profile of **SS** is relatively invariant between 30–90 °C but changes as the sample reaches 120 °C. Figure 2 shows that the overall PXRD pattern became significantly sharper with more intense lines indicating higher crystallinity.

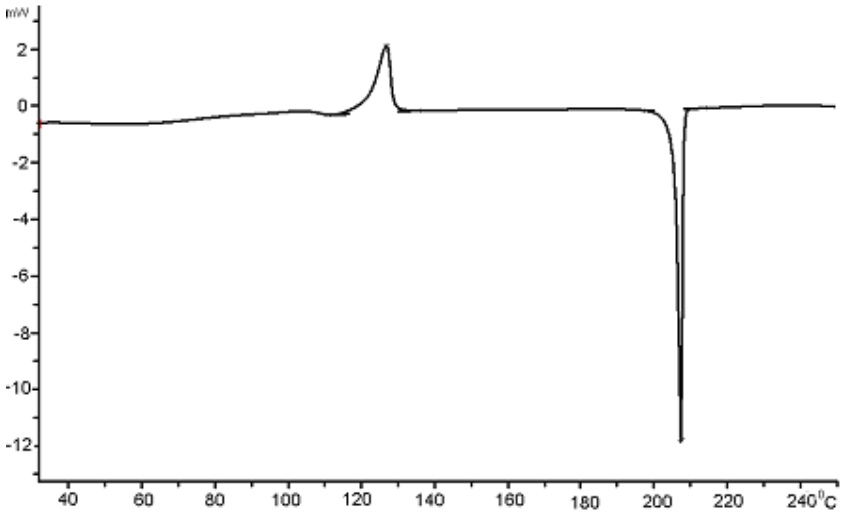

Figure 1. DSC traces of the ground **SS** recorded at a heating rate of 5 °C min^{-1}.Note the exothermic region at 120 °C showing the phase transformation amorphous **SS** → crystalline **SS**.

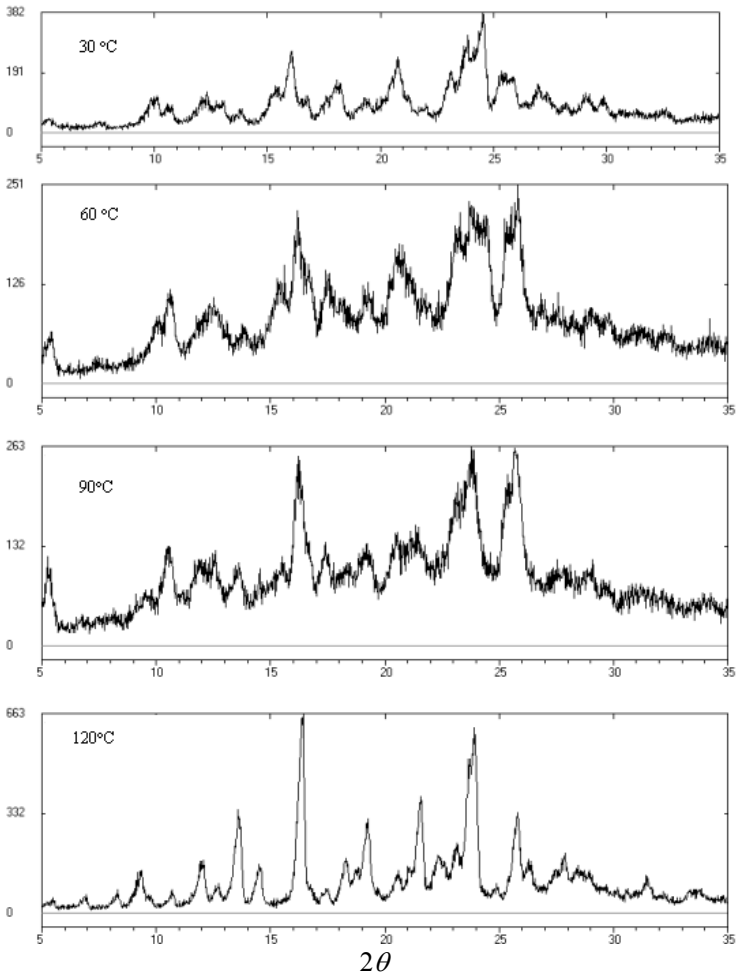

Figure 2. X-ray Powder diffraction patterns of **SS** recorded at different temperatures during the heating experiment. The sample, which is a mixture of amorphous and crystalline forms at room temperature, transforms to crystalline **SS** at ca. 120 °C. Note the increase in intensity of peaks and overall simplification of profile at higher temperature.

Yellow coloured prismatic crystals of **SS** apohost were obtained serendipitously while heating the DMSO solvate of **SS** at 150 ºC. **SS** apohost crystallizes in the centrosymmetric space group $P\bar{1}$ with one $(\text{sildenafil})^{+}$ cation and one $(\text{saccharin})^{-}$ anion in the asymmetric unit. The crystal structure of **SS** apohost contains mainly two types of intermolecular interactions. The first is an $N^{(+)}$–H…$N^{(-)}$ interaction between $N^{(+)}$–H of

$(sildenafil)^{+}$ and $N^{(-)}$ of $(saccharin)^{-}$ that forms a **SS** unit and the other is a strong C–H…O interaction that join these **SS** units. Each **SS** unit forms an fourteen membered supramolecular synthon **I**, consisting of two $N^{(+)}$–H…$N^{(-)}$ and two C–H…O hydrogen bonds between two $(sildenafil)^{+}$ and two $(saccharin)^{-}$ ions (Scheme 2). The second distinctive pattern is a supramolecular synthon **II**, consisting of four C–H…O hydrogen bonds (Scheme 2). Figure 3 shows the packing diagram of **SS** apohost and the two main patterns of interactions present within. In the crystal structure of the apohost, the pyrazolopyrimidone ring system and the benzene ring are almost coplanar, enabling an intramolecular N–H…O hydrogen bond between the pyrazolopyrimidone N–H group and the O-atom of the ethoxy group (Scheme 2).

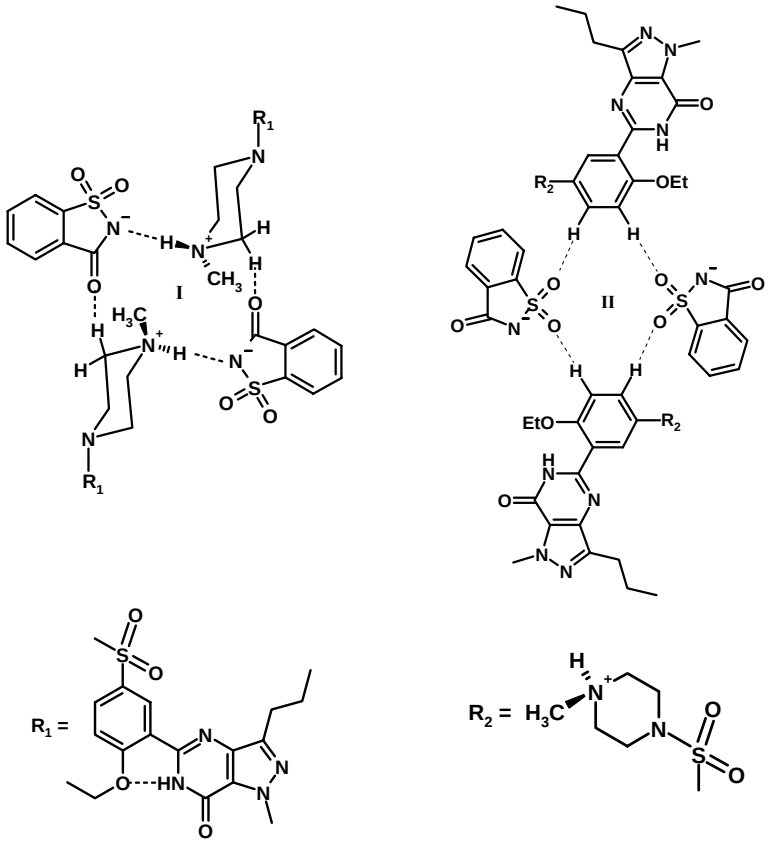

Scheme 2. Supramolecular synthon **I** and **II** in **SS** apohost. Note the intramolecular N–H…O hydrogen bond between the pyrazolopyrimidone N–H group and the O- atom of the ethoxy group.

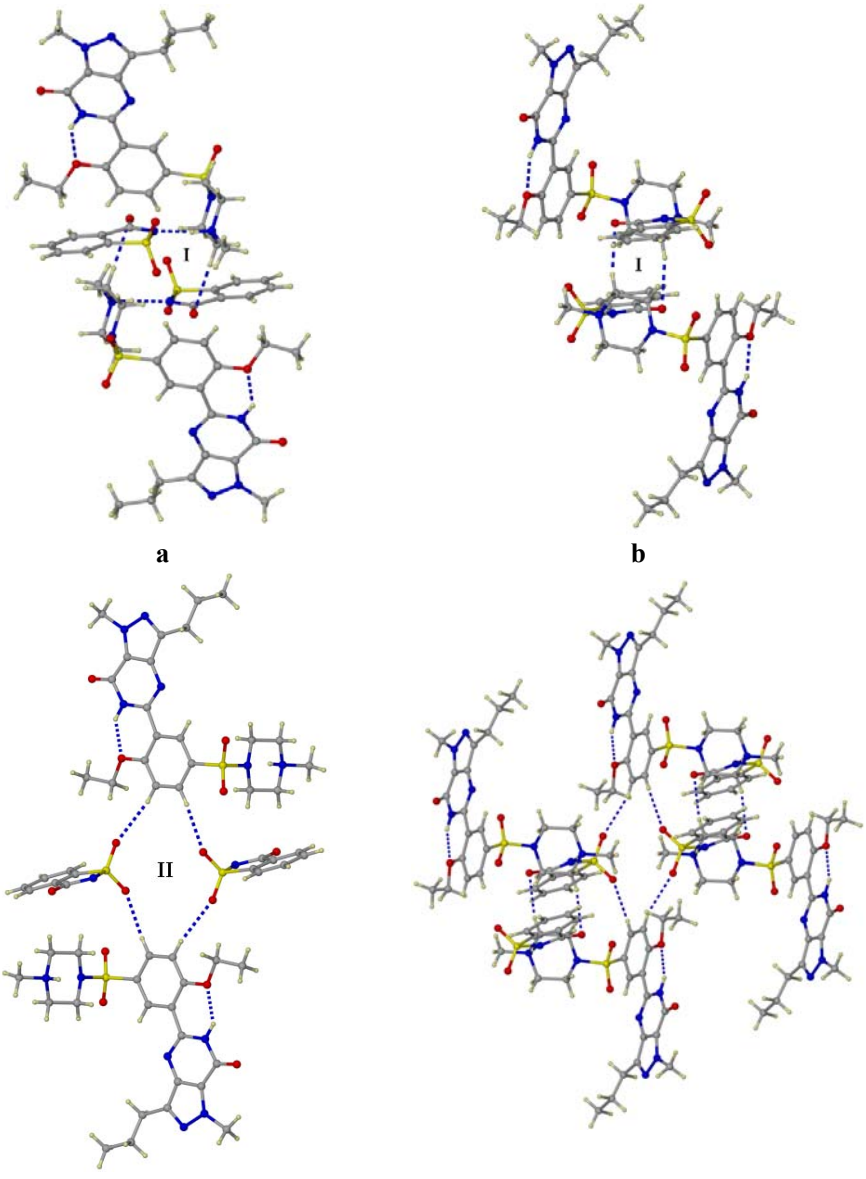

Figure 3. (a) $N^{(+)}$–H…$N^{(-)}$ and C–H…O tetramer synthon **I** in the crystal structure of **SS** apohost, (b) a different view of synthon **I**, (c) fourteen membered supramolecular synthon **II** consisting of four C–H…O interactions and (d) packing diagram of **SS** apohost. Note the intra molecular N–H…O hydrogen bond

Rietveld refinement (R_p = 19.39, R_{wp} = 26.81) of the experimental powder patterns with respect to the simulated peaks [6.7] of the crystal structure confirms that heating amorphous **SS** to a pre-melting temperature of 120 °C transforms amorphous **SS** to > 95% crystalline purity (Figure 4).

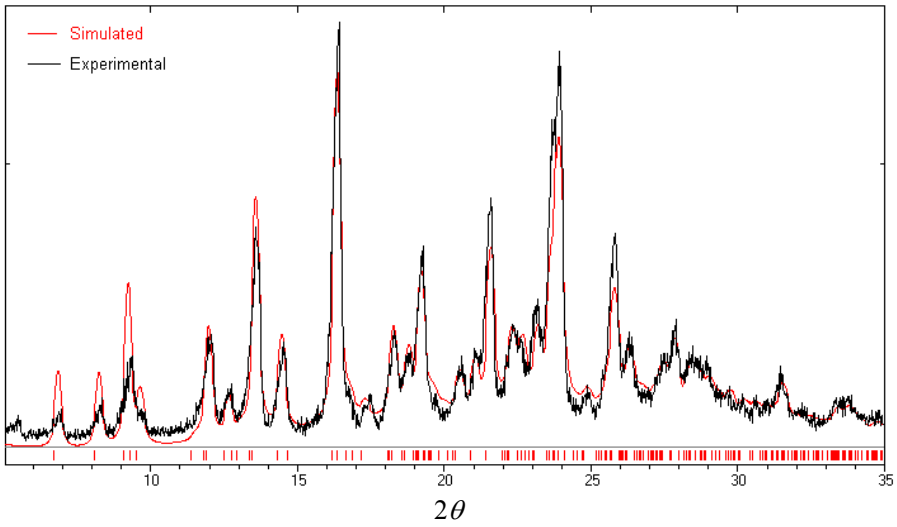

Figure 4. Experimental powder XRD of **SS** apohost at 120 °C (black line) matches with the calculated powder pattern of **SS** apohost (red line). Rietveld refinement in Powder Cell 2.3: R_p = 19.39, R_{wp} = 26.81. The starting solid was a mixture of amorphous and crystalline forms shown in Figure 2.

6.3 Isostructural solvates of SS

SS was crystallized from several solvent molecules of different size, shape and symmetry. Diffraction quality single crystals appeared after one or two days at room temperature, and were characterized by single crystal X-ray diffraction. TGA confirmed the stoichiometry of host and guest, and DSC confirmed the temperature of guest release from the host framework. Host/guest stoichiometry determined from X-ray structure matches with the ratio from weight loss in TGA for all solvates except for the MeOH solvate. All the solvates, with the exception of the methanol solvate, are isostructural with space group $P\bar{1}$ and similar unit cell parameters and similar arrangements of the host molecules in the respective unit cells. Guest atoms are disordered in some solvates.

Guest disorder may be due to the reason that: (1) point group symmetry of the guest is lower than the site symmetry of the void; and/or (2) the guest does not fit tightly enough in the available cavity due to poor host…guest interactions.

In the crystalline saccharinate, two $(sildenafil)^{+}$ and two $(saccharin)^{-}$ ions are connected with $N^{(+)}$–H…$N^{(-)}$ and C–H…O=S hydrogen bonds to form a centrosymmetric tetramer synthon **III** (Scheme 3). In these solvates, synthon **III** is the basic structural unit and is probably the kinetically relevant synthon (Figure 5). Each of these tetramer synthons is connected to the other by two distinct sets of centrosymmetric C–H…O=C hydrogen bonds to form a hexagonal cavity (Figure 6). It would appear that several strong intermolecular C–H…O hydrogen bonds (*d*, 2.23–2.44 Å) stabilize these hexagonal host frameworks. These hexagonal cavities are linked along [100] by short and linear C–H…O bonds (*d*, 2.24 Å; θ, 173.9°) to complete the structure. These C–H…O bonds are from the aromatic C–H of the $(sildenafil)^{+}$ cation to the C=O of $(saccharin)^{-}$ anion. Two of these hexagonal cavities share one common face and propagate in one dimension to generate an independent 1D cage structure (Figure 7). The interaction between two independent 1D cage structures is therefore the interdigitated stacking shown in Figure 7, with a separation of 9 Å. In these cages are located the guest molecules further stabilized by host…guest C–H…O hydrogen bonds.

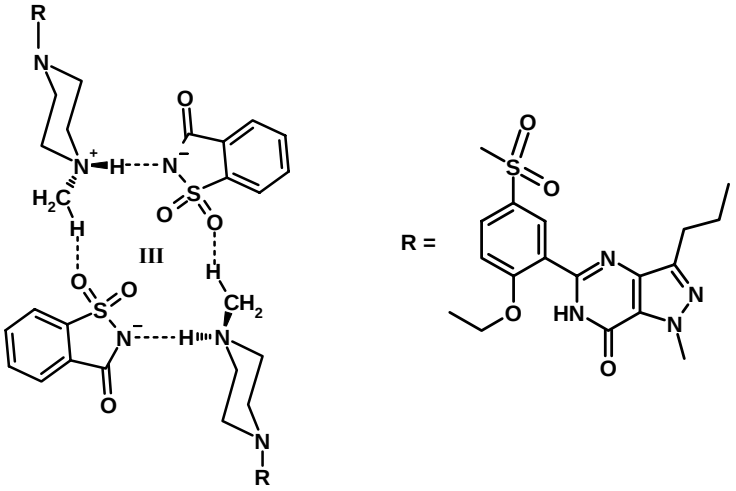

Scheme 3. Supramolecular synthon **III** consisting of $N^{(+)}$–H… $N^{(-)}$ and C–H…O interactions.

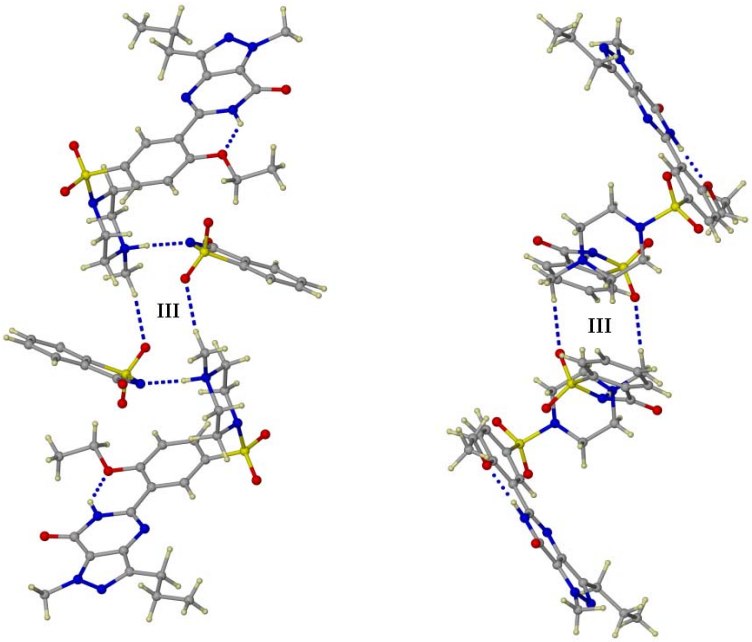

Figure 5. Tetramer synthon **III** consists of $N^{(+)}$–H…$N^{(-)}$ and C–H…O hydrogen bonds in various solvates of **SS**.

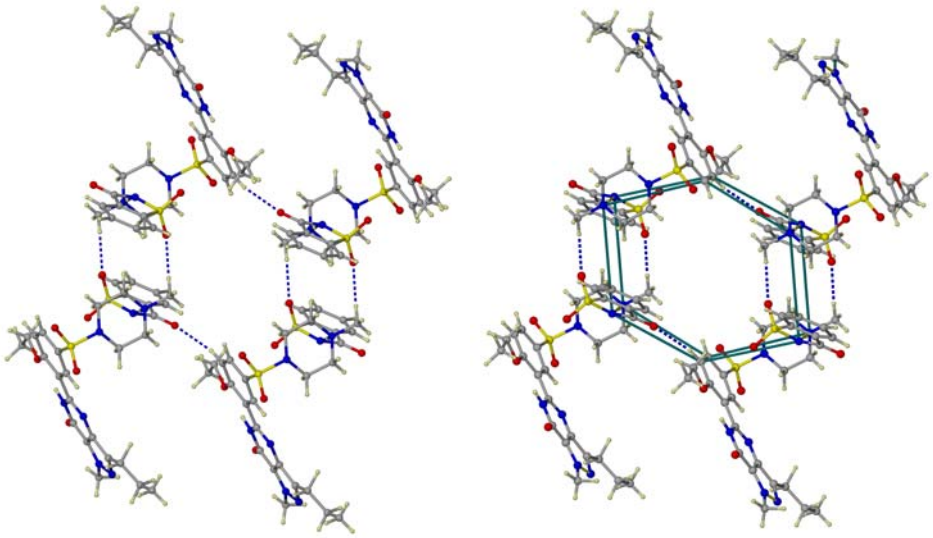

Figure 6. Packing diagram of the host framework in the isostructural solvates of **SS** down [001] to show the hexagonal cavity. Ordered/disordered guest molecules are present at the surface or inside these hexagonal voids.

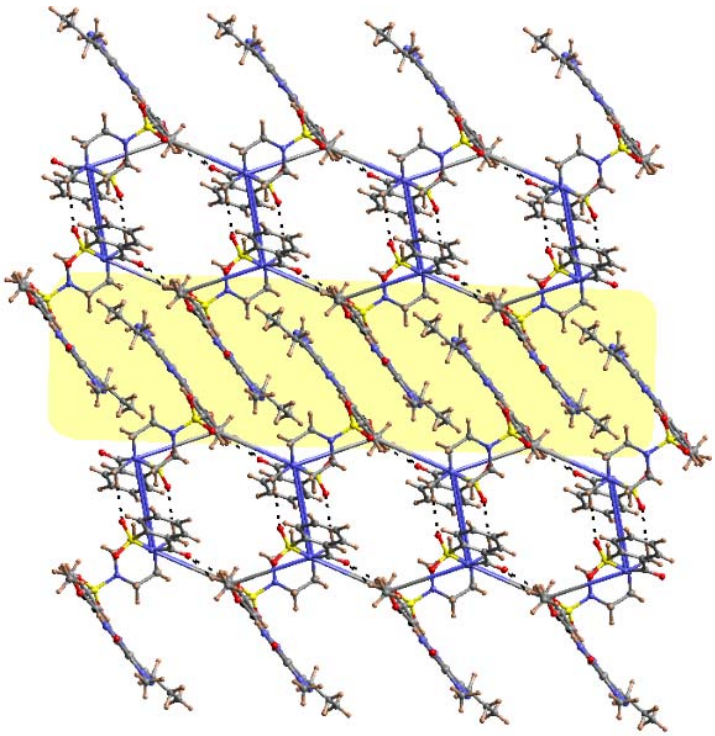

Figure 7. Hexagonal cavities in the solvates of **SS** viewed down the *c*-axis illustrating the overall 2-D network. The stacking region is highlighted. Guest molecules are removed to show the cavity.

It is interesting to note that the cavity sizes in all these solvates are same irrespective of the guest size. There is a variation of the solute-solvent ratio among these isostructural solvates. This solute-solvent ratio varies because the size of the guest is different whereas the hexagonal cavity is fixed. Solvents with smaller volume like acetonitrile, nitromethane and formamide occupy the surface of the cavity. There are two of these solvents in each cavity and these two solvents are inversion related. Solvents that are bigger in size like DMSO, DMF, THF, pyrrolidinone, ethanol, 1,4-dioxane and ethylene glycol are buried in the cavity. These solvents occupy the special position (***i***) in the unit cell even if solvents like DMSO, DMF, THF, pyrrolidinone and ethanol lack a molecular inversion center. As a result, such solvents are disordered over two positions. Water being the smallest sized solvent in the series, sits inside the hexagonal cavity. In

all these isostructural solvates, intramolecular N–H…O hydrogen bond between the pyrazolopyrimidone N–H group and the O-atom of the ethoxy group of the $(sildenafil)^+$ cation is also observed. To summarize, isostructural solvates of sildenafil saccharinate studied in this chapter can be divided into two groups, based on the order/disorder of the guest molecules and host–guest stoichiometry: (i) nitromethane, acetonitrile, formamide, ethylene glycol, 1,4-dioxane and water (guest molecule is ordered) (ii) DMSO, THF, DMF, ethanol, and pyrrolidinone (guest molecule is disordered).

6.3.1 Nitromethane solvate, (SS).(CH_3NO_2)

SS crystallizes as a 1:1 nitromethane solvate when a saturated solution of **SS** (prepared by grinding) in nitromethane is kept overnight at room temperature. It takes the triclinic space group, $P\bar{1}$, with one $(sildenafil)^+$ cation, one $(saccharin)^-$ anion and one nitromethane molecule in the asymmetric unit. The tetramer synthon **III** between two $(sildenafil)^+$ and two $(saccharin)^-$ ions is the basic structural unit here. Two of these tetrameric units self assemble in 2D via two C–H…O hydrogen bonds to form the hexagonal cavity (Figure 8). Two nitromethane molecules occupy the surface of this cavity and complete the solute–solvent cluster. Self-assembly of host molecules in all these isostructural solvates with hexagonal voids of dimensions c.a. 5.91 Å×5.69 Å is mediated by the $N^{(+)}$–H…$N^{(-)}$ and C–H…O tetramer synthon **III**. The ordered nitromethane guest bonds to the host via two C–H…O interactions (*d*, 2.27 Å; θ, 167.3°). These solute–solvent clusters propagate in 2D as a layer (Figure 7). It is presumed that by reorganizing this hexagonal cage framework, host molecules are able to wrap around the guest molecule more tightly, i.e., the crystal structure achieves more efficient close packing compared to the alternative of an open apohost structure. This could be the reason that this compound crystallizes from these solvents with solvent molecules trapped inside the crystal lattice.

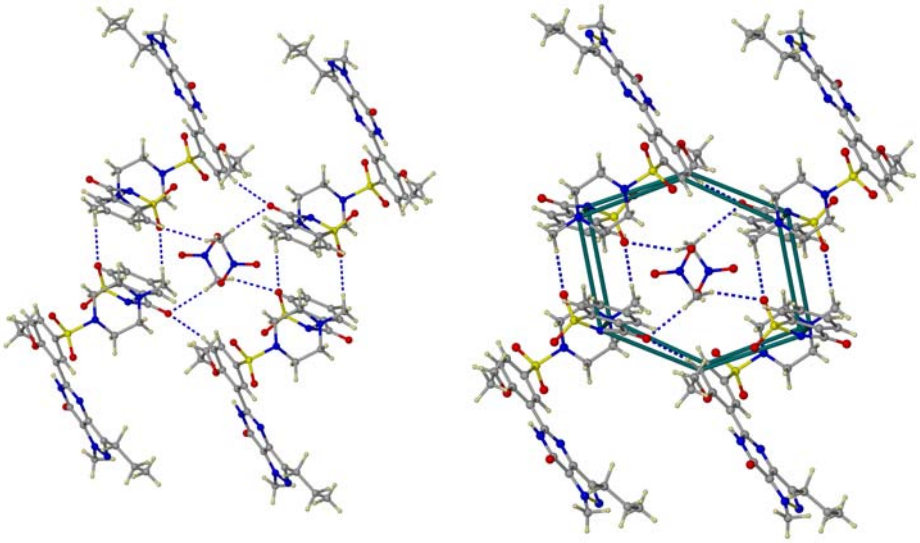

Figure 8. Crystal structure of (**SS**).(CH_3NO_2) down [001] to show the hexagonal cavity. Ordered nitromethane guest molecules are present on the surface of the cavity.

6.3.2 Formamide solvate, (SS).($HCONH_2$)

The packing of (**SS**).($HCONH_2$) is similar to that of (**SS**).(CH_3NO_2) with synthon **III** being the basic structural unit and with the similar hexagonal cavity. The 1:1 solute–solvent module is again found and these modules are connected to each other via C–H…O hydrogen bonds (*d*, 2.28 Å; *θ*, 161.0°). Two formamide molecules occupy the surface of this hexagonal cavity and are inversion related to each other (Figure 9a). Host…guest C–H…O and N–H…O hydrogen bonds further stabilize the structure.

6.3.3 Acetonitrile solvate, (SS).(CH_3CN)

The 1:1 solute–solvent cluster is again found with two acetonitrile molecules occupying the surface of the hexagonal cavity. The structure is triclinic and centrosymmetric and from a packing viewpoint it is hardly distinguishable from the 1:1 solvates with CH_3NO_2 and CH_3CN (Figure 9b).

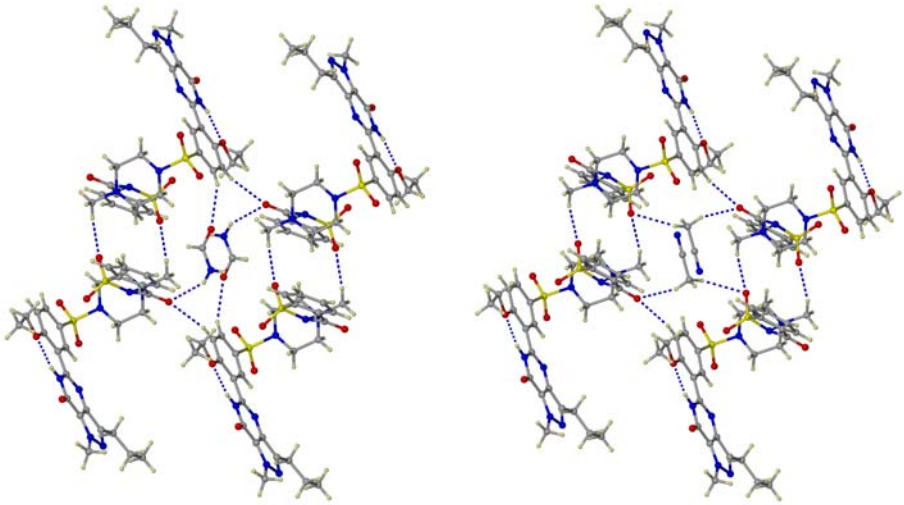

a **b**

Figure 9. (a) Packing diagram of (**SS**).($HCONH_2$) and (b) (**SS**).(CH_3CN) down [001] to show the hexagonal cavity. Ordered nitromethane and acetonitrile guest molecules are present on the surface of the cavity.

6.3.4 Ethylene glycol solvate, $(SS)_2.(HOCH_2CH_2OH)$

This is a variation of the 1:1 solvate in which the centrosymmetric guest molecule occupies the special position in the crystal lattice. As a result, there is a half molecule of ethylene glycol in the crystallographic asymmetric unit along with one $(sildenafil)^+$ cation and one $(saccharin)^-$ anion. The guest is trapped inside the hexagonal cavity instead of just sitting on its surface and it makes only weak C–H…O hydrogen bonds with the host (Figure 10).

It is not unusual to encounter a family of host–guest systems in which the host lattice is invariant. However, it is quite unusual for an organic host that is so very acceptor rich (O=C and SO_2) to trap an O–H donor rich guest like ethylene glycol without any conventional hydrogen bond. It is readily accepted that for all types of crystal structures wherein the molecule contains activated donors like N–H and O–H and activated acceptors like C=O it will form N–H…O or O–H…O interactions are formed if the system does not suffer from any steric constraints [6.8]. So far there are only two examples in the literature where there are activated donor and acceptor groups present in a sterically unhindered situation and yet no conventional or unconventional hydrogen

bonding is found [6.9]. It is interesting to note that ethylene glycol has been trapped in its less stable staggered conformation as a solvate of the title host. The ethylene glycol molecule adopts the more stable gauche conformation in its crystal structure ($P2_12_12_1$, Z' = 1) [6.10]. However, among eleven ethylene glycol solvates reported in the CSD [1.18] (version 5.26, May 2005), the molecule adopts the more stable gauche conformation in three cases only. Figure 11 shows two different conformations of ethylene glycol. The dihedral angle between the two best planes in the gauche and staggered conformers is 65° and 180°. The energy difference between the gauche and the staggered conformations was estimated to be 3.2 kcal mol^{-1} (DFT) and 2.02 kcal mol^{-1} (HF).

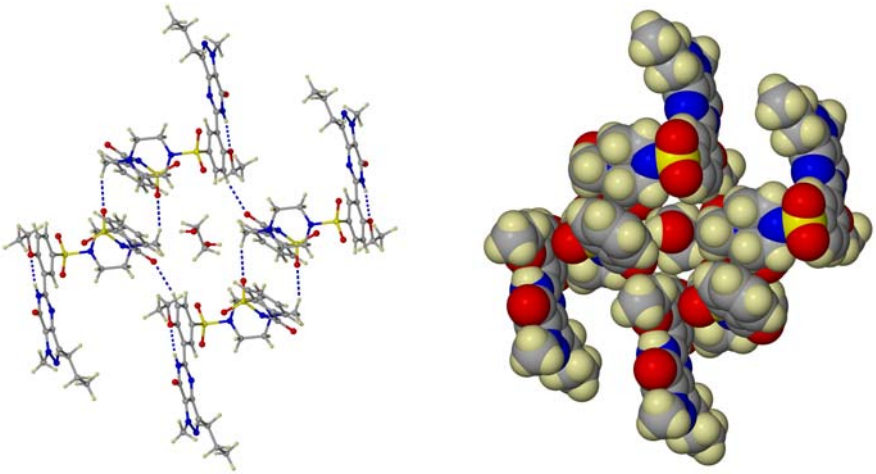

Figure 10. Crystal structure of (**SS**)$_2$.(HOC_2H_4OH) down [001] to show the hexagonal cavity. Ordered ethylene glycol guest molecule occupies the void between two **SS** tetramer. The space fill model has been shown in the right hand side.

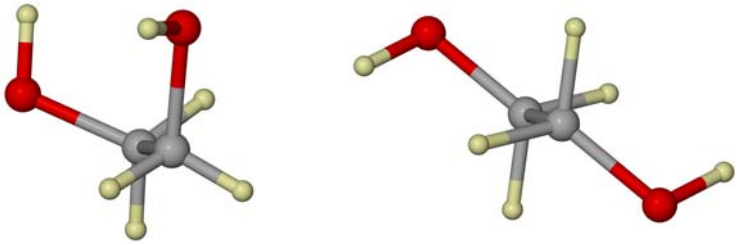

Figure 11. Gauche, (left) and staggered, (right) conformations of ethylene glycol.

6.3.5 1,4-dioxane solvate, $(SS)_2.(C_4H_8O_2)$

Like the ethylene glycol solvate this is also a variation of the 1:1 solvate. The 1,4-dioxane molecule occupies a special position and the host–guest domains are stabilized by weak C–H…O hydrogen bonds (Figure 12).

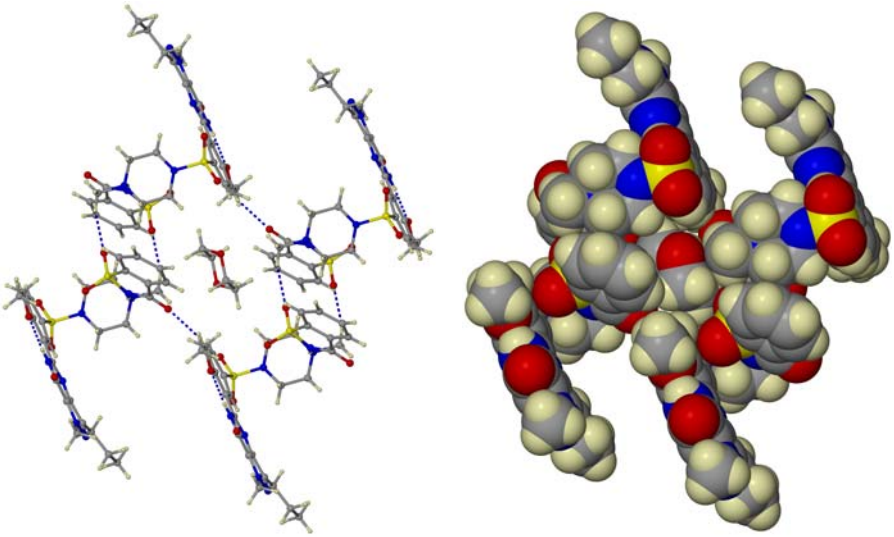

Figure 12. Crystal structure of (**SS**)$_2$.(1,4-dioxane) down [001] to show the hexagonal cavity. Ordered 1,4-dioxane molecule occupies the void between two **SS** tetramer. The space fill model has been shown in the right hand side.

6.3.6 Sildenafil saccharinate hydrate, $(SS).(H_2O)_2$

SS was crystallized from water, a solvent that is smaller in size than the other solvents tried so far. The asymmetric unit of **SS** hydrate contains two water molecules instead of one. The crystal structure of (**SS**).$(H_2O)_2$ is isostructural to the solvates described so far and with an identical arrangement of host atoms in the crystal lattice (Figure 13). Since the cavity size is fixed and water molecules are smaller in size, four water molecules self assemble inside a cavity to form an O–H…O (*d*, 1.88 Å; *θ*, 146.6°) tetramer. Unlike other solvates**,** there is an O–H…O interaction (*d*, 1.72 Å; *θ*, 172.5°) between the solute and the solvent.

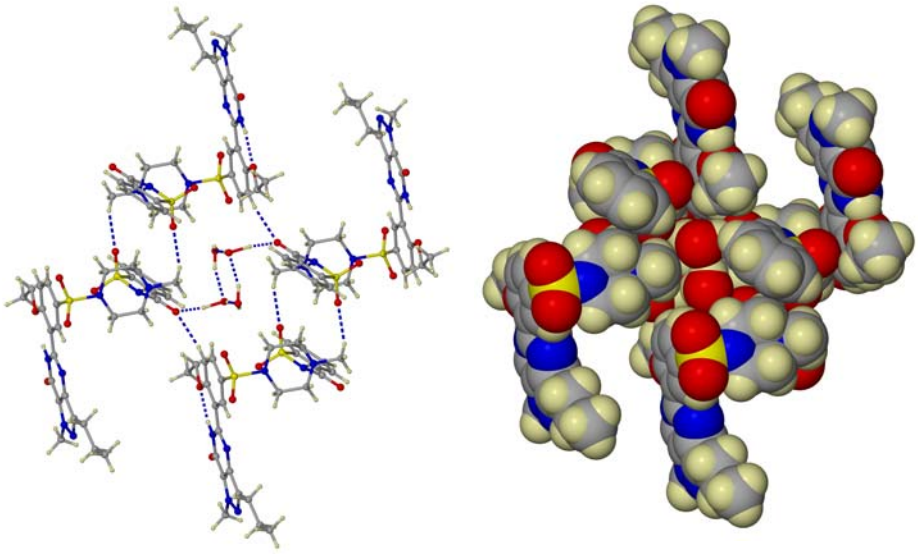

Figure 13. Crystal structure of (**SS**).$(H_2O)_2$ down the *c*-axis to show the hexagonal cavity like other solvates. Four water molecules occupy the voids between two **SS** tetramer to form an O–H…O tetramer.

6.3.7 Dimethylformamide solvate, $(SS)_2.(C_3H_7NO)$

In a recent CSD study, it was pointed out that DMF has the highest tendency for inclusion in crystals because of its multi-point recognition *via* strong and weak hydrogen bonding with the solute/host molecule [1.46]. The crystal structure of $(\mathbf{SS})_2$.(DMF) is also triclinic and centrosymmetric like other solvates. The guest (DMF) molecule is disordered with a 50% site occupancy factor. Although the C=O group in DMF is a potential acceptor there are no strong hydrogen bonds between solute and solvent (Figure 14a).

6.3.8 Tetrahydrofuran solvate, $(SS)_2.(C_4H_8O)$

In this structure too, the 2:1 solute–solvent module is found. Like other solvates, there is a plethora of strong C–H…O interactions (Figure 14b). The THF molecule is inside the hexagonal cavity and is disordered with a 50% site occupancy factor. The host structure is hardly distinguishable from the other solvates.

6.3.9 Ethanol solvate, $(SS)_2.(C_2H_5OH)$

The electron density in the host cavity is diffused for $(\mathbf{SS})_2$.(EtOH) because the guest atoms are disordered. It is therefore difficult to reliably determine the host: guest stoichiometry from X-ray data alone. TGA measurements confirmed the 2:1 host/guest stoichiometry. The R factor for this structure is slightly higher because of severe guest disorder (Figure 14c).

6.3.10 Dimethylsulfoxide solvate, $(SS)_2.(C_2H_6SO)$

DMSO like DMF and dioxane form solvates very easily because it interacts with the solute *via* multi point recognition of strong and weak hydrogen bonding. DMSO solvate of **SS** crystallizes in the centrosymmetric space group $P\bar{1}$. In this structure too, the 2:1 solute–solvent module is found. The DMSO molecule is inside the cavity and lies on an inversion centre and is disordered over two positions with 50% site occupancy factor (Figure 14d).

6.3.11 Pyrrolidinone solvate, $(SS)_2.(C_4H_7NO)$

Considering the crystal structure of other disordered solvates, it was expected that the guest atoms in the crystal structure of $(\mathbf{SS})_2$.(pyrrolidinone) would also be disordered. The 2:1 solute–solvent module is found. The pyrrolidinone molecule is inside the cavity and is disordered over two positions with a 50% site occupancy factor (Figure 14e).

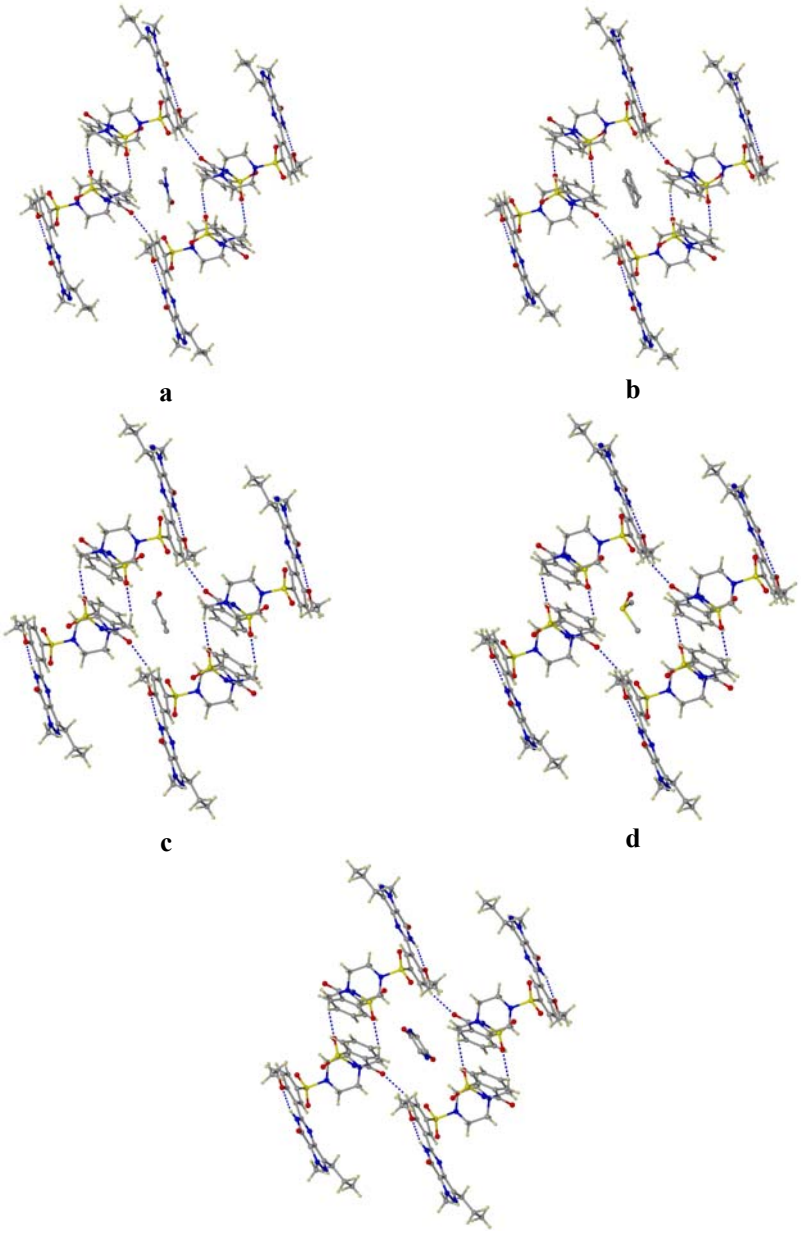

Figure 14. Crystal structure of (a) (**SS**)$_2$.(DMF), (b) (**SS**)$_2$.(THF), (c) (**SS**)$_2$.(EtOH), (d) (**SS**)$_2$.(DMSO), and (e) (**SS**)$_2$.(pyrrolidinone) down the *c*-axis to show the hexagonal cavity like other solvates. Guest molecules occupy the inversion centre in the crystal and are disordered.

The dimensions of the unit cell of these solvates, especially the size of the cavity formed do not depend on the volume of the solvent molecule, but on the nature and the strength of the (sildenafil)$^+$ cation and (saccharin)$^-$ anion interactions. As a result, solvents those are larger in size than the cavity formed by (sildenafil)$^+$ cation and (saccharin)$^-$ anion (*viz* iso-amylalcohol), do not yield any solvated crystal. **SS** crystallizes in the unsolvated form when crystallized from iso-amyl alcohol. In most of the cases, there are several weak C–H…O interactions between the host and the guest. The overall effect of the geometry of the solvent molecule and the strength of the solute-solvent interactions is reflected in the higher value of the packing coefficient of these solvates (Table 1). A higher C_k value (~ 0.70 in all these solvates compared to 0.68 for the apohost) indicates a more compact packing, which may arise either from a larger volume of the solvent molecule or from stronger solute–solvent interactions. To summarize, one can also say that a number of host…guest C–H…O interactions, and a more compact packing drive **SS** to crystallize in this hexagonal cage lattice with solvent molecules occupying the surface or interior of the cavity.

Table 1. Packing coefficients of different solvates with/without solvent.

Guest Molecule	n	Packing co-efficient
Nitromethane	1	0.690
Acetonitrile	1	0.702
Water	1	0.711
Formamide	1	0.684
Ethylene glycol	0.5	0.679
apohost	–	0.680

There is a structural similarity between synthon **III** of these isostructural solvates and the tetramer synthon **I** of the **SS** apohost. In fact a subtle variation or relationship between synthons **I** and **III** can be seen (Figure 15). A slight movement of the **SS** unit will generate synthon **III** from synthon **I**. It is to be noted here that all these isostructral solvates lose the guest molecules while heating and the resulting polycrystalline mass is the **SS** apohost [6.11]. One can say that organic host compound **SS** undergoes a phase-transition upon guest release. In order to actively facilitate this dynamic process, the host molecules undergo significant positional and/or orientational rearrangement. This host–

guest→host lattice transformation is triggered by a rearrangement of several C–H…O interactions between the molecular components.

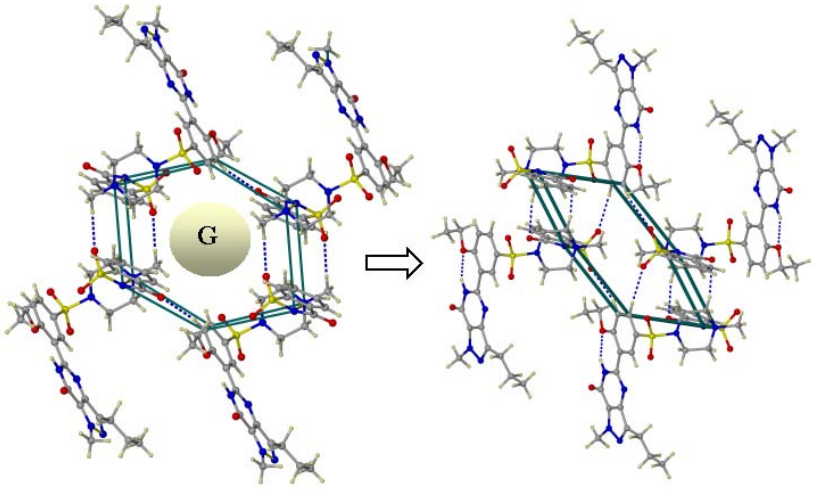

Figure 15. Relationship between the crystal structure of the apohost and different solvates. Note the shape of the hexagonal cavity upon guest loss.

The crystal structures of different solvates of **SS** were analyzed in terms of C–H…O interactions. Figure 16 shows the *d*-θ scatter plot for the C–H…O interactions in these isostructural solvates and the apohost. The C–H…O interactions are strong. The combination of a number of short C–H…O interactions and a sufficient amount of close packing stabilizes the structure.

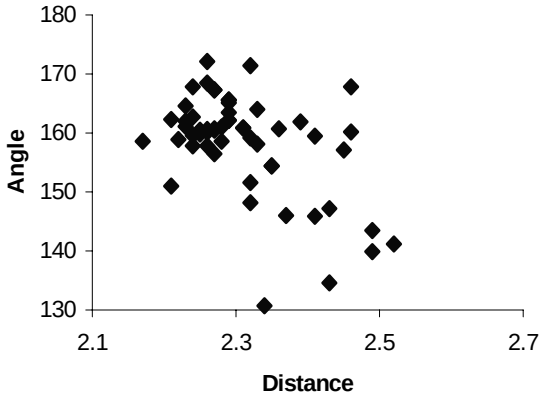

Figure 16. *d*-θ scatter plot for the C–H…O interactions in the isostructural solvates of **SS** and in the apohost.

6.4 Conformational pseudopolymorphism

The crystal structure of sildenafil saccharinate methanolate is shown in figure 17. (**SS**).(MeOH) crystallizes in the monoclinic space group *C*2/*c*. The asymmetric unit contains one $(sildenafil)^+$ cation, one $(saccharin)^-$ anion and one methanol molecule. (**SS**).(MeOH) is not isostructural with other solvates as solvent molecules actively participate in structural organization instead of just playing a space-filling role. In this solvate, the hexagonal cavity that is formed by self-association of $(sildenafil)^+$ cation and $(saccharin)^-$ anion in other solvates is absent. In the isostructural solvates and in the apohost, $(sildenafil)^+$ cations and $(saccharin)^-$ anions are hydrogen bonded to each other via $N^{(+)}$–H…$N^{(-)}$ hydrogen bonds. However, in the methanol solvate, two methanol molecules interleave between the two $(sildenafil)^+$ and $(saccharin)^-$ modules via $N^{(+)}$–H…O (*d*, 1.69 Å; θ, 168.8°) and O–H…$N^{(-)}$ (*d*, 1.75 Å; θ, 164.6°) bonds to give a different structure (Figure 17). Two $(sildenafil)^+$ cations are also connected to each other by an N–H…O dimer synthon. $(Sildenafil)^+$ cations and $(saccharin)^-$ anions are connected to each other via C–H…O=S hydrogen bonds. It is interesting to note that a $N^{(+)}$–H…$N^{(-)}$ hydrogen bond which contains more ionic character is replaced by one $N^{(+)}$–H…O and an O–H…$N^{(-)}$ hydrogen bond due to solvent incorporation. In the crystal structure of the methanolate, the pyrazolopyrimidone ring system and the benzene ring are not coplanar. As a result, the intramolecular N–H…O hydrogen bond (that is seen in the other solvates) between the pyrazolopyrimidone N–H group and the O-atom of the ethoxy group is absent. Energy difference between the coplanar and the twisted conformation of the $(sildenafil)^+$ cation is 3.21 kcal mol^{-1}. This results in the structural variation between the (**SS**).(MeOH) and these isostructural solvates. As the structural variation is associated with the conformational variation of the major component in the crystal this phenomenon could also be termed as *conformational pseudopolymorphism* [5.4] (Figure 18).

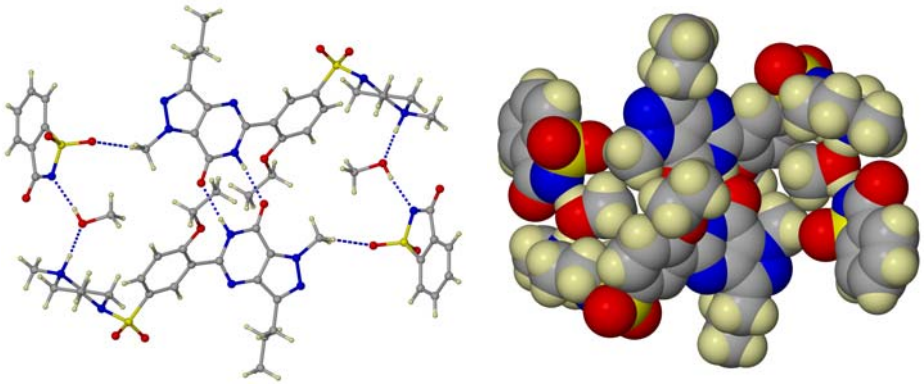

Figure 17. Packing diagram of (**SS**).(MeOH) down the *b* axis. Note the N–H…O dimer synthon unlike other solvates. Methanol molecules interleaves between two **SS** units.

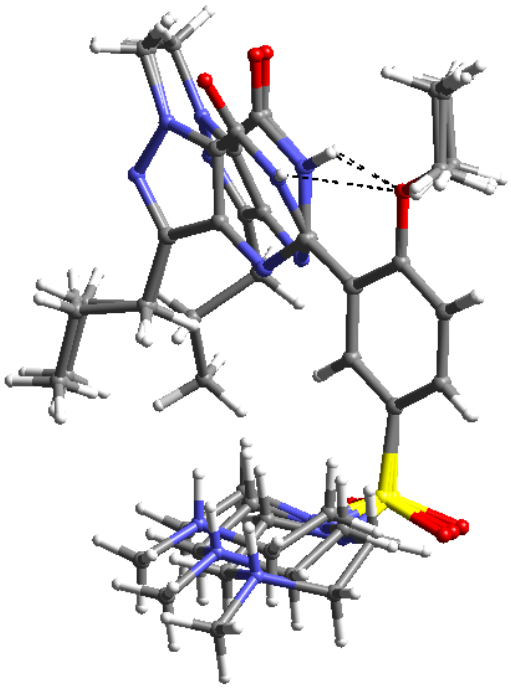

Figure 18. Overlay diagram of $(\text{sildenafil})^{+}$ cation in **SS**.(MeOH), (**SS**) (H_2O) and in **SS** apohost. Note the conformational difference between pyrazolopyrimidone ring system and the benzene ring.

Table 2. Geometrical parameters of H-bridges of the solvates in this study.

Compound	H-bridge	*d*/Å (H…A)[a]	*D*/Å (X…A)	*θ*/deg ∠X–H…A
SS	N–H…N	1.75	2.754(3)	173.7
	N–H…O	1.85	2.653(3)	134.4
	C–H…O	2.21	3.197(5)	151.0
	C–H…O	2.33	3.363(4)	158.1
	C–H…O	2.39	3.440(4)	161.9
	C–H…O	2.33	3.379(4)	164.0
	C–H…O	2.43	3.388(4)	147.2
(SS).(CH_3NO_2)	N–H…N	1.77	2.781(4)	177.9
	N–H…O	1.85	2.675(4)	136.5
	C–H…O	2.26	3.324(4)	168.5
	C–H…O	2.29	3.337(4)	162.2
	C–H…O	2.27	3.332(4)	167.3
	C–H…O	2.32	3.290(4)	148.2
	C–H…O	2.35	3.356(4)	154.4
(SS).(CH_3CN)	N–H…N	1.73	2.739(2)	175.2
	N–H…O	1.79	2.634(2)	138.2
	C–H…O	2.17	3.204(2)	158.6
	C–H…O	2.24	3.294(2)	162.7
	C–H…O	2.26	3.297(2)	160.6
	C–H…O	2.27	3.249(2)	156.5
	C–H…O	2.27	3.332(4)	167.3
	C–H…O	2.35	3.356(4)	154.4
	C–H…O	2.45	2.895(2)	103.3
(SS).($HCONH_2$)	N–H…N	1.77	2.775(3)	176.1
	N–H…O	1.83	2.647(2)	136.2
	C–H…O	2.26	3.337(3)	172.1
	C–H…O	2.26	3.290(3)	157.8
	C–H…O	2.28	3.326(3)	161.0
	C–H…O	2.37	3.323(3)	146.0
$(SS)_2$.(HOC_2H_4OH)	N–H…N	1.76	2.765(3)	174.3
	N–H…O	1.82	2.644(3)	136.7
	C–H…O	2.23	3.278(4)	162.0
	C–H…O	2.23	3.287(4)	164.6
	C–H…O	2.31	3.351(4)	160.9
$(SS)_2$.($C_4H_8O_2$)	N–H…N	1.76	2.765(3)	174.3

	N–H…O	1.82	2.644(3)	136.7
	C–H…O	2.23	3.278(4)	162.0
	C–H…O	2.23	3.287(4)	164.6
	C–H…O	2.31	3.351(4)	160.9
(SS).(H_2O)$_2$	N–H…N	1.75	2.755(3)	177.6
	N–H…O	1.83	2.652(3)	136.0
	O–H…O	1.72	2.698(4)	172.5
	O–H…O	2.17	3.154(5)	174.4
	O–H…O	2.26	3.154(5)	151.1
	C–H…O	2.22	3.252(4)	158.9
	C–H…O	2.24	3.302(4)	167.8
	C–H…O	2.28	3.314(4)	158.6
	C–H…O	2.41	3.450(3)	159.5
(SS)$_2$.(C_2H_6SO)	N–H…N	1.81	2.773(9)	158.8
	N–H…O	1.87	2.686(8)	136.0
	C–H…O	2.25	3.286(9)	159.8
	C–H…O	2.31	3.347(10)	160.8
	C–H…O	2.32	3.349(9)	159.2
	C–H…O	2.43	3.284(14)	134.6
	C–H…O	2.52	3.430(9)	141.2
(SS)$_2$.(C_4H_7NO)	N–H…N	1.74	2.736(5)	170.0
	N–H…O	1.86	2.651(5)	132.7
	C–H…O	2.29	3.346(7)	165.1
	C–H…O	2.24	3.265(6)	157.8
	C–H…O	2.29	3.348(7)	165.6
	C–H…O	2.34	3.151(2)	130.7
	C–H…O	2.49	3.423(6)	143.5
(SS)$_2$.(C_4H_8O)	N–H…N	1.72	2.729(3)	175.4
	N–H…O	1.84	2.651(2)	135.2
	C–H…O	2.25	3.286(3)	160.5
	C–H…O	2.29	3.348(3)	163.5
	C–H…O	2.29	3.348(7)	165.6
	C–H…O	2.29	3.344(3)	162.1
	C–H…O	2.47	3.230(3)	126.3
(SS)$_2$.(C_2H_5OH)	N–H…N	1.75	2.751(3)	175.8
	N–H…O	1.86	2.648(3)	132.9
	C–H…O	2.23	3.273(3)	161.1
	C–H…O	2.27	3.312(4)	160.5
	C–H…O	2.24	3.277(3)	159.6

	C–H…O	2.39	3.191(7)	129.5
	C–H…O	2.45	3.470(3)	157.1
$(SS)_2.(C_3H_7NO)$	N–H…N	1.72	2.726(2)	175.9
	N–H…O	1.85	2.651(2)	134.2
	C–H…O	2.27	3.310(2)	160.7
	C–H…O	2.21	3.256(2)	162.3
	C–H…O	2.26	3.301(2)	160.1
	C–H…O	2.49	3.393(2)	139.9
$(SS)_2.(CH_3OH)$	N–H…O	1.69	2.690(6)	168.8
	N–H…O	1.83	2.800(5)	159.4
	O–H…N	1.76	2.715(6)	164.6
	C–H…O	2.32	3.392(6)	171.4
	C–H…O	2.32	3.308(6)	151.6
	C–H…O	2.36	3.400(6)	160.7
	C–H…O	2.46	3.499(6)	160.2
	C–H…O	2.46	3.530(7)	167.8
	C–H…O	2.41	3.365(6)	145.9

[a] O–H, N–H and C–H distances are neutron normalized to 0.983, 1.009 and 1.083 Å.

Bernstein, in his recent article, indicated his lack of enthusiasm for the continued use of the term pseudopolymorphism [1.61b]. According to him "…. scientists must be precise about definitions, and I am of the opinion that, *pseudo*polymorph is a misnomer. Solvates and hydrates are just that–they are not *pseudo* (as Seddon quoted the definition) anything, and they should be called what they are". However, it is quite surprising to note his silence about the usage of other terms such as inclusion compounds, host–guest systems or lattice inclusion hosts, clathrates and cavitands. Is only pseudopolymorph a misnomer and the other terms are all correct, as they are not *pseudo* anything? In the previous chapter, the validity of the terminology *pseudopolymorphism* has been discussed. Desiraju has pointed out that the term *pseudopolymorphism* is in use in the literature and one cannot deny its existence [1.62]. Although several researchers (including ourselves) had commented about the validity/invalidity of this terminology, yet so far there are very few examples where the validity of this terminology has been analysed structurally. Crystal structures of different solvates of sildenafil saccharinate are such an example that show the importance of this terminology.

Pseudopolymorphs are originally defined as solvated forms of a compound, with different crystal structures and/or difference in the nature of the included solvent [1.60]. That means the crystal structure of an unsolvated compound changes after solvent inclusion. The included solvent could be same or different. Here, the isostructural solvates of sildenafil saccharinate are all different from the crystal structure of the apohost although they are of similar type among themselves. Hence, they can be called as pseudopolymorphs according to the literature definition. One can argue that the sildenafil saccharinate apohost and the corresponding isostructural solvates could better be called 'solvates' instead of 'pseudopolymorphs' because there is not much structural variation among these solvates except the nature of the included solvent and the stoichiometry. However, the totally different crystal structure and the physicochemical behaviour of the sildenafil saccharinate methanolate compared to the other solvates and the apohost will justify the usage of the term pseudopolymorphism in this series.

6.5 X-ray powder diffraction

The powder diffraction patterns of these solvates, show that these solvates are stable at room temperature and the bulk sample contains a single phase. Figure 18 shows the X-ray powder diffraction patterns of sildenafil saccharinate hydrate as a representative case. Rietveld refinement (R_p = 18.39, R_{wp} = 24.81) of the experimental powder patterns with respect to the simulated peaks of the crystal structure gives an idea about the purity of the sample.

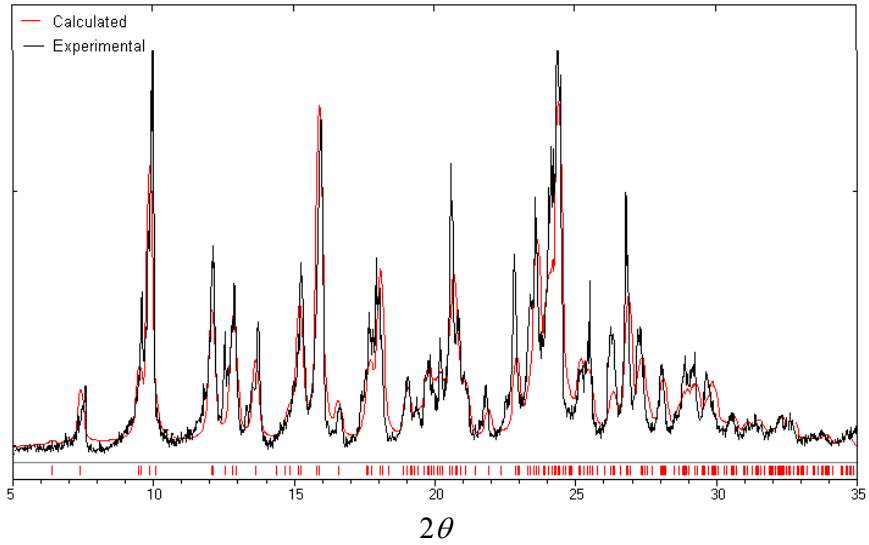

Figure 19. Experimental powder XRD of (**SS**).$(H_2O)_2$ at room temperature (black line) matches with the powder pattern calculated from the crystal structure (red line). Rietveld refinement in Powder Cell 2.3: R_p = 18.39, R_{wp} = 24.81.

Variable temperature PXRD measurements were carried out to confirm the thermal behavior of all these solvates [6.12]. When crystals of sildenafil saccharinate hydrate were heated in a stepwise manner from room temperature to 90 ºC, they became opaque. The polycrystalline sample obtained gave a new diffraction pattern compared to the PXRD patterns of the hydrate. Rietveld refinement of the PXRD patterns of the polycrystalline sample confirmed that this process leads to the unsolvated sildenafil saccharinate (apohost), with no detectable amount of hydrate remaining (Figure 19). The good agreement between calculated and experimental PXRD patterns in the final Rietveld refinement (R_p = 20.39, R_{wp} = 27.81) vindicates the correctness of the argument. PXRD data for other solvates (except $HCONH_2$ and ethylene glycol) after heating to the respective solvent loss temperature shows the complete solvate→ apohost conversion.

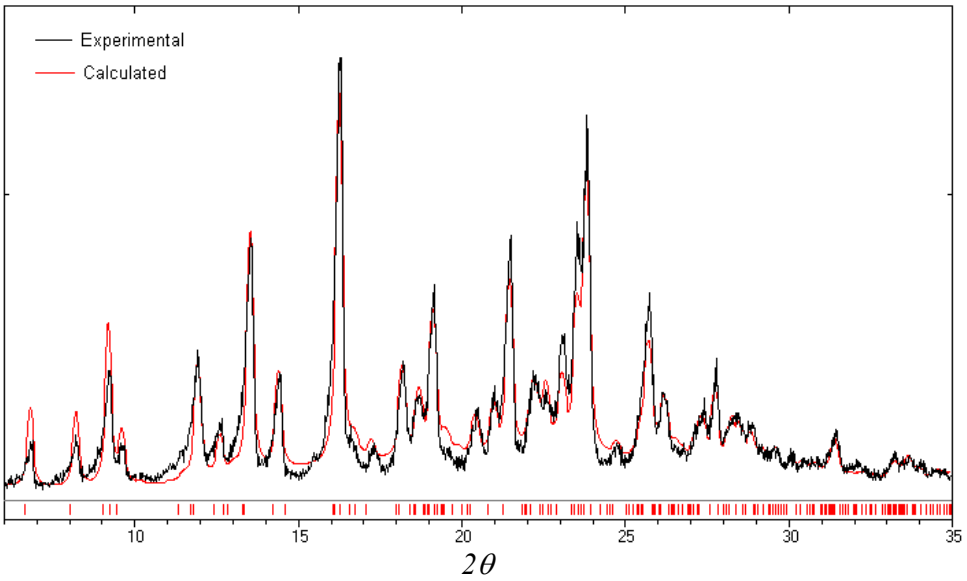

Figure 20. Experimental powder XRD of **(SS).**$(H_2O)_2$, after heating the sample at 100 °C for 2 hours, (black line) matches with the calculated powder pattern of apohost (red line). Rietveld refinement in Powder Cell 2.3: $R_p = 20.39$, $R_{wp} = 27.81$.

6.6 Thermal analysis

Of the 12 crystal structures described in this chapter, only the nitromethane, acetonitrile, 1,4-dioxane, formamide, water, ethylene glycol and methanol guests are ordered, whereas other guest molecules are disordered. Several authors have emphasized the importance of TGA and DSC measurements on host–guest compounds to obtain valuable information about host framework stability, guest enclathration specificity, host…guest binding and enthalpy of guest release [1.62]. TGA measurements confirm the host/guest stoichiometry obtained from the site occupancy of atoms in X-ray structures. It is sometimes difficult to locate and accurately assign the occupancy of disordered guest atoms from difference Fourier maps, particularly for heavily disordered guests. TGA shows that release of guest from the host framework occurs at the first endotherm temperature in DSC. The second endotherm at ~ 208 °C corresponds to the melting of pure sildenafil saccharinate host (Figure 20). Evolution of methanol occurs at 40-60 °C because host molecules do not surround the guest in the cage architecture like other solvates. The T_{onset} values are much higher than the normal boiling point of the

guest for EtOH (121 °C), 1,4-dioxane (166 °C), CH_3CN (158 °C), CH_3NO_2 (132 °C), THF (92 °C) and DMF (165 °C). This could be due to the tight binding of these guests in the hexagonal cage of sildenafil saccharinate. Similarly T_{onset} values are much lower than the normal boiling point of the guest for H_2O (76 °C) ethylene glycol (144 °C) and DMSO (149 °C). The reason for this unusual T_{onset} values is still unclear. T_{onset} and T_{bp} values for all the guest molecules are listed in Table 3.

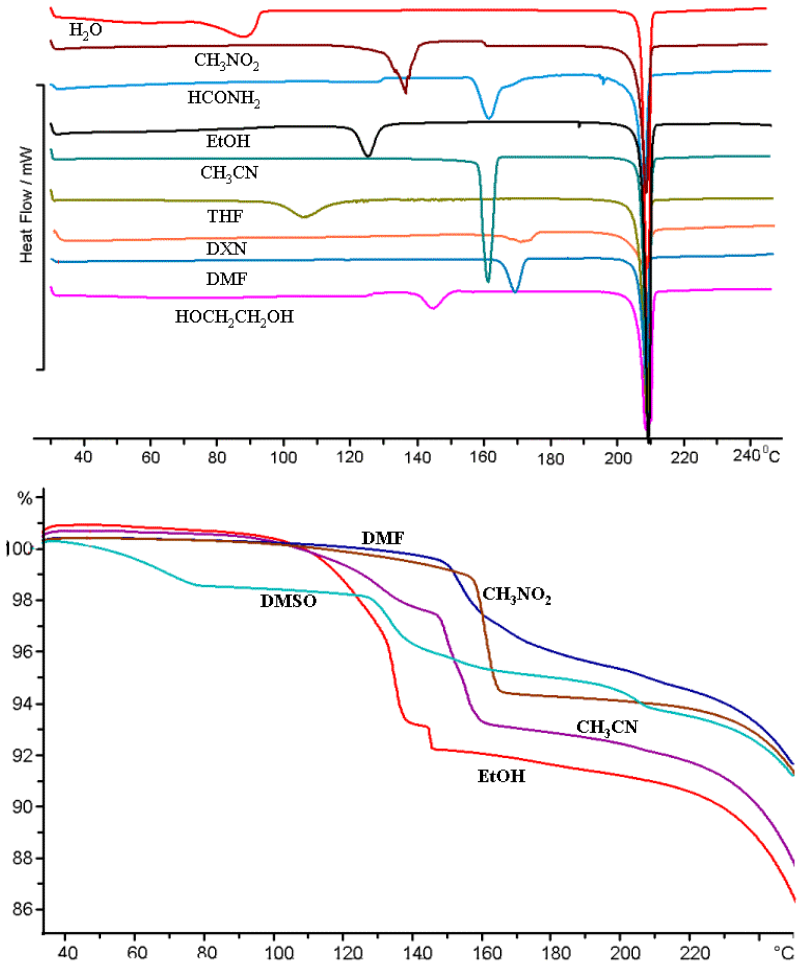

Figure 21. DSC/TGA for some of the isostructural solvates of **SS**. The first endotherm corresponds to guest loss and the second endotherm is melting of the apohost.

Table 3. Thermal analysis (TGA and DSC) on some solvates of **SS**.

Solvent	Observed weight loss from TG/%	Calculated weight loss from host : guest ratio in X-ray(%)	Guest release T_{on}/°C	B p of guest/°C	ΔH/J g^{-1} (for guest release)
CH_3NO_2	8.75	8.47 (1:1)	136	102	57.81
CH_3CN	5.54	5.89 (1:1)	160	81	108.26
H_2O	5.91	5.16 (1:2)	88	100	34.75
HOC_2H_4OH	4.82	4.50 (2:1)	148	198	41.38
DMF	4.69	5.29 (2:1)	172	153	43.38
DMSO	4.63	5.69 (2:1)	153	189	22.75
EtOH	3.28	3.39 (2:1)	124	78	34.39
THF	6.64	5.12 (2:1)	105	65	25.83
1,4 dioxane	6.8	6.19 (2:1)	117	97	15.19
Pyrrolidinone	6.3	5.98 (2:1)	157	180	58.49
MeOH[a]	–	– (1:1)	43	65	–

[a] TGA of methanol solvate was difficult to measure as it was unstable at room temperature

6.7 Calculations

Lattice energies were calculated by minimizing the experimental X-ray structure in Cerius^2 (Dreiding2.21) [2.9]. Since the space group, crystal packing and number of host molecules are same in all the structures, lattice energies were calculated to get a qualitative picture of hydrogen bonding energy in all these solvates. Minimized crystal lattice energies for the host and host–guest crystal structures are listed in Table 4. According to lattice-energy minimizations, the crystal structures of solvated forms are found to be more stable than the apohost structure (~ 370 kcal mol^{-1} and 333.1 kcal mol^{-1} respectively). This result is in agreement with the observation that **SS** upon crystallization form common solvents yields solvated crystals rather than the apohost.

Table 4. Lattice energy calculations on solvates of **SS** in Cerius^2 (Drieding2.21).

Guest molecule	n	Solvent surface Area Å^2/u.c	Solvent Volume Å^3/u.c	H-bond energy		vdW energy		Total energy	
				with solvent	without solvent	with solvent	without solvent	with solvent	without solvent
CH_3NO_2	1	76.31	51.65	–7.11	–6.84	–132.2	–113.2	–373.8	–292.9
CH_3CN	1	66.57	44.96	–7.28	–7.17	–135.9	–116.9	–346.8	–302,3
H_2O	1	38.68	21.62	–28.29	–6.70	–108.7	–119.7	–405.0	–305.7
$HCONH_2$	1	62.10	40.66	–16.23	–7.26	–127.9	–120.4	–373.6	–296.4
OHC_2H_4OH	0.5	82.89	57.43	–10.85	–6.90	–130.1	–119.1	–343.2	–303.1
apohost	–	–	–	–	–6.17	–	–129.6	–	–333.1

The following observations are noteworthy in this series: (i) amorphous **SS** converts to crystalline **SS** while heating; (ii) **SS** forms isostructural solvates while crystallizing form a variety of solvents; (iii) all these isostructural solvates form an $N^{(+)}$–H…$N^{(-)}$ and C–H…O tetramer synthon **III**; (iv) these tetramer synthons joins with each other with a C–H…O hydrogen bond to form a hexagonal cavity; (v) the dimensions of the host cavity in these solvates are same; (vi) crystal structures of these solvates do not depend on the solvent molecule. In the nucleation stage the host cavity forms first and the guest molecules does the space-filling role; (vii) donor rich guest ethylene glycol sits in the hexagonal cavity without any conventional hydrogen bond; (viii) however, single crystals of the solvates could only be isolated when there is a solvent inclusion inside these hexagonal cavity; (ix) PXRD suggests that these isostructural solvates while heating converts to the same apohost structure.

6.8 Conclusions

A traditional view is that host lattices must be assembled with strong hydrogen bonds to sustain the open architecture for guest inclusion. However, recent literature examples demonstrate that weak hydrogen bonds can also be considered as effective design elements in the crystal engineering of host lattices. An advantage of using hydrogen bonding in host design is that stronger hydrogen bonds provide robustness to the host framework while the weak interactions give flexibility and adaptivity. Multiple solvates have been reported for a variety of compounds, but the solvates of sildenafil saccharinate invariably show a large degree of isostructurality. Solid-state structural aspects of sildenafil saccharinate are versatile and we tried to investigate why this compound forms solvates only with those solvents in which it is soluble. Several new pseudopolymorphs/solvates, of sildenafil saccharinate have been obtained. A notable conclusion of this work, and one that could be of general significance is that the term pseudopolymorph is in general a good terminology that defines different structural and physicochemical behaviour of different solvates. Much careful experimental work may be required to obtain new pseudopolymorphs. To this end, the solvate forming propensities of sildenafil citrate has been examined. Preliminary experiments indicate

that it does not form many solvates as extensively as sildenafil saccharinate. Further studies should help to elucidate which forces direct the structural motif observed here and whether this compound is selective towards the polar solvents or not.

6.9 Experimental section

Sample preparation and crystallization

Sildenafil was obtained as complimentary sample from local pharmaceutical company. Saccharin was purchased from Loba chemicals and recrystallized from acetone prior to use. In all experiments the components were well ground and dissolved in appropriate solvents. Solvates of **SS** were obtained by slow cooling of a saturated solution of **SS** and the corresponding guest/solvent. Single crystals appeared after one or two days at room temperature. Melting points are recorded on Fisher–Johns apparatus and also calculated from the onset temperature of endotherm in DSC.

SS ^{1}H NMR ($CDCl_3$): δ 10.85 (s, 1H), 8.57 (d, 1H), 7.84 (m, 1H), 7.65 (m, 4H), 7.16 (d, 1H), 4.30 (s, 5H), 3.49 (m, 8H), 2.94 (m, 2H), 2.85 (s, 3H), 1.86 (m, 2H), 1.58 (m, 3H), 1.05 (m, 3H); IR (cm^{-1}) 3298, 2959, 1695, 1657, 1581 1456, 1359, 1287, 1149, 1028.
Mp: 208 °C

X-ray crystallography

The X-ray data of **SS** apohost and all its solvates were collected at the University of Hyderabad. Intensity data were collected on a Bruker Nonius Smart Apex CCD with graphite monochromated Mo-K_α radiation at 100K [2.7]. The structures were solved by direct methods and refined anisotropically by full-matrix least-squares method using the Shelxtl 6.14 software package [2.8]. The relevant crystallographic information is given in the appendix.

Thermal analysis

Differential scanning calorimetry (DSC) was performed on Mettler Toledo DSC 822e module and Thermogravimetry (TG) was performed on Mettler Toledo

TGA/SDTA 851e module. Crystals taken from the mother liquor were blotted dry on filter paper and placed in open alumina pans for TG experiment and in crimped but vented aluminum sample pans for DSC experiment. Sample size in each case was 5-10 mg. The temperature range was typically 25-250 °C at a heating rate of 0.5 °C min^{-1}. The samples were purged with a stream of nitrogen flowing at 150 mL min^{-1} for DSC and 50 mL min^{-1} for TG. The TG instrument was coupled to a Bruker Tensor FT-IR spectrometer via a heated transfer line for EGA (evolved gas analysis).

X-ray powder diffraction

Powder X-ray diffractions (PXRD) were recorded on a PNAlytical 1830 (Philips Systems Inc) diffractometer using Cu K_α X-radiation at 35 kV and 25 mA. Diffraction patterns were collected over a range of 5-45 °2θ at a scan rate of 1 °2θ min^{-1}. The software Powder Cell 2.3 was used for Rietveld refinement.

Calculations

All calculations were carried out on Indigo Solid Impact and Indy workstations from Silicon Graphics [2.9]. Dreiding 2.21 force field with the charge equilibration option was used for crystal-packing energy calculations (Cerius^2). All interatomic distances, packing coefficients and related calculations were carried out with the PLATON programme [2.10].

CHAPTER SEVEN

STRUCTURAL STUDIES OF THE SYSTEM $(Na^+)(saccharinate^-)(H_2O)_n$. A MODEL FOR CRYSTALLIZATION

7.1 Introduction

Crystallization may be viewed as a supramolecular reaction and in analogy to the molecular processes, the nucleation step in the crystallization may be likened to a transition state [1.36]. Nucleation of crystals from solution is of great importance since crystallization is the primary method for the preparation and purification of industrially important chemicals such as pharmaceuticals, explosives, dyes and photographic materials. Various factors should be considered in trying to understand crystallization process and the formation of structured clusters in solution prior to crystallization. These are, for example, interactions between the structures of growing surfaces and the solvent, as well as solvent…solvent, solvent…solute and solute…solute interactions [1.38].

Saccharin (*o*-sulfobenzimide, sac) was first prepared by Fahlberg and Remsen in 1879, and its salts have been used as sweeteners for more than 125 years [7.1]. Current annual worldwide consumption of sodium saccharin dihydrate, **1**, $(Na^+)(sac^-)(H_2O)_2$, the most common form of saccharin and also referred to as sodium saccharinate dihydrate, exceeds 30,000 tons. The substance is 500 times sweeter than sucrose and finds extensive use as a non-calorific tabletop sweetener, in foods and beverages, in personal care products and in a variety of non-food applications. It is one of the most thoroughly tested of food ingredients and has the approval of WHO after a century of safe use. In recent years, there has been increased interest in the reactivity and structural properties of metal saccharinates due to the potential use of saccharin as an antidote for metal poisoning in the human body [7.2]. The corresponding deprotonated saccharinate anion (sac^-) acts as a polyfunctional ligand due to the presence of the imino nitrogen, carbonyl oxygen, and sulfonyl oxygen atoms [7.3].

Saccharin is a moderately strong acid and the thermal properties and crystal structures of different metal saccharinates have been discussed in a number of papers. An

early work by Magri et al. describes the thermal decomposition of $(Co^{+2})(sac^{-})_2(H2O)_6$ and $(Cu^{+2})(sac^{-})_2(H_2O)_5$ [7.4]. A systematic re-investigation of the thermal decomposition of saccharinates of type $[M(H_2O)_4(sac)_2]\bullet 2H_2O$ (M = Mn, Fe, Co, Ni, Cu, Zn) together with a kinetic analysis of the dehydration process was undertaken by Içbudak and co-workers [7.5]. Naumov et al. have recently investigated the thermal decompositions of the four saccharinates, $(K^{+})_3(sac^{-})_3(H_2O)_2$, $(Na^{+})_3(sac^{-})_3(H_2O)_2$, $(Rb^{+})_2(sac^{-})_2(H_2O)$, and $(NH_4^{+})(sac^{-})$ by means of thermogravimetric (TG) and by DSC methods and interpreted the dehydration and decomposition pathways of these metal saccharinates with respect to their crystal structures [7.6].

Despite of their wide commercial use, primarily as artificial sweetening agents (especially saccharinates of Na^{+} and K^{+}), not much is known about the crystal structures of saccharinates of the alkali metals. Up to date, the X-ray crystal structures only of $(Na^{+})_3(sac^{-})_3(H_2O)_2$, **2**, [7.7] and the mixed salt $(K^{+})_2(Na^{+})(sac^{-})_3(H_2O)_2$, **3**, [7.6] have been reported. In this chapter, the crystal structures of $(K^{+})_3(sac^{-})_3(H_2O)_{2.33}$, **4**, and anhydrous sodium saccharinate have been described. These structures taken together give an idea of the packing landscape of saccharinates.

Jovanovski and Kamenar crystallized **1** (prepared from sac and aqueous Na_2CO_3 by the method of Defournel) from EtOH and determined the structure of the triclinic hydrate, **2**, $(Na^{+})_3(sac^{-})_3(H_2O)_2$ that resulted. Naumov et al. crystallized **1** from water, according to the method of Jovanovski et al [7.8]. However, they mentioned this "monoclinic form" as a substance that contains more than two molecules of water per formula unit. According to them this substance could not be considered as a dihydrate. Later they independently published the crystal structure of dihydrate **1** while this present work was being refereed [7.9].

Solvation is an integral part of crystallization. In the previous chapters, there have been discussions about the structural aspects of different solvates and pseudopolymorphs and it was concluded that solvation could be considered as "interrupted crystallization" [1.45]. The complex structure of **1** has several unusual features, which could have implications for the mechanism of crystallization, and which justify the consideration of crystallization as a supramolecular reaction.

7.2 Crystal structure of $(Na^+)_{16}(sac^-)_{16}(H_2O)_{30}$, 1

Crystallization of the commercially available sodium saccharinate from water routinely yielded **1**. Indeed the commercial sample is also identical to **1** and crystals could also be selected easily from the commercial sample for X-ray work. The monoclinic crystals diffract well and the structure was determined (Figure 1). The material is essentially not even a dihydrate but rather $(Na^+)_{16}(sac^-)_{16}(H_2O)_{30}$ which is equivalent to $(Na^+)(sac^-)(H_2O)_{1.875}$. The unit cell is large (15614 $Å^3$ at room temperature, $P2_1/n$, Z = 4) and the above formula gives the number of species (362 atoms, 238 non-H atoms) in the crystallographic asymmetric unit. The asymmetric unit is not the largest reported but is still of substantial size and complexity [7.10]. The 64 Na^+ cations, 64 sac^- anions and 120 water molecules in the unit cell make this crystal structure one of the largest and most complex for ions/molecules that are as small and simple as these. Figure 1 shows that the structure may be demarcated into "regular" and "irregular" regions. In the former domain, the saccharinate anions are nearly parallel and stacked, the Na^+ ions are hexacoordinated with water and sac^-, and the water molecules are efficiently hydrogen bonded. In the irregular region, there is disorder of sac^-, Na^+ (some of which is not necessarily hexacoordinated) and water (some of which is ill-resolved). The X-ray data obtained were good and extended to high resolution (2θ = 52°). There was no suggestion of modulation or superstructures, and R-value (0.045) was good and the modeling of the disorder was satisfactory.

The regular region of the structure consists of ten sac^- anions, which are arranged in a stack of five water bridged hydrogen bonded pairs with an average plane…plane perpendicular distance of 3.69 Å (Figure 1). Two water molecules are involved in each saccharinate pair via strong O–H…N^- hydrogen bonds (D = 2.85 Å and θ=165.8°). Cross-linking of the pairs is with octahedrally coordinated Na^+ (mean Na^+…O distance 2.39 Å). The result is a compact, finite arrangement of sac^-, Na^+ and water in the form of three supramolecular cubes and two half-cubes. Further connections with Na^+ and water in an elaborate network of hydrogen bonds and Na^+…O interactions complete the arrangement. In the irregular region, the six sac^- anions are no longer parallel. They, along with Na^+ and water, are positionally and/or orientationally

disordered (Figure 2). There is some variation in the occupancies of these species between crystal to crystal and possibly between one temperature and another (Figure 3). Overall, the structure determinations had been carried out for 4 crystals at 4 different temperatures (total 8 data sets collected at 100K, 150K, 200K and 298K). The conclusion is that there is appreciable mobility of the species in this irregular region. This provides another unusual feature of this crystal structure. A part of it, the regular region resembles a conventional crystal, but another and adjacent part, the irregular region has "solution-like" characteristics. It could be considered that hydrate, **1** is in a state of "incipient crystallization".

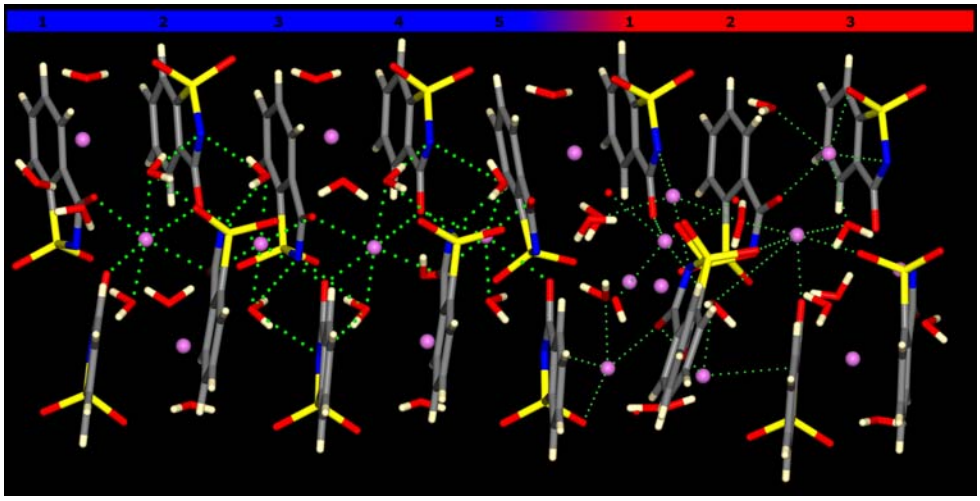

Figure 1. Asymmetric unit of dihydrate **1**. The regular regions are on the left side and the irregular regions on the right. Note the finite supramolecular cube arrangement.

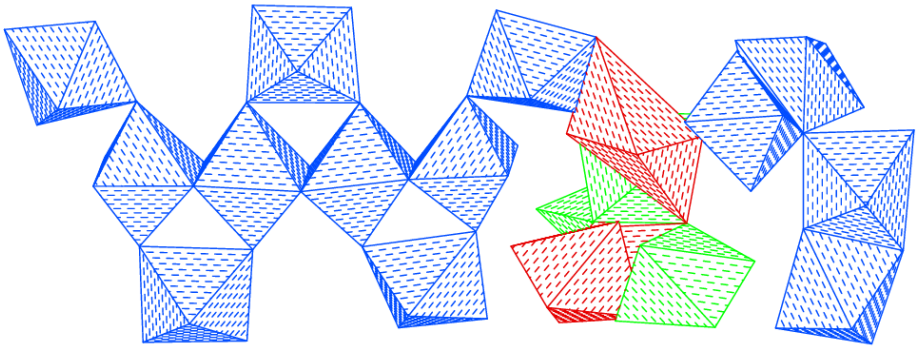

Figure 2. Polyhedral representation of **1** with Na^{+} ions in the centre of each polyhedron and the O/N-atoms at the vertices. In the regular region (left) four octahedra are edge-shared and bridged by three regular octahedra via corner-sharing. Two more corner-shared octahedra bridge the regular and irregular portions. Colour codes: Blue (6-coordination), Red (7-coordination), Green (5-coordination).

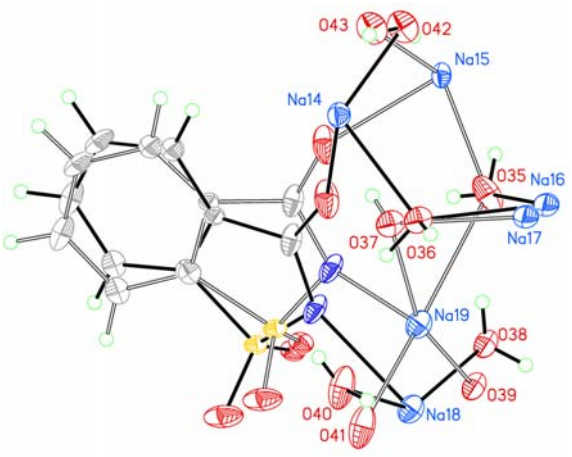

Figure 3. The disordered atoms in **1** showing alternative positions. Na18 and Na19 are 1.543 Å, Na16 and Na17 0.978 Å and Na14 and Na15 3.028 Å apart. Especially the $N^{(-)}$...Na coordinative bond 2.603/2.426 to disordered Na18 and Na19 leads to disorder in saccharinate residue 13.

7.3 Equilibrium with water

The most interesting feature of structure **1** is that it can exist in equilibrium with water (Figure 4). When a crystal is placed in the proximity (10-12 mm) of a single drop of water in a closed environment (covered in a petri dish), it absorbs water rapidly (1-5 min). Further exposure to the vapour (5-15 min) results in dissolution, which is followed

by rapid recrystallization if the water-saturated environment is absent (cover of petri dish removed). A crystal of **1** for which X-ray data were collected, was exposed to water vapour for approximately 10 minutes inside a desiccator and it was mounted on the diffractometer for data collection. Although the crystal shape was considerably altered, data collection proceeded normally and the structure obtained was as observed prior to this "watering" treatment. Figure 5 shows the snapshot pictures of the crystal, mounted in the goniometer, before and after this "watering" treatment. Rotation photographs taken prior to the data collection for this watered crystal indicate that there is enough crystallinity in the sample to go for data collection. Interestingly, the orientations of the crystal axes before and after the watering do not differ by more than 3°, indicating that this is not a case of dissolution and recrystallization, but rather that the crystal of **1** is bathed in the adhering saturated solution as shown in Figure 5. In this connection, it is not clear if Naumov et al. had accidentally examined the "watered" crystals when they stated that the dihydrate contains more than two molecules of water in the formula unit. In hindsight, it would appear that Naumov et al. in their 2000 paper were examining the same substance as in the present study.

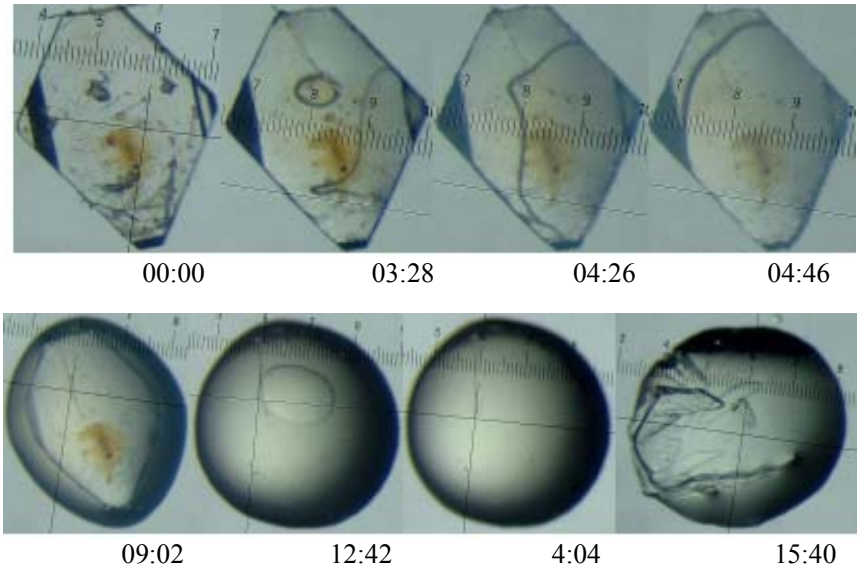

Figure 4. Different phases of **1** during the watering treatment. The numbers refer to the time in minutes.

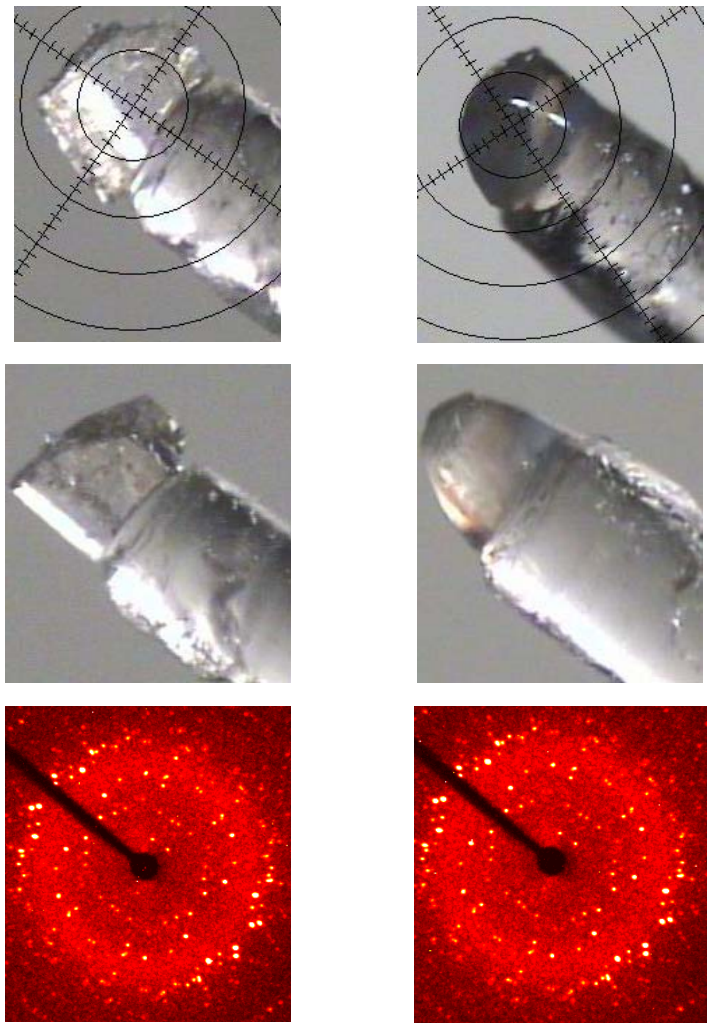

Figure 5. Snapshot pictures of the crystal before (left) and after (right) "watering" treatment. These pictures were taken when the crystal was mounted on a goniometer. The last photograph in each column shows the rotation frame in each case.

7.4 Structural landscape in the system $(Na^{+}/K^{+})(saccharinate^{-})(water)_n$

The structural landscape [1.37] that is encountered during the crystallization of a molecular solid from solvent could be considered to begin with solute-solvent clusters, where solute and solvent are associated with each other via supramolecular synthons,

followed by nucleation and finally, the appearance of metastable (kinetic) crystals that yield eventually to more stable (thermodynamic) form. Solvation is an integral part of crystallization and hydrate **1** can be considered as a high-energy solvate of **2** as it is evenly poised between solution and hydrate **2**. However, it is difficult to find the exact mechanism of **1**→**2** conversion as the crystal structure of **1** contains almost 3 times more water compared to **2**. To get an idea about this entire process, the packing landscape for the system $(Na^+)(sac^-)(H_2O)_n$, (n varies from 0.78 to 0.00) has been analysed (Figure 6).

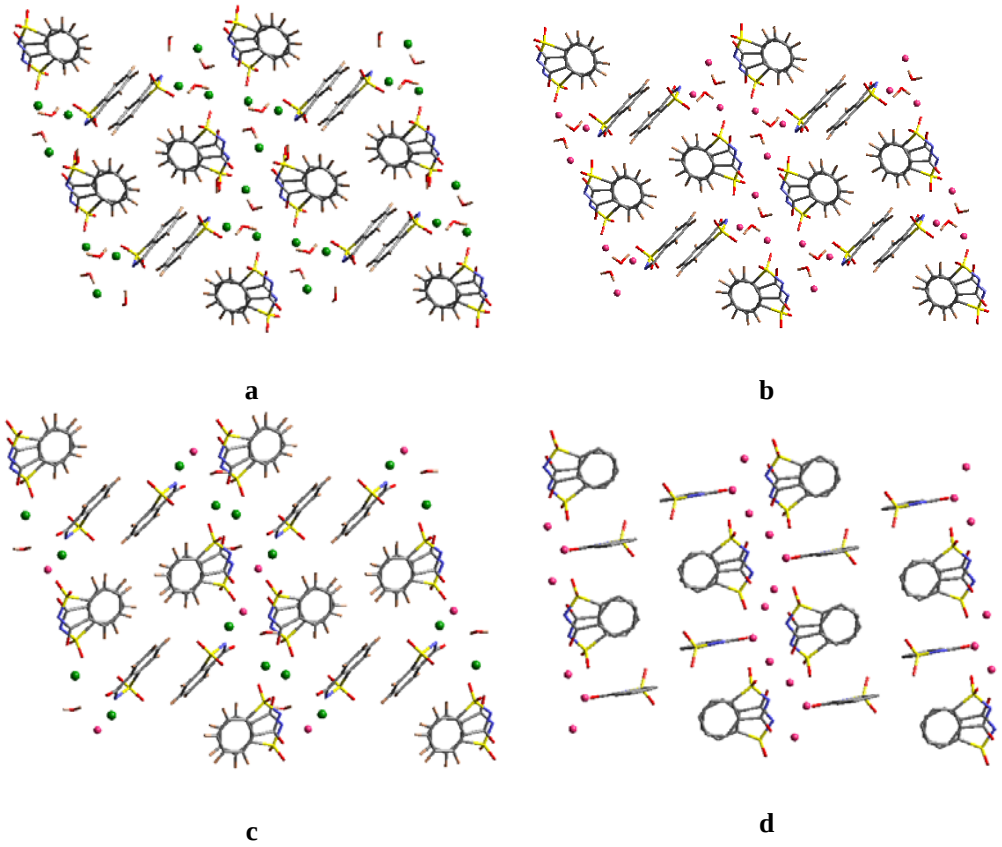

Figure 6. Packing landscape in the system (Na^+/K^+)(saccharinate$^-$)$(water)_n$, (a) water rich $(K)_3(sac)_3(H_2O)_{2.33}$, **4**, (b) Jovanovski-Kamenar hydrate, **2**, $(Na)_3(sac)_3(H_2O)_2$, (c) water poor $(Na^+)(K^+)_2(sac^-)_3(H_2O)$, **3**, (d) anhydrate, $(Na)(sac^-)$. Notice the similarity in packing in these cases. Na^+/K^+ ions are shown as red/green solid spheres.

7.4.1 Crystal structure of Na_3 (saccharinate)$_3$ $(H_2O)_2$, 2

The unit cell of **2** (1204 Å^3, $P\bar{1}$) is much smaller compared to hydrate **1** and the number of species in the crystallographic asymmetric unit (57 atoms, 41 non-H atoms) is also less. There are 6 Na^+ cations, 6 sac^- anions and 4 water molecules in the unit cell. Although this water poor form, **2** is structurally quite different from **1**, yet one can find some resemblance between the synthons in these two hydrates (Figure 7). First synthon is comprised of strong O–H…N$^{(-)}$ interaction between one hydroxyl proton of water molecule and the nitrogen atom of sac^- ion. This synthon is basically half of the O–H…N$^{(-)}$ square synthon that is seen in hydrate **1**. The second synthon is a S═O…H–O–H…O═C hydrogen bonding synthon that interlinks two parallel sac^- anions via a water molecule. Among the notable dissimilarities between the packing of **1** and **2** is the registry of molecules in the stack. Paired sac^- anions in **1** have the SO_2 groups on the same side while in **2** each pair has an SO_2 and CO group on the same side (Figure 8).

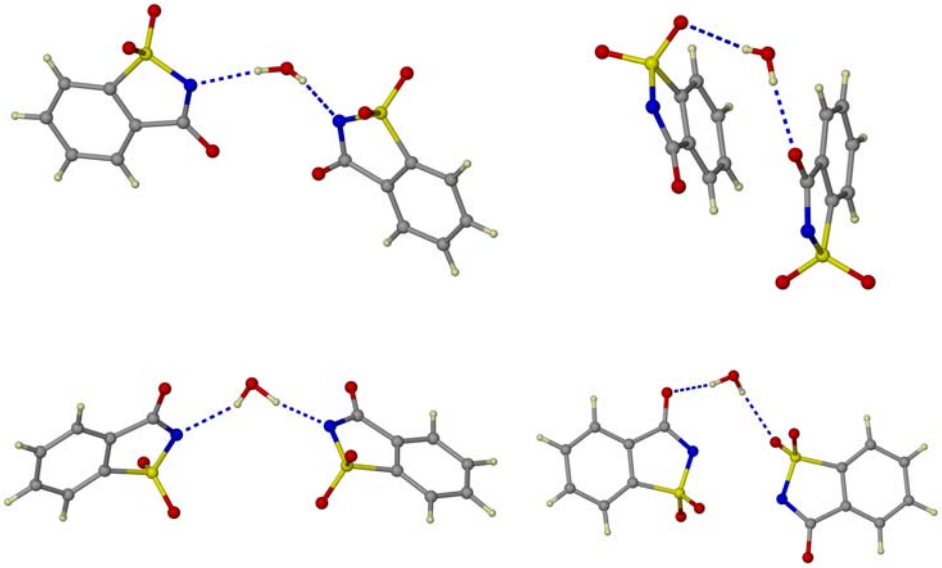

Figure 7. Conserved supramolecular synthons in dihydrate **1** (top) and the Jovanovski-Kamenar hydrate **2** (bottom).

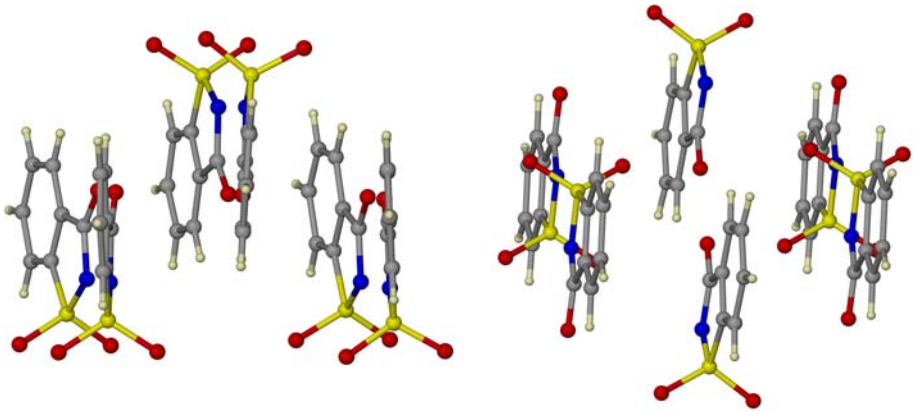

Figure 8. Orientation of SO_2 and CO groups in hydrate, **1** (left) and hydrate, **2** (right). Note that the SO_2 groups on the same side of CO group in **1** while in **2** they are in the opposite side.

7.4.2 Crystal Structure of $(Na^+)(K^+)_2(sac^-)_3(H_2O)$, 3

A mixed Na-K water-poor hydrate, $(Na^+)(K^+)_2(sac^-)_3(H_2O)$, **3**, has also been analysed. $(Na^+)(K^+)_2(sac^-)_3(H_2O)$ crystallizes in the centrosymmetric space group $P\bar{1}$ [7.11]. The unit cell is small (1260 $Å^3$) like **2** and the above formula gives the number of species in the crystallographic asymmetric unit. This structure has not been obtained for sodium saccharinate, but adopting the idea of a packing landscape it looks like a good model for the putative $(Na^+)_3(sac^-)_3(H_2O)$. There are 2 Na^+ and 4 K^+ cations, 6 sac^- anions and 2 water molecules in the unit cell. Arrangements of Na^+/K^+ cations and sac^- anions in the unit cell are similar compared to **2** (Figure 6). However, as the system becomes more water-poor, intermolecular interactions and supramolecular synthons change to some extent. Lack of H-bond donor molecules in this water-poor environment gives rise to a C═O…H–O–H…O═C supramolecular synthon (Figure 9a).

7.4.3 Crystal Structure of $(K^+)_3(sac^-)_3(H_2O)$, 4

When a mixture of saccharin and K_2CO_3 was crystallized from water, a potassium saccharinate $(K^+)_3(sac^-)_3(H_2O)_{2.33}$, **4**, was obtained [7.12]. The structure of **4** is shown in figure 6 and in keeping with the theme of a packing landscape for the system $(Na^+)(sac^-)(H_2O)_n$, it would be a very good model for a water-rich pseudopolymorph of

hydrate **2**. The unit cell volume (1365 $Å^3$) is larger when compared to the hydrates **2** and **3**. Structural analysis of **4** reveals that it contains the S═O…H–O–H…O═C supramolecular synthon that connects two sac^- anions as in hydrate, **2** (Figure 9b).

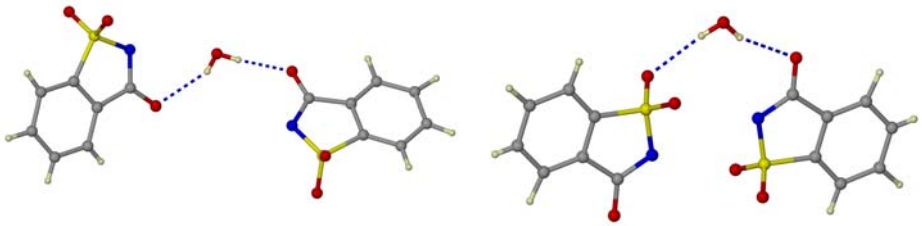

a **b**

Figure 9. Supramolecular synthons in hydrate, **3** (left) and the hydrate, **4** (right).

7.4.4 Crystal Structure of the anhydrate

Crystals of the anhydrate were obtained while cooling a melt of the commercial sample of **1** and the structure was confirmed with Rietveld refinement of the calculated powder pattern against the experimental powder pattern. The resemblance of the packing of the anhydrate to that of the hydrate **2** also provides confirmation of its structure. Arrangements of Na^+ cations and saccharinate anions in the unit cell (1212 $Å^3$) of the anhydrate closely resemble to that of hydrates **2**, **3** and **4** (Figure 6). This structure is devoid of any H–bonded supramolecular synthon due to the lack of water molecules. It is interesting to note that as the water content in the $(Na^+)(sac^-)(H_2O)_n$, system decreases, the distance between two orthogonal sac^- anions increases. This happens because more space is available in this series of closely related structures.

The exact meaning of the word 'landscape' is 'all the visible features of the area of a land' and the interpretation of the term *structural landscape* can be subjective. The crystal structures of $(Na^+/K^+)(sac^-)(water)_n$ help one to understand the structural modulations in this family of crystals and is a measure of the structural space encountered during crystallization itself. All the visible/invisible features during the crystallization of sodium saccharinate can be understood or implied from this structural

landscape. On the other hand, the landscape also represents the packing patterns of alkali metal saccharinates in general. The other constituents like Na^+/K^+ and water are supramolecular constituents and a change of stoichiometries of Na^+/K^+ and water could be termed as a supramolecular perturbation (pseudopolymorphism).

Table 1. Geometrical parameters of H- bridges of the hydrates in this study.

Hydrate	H-bridge	*d*/Å (H…A)[a]	*D*/Å (X…A)	*θ*/deg ∠X–H…A
1	O–H…O	1.83	2.794(3)	166.6
	O–H…O	1.79	2.769(3)	168.7
	O–H…O	1.97	2.946(3)	170.8
	O–H…O	1.88	2.863(3)	177.3
	O–H…O	1.87	2.857(3)	178.4
	O–H…O	1.98	2.949(3)	169.8
	O–H…O	1.93	2.902(3)	171.6
	O–H…N	1.97	2.953(3)	177.8
	O–H…N	2.11	3.073(3)	167.1
	O–H…N	1.89	2.848(3)	164.9
	O–H…N	1.87	2.838(3)	167.4
	O–H…N	1.94	2.885(3)	159.5
	O–H…N	1.88	2.850(3)	168.9
	O–H…N	1.91	2.860(3)	163.1
2	O–H…N	1.87	2.835(4)	165.8
	O–H…N	2.02	2.868(3)	142.2
	O–H…O	1.78	2.745(3)	166.9
	O–H…O	2.29	3.337(4)	162.2
	C–H…N	2.01	2.908(5)	151.4
3	O–H…O	1.98	2.847(4)	143.1
	O–H…O	1.75	2.718(4)	170.5
4	O–H…O	1.89	2.845(2)	166.1
	O–H…O	2.03	2.973(2)	159.9
	O–H…N	2.11	3.057(3)	160.8
	O–H…N	2.09	2.979(3)	149.1

[a] O–H and C–H distances are neutron normalized to 0.983, 1.083 Å.

7.5 TGA/DSC

The other unusual feature of crystalline **1** is that it loses water readily. Crystals of **1** are stable for months if stored in a closed vessel and not allowed to suffer

mechanical damage. However, if they are exposed to dry air, placed in an evacuated container or coarsely ground, they turn opaque. It is remarkable that a solid that is so deliquescent in a water-rich environment is so efflorescent in a water-poor environment like dry N_2 flow, heating or standing in the open air. TGA and DSC of **1** were carried out and it was observed that the water loss occurs in two stages (Figure 10). The first stage begins as low as 35 °C and is essentially complete by 47 °C to yield hydrate, **2**, the structure of which has been discussed earlier in this chapter. This was confirmed by X-ray powder diffraction. The second stage of water loss (**2** to anhydrate) occurs between 100 and 116 °C. Figure 11 shows that dry N_2 flow on crystalline **1** can also yield hydrate **2**. TGA experiments of different samples of hydrate, **1**, obtained from different crystallization batches always showed that the water loss occurs in two stages. It was surprising to note that at least in one case, the dehydration occurred in a single step (Figure 12). DSC scans were performed at a heating rate 0.5 ˚C min^{-1}. DSC traces show that first stage of water loss in between 35 °C and 47 °C is an overlap of two or more endotherms (Figure 13).

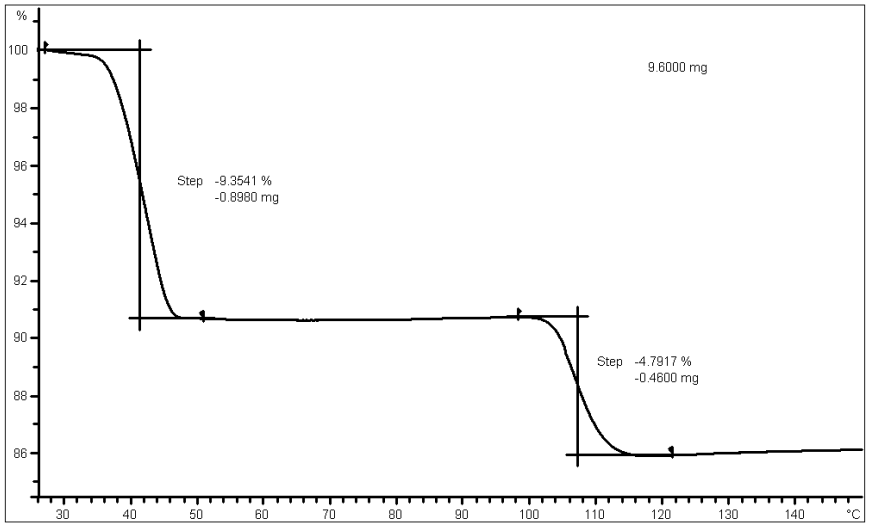

Figure 10. TGA of hydrate **1** at heating rate 0.5 ˚C min^{-1}. The first step starts at 34 ˚C and is over at 47˚ C to give the Jovanovski-Kamenar hydrate, **2**. Hydrate, **2** loses water again in the temperature range 100 to 116 ˚C to give the anhydrate.

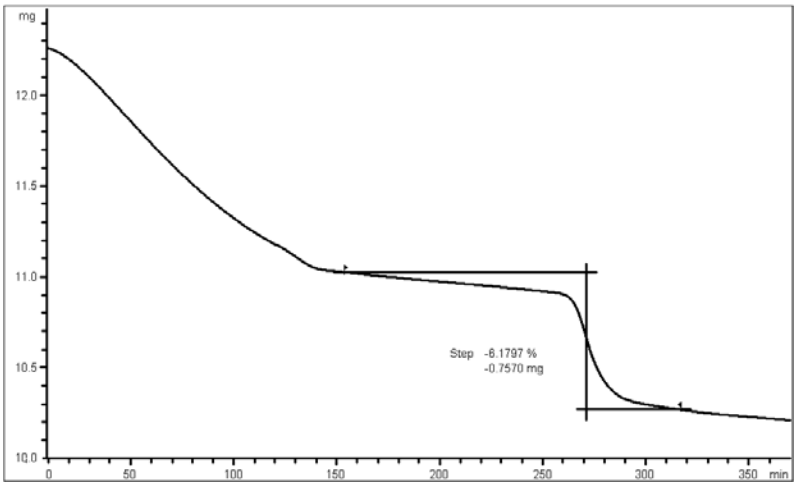

Figure 11. TGA of hydrate **1**. The first step is under dry N_2 flow (150 min) at room temperature to give the Jovanovski-Kamenar hydrate, **2**. Hydrate, **2** loses water again in the temperature range 100 to 116 ˚C to give the anhydrate.

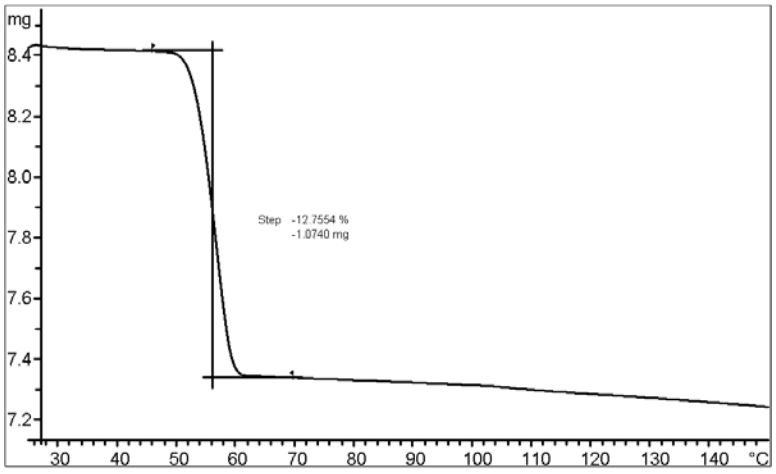

Figure 12. TGA of hydrate **1** after the watering treatment. The entire water loss occurs in a single step in the temperature range 50 to 60 ˚C to give the anhydrate.

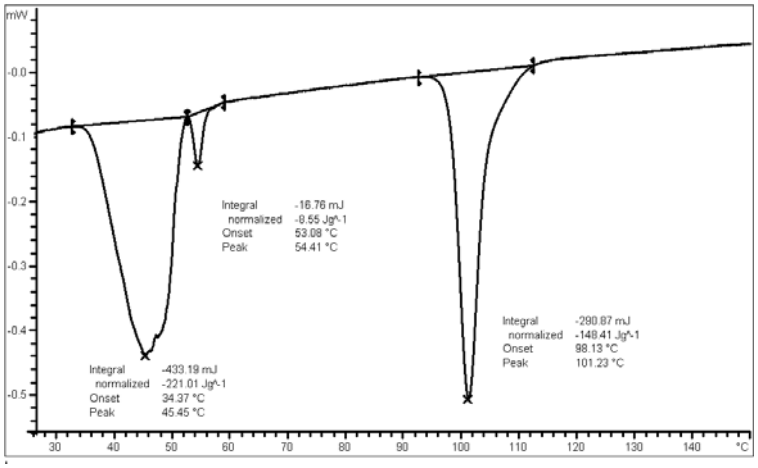

Figure 13. DSC of hydrate **1** at heating rate 0.5 ˚C min^{-1}. The first peak appears at 45 ˚C with a shoulder at 55 ˚C corresponding to the first water loss. Hydrate, **2**, again loses water at 100 ˚C to give the anhydrate.

7.6 X-ray powder diffraction

IR spectra of the sample obtained while recrystallization of sodium saccharinate from dry ethanol (procedure for preparation of hydrate, **2**) and the final spectra obtained after moderate heating of hydrate, **1** are nearly identical. X-ray powder diffraction data was collected after heating hydrate, **1** at 40 °C for 2h. To ascertain the identity and the purity of the observed phases and to investigate the phase transition, Rietveld profile fitting was performed on all the patterns collected [7.13]. The parameters refined included unit cell parameters, sample displacement, background terms, a peak shape asymmetry term, and an overall temperature factor. Rietveld refinement was performed with the co-ordinates of **2** obtained in the single crystal study against the experimental X-ray powder patterns of **1** after heating. Satisfactory refinement (R_P = 27.97, R_{wP} = 42.15) confirms the complete conversion of **1→2** (Figure 14). The second stage of water loss from **2** to anhydrate occurs between 100 and 116 °C. The crystal structure of the anhydrate has not been reported previously. Crystals of anhydrate was obtained while cooling a melt of the commercial sample. These crystals were small and poorly diffracting and the structural model obtained was of necessarily limited accuracy (R = 0.19). However, this model was confirmed with Rietveld refinement (R_P = 24.78, Rw_P =

33.91) of the co-ordinates obtained in the single crystal study against the X-ray powder patterns of the anhydrate (Figure 15).

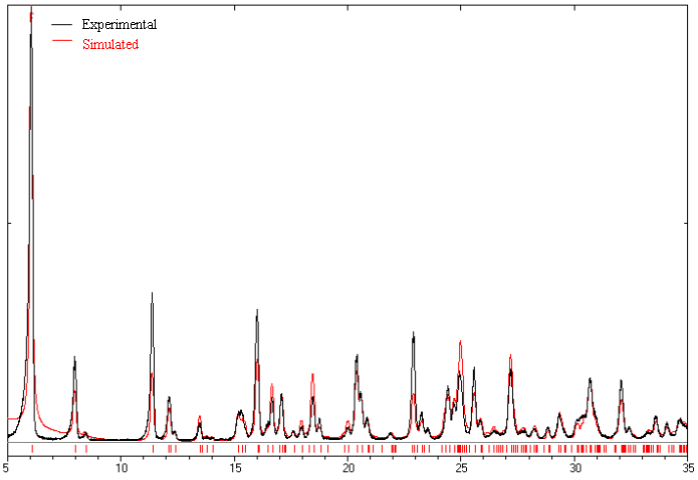

Figure 14. X-ray powder patterns of the sample obtained after heating crystals of **1** at 40 ˚C for 2 h. Rietveld refinement has been carried out with respect to the co-ordinates obtained in the single crystal study of **2**.

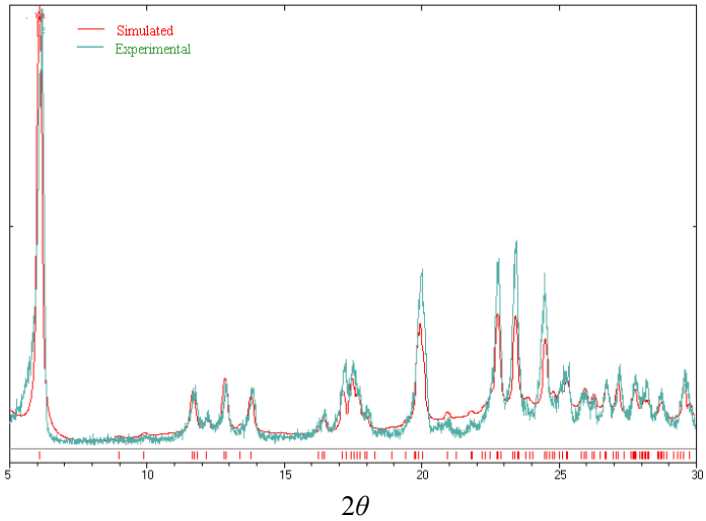

Figure 15. X-ray powder patterns of sodium saccharinate anhydrate obtained from the melt. Rietveld refinement has been carried out with respect to the co-ordinates of anhydrate.

7.7 Hot stage microscopy

Due to the role played by these water molecules in the structural cohesion, this water loss for the **1→2** conversion is likely to be accompanied by the complete change in crystal structure, which at the macroscopic level appears to be the opaqueness of the crystal.

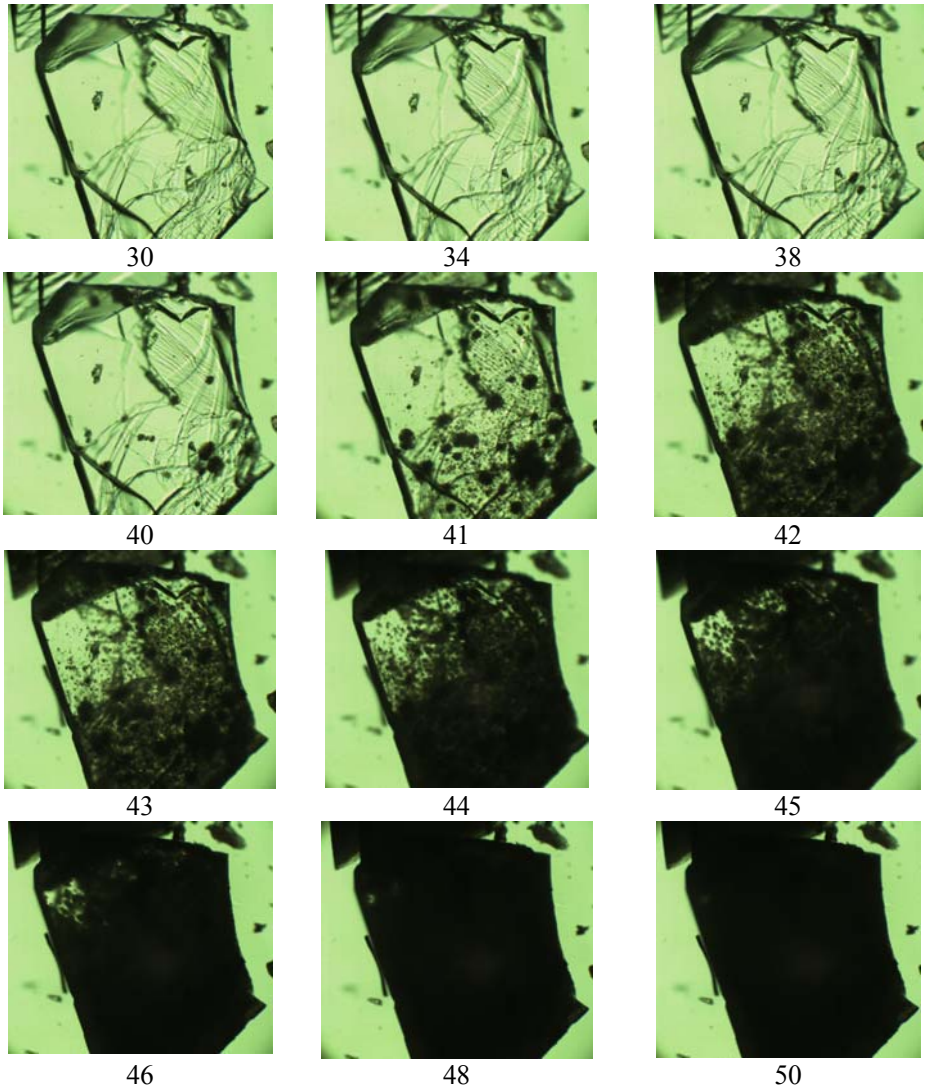

Figure 16. HSM pictures during the 1→2conversion. External features of the once opaque crystals do not change during further heating.

Although TGA and DSC emphasize that water loss form hydrate **1**, occurs in two stages, hot stage microscopy indicates that it becomes completely opaque at 50 ˚C. Further heating of the sample does not change the external nature of the crystals. Samples were loaded on a glass slide, placed on the hot bench of a Kofler hot stage microscope (Wagner and Munz) and heated at a rate of 1˚C min^{-1}. The snapshot pictures below represent the phase change of hydrate **1** up to 50˚C. The numbers refer to the temperature in °C.

7.8 Transformation between hydrates 1→2

In summary, the four structures listed so far (**2**, **3**, **4**, anhydrate) are all very similar. In every case, the positions of Na^+/K^+ and sac^- ions are almost same, and there are variable amounts of water, ranging from 0.78 water molecules per formula unit of metal saccharinate in **4**, to 0.66 in hydrate **2**, to 0.33 in the mixed Na-K hydrate **3**, to zero in the anhydrate. The structure of dihydrate **1**, which has 1.875 formula units of water per formula unit of sodium saccharinate, is quite different from these four, which constitute a related set. Therefore, the transformation of structural significance is the loss of water from **1** to form the Jovanovski-Kamenar hydrate **2**.

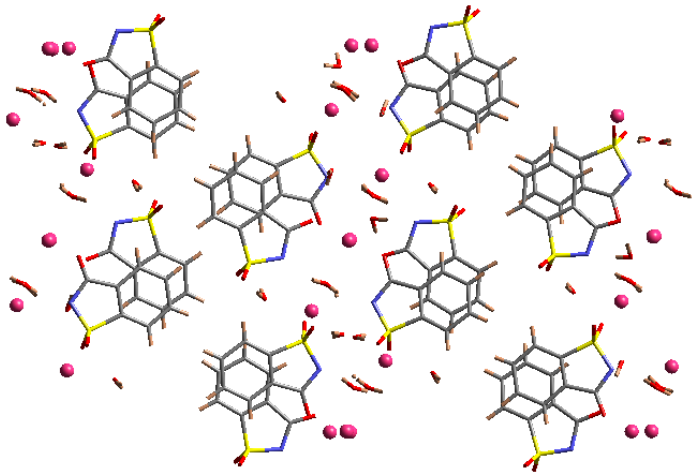

Figure 17. Crystal structure of dihydrate **1**, looking down the stacking direction.

Inspection of the crystal structures of **1** and **2** (Figures 17, 6b) shows that while the sac^- residues in **1** are all nearly parallel, those in **2** occur in two groups that are perpendicular to each another. The stacking of residues in the infinite stack down [001] bears a close resemblance to that in the regular domains of hydrate **1**. The metal ions and the water molecules fill up the space between these stacked saccharinate columns. The residues that occur as discrete dimers in **2**, perpendicular to the infinite stack, are in a stoichiometry that is half of the residues in the infinite stack. This 2:1 stoichiometry of residues in **2** is reminiscent of the 5:3 demarcation of sac^- residues in the regular and irregular regions of dihydrate **1**, and is suggestive of a possible mechanism for the **1**→**2** conversion. Water loss from the infinite channels in water-rich **1** would allow for the relative motion between stacks. Removal of the loosely bound water molecules from the unit cell of hydrate, **1** during the first step, induced either by heating or by evacuation, causes the saccharinate ions to slide out of the stacks, presumably in the direction of their sulfonyl functional groups and towards the voids produced by the leaving water molecules. The cartoon depiction of events (Figure 18) is a good possibility because it is being proposed that maximum movement of residues occurs in those regions of **1** where the arrangement is the least regular and where molecular motion is already expected to be facile. This sliding possibly results in differentiation of the saccharinate ions into two groups, which differ in their distances to the metal. DSC result indicates that even the water molecules in the "disordered" or "less ordered" region can be demarcated into different parts. Some are more disordered and some are less. This is probably the reason why the DSC endotherm for the first stage of water loss shows an overlap of two or more endotherms. Additionally, it is noted that selected supramolecular synthons in dihydrate **1** are retained in the Jovanovski-Kamenar hydrate. The stacked synthons in the regular domains of **1** are preserved as mentioned above. Hydrogen bonded synthons in the irregular domains of **1** are also conserved in **2** (Figure 7). The fact that these synthons are carried over into **2** even as there is much structural reorganization is in keeping with the idea of synthons as kinetically significant units that are preserved through all stages of crystallization [7.14].

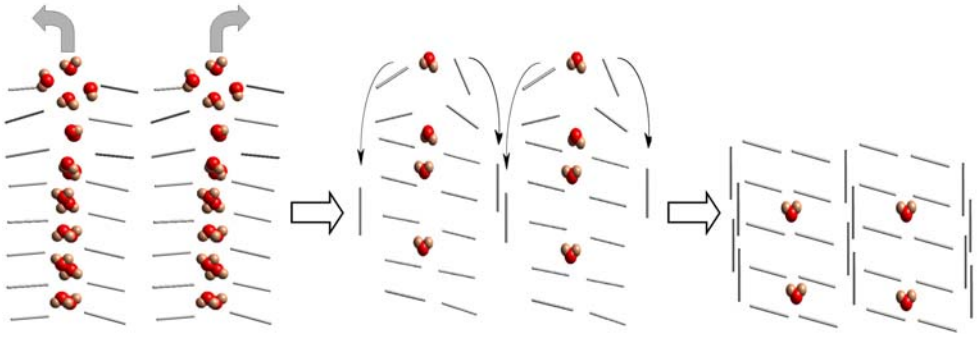

Figure 18. Transformation between hydrates **1**→**2**. Notice that all sac^- anions are nearly parallel in **1** while they adopt two orientations in **2**.

To summarize, one can say that the key step of the dehydration process of hydrate, **1** is the cooperative departure of water molecules along the channels in between the saccharinate layers. Smooth dehydration conditions here allow a departure of water molecules from hydrate, **1**, followed by a structural reorganization step leading to the nearest possible crystalline packing i.e. hydrate, **2**. Moreover, it can be stated that the resulting packing of **2** is determined by the way in which water loss occurs in the initial hydrated structure. So a part of the structural information is preserved, although the gross packing in **2** is different from **1**. When dehydration is induced by heating/grinding, the reorganization of the sac^- ions results in the formation of the hydrate, **2**. Further heating is required to induce the phase transformation towards the stable anhydrous form.

The very easy solubility of **1** in water, the retention of crystallinity of the watered crystal and the rapid recrystallization of the just dissolved crystal, when taken along with the high water content of **1** and the presence of the irregular disordered domains in it indicate a crystal that is very close to the dissolution point. At the same time, the easy loss of water from **1** (water loss from hydrate at 34 °C is very uncommon) and its conversion to **2** indicates that hydrate **1** is a species that is poised between the solution and hydrate **2**. Although **1** is technically speaking, a hydrate, its unusual structure and equally facile water loss and water gain indicates that it is closer to a crystal nucleus than has been observed previously. It is noted that the solubility of hydrate **1** at 27 °C is 120.3 g in 100 g water [7.15]. This is equivalent to a stoichiometry

of $(Na^{+})(sac^{-})(H_2O)_{13}$. Accordingly, the saturated solution of the substance contains only about seven times the amount of water as crystalline **1**.

7.9 CSD study

A CSD search [1.18] was performed (Version 5.26, May 2005) for large unit cells and 592 hits where found where the unit cell volume is greater than 10000 Å^3.

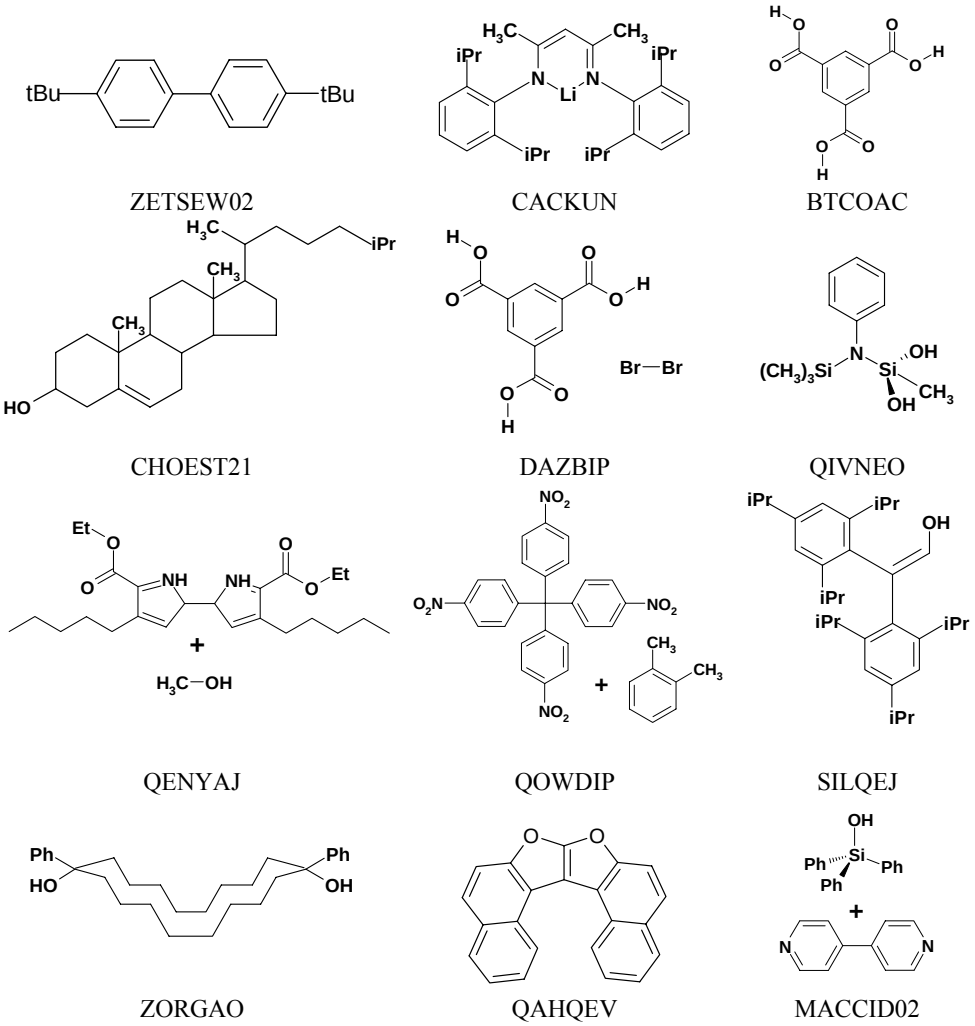

Scheme 1. Schematic drawing of some small molecules that adopt the low symmetry space groups yet posses a cell volume higher than 10000 Å^3.

Of these, only a handful correspond to cases where small molecules adopt low symmetry space groups (typical examples are MACCID02, QOWDIP and ZETSEW02). The molecular structures of some of these compounds are given in Scheme 1. Figure 19 shows the histograms of number of molecules vs unit cell volumes of 592 large crystal structures.

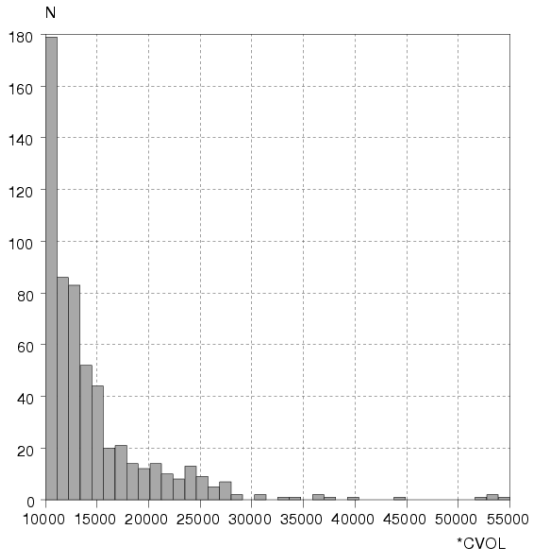

Figure 19. Histogram of number of molecules vs. unit cell volumes of 592 large crystal structures.

The CSD search gives some hints about these high Z′ structures. Firstly, one can say that high Z′ often leads to high unit cell volume but not necessarily vice versa. However, it is to be noted that a high symmetry space group or a high molecular size can also lead to high unit cell volume. Among these high Z′ structures, only a few have large volume, small constituents and low symmetry space groups. Scheme 1 gives the molecular structures and table 2 gives the relevant crystallographic information of those small molecules that adopt low symmetry space groups and yet have a unit cell volume greater than 10000 $Å^3$. It is interesting to note that disorder is quite common among these latter structures. Similarly, there is no lower Z′ equivalent of the same structure (except MACCID02) to understand if these crystal structures really represent stages in a pathway towards more stable crystals or not.

Table 2. Crystallographic information of some small molecules that adopt the low symmetry space groups yet posses a cell volume higher than 10000 Å^3

Refcode	Space group	Cell Volume	Z'	R-factor	Disorder
ZETSEW02	$C2/c$	20407.2	6	8.8	√
CACKUN	$P2_1/c$	17022.3	6	8.9	√
BTCOAC	$C2/c$	11557.7	6	6.9	√
CHOEST21	$P\bar{1}$	10151.2	16	6.4	√
DAZBIP	$C2/c$	11584.8	6	11.1	√
QIVNEO	$P2/c$	12155.5	6	8.7	-
QENYAJ	$P2_1/n$	10707.8	4	12.4	√
QOWDIP	$C2/c$	11815.4	1	7.6	-
SILQEJ	$P2_1/c$	12339.7	4	9.9	-
ZORGAO	$P2_1/n$	10826.2	4	7.6	√
QAHQEV	Cc	11564.8	8	10.1	√
MACCID02	$P\bar{1}$	13671.3	4	14.2	√

The appearance of high Z′ crystal structures has been noted and discussed regularly. The occurrence of high Z′ structures among alcohols and phenols has been rationalised by Brock and Duncan [7.16]. A very important account in this respect is by Steed, who has made valuable comments on several aspects of the phenomenon [1.46]. Nangia and co-workers in their recent study of polymorphism of 4,4-diphenyl-2,5-cyclohexadienone have noted that the strength of C–H…O interactions in promoting $Z' > 1$ for flexible molecules expands the prototype examples of alcohols and phenols to new categories of crystal structures stabilized by weak hydrogen bonds [1.47]. It is however, Desiraju, who has suggested that the high Z′ structures are often pseudosymmetric with the multiple molecules in the asymmetric unit being sometimes related to each other by local symmetry elements. So such crystals may represent stages in a pathway towards more stable crystals where the symmetry is more neatly expressed. According to him " From the crystallographic viewpoint, the very occasional appearance of large unit cells, possibly with solvent incorporated in the structure and the presence of multiple molecules in the asymmetric unit (Z′>1) is reflective of 'frozen' or interrupted crystallization" [1.45d]. It is interesting to note that these high Z′ structures mentioned above are often found as disordered or solvated. Solvation can be termed as "interrupted

crystallization". However it is difficult to interpret if structural disorder is related to the crystallization or not.

7.10 Conclusions

It is well known that many aspects of the crystallization process are still in the realm of conjecture, although there have been some attempts to monitor directly the early stages of crystallization via different experimental methods. The structure of hydrate, **1** is a good model for nucleation in the crystallization of the hydrate, **2** from water. Dihydrate, **1** is an unusual metastable hydrate that is structurally related to both the solution and to the more stable crystalline sodium saccharinate hydrates, **2-4** and to the anhydrate. The present chapter illustrates that the understanding of the nucleation and crystallization mechanism requires detailed and accurate investigations, using a combination of complementary techniques associated with structural data. The crystal structure of **1** represents as good an approximation to what a crystal nucleus looks like, as can be obtained presently [7.17]. Remarkably, a species that is in such delicate equilibrium with the solution is able to diffract so well. This is because of the rigidity that is imparted to the system by the several hydrogen bonds and Na^{+}…O interactions formed by water [7.18]. Indeed, the very existence and easy observation of this unique structure owes to the presence of the large excess of water. In summary, dihydrate, **1** appears to be a good model for the structure of a nucleus in the crystallization reaction. The work described in this chapter also shows that the elements of long-range order are likely to be present in crystal nuclei, at least the ones that correspond to late transition states. Further investigations are in progress, with new structural data, to study the influence of various physical parameters on the thermal behaviour of these saccharinates, and to improve the characterization of the new solvates.

7.11 Experimental section

Crystallization

In all experiments the components were well ground and dissolved in appropriate solvents. Melting points were recorded on Fisher–Johns apparatus and also

calculated from the onset temperature of endotherm in DSC. All these compounds were characterized with IR (Jasco 5300) spectra. Experimental photographs for the watering treatment were taken from a Leica optical microscope using a digital camera. Interval between each snapshot was kept at ~10 seconds.

$(Na^+)_{16}(sac^-)_{16}(H_2O)_{30}$, 1 : Crystals of dihydrate, **1** were grown from a saturated solution sodium saccharinate in water at room temperature. The commercial sample available in the market is identical to **1** and crystals could also be selected easily from the commercial sample for X-ray work. M.p. 363 ºC; IR (KBr): 3485, 3361, 3161, 1690, 1404, 1236, 1032, 852, 653 cm^{-1}.

$(Na^+)_3(sac^-)_3(H_2O)_2$, 2 : Crystals of hydrate, **2** were grown from a saturated solution of commercially available sodium saccharinate in dry ethanol at room temperature. M.p. 364 ºC; IR (KBr): 3390, 3361, 3869, 1690, 1404, 1236, 1032, 852, 653 cm^{-1}.

$(K^+)_3(sac^-)_3(H_2O)_{2.33}$, 4 : When a mixture of saccharin and K_2CO_3 crystallized from water, a potassium saccharinate $(K^+)_3(sac^-)_3(H_2O)_{2.33}$, **4**, was obtained. M.p. 346 ºC; IR (KBr): 3385, 3161, 1686, 1404, 1236, 1032, 852, 653 cm^{-1}.

$(Na^+)_3(sac^-)_3$: Crystals of anhydrate was obtained while cooling a melt of the commercial sample. M.p. 364 ºC; IR (KBr): 3161, 1686, 1404, 1236, 1032, 852, 653 cm^{-1}.

Thermal analysis

Differential scanning calorimetry (DSC) was performed on Mettler Toledo DSC 822e module and Thermogravimetry (TG) was performed on Mettler Toledo TGA/SDTA 851e module. Crystals taken from the mother liquor were blotted dry on filter paper and placed in open alumina pans for TG experiment and in crimped but vented aluminum sample pans for DSC experiment. Sample size in each case was 5-10 mg. The temperature range was typically 25-250 °C at a heating rate of 0.5 °C min^{-1}. The samples were purged with a stream of nitrogen flowing at 150 mL min^{-1} for DSC and 50 mL min^{-1} for TG.

X-ray crystallography

The X-ray data of dihydrate **1**, hydrates **2**, **3**, **4** and anhydrate were collected at the University of Hyderabad. Intensity data were collected on a Bruker Nonius Smart Apex CCD with graphite monochromated Mo-K_α radiation at 100K 150K, 200K and 298K [2.7]. The structures were solved by direct methods and refined anisotropically by full-matrix least-squares method using the Shelxtl 6.14 software package [2.8]. The relevant crystallographic information is given in the appendix.

X-ray powder diffraction

Powder X-ray diffractions (PXRD) were recorded on a PNAlytical 1830 (Philips Systems Inc) diffractometer using Cu K_α X-radiation at 35 kV and 25 mA. Diffraction patterns were collected over a range of 5-45 °2θ at a scan rate of 1 °2θ min^{-1}. The software Powder Cell 2.3 was used for Rietveld refinement.

Hot stage microscope

A Kofler hot stage microscope (Wagner and Munz) was used. The temperature and heating rate were monitored by a digital thermometer. Pictures were taken by a digital camera attached to the microscope and processed with the Motic software.

Calculations

All calculations were carried out on Indigo Solid Impact and Indy workstations from Silicon Graphics [2.9]. All interatomic distances and related calculations were carried out with the PLATON programme [2.10].

CHAPTER EIGHT
SUMMARY AND OUTLOOK

The crystal structure determines key solid-state properties such as bioavailability, stability and dissolution rate of pharmaceutical solids, performance of electronic and microporous materials and non-linear optics. Hence, predicting and understanding the phenomenon of crystallization is of great scientific and technological importance. However, it is quite difficult to understand the molecular self-assembly processes that occur at the time of nucleation. As a result, the ability to monitor the nucleation process experimentally during crystallization still remains a distant goal despite an intensive worldwide effort. In this regard, I feel that structural analysis of solvated crystals is a good choice to understand crystal nucleation, because solvation is an interruption of the crystallization process. A considerable amount of work has been done so far to monitor different physiochemical aspects of solvated crystals. However, there has been almost no effort till date to analyze the crystal structures of solvates in terms of these supramolecular synthons to understand the crystallization process itself. Throughout this thesis, I have tried to draw connections between molecular aggregation in solution, the nature of intermolecular interactions in the nucleation stage and the supramolecular synthons in the resulting crystal. It is well known that the formation of an unsolvated crystal from solvent requires that solute–solvent interactions be replaced by solute–solute interactions. Accordingly, strong solute–solvent interactions may lead to nucleation of solvated crystals. So structural analysis of solvated crystals could give us a hint about the packing landscape during crystal nucleation that ends in an unsolvated crystal structure.

In Chapters 2 and 3, synthon robustness, solid-state architecture, the existence of weak intramolecular interactions and their effects in modulating a supramolecular synthon in a series of substituted *gem*-alkynols are described. The *gem*-alkynols are known for their supramolecular inconsistency because of the juxtaposition of two hydrogen bond donors (O–**H**, C≡C–**H**) and two hydrogen bond acceptors (**O**–H, **C≡C**–

H) in the same C-atom. In these two chapters, the crystal structures of 24 cyclic and fused ring *gem*-alkynols have been analysed to explore the relationships between molecular functionality and crystal packing. Also, various features of a rare intramolecular O–H…Cl–C interaction have been studied using crystallographic, spectroscopic and computational methods. The hydrogen bonds are arranged in most of these structures to give two centrosymmetric synthons, which are noteworthy for their robustness. A new synthon, which is a hybrid of these two centrosymmetric synthons, is also observed. It has been observed that chloro substitution is, in general, more aggressive than methyl substitution and that almost all of the Cl-substituted compounds contain an entirely different synthon compared to these previously observed synthons. The O–H…Cl–C interaction fares surprisingly well in this family of compounds even in the presence of competing stronger acceptors. It is noteworthy that large synthons like **I**, **II** and ***H***, which occur frequently, constitute the most useful structural domains in this crystal family. Overall, the crystal structures described in these chapters show an unusual degree of modularity for compounds that generally form interactions that are weak and variable.

The factors, which have been described in Chapters 2 and 3 are the key elements to understand the solvation phenomenon and this has been detailed in Chapters 4, 5 and 6. The discussion starts with the molecule 15DDDA that has an inversion centre as the only molecular symmetry element and yet the molecule does not occupy this site symmetry in the crystal (space group $P2_1/n$). The reason for this very unusual occurrence is the crowded environment of the hydrogen bond donors and acceptors that leads to less than optimum hydrogen bonding. Based on the hypothesis that hydrogen bonding is less than satisfactory in the crystal structure of this compound, pseudopolymorphs have been prepared with strong hydrogen bond accepting solvents like dipolar aprotic and amine solvents. In the crystal structures of different pseudopolymorphs of 15DDDA, the molecule is able to occupy an ***i*** site and form strong and linear O–H…O, O–H…N and N–H…O hydrogen bonds with the solvent molecules. This sufficiently uncommon occurrence is discussed in detail in Chapter 4. Competition experiments show that a

smaller solvent molecule with a greater hydrogen bond accepting ability is included more readily and that the hydrogen bonds formed are correspondingly better.

In Chapter 5, a unique observation of both gauche and staggered rotamers of diethylamine, in two distinct 1:1 solvates of the host compound, *cis*-15DDDA are described. In both solvates, there is an infinite cooperative array of O–H…N–H…O–H…O interactions between the solute and the solvent. The energy difference between two conformers, is of the order of ~ 4 kJ mol^{-1}. These conformational pseudopolymorphs appear concomitantly and these crystal structures are the first example of solvates in which both stable and unstable conformations of a solvent have been reported within the same host.

Chapter 6 describes the crystal structures of 12 solvates of the saccharin salt of the anti-impotency drug sildenafil (Viagra). A mixture of crystalline and amorphous forms of sildenafil saccharinate (**SS**) was prepared by grinding 1:1 molar proportions of sildenafil and saccharin, and this mixture crystallizes while heating. All the inclusion complexes of **SS**, except the one with methanol, are isostructural. Various host–guest C–H…O or O–H…O interactions stabilize the structures. The hexagonal cage structure of host atoms in all these solvates is stabilized by a 14 membered supramolecular synthon. The host/guest stoichiometry determined from the X-ray structure matches with the ratio from weight loss in TGA for all solvates except the MeOH solvate. The MeOH solvate has a different crystal packing in space group *C*2/*c*, wherein two methanol molecules interleave between a $(sildenafil)^{+}$ cation and a $(saccharin)^{-}$ anion.

It is well known that crystallization begins with solute–solvent aggregates that contain solute–solute, solute–solvent and solvent–solvent interactions. However, during the final stages of crystallization, the entropic gain in eliminating solvent molecules from these aggregates into the bulk solution, and the simultaneous enthalpic gain in forming stable solute species that contain robust supramolecular synthons leads to the solvent free crystals. Crystallization of 15DDDA, *cis*-15DDDA and **SS** apohost will come into this category. Now, if a solvent is trapped inside the crystal lattice, say because of multipoint recognition between the solute and the solvent, what we get is a solvate or pseudopolymorph. Using the concept of the Bürgi-Dunitz [2.4a] type of structure

correlation, one can say that these solvated crystals are an image of an interrupted crystallization and that they give us an idea as to how a solute–solvent cluster may look like during the early stages of crystallization. We can understand structural aspects of solvation by studying solid-state architecture of different pseudopolymorphs in the *gem*-alkynol family. These pseudopolymorphs also give us an idea of different packing possibilities during the early stages of crystallization.

The crystal structure of sodium saccharinate dihydrate, **1** that has been described in Chapter 7 essentially validates these ideas. This complex structure has several unusual features, which could have implications for the mechanism of crystallization. Structural analysis reveals that the stoichiometry of the material is $(Na^+)_{16}(sac^-)_{16}(H_2O)_{30}$. The asymmetric unit has 362 atoms and much water, and the crystal contains ordered and disordered regions. Before this thesis, the X-ray crystal structures of only $(Na^+)_3(sac^-)_3(H_2O)_2$, **2**, and the mixed salt $(K^+)_2(Na^+)(sac^-)_3(H_2O)_2$, **3**, were reported. In this chapter, the crystal structures of $(K^+)_3(sac^-)_3(H_2O)_{2.33}$, **4**, and anhydrous sodium saccharinate have also been described. Together, these structures give an idea of packing landscape of saccharinate anion during crystallization. The unusual feature of hydrate, **1** is that it can exist in equilibrium with water and that it dehydrates in two stages. The first stage occurs between 35-47 °C to yield hydrate **2**. The second stage of water loss (**2** to anhydrate) occurs between 100 and 116 °C. Further, there are only a handful of structures reported in the CSD that correspond to cases where small molecules adopt low symmetry space groups. The present structure is therefore unique.

The terminology for the description of solid-state molecular structures is unsatisfactory, even for single component systems. In this thesis, I tried to address some terminology and nomenclature issue. Consideration of the multitude of structures displayed by the solvates listed in Nangia and Desiraju's paper raises the question as to whether the present nomenclature is even less adequate for the greater complexity inherent in two-component systems [1.49]. There has been considerable recent debate and discussion in *Crystal Growth & Design* on the use of the word *pseudopolymorph*. This debate has started after Desiraju's article in *CrystEngComm*, where he mentioned his acceptance of the term *pseudopolymorph* [5.8a]. Seddon then argued that the words

pseudopolymorph and *pseudopolymorphism* are incorrect and should be avoided [5.8c]. Desiraju's reply to Seddon's comment was that pseudopolymorphism is still the best of all possible names [5.8d]. The next article during this exchange of comments was by Bernstein who agreed with Seddon that the term *pseudopolymorph* was a misnomer [5.8e]. It is, however, Nangia, who explains that the meaning of these words are clear enough to a room full of researchers from several related fields of crystal engineering, pharmaceutical R&D, crystallography, materials science and biochemistry [5.8f]. He has correctly emphasized that "Even if a different name is agreed upon (say solvate) through some consensus there is no guarantee that chemists will switch to that name because they are by now very familiar with the terms *pseudopolymorph* and *pseudopolymorphism*". Several authors like Haleblian, McCrone, Dunitz and Threlfall, have argued against the use of the term *pseudopolymorphism* [5.11]. In spite of their objections to the use of the term *pseudopolymorphism* to describe solvated structures of a material, the term seems to have gained in general acceptance, especially in the pharmaceutical industry both in characterization and production/processing aspects [5.12]. This gives an idea that the most important reason for retaining the term *pseudopolymorph* is now more than merely scientific. The term now has entered into the legal lexicon in recent court battles involving major pharmaceutical companies and this is emphasized by Nangia.

There is some similarity in the usage of the terms *pseudopolymorph* and *cocrystal*. Both these terms gained easy acceptance although both of them have their own scientific limitations. Desiraju feels that both these terms *pseudopolymorph* and *cocrystal* are not totally correct. However, he maintains that the former contains more scientific virtues than the latter and that is why the term *pseudopolymorph* should stay whereas the term *cocrystal* should at least be modified to *co-crystal* if not totally avoided. I feel that terms like *host–guest compounds*, *clathrates*, *inclusion compounds,* and *pseudopolymorphs* cannot be immediately replaced by the term *solvate* although they come under the common umbrella of solvation. Each of these terms signifies something different compared to the others and the term *solvate* alone cannot cover all these facts. Desiraju states "…. if something is scientifically suspect it must go, howsoever popular it might be. What is easy is sometimes not what is best" [5.8a]. Yet, I feel that both these

terms *pseudopolymorph* and *cocrystal* will stay on because scientists are now used to these two terms. All we can and should do is to watch that in future things get as clear as possible while using these terminologies.

An important aspect of crystal engineering is to understand and attempt to control the manner in which molecules are arranged in the crystal lattice through supramolecular synthons. An effort has been made throughout this thesis to use the idea of the supramolecular synthon to understand the packing landscape during crystallization. To summarize, it could be said that future research in this area should be directed to obtain even more control over the understanding of the self-assembly of molecules during the all-important early stages of crystallization.

List of Publications

1. Dilemmas in crystallization. The 'unusual' behaviour of *trans*-1,5-dichloro-9,10-diethynyl-9,10-dihydroanthracene-9,10-diol and the more 'normal' behaviour of its pseudopolymorphs with dipolar aprotic solvents.
   Rahul Banerjee, Gautam R. Desiraju, Raju Mondal, Andrei. S. Batsanov, Charlotte K. Broder and Judith A. K. Howard
   Helv. Chim. Acta, **2003**, 86, 1339-1351.

2. Organic chlorine as a hydrogen-bridge acceptor. Evidence for the existence of intramolecular O–H…Cl–C interactions in some *gem*-alkynols.
   Rahul Banerjee, Gautam R. Desiraju, Raju Mondal and Judith A. K. Howard
   Chem. Eur. J., **2004**, 10, 3373-3383.

3. Gauche and staggered forms of diethylamine in solvates of 1,5-dichloro-cis-9,10-diethynyl-9,10-dihydroanthracene-9,10-diol. A case of conformational pseudopolymorphism?
   Raju Mondal, Judith A. K. Howard, **Rahul Banerjee** and Gautam R. Desiraju
   Chem. Commun., **2004**, 644-645.

4. (4-Ethynylphenyl)methoxymethanimine
   Archan Dey and Rahul Banerjee
   Acta Cryst. **2004**, E60, o2117-2118.

5. Hexagonal host framework of *sym*-aryloxytriazines stabilised by weak intermolecular interactions.
   Binoy K. Saha, Srinivasulu Aitipamula, **Rahul Banerjee**, Ashwini Nangia, Ram K. R. Jetti, Roland Boese, Chi-Keung. Lam and Thomas C. W. Mak
   Mol. Cryst. Liq. Cryst. **2005**, 440, 295-316.

6. Saccharin as a salt former. Enhanced solubilities of saccharinates of active pharmaceutical ingredients.
   Prashant M. Bhatt, Nittala V. Ravindra, **Rahul Banerjee** and Gautam R. Desiraju
   Chem. Commun., **2005**, 1073-1075.

7. Structural studies of the system Na(saccharinate)•*n* (H_2O): A model for crystallization
   Rahul Banerjee, Prashant M. Bhatt, Michael T. Kirchner and Gautam R. Desiraju
   Angew. Chem. Int. Ed., **2005**, 44, 2515-2520. (VIP)

8. Saccharin salts of active pharmaceutical ingredients, their crystal structures, and increased water solubilities.
   Rahul Banerjee, Prashant M. Bhatt, Nittala V. Ravindra and Gautam R. Desiraju.
   Cryst. Growth & Design, **2005**, 5, 2299-2309.

9. Synthon evolution and unit cell evolution during crystallisation. A study of symmetry -independent molecules (Z´>1) in crystals of some hydroxy compounds.
   Dinabandhu Das, **Rahul Banerjee**, Raju Mondal, Judith A. K. Howard, Roland Boese and Gautam R. Desiraju
   Chem. Commun., **2006**, *5*, 555.

10. Conformational, concomitant polymorphs of 4,4-diphenyl-2,5-cyclohexadienone. Conformation and lattice energy compensation in kinetic and thermodynamic forms.
    Saikat Roy, **Rahul Banerjee**, Ashwini Nangia and Gert J. Kruger
    Chem. Eur. J., **2006** (*in press*).

11. Synthon robustness and solid state architecture in substituted *gem*-alkynols.
    Rahul Banerjee, Raju Mondal, Judith A. K. Howard and Gautam R. Desiraju
    Cryst. Growth & Design, **2006**, (*in press*).

12. Pseudopolymorphism in sildenafil saccharinate. A new host material.
    Rahul Banerjee, Prashant M. Bhatt, and Gautam R. Desiraju
    (*in preparation*)

13. Crystal structure of desloratadine. A tricyclic antihistaminic drug.
    Prashant M. Bhatt, **Rahul Banerjee** and Gautam R. Desiraju
    (*in preparation*)

14. A different approach of solvent-drop grinding method. Preparation of an unusually stable amorphous form desloratadine saccharinate.
    Prashant M. Bhatt, **Rahul Banerjee** and Gautam R. Desiraju
    (*in preparation*)

15. Solvent free supramolecular synthesis of some acid and amide cocrystals.
    L. Sreenivas Reddy, **Rahul Banerjee**, Prashant M. Bhatt, Gert. J. Kruger and Ashwini Nangia
    (*in preparation*)

REFERENCES AND NOTES

CHAPTER ONE

[1.1] (a) E. J. Corey and X. M. Cheng, *The Logic of Chemical Synthesis*, Wiley: New York, **1989**. (b) D. Seebach, *Angew. Chem. Int. Ed. Engl.*, **1990**, *29*, 1320. (c) K. C. Nicolaou and E. J. Sorensen, *Classics in Total Synthesis*, VCH: Weinheim, **1995**. (d) K. C. Nicolaou, D. Vourloumis, N. Winssinger and P. S. Baran, *Angew. Chem. Int. Ed.*, **2000**, *39*, 44. (e) S. J. Danishefsky and J. R. Allen, *Angew. Chem. Int. Ed.*, **2000**, *39*, 836.

[1.2] (a) G. M. Whitesides, E. E. Simanek, J. P. Mathias, C. T. Seto, D. N. Chin, M. Mammen and D. M. Gordon, *Acc. Chem. Res.*, **1995**, *28*, 37. (b) M. C. T. Fyfe and J. F. Stoddart, *Acc. Chem. Res.*, **1997**, *30*, 393. (c) M. D. Hollingsworth, *Science*, **2002**, *295*, 2410. (d) M. Morimoto, S. Kobatake and M. Irie, *J. Am. Chem. Soc.*, **2003**, *125*, 11080. (e) J. L. Atwood, L. J. Barbour and A. Jerga, *Angew. Chem. Int. Ed.*, **2004**, *43*, 2948. (f) K. Sada, K. Inoue, T. Tanaka, A. Tanaka, A. Epergyes, S. Nagahama, A. Matsumoto and M. Miyata, *J. Am. Chem. Soc.*, **2004**, *126*, 1764. (g) H. Zhao, Y. H. Li, X. S. Wang, Z. R. Qu, L. Z. Wang, R. G. Xiong, B. F. Abrahams and Z. Xue, *Chem. Eur. J.*, **2004**, *10*, 2386. (h) D. Laliberte, T. Maris and J. D. Wuest, *J. Org. Chem.*, **2004**, *69*, 1776. (i) D. K. Kumar, D. A. Jose, P. Dastidar and A. Das, *Chem. Mater.*, **2004**, *16*, 2332. (j) M. Fourmigué and P. Batail, *Chem. Rev.*, **2004**, *104*, 5379. (k) S. Iyengar and M. C. Biewer, *Cryst. Growth Des.*, **2005**, *5*, 2043. (l) S. M. Curtis, N. Le, F. W. Fowler and J. W. Lauher, *Cryst. Growth Des.*, **2005**, *5*, 2313. (m) Y. Morita, T. Murata, K. Fukui, S. Yamada, K. Sato, D. Shiomi, T. Takui, H. Kitagawa, H. Yamochi, G. Saito and K. Nakasuji, *J. Org. Chem.*, **2005**, *70*, 2739.

[1.3] (a) *Design of Organic Solids*; E. Weber, Ed.; *Topics in Current Chemistry*; Springer: Berlin, vol. 198, **1998**. (b) E. Pidcock and W. D. S. Motherwell, *Cryst. Growth Des.*, **2005**, *5*, 2232. (c) M. Du, Z. H. Zhang and X. J Zhao, *Cryst. Growth Des.*, **2005**, *5*, 1199. (d) S. Takahashi, T. Katagiri and K.

Uneyama, *Chem*. *Commun*., **2005**, 3658. (e) R. A. Weatherhead-Kloster, H. D. Selby, W. B. Miller and E. A. Mash, *J*. *Org*. *Chem*., **2005**, *70*, 8693.

[1.4] G. R. Desiraju, *Crystal Engineering*. *The Design of Organic Solids*, Elsevier: Amsterdam, **1989**. Selected other references and reviews on crystal engineering of organic molecular solids include: (a) *The Crystal as a Supramolecular Entity*: *Perspectives in Supramolecular Chemistry*, vol. 2; G. R. Desiraju, Ed.; Wiley: Chichester, **1996**. (b) *Comprehensive Supramolecular Chemistry*, J. L. Atwood, J. E. D. Davies, D. D. MacNicol and F. Vögtle, Eds.; Pergamon: Oxford, vols. 6, 7, 9, 10, **1996**. (c) *Crystal Engineering*: *From Molecules and Crystals To Materials*, D. Braga and A. G. Orpen, Eds.; NATO ASI Series Kluwer: Dordrecht, Netherlands, **1999**. (d) *Crystal Engineering*: *The Design and Application of Functional Solids*, K. R. Seddon and M. J. Zaworotko, Eds.; NATO ASI Series Kluwer: Dordrecht, Netherlands, **1999**. (e) J. W. Steed and J. L. Atwood, *Supramolecular Chemistry*, Wiley: Chichester, **2000**, *11*, pp. 389–463. (f) C. V. K. Sharma, *Cryst*. *Growth Des*., **2002**, *2*, 465. (g) *Crystal Design*. *Structure and Function*: *Perspectives in Supramolecular Chemistry,* vol. 7; G. R. Desiraju, Ed.; Wiley: Chichester, **2003**. (h) B. Kahr, *Cryst*. *Growth Des*., **2004**, *4*, 3. (i) M. W. Hosseini, *Acc*. *Chem*. *Res*., **2005**, *38*, 313. (j) D. Braga, L. Brammer and N. R. Champness, *CrystEngComm,* **2005**, *1*, 1.

[1.5] (a) J. -M. Lehn, *Angew*. *Chem*. *Int*. *Ed*., **1990**, *29*, 1304. (b) J. -M. Lehn, *Supramolecular Chemistry*: *Concepts and Perspectives*, VCH: Weinheim, **1995**. (c) G. R. Desiraju, *Nature (London)*, **2001**, *412*, 397. (d) D. N. Reinhoudt and M. Crego-Calama, *Science*, **2002**, *295*, 2403.

[1.6] (a) *Organic Solid State Chemistry*, G. R. Desiraju, Ed.; *Studies in Organic Chemistry*, Elsevier: Amsterdam, **1987**. (b) P. W. Baures, A. M. Beatty, M. Dhanasekaran, B. A. Helfrich, W. P. Segarra and J. Desper, *J*. *Am*. *Chem*. *Soc*., **2002**, *124*, 11315. (c) C. K. Broder, M. G. Davidson, V. T. Forsyth, J. A. K. Howard, S. Lamb and S. A. Mason, *Cryst*. *Growth Des*., **2002**, *2*, 163. (d) S. Zhu, C. Xing, W. Xu, G. Jin and Z. Li, *Cryst*. *Growth Des*., **2004**, *4*, 53. (e) A.

R. Choudhury and T. N. Guru Row, *Cryst. Growth Des*., **2004**, *4*, 47. (f) A. Angeloni, P. C. Crawford, A. G. Orpen, T. J. Podesta and B. J. Shore, *Chem. Eur. J*., **2004**, *10*, 3783. (g) L. S. Reddy, S. Basavoju, V. R. Vangala and A. Nangia, *Cryst. Growth Des*., **2006**, *6*, 161. (h) I. E. D. Vega, P. A. Gale, M. E. Light and S. J. Loeb, *Chem. Commun*., **2005**, 4913. (i) F. F. Said, T. G. Ong, G. P. A. Yap and D. Richeson, *Cryst. Growth Des*., **2005**, *5*, 1881. (j) P. Metrangolo, H. Neukirch, T. Pilati and G. Resnati, *Acc. Chem. Res*., **2005**, *38*, 386.

[1.7] (a) G. R. Desiraju, *Angew. Chem., Int. Ed. Engl*., **1995**, *34*, 2311. (b) C. B. Aakeröy, *Acta Crystallogr*., **1997**, *B53*, 569. (c) G. R. Desiraju, *Chem. Commun*., **1997**, 1475. (d) A. Nangia and G. R. Desiraju, *Top. Curr. Chem*., **1998**, *198*, 57. (e) A. Nangia and G. R. Desiraju, *Acta Crystallogr*., **1998**, *A54*, 934. (f) W. D. S. Motherwell, G. P. Shields and F. H. Allen, *Acta Crystallogr*., **1999**, *B55*, 1044. (g) G. R. Desiraju, *Stimulating Concepts in Chemistry*; F. Vögtle, J. F. Stoddart and M. Shibasaki, Eds.; Wiley-VCH: **2000**, pp 293−308. (h) M. J. Zaworotko, *Chem. Commun*., **2001**, 1. (i) A. F. Williams, *Supramolecular Synthons*: *Encyclopedia of Supramolecular Chemistry*, J. L. Atwood and J. Steed, Eds.; **2004**. (j) T. Gelbrich and M. B. Hursthouse, *CrystEngComm*, **2005**, *53*, 324.

[1.8] E. J. Corey, *Pure Appl. Chem.*, **1967**. *14*. 19.

[1.9] E. J. Corey, *Chem.Soc. Rev.*, **1988.** *17.* 111.

[1.10] (a) W. Vanspeybrouck, W. A. Herrebout, B. J. van der Veken, J. Lundell and R. N. Perutz, *J. Phys. Chem. B*, **2003**, *107*, 13855. (b) V. Balamurugan, W. Jacob, J. Mukherjee and R. Mukherjee, *CrystEngComm*, **2004**, *6*, 396. (c) D. R. Turner, B. Smith, A. E. Goeta, I. R. Evans, D. A. Tocher, J. A. K. Howard and J. W. Steed, *CrystEngComm*, **2004**, *103*, 633. (d) N. S. Begum, C. R. Girija, M. N. Mallya and G. Nagendrappa, *J. Mol. Struct*., **2005**, *751*, 127. (e) J. N. Moorthy, R. Natarajan and P. Venugopalan, *J. Mol. Struct*., **2005**, *741*, 107. (f) P. Rodríguez-Cuamatzi, O. I. Arillo-Flores, M. I. Bernal-Uruchurtu and H. Höpfl, *Cryst. Growth Des*., **2005**, *5*, 167.

[1.11] (a) V. R. Thalladi, B. S. Goud, V. J. Hoy, F. H. Allen, J. A. K. Howard and G. R. Desiraju, *Chem. Commun*., **1996**, *3*, 401. (b) P. J. Langely, J. Hulliger, R. Thaimattam and G. R. Desiraju, *New J. Chem.,* **1998**, *22*, 1307. (c) J. M. A. Robinson, D. Philp, B. M. Kariuki and K. D. M. Harris, *Chem. Commun.*, **1999**, 329. (d) J. M. A. Robinson, D. Philp, K. D. M. Harris and B. M. Kariuki, *New J. Chem.,* **2000**, *24*, 799. (e) P. K. Thallapally, K. Chakraborty, A. K. Katz, H. L. Carrell, S. Kotha and G. R. Desiraju, *CrystEngComm*, **2001**, *31*, 134.

[1.12] X. Gao, T. Friscic and L. R. MacGillivray, *Angew. Chem. Int. Ed*., **2004**, *43*, 232.

[1.13] (a) M. Simard, D. Su and J. D. Wuest, *J. Am. Chem. Soc.*, **1991**, *113*, 4696. (b) P. Grosshans, A. Jouaiti, V. Bulach, J. -M. Planeix, M. W. Hosseini and J. -F. Nicoud, *Chem. Commun.*, **2003**, 1336. (c) M. W. Hosseini, *CrystEngComm*, **2004**, *6*, 318. (d) M. W. Hosseini, *Chem. Commun.*, **2005**, 5825. (e) J. D. Wuest, *Chem. Commun.*, **2005**, 5830

[1.14] R. J. Davey, K. Allen, N. Blagden, W. I. Cross, H. F. Lieberman, M. J. Quayle, S. Righini, L. Seton and G. J. T. Tiddy, *CrystEngComm*, **2002**, *4*, 257.

[1.15] (a) J. A. R. P. Sarma and G. R. Desiraju, *Cryst. Growth Des*., **2002**, *2*, 93. (b) S. L. Price, *Crystal Structure Prediction*: *Encyclopedia of Supramolecular Chemistry*, J. L. Atwood and J. Steed, Eds.; **2004**. (c) A. Dey, M. T. Kirchner, V. R. Vangala, G. R. Desiraju, R. Mondal and J. A. K. Howard, *J. Am. Chem. Soc*., **2005**, *127*, 10545.

[1.16] (a) N. L. Rosi, J. Kim, M. Eddaoudi, B. Chen, M. O'Keeffe and O. M. Yaghi, *J. Am. Chem. Soc*., **2005**, *127*, 1504. (b) N. W. Ockwig, O. Delgado-Friedrichs, M. O'Keeffe and O. M. Yaghi, *Acc. Chem. Res*., **2005**, *38*, 176.

[1.17] (a) K. K. Arora and V. R. Pedireddi, *J. Org. Chem.*, **2003**, *68*, 9177. (b) A. Ballabh, D. R. Trivedi, P. Dastidar and A. Das, *Cryst. Growth Des*., **2005**, *5*, 1545. (c) M. Du, Z. H. Zhang, X. J. Zhao and H. Cai, *Cryst. Growth Des*., **2005**, *5*, 1247. (d) D. Kong, A. Clearfield and J. Zon, *Cryst. Growth Des*., **2005**, *5*, 1767. (e) S. Upreti and A. Ramanan, *Cryst. Growth Des*., **2005**, *5*,

1837. (f) M. O. Awaleh, A. Badia and F. Brisse, *Cryst*. *Growth Des*., **2005**, *5*, 1897. (g) B. R. Bhogala, P. Vishweshwar and A. Nangia, *Cryst*. *Growth Des*., **2005**, *5*, 1271.

[1.18] (a) F. H. Allen and O. Kennard, *Chem*. *Des*. *Automat*. *News*, **1993**, *8*, 31. (b) F. H. Allen, W. D. S. Motherwell, P. R. Raithby, G. P. Shields and R. Taylor, *New J*. *Chem*., **1999**, *23*, 25. (c) F. H. Allen, *Acta Crystallogr*., **2002**, *B58*, 380. (d) A. Nangia, *CrystEngComm*, **2002**, *4*, 93. (e) F. H. Allen and R. Taylor, *Chem*. *Soc*. *Rev*., **2004**, *33*, 463.

[1.19] (a) Ö. Almarsson and M. J. Zaworotko, *Chem*. *Commun*., **2004**, 1889. (b) P. Vishweshwar, J. A. McMahon and M. J. Zaworotko, *Crystal Engineering of Pharmaceutical Co-Crystals*: *Frontiers in Crystal Engineering*, E. Tiekink and J. J. Vittal, Eds.; Wiley: Chichester; UK, **2005**.

[1.20] (a) K. C. W. Chong, J. Sivaguru, T. Shichi, Y. Yoshimi, V. Ramamurthy and J. R. Scheffer, *J*. *Am*. *Chem*. *Soc*., **2002**, *124*, 2858. (b) P. R. Schreiner, *Chem*. *Soc*. *Rev*., **2003**, *32*, 289. (c) Y. Huang, A. K. Unni, A. N. Thadani and V. H Rawal, *Nature*, **2003,** *424*, 146. (d) A. Natarajan, J. T. Mague, K. Venkatesan and V. Ramamurthy, *Org*. *Lett*., **2005**, *10*, 1895.

[1.21] (a) J. Zyss and J. -F. Nicoud, *Curr. Opin. Solid State Mater. Sci*., **1996**, *1*, 533. (b) C. F. V. Nostrum and R. J. M. Notle, *Chem. Commun*., **1996**, 2385. (c) O. Kahn, *Curr. Opin. Solid State Mater. Sci*., **1996**, *1*, 547. (d) N. Bowden, A. Rerfort, J. Carbeck and G. M. Whitesides, *Science*, **1997**, *276*, 233. (e) M .J. Zaworotko, *Angew. Chem*., *Int. Ed*., **2000**, *39*, 220. (f) P. K. Thallapally, G. R. Desiraju, M. Bagieu-Beucher, R. Masse, C. Bourgogne and J. F. Nicoud, *Chem*. *Commun*., **2002**, 1052.

[1.22] (a) V. A. Russel, C. C. Evans, W. Li and M. D. Ward, *Science*, **1997**, *276*, 575. (b) K. T. Holman, A. M. Pivovar and M. D. Ward, *Science*, **2001**, *294*, 1907.

[1.23] D. J. Crouch, P. J. Skabara, M. Heeney, I. McCulloch, S. J. Coles and M. B. Hursthouse, *Chem*. *Commun*., **2005**, 1465.

[1.24] (a) G. Klebe, *J*. *Mol*. *Biol*., **1994**, *237*, 212. (b) S. Sarkhel and G. R. Desiraju, *Proteins*, **2003**, *3*, 675.

[1.25] (a) G. A. Jeffrey and W. Saenger, *Hydrogen Bonding in Biological Structures*, Springer: Berlin, **1991**. (b) D. Hadzi, *Theoretical Treatments of Hydrogen Bonding*, Wiley: Chichester, **1997**. (c) G. A. Jeffrey, *An Introduction to Hydrogen Bonding*, Oxford University Press: Oxford, **1997**. (d) G. R. Desiraju and T. Steiner, *The Weak Hydrogen Bond in Structural Chemistry and Biology*, Oxford University Press: Oxford, **1999**. (e) T. Steiner, *Angew. Chem. Int. Ed. Engl.*, **2002**, *41*, 48. (f) J. Martz, E. Graf, A. D. Cian and M. W. Hosseini, in *Crystal Design and Function, Perspectives in Supramolecular Chemistry*, vol. 7, G. R. Desiraju, Ed.; Wiley: Chichester, **2003**, pp. 177-209.

[1.26] (a) R. E. Meléndez and A. D. Hamilton, *Topics in Current Chemistry*, "*Design of Organic Solids*", vol. 198, E. Weber, Ed.; **1998**, pp 97-130. (b) G. T. R. Palmore and J. C. MacDonald, *The Amide Linkage*: *Selected Structural Aspects in Chemistry, Biochemistry, and Materials Science*, A. Greenberg, C. M. Breneman and J. F. Liebman, Eds.; Wiley: New York, **2000**. (c) J. N. Moorthy, R. Natarajan, P. Mal and P. Venugopalan, *J. Am. Chem. Soc.*, **2002**, *124*, 6530. (d) P. W. Baures, J. R. Rush, A. V. Wiznycia, J. Desper, B. A. Helfrich and A. M. Beatty, *Cryst. Growth Des.*, **2002**, *2*, 653. (e) P. Gilli, V. Bertolasi, L. Pretto, A. Lyćka and G. Gilli, *J. Am. Chem. Soc.*, **2002**, *124*, 13554. (f) V. S. S. Kumar, A. Nangia, M. T. Kirchner and R. Boese, *New J. Chem.*, **2003**, *27*, 224. (g) J. -H. Fournier, T. Maris, J. D. Wuest, W. Guo and E. Galoppini, *J. Am. Chem. Soc.*, **2003**, *125*, 1002. (h) A. D. Bond, *New J. Chem.*, **2004**, *28*, 104. (i) S. Perruchas, K. Boubekeur and P. Batail, *Cryst. Growth Des.*, **2005**, *5*, 1585. (j) B. K. Saha, A. Nangia and M. Jaskólski, *CrystEngComm*, **2005**, *7*, 355. (k) V. R. Vangala, R. Mondal, C. K. Broder, J. A. K. Howard and G. R. Desiraju, *Cryst. Growth Des.*, **2005**, *5*, 99.

[1.27] (a) P. Gilli, V. Ferretti, V. Bertolasi and G. Gilli, *J. Am. Chem. Soc.*, **1994**, *116*, 909. (b) T. Steiner and W. Saenger, *Acta Crystallogr.*, **1994**, *B50*, 348. (c) C. Flensburg, S. Larsen and R. F. Stewart, *J. Phys. Chem.*, **1995**, *99*, 10130. (d) P. R. Mallinson, K. Woźniak, G. T. Smith and K. L. McCormack, *J. Am. Chem. Soc.*, **1997**, *119*, 11502. (e) T. Steiner, *J. Phys. Chem. A*, **1998**, *102*, 7041. (f)

P. Gilli, V. Bertolasi, V. Ferretti and G. Gilli, *J. Am. Chem. Soc.*, **2000**, *122*, 10405. (g) P. Vishweshwar, N. J. Babu, A Nangia, S. A. Mason, H. Puschmann, R. Mondal and J. A. K. Howard, *J. Phys. Chem. A*, **2004**, *108*, 9406. (h) M. D. Ward, *Chem. Commun.*, **2005**, 5838.

[1.28] (a) P. W. Baures, A. M. Beatty, M. Dhanasekaran, B. A. Helfrich, W. Pe´rez-Segarra and J. Desper, *J. Am. Chem. Soc.*, **2002**, *124*, 11315. (b) Y. Nishiyama, J. Sugiyama, H. Chanzy and P. Langan, *J. Am. Chem. Soc.*, **2003**, *125*, 14300. (c) M. Jarvis, *Nature*, **2003**, *426*, 611. (d) R. Boese, M. T. Kirchner, W. E. Billups and L. R. Norman, *Angew. Chem. Int. Ed.*, **2003**, *42*, 1961. (e) D. Das, R. K. R. Jetti, R. Boese and G. R. Desiraju, *Cryst. Growth Des.*, **2003**, *3*, 675. (f) A. D. Santis, A. Forni, R. Liantonio, P. Metrangolo, T. Pilati and G. Resnati, *Chem. Eur. J.*, **2003**, *9*, 3974. (g) K. J. Wallace, W. J. Belcher, D. R. Turner, K. F. Syed and J. W. Steed *J. Am. Chem. Soc.*, **2003**, *125*, 9699. (h) E. A. Meyer, R. K. Castellano and F. Diederich, *Angew. Chem., Int. Ed.*, **2003**, *42*, 1210. (i) M. Fourmigué and P. Batail, *Chem. Rev.*, **2004,** *104*, 5379.

[1.29] (a) R. D. Green, *Hydrogen Bonding by C-H Groups*, McMillan: London, **1974**. (b) R. Taylor and O. Kennard, *J. Am. Chem. Soc.*, **1982**, *104*, 5063. (c) G. R. Desiraju, *Acc. Chem. Res.*, **1996**, *29*, 441. (d) T. Steiner, *Chem. Commun.*, **1997**, 727. (e) G. R. Desiraju, *Chem. Commun.*, **2005**, 2995.

[1.30] (a) M. F. Richardson, Q. -C. Yang, E. N. Bregger and J. D. Dunitz, *Acta Crystallogr.*, **1990**, *B46*, 653. (b) J. A. K. Howard, V. J. Hoy, D. O'Hagan and G. T. Smith, *Tetrahedron*, **1996,** *52*, 12613. (c) V. R. Thalladi, H. -C. Weiss, D. Bläser, R. Boese, A. Nangia and G. R. Desiraju, *J. Am. Chem. Soc.*, **1998**, *120*, 8702. (d) W. Caminati, S. Melandri, P. Moreschini and P. G. Favero, *Angew. Chem. Int. Ed.* **1999**, *38*, 2924. (e) Y. Tatamitani, B. Liu, J. Shimada, T. Ogata, P. Ottaviani, A. Maris, W. Caminati and J. L. Alonso, *J. Am. Chem. Soc.*, **2002**, *124*, 2739. (f) J. L. Alonso, S. AntolLnez, S. Blanco, A. Lesarri, J. C. Lipez and W. Caminati, *J. Am. Chem. Soc.*, **2004**, *126*, 3244.

[1.31] (a) P. K. Thallapally and A. Nangia, *CrystEngComm*, **2001**, *27*, 1. (b) L. Brammer, E. A. Bruton and P. Sherwood, *Cryst. Growth Des.*, **2001**, *1*, 277. (c)

F. Zordan, L. Brammer and P. Sherwood, *J. Am. Chem. Soc*., **2005**, *127*, 5979. (d) F. Zordan, S. L. Purver, H. Adams and L. Brammer, *CrystEngComm*, **2005**, *7*, 350. (e) K. Reichenbächer, H. I. Süss and J. Hulliger, *Chem. Soc. Rev*., **2005**, *34*, 22.

[1.32] (a) M. L. Huggins, *J. Org. Chem*., **1936**, *1*, 405. (b) G. R. Desiraju, *Acc. Chem. Res*., **2002**, *35*, 565. (c) I. H.-Kryspin, G. Haufe and S. Grimme, *Chem. Eur. J*., **2004**, *10*, 3411.

[1.33] (a) S. S. Kuduva, D. Bläser, R. Boese and G. R. Desiraju, *Struct. Chem.,* **2001**, *12*, 259. (b) S. S. Kuduva, D. Bläser, R. Boese and G. R. Desiraju, *J. Org. Chem.*, **2001**, *66*, 1621. (c) A. Forni, P. Metrangolo, T. Pilati and G. Resnati, *Cryst. Growth Des*., **2004**, *4*, 291. (d) C. M. L. V. Velde, L. -J. Chen, J. K. Baeke, M. Moens, P. Dieltiens, H. J. Geise, M. Zeller, A. D. Hunter and F. Blockhuys, *Cryst. Growth Des*., **2005**, *5*, 167.

[1.34] (a) F. H. Allen, J. A. K. Howard, V. J. Hoy, G. R. Desiraju, D. S. Reddy and C. C. Wilson, *J. Am. Chem. Soc*., **1996**, *118*, 4081. (b) N. N. L. Madhavi, G. R. Desiraju, C. Bilton, J. A. K. Howard and F. H. Allen, *Acta Crystallogr*., **2000**, *B56*, 1063. (c) C. Bilton, J. A. K. Howard, N. N. L. Madhavi, A. Nangia, G. R. Desiraju and F. H. Allen, *Acta Crystallogr*., **2000**, *B56*, 1071. (d) N. N. L. Madhavi, C. Bilton, J. A. K. Howard, F. H. Allen, A. Nangia and G. R. Desiraju, *New J. Chem*., **2000**, *24*, 1.

[1.35] (a) C. V. K. Sharma and A. Clearfield, *J. Am. Chem. Soc*., **2000**, *122*, 4394. (b) V. R. Vangala, B. R. Bhogala, A. Dey, G. R. Desiraju, C. K. Broder, P. S. Smith, R. Mondal, J. A. K. Howard and C. C. Wilson, *J. Am. Chem. Soc*., **2003**, *125*, 14495. (c) B. -Q. Ma and P. Coppens, *Chem. Commun*., **2004**, 932.

[1.36] (a) W. Ostwald, *Z. Phys. Chem*., **1897**, *22*, 289. (b) M. Volmer, *Kinetic der Phasenbildung*, Steinkopf: Leipzig, **1939**. (c) A. C. Zettlemoyer, *Nucleation*, Dekker: New York, **1969**. (d) B. Lewis, *Nucleation and Growth Theory*: *Crystal Growth*, B. R., Pamplin, Ed.; Pergamon: Oxford, **1980**. (e) R. J. Davey and J. Garside, *From Molecules to Crystallizers*, Oxford University Press: Oxford, U.K., **2000**. (f) J. H. ter Horst, H. J. M. Kramer and P. J. Jansens,

Cryst. *Growth Des*., **2002**, *2*, 351. (g) J. Drenth, K. Dijkstra, C. Haas, J. Leppert and O. Ohlenschlager, *J. Phys*. *Chem*. *B*, **2003**, *107,* 4203. (h) C. S. Towler, R. J. Davey, R. W. Lancaster, and C. J. Price, *J. Am*. *Chem*. *Soc*., **2004**, *126*, 13347.

[1.37] (a) R. J. Davey, N. Blagden, S. Righini, H. Alison, M. J. Quayle and S. Fuller, *Cryst*. *Growth Des*., **2001**, *1*, 59. (b) H. Groen and K. J. Roberts, *J. Phys*. *Chem*. *B*, **2001**, *105*, 10723. (c) R. J. Davey, N. Blagden, S. Righini, H. Alison and E. S. Ferrari, *J. Phys. Chem. B*., **2002**, *106*, 1954. (d) R. J. Davey, W. Liu, M. J. Quayle, and G. J. T. Tiddy, *Cryst. Growth Des.*, **2002**, *4*, 269. (e) N. Blagden and R. J. Davey, *Cryst*. *Growth Des*., **2003**, *3*, 873. (f) W. I. F. David, K. Shankland, C. R. Pulham, N. Blagden, R. J. Davey and M. Song , *Angew*. *Chem*. *Int*. *Ed*., **2005**, *44*, 2.

[1.38] (a) I. Weissbuch, M. Lahav and L. Leiserowitz, *Cryst. Growth Des.* **2003**, *3*, 125. (b) I. Weissbuch, V. Y. Torbeev, L. Leiserowitz and M. Lahav, *Angew*. *Chem*. *Int*. *Ed*., **2005**, *44*, 3226.

[1.39] (a) A. S. Myerson and P. Y. Lo, *J. Cryst. Growth*, **1990**, *99*, 1048. (b) A. S. Myerson and P. Y. Lo, *J. Cryst. Growth*, **1991**, *110*, 26. (c) R. M. Ginde and A. S. Myerson, *J. Cryst. Growth*, **1992**, *116*, 41. (d) A. S. Myerson and R. M. Ginde, *Handbook of Industrial Crystallization*, A. S. Myerson, Ed.; Butterworth-Heinemann: Stoneham, MA, **1992**.

[1.40] (a) S. Devarakonda, J. M. B. Evans and A. S. Myerson, *Cryst*. *Growth Des*., **2003**, *3*, 741. (b) S. Ueno, R. I. Ristic, K. Higaki and K. Sato, *J. Phys. Chem. B*., **2003**, *107,* 4927. (c) S. Chattopadhyay, D. Erdemir, J. M. B. Evans, J. Ilavsky, H. Amenitsch, C. U. Segre and A. S. Myerson, *Cryst. Growth Des.*, **2005**, *5*, 523.

[1.41] S. Martini, M. L. Herrera and R. W. Hartel, *J. Agric. Food Chem.*, **2001**, *49*, 3223.

[1.42] L. G. M. Beekmans, R. Vallee and G. J. Vancso, *Macromolecules*, **2002**, *35*, 9383.

[1.43] S. Datta and D. J. W. Grant, *Cryst*. *Growth Des*., **2003**, *3*, 1351.

[1.44] (a) N. Padmaja, S. Ramakumar and M. A. Viswamitra, *Acta Crystallogr.*, **1990**, *A46*, 725. (b) G. R. Desiraju, J. C. Calabrese and R. L. Harlow, *Acta Crystallogr.*, **1991**, *B47*, 77. (c) A. J. C. Wilson, *Acta Crystallogr.*, **1993**, *A49*, 795. (d) C. P. Brock, *J. Res. Natl. Inst. Stand. Technol*., **1996**, *101*, 321. (e) S. Kumar, K. Subramanian, R. Srinivasan, K. Rajagopalan, A. M. M. Schreurs, J. Kroon and T. Steiner, *J. Mol. Struct*., **2000**, *520*, 131.

[1.45] (a) R. Banerjee, P. M. Bhatt, M. T. Kirchner and G. R. Desiraju, *Angew. Chem. Int. Ed*., **2005**, *44*, 2515. (b) S. Parveen, R. J. Davey, G. Dent and R. G. Pritchard, *Chem. Commun*., **2005**, 1531. (c) R. Mondal and J. A. K. Howard, *CrystEngComm*, **2005**, 462. (d) D. Das, R. Banerjee, R. Mondal, J. A. K. Howard, R. Boese and G. R. Desiraju, *Chem*. *Commun*., **2006**, doi: 10.1039/b514076e

[1.46] J. W. Steed, *CrystEngComm*, **2003**, *5*, 169.

[1.47] V. S. S. Kumar, A. Addlagatta, A. Nangia, W. T. Robinson, C. K. Broder, R. Mondal, I. R. Evans, J. A. K. Howard and F. H. Allen, *Angew*. *Chem*. *Int*. *Ed*., **2002**, *41*, 3848.

[1.48] (a) K. E. Plass, K. Kim and A. J. Matzger, *J. Am. Chem. Soc.*, **2004**, *126*, 9042. (b) C. P. Price, A. L. Grzesiak and A. J. Matzger, *J. Am. Chem. Soc.*, **2005**, *127*, 5512.

[1.49] A. Nangia and G. R. Desiraju, *Chem*.*Commun*., **1999**, 605.

[1.50] (a) T. L. Threlfall, *Org*. *Process Res*. *Dev*., **2000**, *4*, 384. (b) S. Garnier, S. Petit and G. Coquerel, *J. Thermal Anal. & Calorimetry,* **2002**, *68*, 489. (c) Y. -S. Kim and R. W. Rousseau, *Cryst*. *Growth Des*., **2004**, *4*, 1211. (d) T. Hosokawa, S. Datta, A. R. Sheth, N. R. Brooks, V. G. Young and D. J. W. Grant, *Cryst*. *Growth Des*., **2004**, *4*, 1195. (e) S. Dutta and D. J. W. Grant, *Nat*. *Rev*. *Drug Discovery*, **2004**, *3*, 42. (f) M. R. Caira, T. le-Roex, L. R. Nassimbeni, J. A. Ripmeester and E. Weber, *Org*. *Biomol*. *Chem*., **2004**, *2*, 2299.

[1.51] (a) K. R. Morris and N. Rodriguez-Hornedo, *Encyclopedia of Pharmaceutical Technology*, Marcel Dekker: New York, **1993**. (b) S. R. Byrn, R. R. Pfeiffer

and J. G. Stowell, *Solid-State Chemistry of Drugs*, 2nd ed.; SSCI Inc.: West Lafayette, IN, **1999**. (c) H. G. Brittain, *Methods for the Characterization of Polymorphs and Solvates*. In *Polymorphism in Pharmaceutical Solids*. H. G. Brittain, Ed.; Marcel Dekker Inc.: New York, **1999**. (d) S. H. Neau, *Water-Insoluble Drug Formations*, Ed. R. Liu, Interpharm: Buffalo Grove, **2000**, pp 405–425. (e) M. Puddipeddi, A. T. M. Serajuddin, D. J. W. Grant and P. H. Stahl, in *Handbook of Pharmaceutical Salts: Properties, Selection, and Use*, P. H. Stahl and C. G. Wermuth, Eds; pp 19–38, Wiley: Weinheim, **2002**. (f) C. H. Gu and D. J. W. Grant, in *Handbook of Experimental Pharmacology: Stereochemical Aspects of Drug Action and Disposition*, vol. 153, M. Eichelbaum, B. Testa and A. Somogyi, Eds; Springer: Berlin, **2003**. (g) S. Morissette, Ö. Almarsson, M. Peterson, J. Remenar, M. Read, A. Lemmo, S. Ellis, M. Cima and C. Gardner, *Adv. Drug Deliv. Rev.*, **2004**, *56*, 275.

[1.52] B. Rodríguez-Sponga, C. P. Price, A. Jayasankara, A. J. Matzger and N. Rodríguez Hornedoa, *Adv. Drug Deliv. Rev.*, **2004**, *56*, 241.

[1.53] (a) L. J. Barbour, G. W. Orr and J. L. Atwood, *Nature*, **1998**, *393*, 671. (b) K. A. Udachin and J. A. Ripmeester, *Nature*, **1999**, *397*, 420. (c) L. J. Barbour, G. W. Orr and J. L. Atwood, *Chem. Commun.*, **2000**, 859. (d) R. Ludwig, *Angew. Chem. Int. Ed.*, **2001**, *40*, 1808. (e) J. L. Atwood, L. J. Barbour, T. J. Ness, C. L. Raston and P. L. Raston, *J. Am. Chem. Soc.*, **2001**, *123*, 7192. (f) C. Janiak, T. G. Scharmann and S. A. Mason, *J. Am. Chem. Soc.*, **2002**, *124*, 14010. (g) L. R. Pratt and A. Pohorille, *Chem. Rev.*, **2002**, *102*, 2671. (h) K. Raghuraman, K. K. Katti, L. J. Barbour, N. Pillarsetty, C. L. Barnes and K. V. Katti, *J. Am. Chem. Soc.*, **2003**, *125*, 6955. (i) S. Otto and J. B. F. N. Engberts, *Org. Biomol. Chem.*, **2003**, *1*, 2809. (j) A. I. Kolesnikov, J. -M. Zanotti, C.-K. Loong, P. Thiyagarajan, A. P. Moravsky, R. O. Loutfy and C. J. Burnham, *Phys. Rev. Lett.*, **2004**, *93*, 1. (k) B. -Q. Ma, H.-L. Sun and S. Gao, *Angew. Chem. Int. Ed.*, **2004**, *43*, 1374. (l) B. Sreenivasulu and J. J. Vittal, *Angew. Chem. Int. Ed.*, **2004**, 43, 5769. (m) B. K. Saha and A. Nangia, *Chem. Commun.*, **2005**, 3024. (n) L. Cunha-Silva and J. J. C. Teixeira-Dias, *New J. Chem.*, **2005**, *29*, 1335.

[1.54] (a) R. K. Khankari and D. J. W. Grant, *Thermochim*. *Acta*, **1995**, 61. (b) A. L. Gillon, N. Feeder, R. J. Davey and R. Storey, *Cryst*. *Growth Des*., **2003**, *3*, 663. (c) L.-F. Huanga and W.-Q. Tong, *Adv*. *Drug Deliv*. *Rev*., **2004**, *56*, 321. (d) D. A. Haynes, W. Jones and W. D. S. Motherwell, *CrystEngComm*, **2005**, 462.

[1.55] (a) G. R. Desiraju, *J*. *Chem*. *Soc*., *Chem. Commun*., **1991**, 426. (b) A. L. Gillon, N. Feeder, R. J. Davey and R. Storey, *Cryst*. *Growth Des*., **2003**, *3*, 663.

[1.56] L. Infantes and W. D. S. Motherwell, *CrystEngComm*, **2004**, *4*, 454.

[1.57] (a) S. Petit and G. Coquerel, *Chem*. *Mater*., **1994**, *8*, 2247. (b) L. O. Figura and M. Epple, *J*. *Thermal Anal*., **1995**, *44*, 45. (c) T. D. Dincer, G. M. Parkinson, A. L. Rohl and M. I. Ogden, *J*. *Cryst*. *Growth*, **1999**, *205*, 368. (d) S. L. Raghavan, R. I. Ristic, D. B. Sheen and J. N. Sherwood, *J*. *Pharm*. *Sci*., **2001**, *90*, 823. (e) C.H. Gu and D. J. W. Grant, *J*. *Pharm*. *Sci*., **2001**, 90 1277. (f) S. Garnier, S.Petit and G. Coquerel, *J*. *Thermal Anal*. *& Calorimetry*, **2002**, *68*, 489.

[1.58] A. L. Bingham, D. S. Hughes, M. B. Hursthouse, R. W. Lancaster, S. Tavener and T. L. Threlfall, *Chem*. *Commun*., **2001**, 603.

[1.59] (a) J. L. Atwood, J. E. D. Davies and F. Vogtle, *Comprehensive Supramolecular Chemistry*; Pergammon: New York, **1996**, vol. 6. (b) R. Bishop, *Chem. Soc. Rev.*, **1996**, 311. (c) D. D. MacNicol, F. Toda and R. Bishop, Eds.; *Comprehensive Supramolecular Chemistry*; vol. 6, *Solid-state Supramolecular Chemistry: Crystal Engineering*, Pergamon Press: Oxford, **1996**. (d) E. Zaborowski, H. Zimmermann and S. Vega, *J. Am. Chem. Soc.*, **1998**, *120*, 8113. (e) R. Bishop, *Synlett*., **1999,** *9*, 1351. (f) T. Müller, J. Hulliger, W. Seichter, E. Weber, T. Weber and M. Wübbenhorst, *Chem*. *Eur*. *J*., **2000**, *6*, 54. (g) R. K. R. Jetti, A. Nangia, F. Xue and T. C. W. Mak, *Chem. Commun.*, **2001**, 919. (h) A. Nangia, *Curr. Opin. Solid State Mater. Sci.*, **2001**, *5*, 115. (i) S. Kim, R. Bishop, D. C. Craig, I. G. Dance and M. L. Scudder, *J*. *Org*. *Chem*., **2001**, *67*, 3221. (j) E. Weber, S. Nitsche, A. Wierig and I. Csöregh, *Eur*. *J*. *Org*. *Chem*., **2002**, 856. (k) H. I. Süss, M. Lutz and J.

Hulliger, *CrystEngComm*, **2002**, *4*, 610. (l) R. K. R. Jetti, P. K. Thallapally, C -K. Lam, T. C. W. Mak and A. Nangia, *Chem. Commun.*, **2002**, 952. (m) T. Hertzsch, F. Budde, E. Weber and J. Hulliger, *Angew. Chem. Int. Ed.*, **2002**, *41*, 2281. (n) D. V. Soldatov, E. V. Grachev and J. A. Ripmeester, *Cryst. Growth Des.*, **2002**, *2*, 401. (o) J. L. Atwood, L. J. Barbour and A. Jerga, *Science*, **2002**, *296*, 2367. (p) C. M. Reddy, A. Nangia, C-K. Lam and T. C. W. Mak, *CrystEngComm,* **2002**, *4,* 323. (q) S. Apel, M. Lennartz, L. R. Nassimbeni and E. Weber, *Chem. Eur. J.*, **2002**, *8*, 3678. (r) J. G. Selbo, J. J. Haycraft and C. J. Eckhardt, *J. Phys. Chem. B*, **2003**, 107, 11163. (s) G. V. C. Cave, J. Antesberger, L. J. Barbour, R. M. McKinley and J. L. Atwood, *Angew. Chem. Int. Ed.*, **2004**, *43*, 5263. (t) M. R. Caira, Y. Paul Chang, L. R. Nassimbeni and H. Su, *Org. Biomol. Chem.*, **2004**, *2*, 655. (u) C.-K. Lam and T. C. W. Mak, *J. Am. Chem. Soc.*, **2005**, *127*, 11536. (v) B. K. Saha, R. K. R. Jetti, L. S. Reddy, S. Aitipamula and A. Nangia, *Cryst. Growth Des.*, **2005**, *5*, 887. (w) B. K. Saha, S. Aitipamula, R. Banerjee, A. Nangia, R. K. R. Jetti, R. Boese, C-. K. Lam and T. C. W. Mak, *Mol. Cryst. Liq. Cryst.,* **2005**, *440*, 295.

[1.60] (a) J. A. R. P. Sarma and G. R. Desiraju, In *Crystal Engineering: The Design and Application of Functional Solids*; M. J. Zaworotko and K. R. Seddon, Eds; Kluwer: Dordrecht, **1999**, 325. (b) V. S. S. Kumar, S. S. Kuduva and G. R. Desiraju, *J. Chem. Soc., Perkin Trans. 2*, **1999**, 1069. (c) R. Thaimattam, F. Xue, J. A. R. P. Sarma, T. C. W. Mak and G. R. Desiraju, *J. Am. Chem. Soc.*, **2001**, *123*, 4432. (d) V. S. S. Kumar and A. Nangia, *Chem. Commun.*, **2001**, 2392. (e) K. A. Udachin, G. D. Enright, P. O. Brown and J. A. Ripmeester, *Chem. Commun.*, **2002**, 2162. (f) S. H. Dale, M. R. J. Elsegood and C. Redshaw, *CrystEngComm*, **2003**, *5,* 368. (g) J. Ashmore, R. Bishop, D. C. Craig and M. L. Scudder, *Mendeleev Commun.*, **2003**, *13*, 144. (h) R. Banerjee, G. R. Desiraju, R. Mondal, A. S. Batsanov, C. K. Broder and J. A. K. Howard, *Helv. Chim. Acta*, **2003**, *86*, 1339. (i) Y. -S. Kim and R. W. Rousseau, *Cryst. Growth Des.*, **2004**, *4*, 1211. (j) T. Hosokawa, S. Datta, A. R. Sheth, N. R.

Brooks, V. G. Young and D. J. W. Grant, *Cryst. Growth Des.*, **2004**, *4*, 1195. (k) Y. Imai, T. Sato and R. Kuroda, *Chem. Commun.*, **2005**, 3289.

[1.61] (a) T. L. Threlfall, *Analyst*, **1995**, *120*, 2435. (b) G. R. Desiraju, *Science*, **1997**, *278*, 404. (c) J. Bernstein, R. J. Davey and J. O. Henck, *Angew. Chem., Int. Ed.*, **1999**, 38, 3441. (d) L. Yu, G. A. Stephenson, C. A. Mitchell, C. A. Bunnell, S. V. Snorek, J. J. Bowyer, T. B. Borchardt, J. G. Stowell and S. R. Byrn, *J. Am. Chem. Soc.*, **2000**, *122*, 585. (e) R. Suryanarayanan and S. R. Byrn, *Adv. Drug Deliv. Rev.*, **2001**, *48*, 1. (f) J. Bernstein, *Polymorphism in Molecular Crystals,* Clarendon: Oxford, **2002**. (g) A. Kálmán, L. Fábián, G. Argay, G. Bernáth and Z. C. Gyarmati, *J. Am. Chem. Soc.*, **2003**, *125*, 34. (h) L. Yu, *J. Am. Chem. Soc.*, **2003**, *125*, 6380. (i) A. L. Grzesiak, M. Lang, K. Kim and A. J. Matzger, *J. Pharm. Sci.*, **2003**, *92*, 2260. (j) J. A. McMahon, M. J. Zaworotko and J. F. Remenar, *Chem. Commun.*, **2004**, 278. (k) D. J. W. Grant and S. R. Byrn, *Adv. Drug Deliv. Rev.*, **2004**, *56*, 237. (l) S. Coste, J.-M. Schneider, M.-N. Petit and G. Coquerel, *Cryst. Growth Des.*, **2004**, *4*, 1237. (m) M. R. Caira, S. A. Bourne, W. T. Mhlongo and P. M. Dean, *Chem. Commun.*, **2004**, 2216. (n) V. S. S Kumar, C. F. Pigge and N. P. Rath, *CrystEngComm*, **2004**, *6*, 102. (o) L. Fábián, A. Kálmán, G. Argay, G. Bernáth and Z. C. Gyarmati, *Chem. Commun.*, **2004**, *18*, 2114. (p) C. R. Gardner, C. T. Walsh and Ö. Almarsson, *Nature Rev.*, **2004**, *3*, 926. (q) S. L. Morissette, Ö. Almarsson, M. L. Peterson, J. F. Remenar, M. J. Read, A. V. Lemmo, S. Ellis, M. J. Cima and C. R. Gardner, *Adv. Drug Delivery Rev.*, **2004**, *56*, 275. (r) S. Aitipamula and A. Nangia, *Chem. Commun.*, **2005**, 3159.

[1.62] (a) M. Sorrenti, G. P. Bettinetti and A. Negri, *Thermochim. Acta*, **1998**, *321*, 67. (b) L. R. Nassimbeni, *Acc. Chem. Res.*, **2003**, *28*, 37.

CHAPTER TWO

[2.1] (a) S. G. Fleischman, S. S. Kuduva, J. A. McMahon, B. Moulton, R. B. Walsh, N. Rodriguez-Hornedo and M. J. Zaworotko, *Cryst. Growth Des.*, **2003**, *3*, 909. (b) J. F. Remenar, S. L. Morissette, M. L. Peterson, B. Moulton, J. M.

MacPhee, H. R. Guzmán and Ö. Almarsson, *J. Am. Chem. Soc.*, **2003**, *125*, 8456. (c) N. Shan, A. D. Bond and W. Jones, *New J. Chem.*, **2003**, *27*, 365. (d) L. S. Reddy, A. Nangia and V. M. Lynch, *Cryst. Growth. Des.*, **2004**, *4*, 89. (e) C. B. Aakeröy, J. Desper and B. A. Helfrich, *CrystEngComm*, **2004**, *6*, 19. (f) C. B. Aakeröy and D. J. Salmon, *CrystEngComm*, **2005**, *7*, 439. (g) J. A. Bis and M. J. Zaworotko, *Cryst. Growth Des.*, **2005**, *5*, 1169.

[2.2] (a) G. R. Desiraju and J. A. R. P. Sarma, *Proc. Indian Acad. Sci.*, **1986**, *96*, 599. (b) N. N. L. Madhavi, A. K. Katz, H. L. Carrell, A. Nangia and G. R. Desiraju, *Chem. Commun.*, **1997**, 1953. (c) P. K. Thallapally, K. Chakraborty, H. L. Carrell, S. Kotha and G. R. Desiraju, *Tetrahedron*, **2000**, *56*, 6721. (d) B. Omondi, M. A. Fernandes, M. Layh, D. C. Levendis, J. L. Look and T. S. P. Mkwizu, *CrystEngComm*, **2005**, *7*, 690.

[2.3] R. Parthasarathy and G. R. Desiraju, *J. Am. Chem. Soc.* **1989,** *111*, 8725.

[2.4] (a) J. D. Dunitz, *Thoughts on Crystals as Supramolecules*. In *The Crystal as a Supramolecular Entity*, G. R. Desiraju, Ed.; J. Wiley & Sons: Chichester, **1996**; pp 1-30. (b) J. M. A. Robinson, B. M. Kariuki, K. D. M. Harris, D. Philp, *J. Chem. Soc., Perkin Trans. 2* **1998**, 2459. (c) S. Pekker, E. Kováts, G. Oszlányl, G. Bényel, G. Klupp, G. Bortel, I.; Jakab, E. Jalsovszky, F. Borondics, K. Kamarás, M. Bokor, G. Kriza, K. Tompa and G. Faigel, *Nature Mater.*, **2005**, *4*, 764.

[2.5] (a) W. H. Bragg, *Proc. Phys. Soc.*, (London), **1921**, *34*, 33. (b) W. H. Bragg, *Proc. Phys. Soc.*, (London), **1922**, *35*, 167. (c) J. M. Robertson, *Organic Crystals and Molecules*; Cornell University Press: New York, **1953**, pp 160-161.

[2.6] (a) C. B. Aakeröy, A. M. Beatty and B. A. Helfrich, *J. Am. Chem. Soc.*, **2002**, *124*, 14425. (b) C. B. Aakeröy, J. Desper, B. Leonard and J. F. Urbina, *Cryst. Growth Des.*, **2005**, *5*, 865. (c) C. B. Aakeröy, J. Desper and J. F. Urbina, *Chem. Commun.*, **2005**, 2820.

[2.7] *SMART, Version 5.05*; Bruker AXS, Inc.: Madison, Wisconsin, **1998**.

[2.8] (a) G. M. Sheldrick, *SHELXTL V5.1*; Madison, WI, **1998**. (b) *SAINT, Version 6.2*, Bruker AXS, Inc.: Madison, Wisconsin, **2001**.

[2.9] *Cerius*^{2} suite of software for crystal lattice energy calculation and crystal structure prediction are crystal packer and polymorph predictor. *Cerius*^{2} Program Molecular Simulations, 9685 Scranton Road, San Diego.

[2.10] A. L. Spek, PLATON, Bijvoet Centre for Biomedical Research, Vakgroep Kristal-en Structure-Chemie, University of Utrecht, The Netherlands.

CHAPTER THREE

[3.1] (a) S. L. James, G. Verspui, A. L. Spek and G. van Koten, *Chem. Commun.*, **1996**, 1309. (b) F. Neve and A. Crispini, *Cryst. Growth Des.*, **2001**, *1*, 387. (c) J. -A. van den Berg and K. R. Seddon, *Cryst. Growth Des.*, **2003**, *3*, 643. (d) V. Balamurugan, M. S. Hundal and R. Mukherjee, *Chem. Eur. J.*, **2004**, *10*, 1683. (e) J. Olsen, P. Seiler, B. Wagner, H. Fischer, T. Tschopp, U. Obst-Sander, D. W. Banner, M. Kansy, K. Müller and F. Diederich, *Org. Biomol. Chem.*, **2004**, *2*, 1339. (f) K. Reichenbächer, H. I. Süss and J. Hulliger, *Chem. Soc. Rev.*, **2005**, *34*, 22.

[3.2] C. B. Aakeröy, T. A. Evans, K. R. Seddon and I. Pálinkó, *New J. Chem.*, **1999**, *23*, 145.

[3.3] They also confirmed that when fluorine is a part of an anion, for example, PF_6^-, the fluorine becomes rather good acceptor. J. D. Dunitz and R. Taylor, *Chem. Eur. J.*, **1997**, *3*, 89.

[3.4] (a) S. C. F. Kui, N. Zhu and M. C. W. Chan, *Angew. Chem. Int. Ed.*, **2003**, *42*, 1628. (b) M. C. W. Chan, S. C. F. Kui, J. M. Cole, G. J. McIntyre, S. Matsui, N. Zhu and Ka-Ho Tam, *Chem. Eur. J.*, **2006**, doi: 10.1002/chem.200501054.

[3.5] J. A. Olsen, D. W. Banner, P. Seiler, U. O. Sander, A. D'Arcy, M. Stihle, K. Müller and F. Diederich, *Angew. Chem. Int. Ed.*, **2003**, *42*, 2507.

[3.6] (a) D. Y. Curtin and S. R. Byrn, *J. Am. Chem. Soc.*, **1969**, *91*, 6102. (b) S. R. Byrn, D. Y. Curtin and I. C. Paul, *J. Am. Chem. Soc.*, **1972**, *94*, 890. (c) R. Taylor and O. Kennard, *J. Am. Chem. Soc.*, **1982**, *104*, 5063. (d) M. F.

Richardson, Q. -C. Yang, E. N. Bregger and J. D. Dunitz, *Acta Crystallogr*., **1990**, *B46*, 653.

[3.7] A. Hantzsch, *Chem*. *Ber*., **1915**, *48*, 797.

[3.8] O. R. Wulf, U. Liddel and S. B. Hendricks, *J*. *Am*. *Chem*. *Soc*., **1936**, *58*, 2287.

[3.9] J. E. Burks, D. van der Helm, C. Y. Chang and L. S. Ciereszko, *Acta Crystallogr*., **1977**, *B33*, 704.

[3.10] F. Toda, H. Liu, I. Miyahara and K. Hirotsu, *J*. *Chem*. *Soc*. *Perkin Trans*. *2*, **1997**, *218*, 85.

[3.11] Distances (*d*) in the range 2.00 – 3.00 Å and angle (θ) in the range 120 – 180˚ have been considered. R. Banerjee, G. R. Desiraju, R. Mondal and J. A. K. Howard, *Chem*. *Eur*. *J*., **2004**, *10*, 3373.

[3.12] R. S. Rowland and R. Taylor, *J*. *Phys*. *Chem*., **1996**, *100*, 7384.

[3.13] (a) T. Spaniel, H. Görls and J. Scholz, *Angew*. *Chem*. *Int*. *Ed*., **1998**, *37*, 1862. (b) E. Engeldinger, D. Armspach, D. Matt and P. G. Jones, *Chem*. *Eur*. *J*., **2003**, *9*, 3091.

[3.14] The calculation had been done using the work of Kovács et al. on the blue shifting of C–H…X (X = O, halogen) dimers of formaldehyde, and taking other work on intramolecular/intermolecular hydrogen bond energies as background. (a) A. Kovács, A. Szabó, D. Nemcsok and I. Hargittai, *J*. *Phys*. *Chem*. *A*., **2002**, *106,* 5671. (b) A. Kovács, A. Szabó and I. Hargittai, *Acc*. *Chem*. *Res*., **2002**, *35*, 887. (c) H. Y. Liao and S. Y. Chu, *New J*. *Chem*., **2003**, *27*, 421. (d) P. D. Vaz, M. Nolasco, N. Fonseca, A. M. Amado, A. M. A. Costa, V Félix, M. G. B. Drew, B. J. Goodfellow and P. J. A. Ribeiro-Claro, *Phys*. *Chem*. *Chem*. *Phys*., **2005**, *7*, 3027.

[3.15] Spartan 04 computational methods include Hartree-Fock, density function theory, and Møller-Plesset on an interactive PC interface. www.wavefun.com.

[3.16] M. W. Schmidt, K. K. Baldridge, J. A. Boatz, S. T. Elbert, M. S. Gordon, J. J. Jensen, S. Koseki, N. Matsunaga, K. A. Nguyen, S. Su, T. L. Windus, M. Dupuis and J. A. Montgomery, *J*. *Comput*. *Chem*., **1993**, *14*, 1347.

CHAPTER FOUR

[4.1] (a) W. Nowacki, *Helv. Chim. Acta* **1942,** *25*, 863. (b) W. Nowacki, *Helv. Chim. Acta* **1943,** *26*, 459. (c) A. I. Kitaigorodskii, *Molecular Crystals and Molecules*, Academic Press: New York, **1973**.

[4.2] (a) E. Pidcock and W. D. S. Motherwell, *Cryst. Growth Des*., **2004**, *4*, 611. (b) E. Pidcock and W. D. S. Motherwell, *Cryst. Growth Des*., **2005**, *5*, 2232. (c) J. D. Dunitz and A. Gavezzotti, *Cryst. Growth Des.*, **2005**, *5*, 2180. (d) J. D. Dunitz and A. Gavezzotti, *Angew. Chem. Int. Ed*., **2005**, *44*, 1766.

[4.3] (a) W. D. S. Motherwell, H. L. Ammon, J. D. Dunitz, A. Dzyabchenko, P. Erk, A. Gavezzotti, D. W. M. Hofmann, F. J. J. Leusen, J. P. M. Lommerse, W. T. M. Mooij, S. L. Price, H. A. Scheraga, B. Schweizer, M. U. Schmidt, B. P. van Eijck, P. Verwer and D. E. Williams, *Acta Crystallogr.*, **2002**, *B58*, 647. (b) J. D. Dunitz, *Chem. Commun*., **2003**, 545. (c) A. Gavezzotti, *CrystEngComm*, **2003**, *5*, 429. (d) S. L. Price, *Crystal Structure Prediction*: *Encyclopedia of Supramolecular Chemistry*, J. L. Atwood and J. Steed, Eds.; **2004**, pp 371-379. (e) T. C. Lewis, D. A. Tocher and S. L. Price, *Cryst. Growth Des.*, **2004**, *4*, 979. (f) C. Ouvard and S. L. Price, *Cryst. Growth Des.*, **2004**, *4*, 1119. (g) H. Nowell and S. L. Price, *Acta Crystallogr.* **2005**, *B61*, 558. (h) G. M. Day, W. D. S. Motherwell, H. Ammon, S. X. M. Boerrigter, R. G. Della Valle, E. Venuta, A. Dzyabchenko, J. D. Dunitz, B. Schweizer, B. P. van Eijck, P. Erk, J. C. Facelli, V. E. Bazterra, M. B. Ferraro, D. W. M. Hofmann, F. J. J. Leusen, C. Liang, C. C. Pantelides, P. G. Karamertzanis, S. L. Price, T. C. Lewis, H. Nowell, A. Torrisi, H. A. Scheraga, Y. A. Arnautova, M. U. Schmidt and P. Verwer, *Acta Crystallogr.*, **2005**, *B61*, 511. (i) A. T. Hulme, S. L. Price and D. A. Tocher, *J. Am. Chem. Soc.*, **2005**, *127*, 1116. (j) G. M. Day, W. D. S. Motherwell and W. Jones, *Cryst. Growth Des.*, **2005**, *5*, 1023.

[4.4] L. N. Kuleshova and M. Yu. Antipin, *Russ. Chem. Rev.*, **1999**, *68*, 1. For other references see [1.44], [1.46] and [1.48].

[4.5] (a) G. Filippini and A. Gavezzotti, *Acta Crystallogr.*, **1992**, *B48*, 230. (b) C. P. Brock and J. D. Dunitz, *Chem. Mater.*, **1994**, *6*, 1118. (c) A. Gavezzotti, *Crystallogr. Rev.*, **1998**, *7*, 5.

[4.6] (a) M. D. Hollingsworth, M. E. Brown, M. Dudley, H. Chung, M.L. Peterson and A.C. Hillier, *Angew. Chem. Int. Ed.*, **2002**, *41*, 965. (b) L. R. Nassimbeni and H. Su, *Acta Crystallogr.*, **2002**, *B58*, 251. (c) R. K. R. Jetti, R. Boese, P. K. Thallapally and G. R. Desiraju, *Cryst. Growth Des.*, **2003**, *3*, 1033. For other references see [1.59].

[4.7] (a) J. C. Cole, J. W. Yao, G. P. Shields, W. D. S. Motherwell, F. H. Allen and J. A. K. Howard, *Acta Crystallogr.*, **2001**, *B57*, 88. (b) J. W. Yao, J. C. Cole, E. Pidcock, F. H. Allen, J. A. K. Howard and W. D. S. Motherwell, *Acta Crystallogr.*, **2002**, *B58*, 640.

[4.8] W. D. S. Motherwell, personal communication.

[4.9] R. Boese, G. R. Desiraju, R. K. R. Jetti, I. Ledoux, V. R. Thalladi and J. Zyss, *Struct. Chem.*, **2002**, *13*, 321.

[4.10] In confirmation of the geometrical role of the Cl-group in various compounds generally we note that type-I Cl…Cl interactions are manifestations of pure close packing and that they do not arise from polarization. In contrast, the Cl…Cl contacts of type-II are polarization induced and direction dependent. Selected references on type I and type II contacts include: (a) W. Jones, C. R. Theocharis, J. M. Thomas and G. R. Desiraju, *Chem. Commun.*, **1983**, 1443. (b) R. Parthasarathy and G. R. Desiraju, *J. Am. Chem. Soc.*, **1989**, *111*, 8725. (c) S. L. Price, A. L. Stone, J. Lucas, R. S. Rowland and A. E. Thornley, *J. Am. Chem. Soc.*, **1994**, *116*, 4910. (d) V. R. Pedireddi, D. S. Reddy, B. S. Goud, D. C. Craig, A. D. Rae and G. R. Desiraju, *J. Chem. Soc. Perkin Trans. 2*, **1994**, 2353. (e) O. Navon, J. Bernstein and V. Khodorkovsky, *Angew. Chem. Int. Ed.*, **1997**, *36*, 601. (f) R. K. R. Jetti, P. K. Thallapally, F. Xue, T. C. W. Mak and A. Nangia, *Tetrahedron*, **2000**, *56*, 6707. (g) C. M. Reddy, M. T. Kirchner, R. C. Gundakaram, K. A. Padmanabhan and G. R. Desiraju, *Chem. Eur. J.*, **2006**, doi: 10.1002/chem.200500983

[4.11] (a) V. R. Thalladi, R. Boese, S. Brasselet, I. Ledoux, J. Zyss, R.K.R. Jetti and G. R. Desiraju, *Chem. Commun.*, **1999**, 1639. (b) I. Dance and M. Scudder, *New. J. Chem*., **2001**, *25*, 1500. (c) P. K. Thallapally, K. Chakraborty, A. K. Katz, H. L. Carrell, S. Kotha and G. R. Desiraju, *CrystEngComm*, **2001**, 31.

[4.12] (a) D. S. Reddy, D. C. Craig and G. R. Desiraju, *J. Am. Chem. Soc*., **1996,** *118*, 4090. (b) R. Thaimattam, F. Xue, J. A. R. P. Sarma, T. C. W. Mak and G. R. Desiraju, *J. Am. Chem. Soc.*, **2001**, *123*, 4432. (c) R. Thaimattam, C. V. K. Sharma, A. Clearfield and G. R. Desiraju, *Cryst*. *Growth Des*., **2001**, *1*, 103.

[4.13] (a) C. H. Görbitz and H. -P. Hersleth, *Acta Crystallogr.*, **2000**, *B56*, 1094. (b) F. C. Pigge, Z. Zheng and N. P. Raith, *New. J. Chem.*, **2000**, *24*, 183. (c) J. K. Harper, N. K. Dalley, A. E. Mulgrew, F. G. West and D. M. Grant, *Acta Crystallogr.*, **2001**, *C57*, 64. (d) A. Anthony and G. R. Desiraju, *Supramolecular Chemistry*, **2001**, *13*, 11. (e) D. Cannon, J. N. Low, J. Cobo, S. Molina, M. Nogueras, A. Sánchez and C. Glidewell, *Acta Crystallogr*., **2001**, *C57*, 608.

[4.14] (a) E. Fogassy, M. Ács, F. Faigl, K. Simon, J. Rohonczy and Z. Ecsery, *J. Chem*. *Soc*., *Perkin Trans*. *2*, **1986**, 1881. (b) S. A. Cirkel and R. Boese, *Acta Crystallogr*., **2004**, *A60*, s205.

[4.15] (a) O. Ermer and A. Eling, *J. Chem. Soc., Perkin Trans. 2*, **1994**, 925. (b) S. Hanessian, A. Gomtsyan, M. Simard and S. Roelens, *J. Am. Chem. Soc*., **1994**, *116*, 4495. (c) S. Hanessian, M. Simard and S. Roelens, *J. Am. Chem. Soc*., **1995**, *117*, 7630. (d) S. Hanessian, R. Saladino, R. Margarita and M. Simard, *Chem. Eur. J*., **1999**, *5*, 2169. (e) S. Hanessian and R. Saladino, in *Crystal Design. Structure and Function*. *Perspectives in Supramolecular Chemistry,* G. R. Desiraju, Ed.; Wiley: New York, **2003**, *7*, 77.

CHAPTER FIVE

[5.1] (a) D. V. Soldatov, G. D. Enright and J. A. Ripmeester, *Supramol*. *Chem*., **1999**, *11*, 35. (b) A. N. M. M. Rahman, R. Bishop, D. C. Craig and M. L.

Scudder, *Eur. J. Org. Chem.*, **2003**, 72. (c) V. S. S. Kumar, F. C. Pigge and N. P. Rath, *Cryst. Growth Des.*, **2004**, *4*, 651.

[5.2] (a) K. Nakano, K. Sada and M. Miyata, *Chem. Commun.*, **1996**, 989. (b) B. T. Ibragimov, Z. G. Tiljakov, K. M. Beketov and S. A. Talipov, *J. Inclusion Phenom.*, **1997**, *27*, 99. (c) B. T. Ibragimov, K. K. Makhkamov and K. M. Beketov, *J. Inclusion Phenom.*, **1999**, *35*, 583. (d) L. Paternostre, P. Damman and M. Dosière, *Macromolecules*, **1999**, *32*, 153. (e) K. A. Udachin, G. D. Enright, P. O. Brown and J. A. Ripmeester, *Chem. Commun.*, **2002**, 2162.

[5.3] (a) K. M. Beketov, B. T. Ibragimov, S. A. Talipov, K. Makhkamov and T. F. Aripov, *J. Inclusion Phenom.*, **1997**, *27*, 105. (b) K. M. Beketov, B. T. Ibragimov and S. A. Talipov, *J. Inclusion Phenom.*, **1997**, *28*, 141. (c) R. Mondal, J. A. K. Howard, R. Banerjee and G. R. Desiraju, *Chem. Commun.*, **2004**, 644.

[5.4] (a) R. Glaser, D. Shiftan and M. Drouin, *J. Org. Chem.*, **1999**, *64*, 9217. (b) S. Ahn, B. M. Kariuki and K. D. M. Harris, *Cryst. Growth Des.*, **2001**, *1*, 107. (c) P. Prabakaran, B. Umadevi, P. Panneerselvam, P. T. Muthiah, G. Bocelli and L. Right, *CrystEngComm*, **2003**, *5*, 487. (d) K. Kim, K. E. Plass and A. J. Matzger, *Langmuir*, **2005**, *21*, 647.

[5.5] (a) F. Toda, K. Tanaka and R. Kuroda, *Chem. Commun.*, **1997**, 1227. (b) V. S. S. Kumar and A. Nangia, *Chem. Commun.*, **2001**, 2392. (c) S. Hirano, S. Toyota and F. Toda, *Chem. Commun.*, **2004**, 2354. (d) S. Hirano, S. Toyota, M. Kato and F. Toda, *Chem. Commun.*, **2005**, 3646.

[5.6] Selected reference on conformational polymorph include: (a) J. Bernstein, in *Organic Solid State Chemistry*, G. R. Desiraju ed.; Elsevier: London, **1987**. (b) D. Buttar, M. H. Charlton, R. Docherty and J. Starbuck, *J. Chem. Soc., Perkin Trans. 2*, **1998**, 763. (c) V. S. S. Kumar, A. Addlagatta, A. Nangia, W. T. Robinson, C. K. Broder, R. Mondal, I. R. Evans, J. A. K. Howard and F. H. Allen, *Angew. Chem. Int. Ed.*, **2002**, *41*, 3848. (d) T. V. Timofeeva, G. H. Kuhn, V. V. Nesterov, V. N. Nesterov, D. O. Frazier, B. G. Penn and M. Y. Antipin, *Cryst. Growth Des.*, **2003**, *3*, 383. (e) L. Yu, *Cryst. Growth Des.*,

2003, *3*, 967. (f) V. Ischenko, U. Englert and M. Jansen, *Chem. Eur. J.*, **2005**, *11*, 1375. (g) C. Guo, M. B. Hickey, E. R. Guggenheim, V. Enkelmann and B. M. Foxman, *Chem. Commun.*, **2005**, 2220.

[5.7] D. F. Plusquellic, X. -Q. Tan and D. W. Pratt, *J. Chem. Phys.*, **1992**, *96*, 8026.

[5.8] (a) G. R. Desiraju, *CrystEngComm*, **2003**, *5*, 466. (b) J. D. Dunitz, *CrystEngComm*, **2003**, *5*, 506. (c) K. R. Seddon, *Cryst. Growth Des.*, **2004**, *4*, 1087. (d) G. R. Desiraju, *Cryst. Growth Des.*, **2004**, *4*, 1089. (e) J. Bernstein, *Cryst. Growth Des.*, **2005**, *5*, 661. (f) A. Nangia, *Cryst. Growth Des.*, **2006**, *6*, 2.

[5.9] W. C. McCrone, in *Physics and Chemistry of the Organic Solid State,* vol. 2, D. Fox, M. M. Labes and A. Weissberger Eds.; Wiley Interscience: New York, **1965**, pp. 725-767.

[5.10] (a) A. V. Trask, W. D. S. Motherwell and W. Jones, *Chem. Commun.*, **2004**, 890. (b) T. R. Shattock, P. Vishweshwar, Z. Wang and M. J. Zaworotko, *Cryst. Growth Des.*, **2005**, *5*, 2046.

[5.11] (a) J. Haleblian and W. C. McCrone, *J. Pharm. Sci.*, **1969**, *58*, 911. (b) J. D. Dunitz, *Pure Appl. Chem.,* **1991**. *63*. 177.

[5.12] (a) S. Kitamura, L. C. Chang and J. K. Guillory, *Int. J. Pharm.*, **1994**, *101*, 127. (b) H. Kitaoka, C. Wada, R. Moroi and H. Hakusui, *Chem. Pharm. Bull.*, **1995**, *43*, 649. (c) M. R. Caira, E. W. Peinaar and A. P. Lotter, *Mol. Cryst. Liq. Cryst.*, **1996**, *278*, 241.

CHAPTER SIX

[6.1] E. Weber, *Shape and symmetry in the design of new hosts*. In *Comprehensive Supramolecular Chemistry*; vol. 6, *Solid-state Supramolecular Chemistry: Crystal Engineering*, D. D. MacNicol, F. Toda and R. Bishop, Eds.; Pergamon Press: Oxford, **1996**.

[6.2] (a) N. K. Terrett, A. S. Bell, D. Brown and P. Ellis, *Bioorg. Med. Chem. Lett.*, **1996**, *6*, 1819. (b) A. R. McCullough, *Rev. Urol.*, **2002**, *4*, 26.

[6.3] H. S. Yathirajan, B Nagaraj, P Nagaraja and M. Bolte, *Acta Crystallogr*., **2005**, *E61*, o489.

[6.4] (a) A. Kálman and L. Párkányi, *Adv. Mol. Struct. Res*., **1997**, *3*, 189. (b) U. Rychlewska and B. Warzajtis, *Acta Crystallogr*., **2002**, *B58*, 265. (c) E. Bosch and C. L. Barnes, *Cryst. Growth Des*., **2002**, *2*, 299. (d) R. K. R. Jetti, A. Nangia, F. Xue and T. C. W. Mak, *Chem. Commun*., **2001**, 919. (e) A. Dey, R. K. R. Jetti, R. Boese and G. R. Desiraju, *CrystEngComm*, **2003**, *5*, 248.

[6.5] R. Banerjee, P. M. Bhatt, N. V. Ravindra and G. R. Desiraju., *Cryst. Growth & Design*, **2005**, 2299.

[6.6] (a) K. D. M. Harris, M. Tremayne, P. Lightfoot and P. G. Bruce, *J. Am. Chem. Soc*., **1994**, *116*, 3543. (b) K. D. M. Harris, M. Tremayne and B. M. Kariuki, *Angew. Chem., Int. Ed*., **2001**, *40*, 1626. (c) K. D. M. Harris and E. Y. Cheung, *Chem. Soc. Rev*., **2004**, *33*, 526. (d) C. Baerlocher and L. B. McCusker, *Z. Kristallogr*., **2004**, *216*, 782.

[6.7] The Rietveld refinement was carried out with the program Powder Cell[2.3].

[6.8] G. R. Desiraju, *CrystEngComm*, **2002**, *4*, 499.

[6.9] (a) D. S. Coombes, G. K. Nagi and S. L. Price, *Chem. Phys. Lett*., **1997**, *265*, 532. (b) T. Beyer, T. Lewis and S. L. Price, *CrystEngComm*, **2001**, *3*, 178. (c) W. Liu, C. -H. Lee, H. -W. Li, C. -K. Lam, J. Wang, T. C. W. Mak and D. K. P. Ng, *Chem. Commun*., **2002**, 628.

[6.10] R.Boese and H.-C.Weiss, *Acta Crystallogr*., **1998**, *C54*, 24.

[6.11] Sometimes it may happen that, for some tunnel solvate structures, it may be possible to expel the solvent (guest) molecules with the host tunnel remaining structurally intact; a single crystal of the tunnel solvate would then yield a single crystal of the apohost structure upon desolvation.

[6.12] (a) P. F. Henry, M. T. Weller, and Chick C. Wilson, *Chem. Mater*., **2002**, *14,* 4104. (b) S. Roy, R. Banerjee, A. Nangia, and G. J. Kruger, *Chem. Eur. J*., **2006**, in press.

CHAPTER SEVEN

[7.1] (a) C. Fahlberg and I. Remsen, *Chem. Ber.*, **1879**, *12*, 469. (b) C. Fahlberg and R. List, *Chem. Ber.*, **1887**, *20*, 1597. (c) M. H. Defournel, *Bull. Soc. Chim.*, **1901**, *25*, 322. (d) J. M. Price, C. G. Biava, B. L. Oser, E. E. Vogin, J. Steinfeld and H. L. Ley, *Science*, **1970**, *167*, 1131. (e) E. M. Garland, T. Sakata, M. J. Fisher, T. Masui and M. S. Cohen, *Cancer Res.*, **1989**, *49*, 3789.

[7.2] (a) B. S. Parajón-Costa, E. J. Barana, O. E. Pirob and E. E. Castellano, *Z. Naturforsch.*, **2002**, *57b***,** 43. (b) V. T. Yilmaz, S. Caglar and W. T. A. Harrison, *Transition Metal Chemistry*, **2004**, *29*, 477.

[7.3] (a) P. Naumov and G. Jovanovski, *Struct. Chem.*, **2000**, *10*, 19. (b) P. Naumov and G. Jovanovski, *Vib. Spectrosc.*, **2000**, *24*, 201. (c) P. Naumov and G. Jovanovski, *J. Coord. Chem.* **2001**, *54*, 63. (d) P. Naumov and G. Jovanovski, *Curr. Org. Chem.* **2001**, *5*, 1059. (e) P. Naumov, G. Jovanovski, J. V. Hanna, I. A. Razak, S. Chantrapromma, H.-K. Fun and S. W. Ng, *Inorg. Chem. Commun.*, **2001**, *4*, 766. (f) P. Naumov and G. Jovanovski, *J. Mol. Struct.*, **2001**, *563*, 335. (g) P. Naumov, G. Jovanovski, M. G. B. Drew and S. W. Ng, *Inorg. Chim. Acta*, **2001**, *314*, 154.

[7.4] A. D. Magri, G. D'Ascenzo, S. N. Cesaro and E. Chiacchierini, *Thermochim. Acta*, **1980**, *36*, 279.

[7.5] H. Içbudak, V. T. Yilmaz and H. Ölmez, *J. Thermal. Anal.*, **1998**, *53*, 843.

[7.6] P. Naumov G. Jovanovski, S. Abbrent and L.-E. Tergenius, *Thermochim. Acta*, **2000**, *359*, 123.

[7.7] G. Jovanovski and B. Kamenar, *Cryst. Struct. Commun.*, **1982**, *11*, 247.

[7.8] G. Jovanovski, O. Grupče and B. Šoptrajanov, *J. Mol. Struct.*, **1990**, *219*, 61.

[7.9] P. Naumov, G. Jovanovski, O. Grupče, B. Kaitner, A. D. Rae and S. W. Ng, *Angew. Chem. Int. Ed.*, **2005,** *44*, 1251.

[7.10] S. E. Lister, I. R. Evans, J. A. K. Howard, A. Coelho and J. S. O. Evans, *Chem. Commun.*, **2004**, 2540.

[7.11] K. M. A. Malik, S. Z. Haider and M. A. Hossain, *Acta Crystallogr.*, **1984**, *C40*, 1696.

[7.12] An experiment to ascertain if a K-analogue of dihydrate **1** could be obtained was performed. Failure to obtain dihydrate **1** is hardly surprising and adds to the body of evidence, which suggests that the structure of **1** is truly unusual. The water stoichiometry of 2.33 in this K-salt, **4** contrasts with the results of G. Jovanovski, B. Kaitner, O. Grupče and P. Naumov, *Central Eur. J. Chem*., **2004**, *2*, 254, who report the structure of $(K^{+})_3(sac^{-})_3(H_2O)_2$.

[7.13] The Rietveld refinement was carried out with the program Powder Cell[2.3].

[7.14] G. R. Desiraju, *Nature*, **2003**, *423*, 485.

[7.15] M. L. Mitchell and R. L. Pearson, *Alternative Sweeteners*, L. Nabors and R. C. Gelardi, Eds.; Marcel Dekker: New York, **1991**, pp 127-156.

[7.16] C. P. Brock and L. L. Duncan, *Chem. Mater*, **1994**, *6*, 1307.

[7.17] (a) A. Müller, S. Q. N. Shah, H. Bögge and M. Schmidtmann, *Nature*, **1999**, *397*, 48. (b) T. Liu, E. Diemann, H. Li, A. W. M. Dress and A. Müller, *Nature*, **2003**, *426*, 59.

[7.18] Y. Sugawara, A. Nakamura, Y. Iimura, K. Kobayashi and H. Urabe, *J. Phys. Chem. B*, **2002**, 106, 10363.

ABOUT THE AUTHOR

Rahul Banerjee was born in Sukchar, Kulinpara, a village in 24 Parganas district of West Bengal, India, in 1977. He received his elementary and secondary school education in Ramakrishna Mission, Rahara. After completion of B.Sc. and M.Sc. degrees from Calcutta University, Calcutta, he joined the School of Chemistry, University of Hyderabad for his Ph.D. degree in 2001. He was awarded a research fellowship by the University Grants Commission (JRF and SRF) between 2001-2006.

APPENDIX

Table 1. Crystallographic data for the structures discussed in this thesis.

Chapter 2				
	1b	**1c**	**1d**	**1e**
Empirical formula	$C_{12}H_{12}O_2$	$C_{12}H_{12}O_2$	$C_{14}H_{16}O_2$	$C_{10}H_6Cl_2O_2$
Formula wt.	188.23	188.23	216.28	229.26
Crystal system	Triclinic	Monoclinic	Orthorhombic	Monoclinic
Space group	$P\bar{1}$	$P2_1/c$	$P2_12_12_1$	$P2_1/c$
a [Å]	6.6905(4)	10.8340(3)	32.5783(12)	7.1489(14)
b [Å]	8.6781(6)	10.2757(2)	18.3051(6)	13.333(3)
c [Å]	10.1446(7)	9.7859(2)	25.6653(10)	10.614(2)
α [deg]	70.615(3)	90	90	90
β [deg]	75.058(3)	107.015(1)	90	104.00(3)
γ [deg]	88.865(3)	90	90	90
Z	2	4	24	4
V [Å^3]	535.43(6)	1041.75(4)	15305.5(10)	981.7(3)
D_{calc} [g/cm^3]	1.167	1.200	1.126	1.550
T [K]	120(2)	120(2)	120(2)	120(2)
μ [mm^{-1}]	0.079	0.081	0.074	0.627
2θ range	4.42–55.00	5.58–55.00	4.04–54.92	5.0–55.00
Index ranges	$-8 \le h \le 8$	$-13 \le h \le 14$	$-42 \le h \le 42$	$-9 \le h \le 9$
	$-11 \le k \le 11$	$-13 \le k \le 13$	$-23 \le k \le 23$	$-17 \le k \le 17$
	$-13 \le l \le 13$	$-12 \le l \le 12$	$-33 \le l \le 33$	$-13 \le l \le 13$
N-total	6335	10448	42794	10763
N-independent	2445	2396	8760	2251
N-observed	2141	2013	8176	2011
Parameters	175	175	625	151
R_1	0.0426	0.0373	0.0427	0.0269
wR_2	0.1160	0.1051	0.1067	0.0665
GOF	1.086	1.067	1.055	1.026

Table 1. *Continued…*

Chapter 2				
2b	**2c**	**2d**	**2e**	**2f**
$C_{16}H_{14}O_2$	$C_{14}H_8Cl_2O_2$	$C_{16}H_{14}O_2$	$C_{16}H_{12}Cl_2O_2$	$C_{16}H_{12}Br_2O_2$
238.29	279.12	238.29	307.18	396.08
Triclinic	Monoclinic	Monoclinic	Monoclinic	Orthorhombic
$P\bar{1}$	$P2_1/c$	$P2_1/c$	$P2_1/c$	$P2_12_12_1$
8.4194(3)	7.4303(2)	12.9015(4)	7.4472(15)	9.5729(2)
8.7817(3)	23.2596(5)	10.4113(3)	13.893(3)	10.3511(2)
10.3302(4)	7.5476(2)	9.7922(3)	14.297(3)	15.1691(3)
114.080(1)	90	90	90	90
102.774(2)	110.613(1)	100.768(1)	102.93(3)	90
99.085(2)	90	90	90	90
2	4	4	4	4
653.12(4)	1220.91(5)	1292.14(7)	1441.6(5)	1503.11(5)
1.212	1.518	1.225	1.415	1.750
120(2)	120(2)	120(2)	120(2)	120(2)
0.079	0.520	0.080	0.447	0.539
4.56–57.98	5.86–54.98	3.22–55.00	4.14–55.00	4.76–54.96
$-11 \le h \le 10$	$-9 \le h \le 9$	$-16 \le h \le 16$	$-9 \le h \le 9$	$-12 \le h \le 12$
$-11 \le k \le 11$	$-30 \le k \le 30$	$-13 \le k \le 12$	$-17 \le k \le 18$	$-13 \le k \le 13$
$-14 \le l \le 14$	$-9 \le l \le 9$	$-12 \le l \le 12$	$-18 \le l \le 18$	$-19 \le l \le 19$
8092	16241	13572	15311	17002
3418	2797	2976	3304	3441
2664	2691	2709	3027	3328
201	195	219	229	229
0.0605	0.0244	0.0386	0.0273	0.0148
0.1441	0.0644	0.1049	0.0731	0.0363
1.083	1.034	1.017	1.040	1.047

Table 1. *Continued…*

Chapter 2				
3a	**3b**	**4b**	**4c**	**4d**
$C_{18}H_{12}O_2$	$C_{18}H_{10}Cl_2O_2$	$C_{19}H_{14}O_2$	$C_{20}H_{16}O_2$	$C_{20}H_{16}O_2$
260.3	329.19	274.32	288.32	288.32
Monoclinic	Orthorhombic	Monoclinic	Monoclinic	Monoclinic
$P2_1/c$	$P2_12_12_1$	$P2_1/c$	$P2_1/c$	$P2_1/c$
10.8363(2)	6.7139(1)	10.387(2)	10.4185(2)	7.2871(15)
27.5202(6)	7.4777(1)	29.695(6)	14.8637(3)	13.340(3)
10.3894(2)	29.8603(4)	10.826(2)	9.6570(2)	15.870(3)
90	90	90	90	90
117.119(1)	90	118.15(3)	98.718(1)	96.254(12)
90	90	90	90	90
4	4	4	4	4
2757.67(9)	1499.12(4)	2944.3(10)	1478.18(5)	1533.6(5)
1.254	1.458	1.238	1.296	1.249
120(2)	120(2)	120(2)	120(2)	120(2)
0.081	0.436	0.079	0.083	0.080
4.22–52.00	5.46–54.94	2.74–52.00	3.96–52.00	4.0–58.00
$-13 \le h \le 13$	$-7 \le h \le 8$	$-12 \le h \le 12$	$-13 \le h \le 13$	$-9 \le h \le 9$
$-33 \le k \le 33$	$-9 \le k \le 9$	$-36 \le k \le 36$	$-19 \le k \le 19$	$-18 \le k \le 15$
$-11 \le l \le 12$	$-38 \le l \le 38$	$-13 \le l \le 13$	$-12 \le l \le 12$	$-21 \le l \le 21$
28102	17835	30792	17177	18494
5423	3407	5785	3389	4044
4269	3366	3784	2413	3183
457	231	463	263	263
0.0662	0.0279	0.0773	0.0379	0.0469
0.1700	0.0706	0.1936	0.0976	0.1134
1.263	1.120	1.074	1.050	1.039

Table 1. *Continued…*

Chapter 3				
CDDA	**14DDDA**	**15DDDA**	**18DDDA**	**TDDA**
$C_{18}H_{11}O_2Cl$	$C_{18}H_{10}O_2Cl_2$	$C_{18}H_{10}Cl_2O_2$	$C_{18}H_{10}O_2Cl_2$	$C_{18}H_8O_2Cl_4$
294.72	329.16	329.16	329.16	398.04
Triclinic	Triclinic	Monoclinic	Monoclinic	Monoclinic
$P\bar{1}$	$P\bar{1}$	$P2_1/n$	$C2/c$	$P2_1$
8.4500(17)	6.7496(4)	7.4205(2)	27.597(6)	9.3730(5)
9.2334(18)	7.2021(4)	12.7571(4)	6.8419(14)	9.5301(5)
14.108(3)	15.5160(8)	14.8695(4)	15.099(3)	10.3102(5)
84.52(3)	76.992(2)	90	90	90
89.85(3)	87.075(2)	93.382(1)	101.48(3)	114.559(2)
73.53(3)	74.353(2)	90	90	90
2	2	4	8	2
1050.4(4)	707.63(7)	1405.16(7)	2793.8(10)	837.65(7)
1.398	1.545	1.563	1.565	1.578
120(2)	120(2)	120(2)	120(2)	120(2)
0.273	0.462	0.465	0.468	0.714
4.62 – 54.94	2.70 – 58.10	4.2 – 57.98	5.5 – 54.99	4.34 – 57.97
$-10 \le h \le 10$	$-9 \le h \le 9$	$-10 \le h \le 9$	$-35 \le h \le 35$	$-12 \le h \le 12$
$-11 \le k \le 11$	$-9 \le k \le 9$	$-17 \le k \le 17$	$-8 \le k \le 8$	$-13 \le k \le 13$
$-18 \le l \le 18$	$-21 \le l \le 21$	$-20 \le l \le 20$	$-19 \le l \le 19$	$-14 \le l \le 13$
12642	8590	16581	15923	10227
4803	3693	3207	3211	4398
3970	3175	2702	2886	4344
365	199	239	239	249
0.0408	0.0969	0.0328	0.0350	0.0283
0.1025	0.2786	0.0853	0.0999	0.0748
1.028	1.238	1.031	1.058	1.057

Table 1. *Continued…*

Chapter 3	*Chapter 4*			
15MKA	**(15DDDA) (DMSO)**	**(15DDDA) $(DMSO)_2$**	**(15DDDA) $(HMPA)_2$**	**(15DDDA) $(NMP)_2$**
$C_{16}H_8O_2Cl_2$	$(C_{18}H_{10}Cl_2O_2).(C_2H_6OS)$	$(C_{18}H_{10}Cl_2O_2).(C_2H_6OS)_2$	$(C_{18}H_{10}Cl_2O_2).(C_6H_{18}N_3OP)_2$	$(C_{18}H_{10}Cl_2O_2).(C_5H_9NO)_2$
303.12	407.29	485.42	687.57	527.42
Monoclinic	Triclinic	Triclinic	Triclinic	Triclinic
$P2_1/n$	$P\bar{1}$	$P\bar{1}$	$P\bar{1}$	$P\bar{1}$
7.2693(2)	7.3174(15)	6.6307(5)	8.5057(2)	7.4173(15)
11.5276(3)	9.3646(19)	7.6581(5)	9.7689(2)	9.1696(18)
15.4191(4)	14.222(3)	11.9717(7)	10.7323(2)	9.6472(19)
90	81.14(3)	79.613(2)	86.9450(10)	103.40(3)
98.775(1)	89.16(3)	84.232(2)	77.4350(10)	90.46(3)
90	67.56(3)	67.037(2)	84.8540(10)	102.70(3)
4	2	2	2	2
1276.96(6)	889.0(3)	550.26(6)	866.37(3)	621.5(2)
1.577	1.522	1.465	1.318	1.409
120(2)	120(2)	120(2)	120(2)	120(2)
0.504	0.501	0.512	0.323	0.300
5.34– 55.00	4.76 – 54.98	3.90 –54.98	3.90 –54.98	4.34 –54.98
$-9 \le h \le 9$	$-9 \le h \le 9$	$-8 \le h \le 8$	$-11 \le h \le 12$	$-9 \le h \le 9$
$-14 \le k \le 13$	$-12 \le k \le 11$	$-9 \le k \le 9$	$-12 \le k \le 12$	$-11 \le k \le 11$
$-19 \le l \le 20$	$-18 \le l \le 18$	$-15 \le l \le 15$	$-13 \le l \le 13$	$-12 \le l \le 12$
12801	10782	6206	9911	7131
2925	4079	2530	3965	2848
2436	3749	2385	3727	2701
213	299	233	291	217
0.0348	0.0325	0.0388	0.0325	0.0322
0.0912	0.0895	0.0948	0.0886	0.0871
1.052	1.059	1.061	1.041	1.031

Table 1. *Continued…*

Chapter 4		*Chapter 5*		
(15DDDA) $(DMF)_2$	**$(15DDDA)_2$ $(pyrrolidinone)_2$**	***cis*-15DDDA**	**2a**	**2b**
$(C_{18}H_{10}Cl_2O_2).(C_3H_7NO)_2$	$(C_{18}H_{10}Cl_2O_2).(C_4H_7NO)_2$	$C_{18}H_{10}Cl_2O_2$	$(C_{18}H_{10}Cl_2O_2).(C_4H_{11}N)$	$(C_{18}H_{10}Cl_2O_2).(C_4H_{11}N)$
475.35	325.78	329.16	402.30	402.30
Monoclinic	Triclinic	Monoclinic	Monoclinic	Orthorhombic
$P2_1$	$P\bar{1}$	$P2_1/n$	$P2_1/n$	*Pbca*
120(2)	120(2)	120(2)	120(2)	95(2)
7.3834(3)	7.9147(14)	7.4731(2)	8.1794(2)	14.955(3)
15.3739(8)	9.5545(16)	12.5163(3)	13.6483(4)	13.659(3)
10.3430(5)	11.326(2)	16.2952(5)	18.0272(5)	19.433(4)
90	66.629(6)	90	90	90
102.497(2)	87.797(7)	100.565(1)	96.984(1)	90
90	87.831(7)	90	90	90
2	2	8	4	8
1146.23(9)	785.4(2)	1498.34(7)	1997.53(9)	3969.4(14)
1.377	1.378	1.459	1.338	1.346
0.317	0.252	0.436	0.342	0.344
4.04 –54.96	2.27–27.55	4.12–54.94	3.76–52.00	4.20–55.00
$-9 \le h \le 9$	$-10 \le h \le 10$	$-9 \le h \le 9$	$-10 \le h \le 10$	$-19 \le h \le 19$
$-19 \le k \le 19$	$-12 \le k \le 12$	$-16 \le k \le 16$	$-16 \le k \le 16$	$-17 \le k \le 17$
$-13 \le l \le 13$	$-14 \le l \le 14$	$-21 \le l \le 21$	$-22 \le l \le 22$	$-25 \le l \le 25$
11510	8197	16656	19907	41925
4895	3610	3431	3925	4557
4233	3149	2430	3353	3539
333	272	239	328	328
0.0576	0.0375	0.0539	0.0460	0.0656
0.1539	0.1061	0.1172	0.1063	0.1230
1.182	1.069	1.054	1.105	1.161

Table 1. *Continued…*

Chapter 6				
SS	**(SS) (CH_3NO_2)**	**(SS) (CH_3CN)**	**(SS) ($HCONH_2$)**	**$(SS)_2$ (HOC_2H_4OH)**
($C_{22}H_{31}N_6O_4S$) ($C_7H_4NO_3S$)	($C_{22}H_{31}N_6O_4S$) ($C_7H_4NO_3S$) (CH_3NO_2)	($C_{22}H_{31}N_6O_4S$) ($C_7H_4NO_3S$) (C_2H_3N)	($C_{22}H_{31}N_6O_4S$) ($C_7H_4NO_3S$) (CH_3NO)	($C_{22}H_{31}N_6O_4S$) ($C_7H_4NO_3S$) ($C_2H_6O_2$)
657.76	718.56	698.21	702.53	1377.08
Triclinic	Triclinic	Triclinic	Triclinic	Triclinic
$P\bar{1}$	$P\bar{1}$	$P\bar{1}$	$P\bar{1}$	$P\bar{1}$
10.3848(10)	9.904(3)	9.8766(12)	9.7746(8)	9.8344(10)
11.1915(11)	12.121(3)	11.8949(14)	12.1473(10)	11.9909(12)
14.3155(14)	14.746(4)	14.5924(17)	14.4824(12)	14.4669(14)
80.025(2)	87.369(3)	86.0090(10)	87.0150(10)	85.5520(10)
70.988(2)	75.491(3)	73.1880(10)	75.2760(10)	73.6810(10)
89.912(2)	89.243(3)	89.0450(10)	88.6890(10)	88.6810(10)
2	2	2	2	2
1546.5(3)	1711.9(7)	1637.1(3)	1660.8(2)	1632.3(3)
1.412	1.394	1.418	1.405	1.401
298(2)	100(2)	100(2)	298(2)	298(2)
0.231	0.220	0.223	0.223	0.224
5.2 – 49.4	2.9 – 50.0	3.4 – 50.0	2.9 – 50.0	2.9 – 50.0
$-11 \le h \le 12$	$-10 \le h \le 11$	$-11 \le h \le 11$	$-11 \le h \le 11$	$-11 \le h \le 11$
$-13 \le k \le 13$	$-14 \le k \le 14$	$-14 \le k \le 14$	$-14 \le k \le 14$	$-14 \le k \le 13$
$-17 \le l \le 17$	$-17 \le l \le 17$	$-17 \le l \le 17$	$-17 \le l \le 17$	$-16 \le l \le 17$
11556	9594	16134	15991	14500
5440	5795	5754	5835	5739
3636	4556	5304	5140	4631
418	455	446	446	437
0.0534	0.0573	0.0360	0.0437	0.0496
0.1230	0.1616	0.0931	0.1257	0.1321
1.031	1.067	1.061	1.049	1.053

Table 1. *Continued…*

Chapter 6				
$(SS)_2$ $(C_4H_8O_2)$	**$(SS)\cdot(H_2O)_2$**	**$(SS)_2$ (C_2H_6SO)**	**$(SS)_2$ (C_4H_7NO)**	**$(SS)_2$ (C_4H_8O)**
$(C_{22}H_{31}N_6O_4S)$ $(C_7H_4NO_3S)$ $(C_4H_8O_2)$	$(C_{22}H_{31}N_6O_4S)$ $(C_7H_4NO_3S)$ $(H_2O)_2$	$[(C_{22}H_{31}N_6O_4S)$ $(C_7H_4NO_3S)]_2$ (C_2H_6SO)	$[(C_{22}H_{31}N_6O_4S)$ $(C_7H_4NO_3S)]_2$ (C_4H_7NO)	$[(C_{22}H_{31}N_6O_4S)$ $(C_7H_4NO_3S)]_2$ (C_4H_8O)
1402.84	693.22	1392.92	1400.11	1386.02
Triclinic	Triclinic	Triclinic	Triclinic	Triclinic
$P\bar{1}$	$P\bar{1}$	$P\bar{1}$	$P\bar{1}$	$P\bar{1}$
10.1077(7)	9.6860(9)	9.912(3)	10.0172(14)	9.9555(10)
11.7836(9)	11.8441(11)	11.977(4)	12.0024(17)	11.9824(12)
14.4197(11)	14.4976(13)	14.587(5)	14.510(2)	14.5239(15)
85.1150(10)	93.7430(10)	86.226(5)	85.071(2)	86.1600(10)
71.8480(10)	107.5540(10)	72.561(5)	72.648(2)	72.8820(10)
88.2100(10)	90.2610(10)	89.305(5)	87.666(2)	88.3800(10)
2	2	2	2	2
1626.0(2)	1581.8(3)	1648.5(9)	1658.7(4)	1652.0(3)
1.433	1.457	1.384	1.383	1.407
100(2)	100(2)	100(2)	298(2)	298(2)
0.227	0.234	0.251	0.220	0.221
3.0 – 50.0	3.0 – 50.0	2.9 – 50.0	2.9 – 46.7	2.9 – 50.0
$-12 \le h \le 12$	$-11 \le h \le 10$	$-10 \le h \le 11$	$-11 \le h \le 11$	$-11 \le h \le 11$
$-14 \le k \le 14$	$-14 \le k \le 12$	$-14 \le k \le 14$	$-13 \le k \le 12$	$-14 \le k \le 14$
$-17 \le l \le 17$	$-17 \le l \le 17$	$-17 \le l \le 17$	$-16 \le l \le 16$	$-17 \le l \le 17$
15654	11155	12052	9016	18717
5703	5568	5786	4735	5817
5205	5039	3256	3556	5095
445	459	458	452	451
0.0430	0.0533	0.1066	0.0650	0.0464
0.1100	0.1445	0.2407	0.1802	0.1179
1.034	1.136	1.052	1.085	1.056

Table 1. *Continued…*

Chapter 6			*Chapter 7*	
$(SS)_2$ (C_2H_5OH)	**(SS) (CH_3OH)**	**$(SS)_2$ (C_3H_7NO)**	**1**	**4**
$[(C_{22}H_{31}N_6O_4S)(C_7H_4NO_3S)]_2(C_2H_6O)$	$(C_{22}H_{31}N_6O_4S)(C_7H_4NO_3S)(CH_4O)$	$[(C_{22}H_{31}N_6O_4S)(C_7H_4NO_3S)]_2(C_3H_7NO)$	$Na_{16}(C_7H_4NO_3S)_{16}(H_2O)_{30}$	$K_3(C_7H_4NO_3S)_3(H_2O)_{2.33}$
1360.76	689.11	1387.88	238.94	235.27
Triclinic	Monoclinic	Triclinic	Monoclinic	Triclinic
$P\bar{1}$	$C2/c$	$P\bar{1}$	$P2_1/n$	$P\bar{1}$
100(2)	100(2)	100(2)	100(2)	298(2)
9.7393(13)	40.736(4)	9.8323(8)	18.5918(11)	7.6104(5)
11.8275(16)	8.1842(7)	11.8486(10)	28.3628(16)	12.3049(8)
14.4853(19)	20.6300(18)	14.4885(12)	29.0562(16)	15.4936(10)
93.674(2)	90.00	86.2120(10)	90	72.278(1)
107.399(2)	104.870(2)	72.4360(10)	93.560(2)	86.581(1)
90.050(2)	90.00	89.5080(10)	90	81.229(1)
2	8	2	4	2
1588.6(4)	6647.6(10)	1605.6(2)	15291.7(15)	1365.75(5)
1.442	1.378	1.429	1.661	1.716
0.230	0.220	0.228	0.381	0.794
3.0 – 52.60	4.04 – 50.00	3.0 – 52.60	2.54–52.10	2.76–52.12
$-12 \le h \le 11$	$-41 \le h \le 48$	$-12 \le h \le 11$	$-22 \le h \le 22$	$-9 \le h \le 9$
$-14 \le k \le 14$	$-9 \le h \le 9$	$-12 \le k \le 1\ 4$	$-34 \le k \le 35$	$-15 \le k \le 15$
$-17 \le 1 \le 18$	$-23 \le h \le 19$	$-18 \le l \le 16$	$-35 \le l \le 25$	$-19 \le 1 \le 19$
14780	8262	12397	105833	22602
6326	5371	6457	30081	5369
4824	3237	5810	21746	5029
586	441	460	2385	410
0.0493	0.0720	0.0411	0.0448	0.0312
0.1121	0.1286	0.1096	0.0719	0.0879
1.020	0.977	1.039	1.005	1.095